



UNIVERSITÄT ZU LÜBECK

From the INSTITUTE FOR SYSTEMIC INFLAMMATION RESEARCH

OF THE UNIVERSITY OF LÜBECK

Director: PROF. DR. med. JÖRG KÖHL

**Impact of the complement system and Gab3 on
natural killer cells during *Toxoplasma gondii*
infection**

Dissertation

for Fulfillment of the Requirements for the Doctoral Degree

of the University of Lübeck

From the Department of Natural Sciences

Submitted by:

Fabian Mey

From Minden

Lübeck 2019

First referee: Prof. Dr. med. Jörg Köhl

Second referee: Prof. Dr. rer. nat. Ulrich Schaible

Date of oral examination: 9th October 2019

Approved for printing: 9th October 2019

List of contents

Summary.....	V
Zusammenfassung	VII
1 Introduction	1
1.1 The immune system.....	1
1.1.1 Innate and adaptive immunity	1
1.1.2 The complement system.....	4
1.1.2.1 Activation of the complement system	5
1.1.2.2 Regulation of the complement system	8
1.1.2.3 The anaphylatoxin C5a and its two receptors	8
1.2 IL-12 cytokine family.....	11
1.3 Natural killer cells: key players during early innate immune responses.....	12
1.3.1 Natural killer cell activation and pathogen clearance	12
1.3.2 Dendritic cell – mediated NK cell activation via stimulatory synapse formation	14
1.4 <i>Toxoplasma gondii</i>: an intracellular parasite	15
1.4.1 Biology and life cycle of <i>Toxoplasma gondii</i>	15
1.4.2 The innate immune response against <i>T. gondii</i>	17
1.4.3 The role of NK cells during <i>T. gondii</i> infection	21
1.4.4 The adaptive immune response against <i>T. gondii</i> infection.....	21
1.4.5 The role of the complement system during <i>T. gondii</i> infections	22
1.5 The growth factor receptor-bound protein 2 (Grb-2)-associated binder (Gab) protein family	24
1.5.1 Role and function in signal transduction	24
1.5.2 PH-domain – associated recruitment of Gab proteins	26
1.6 Hypothesis and specific aims.....	27
2 Material and Methods.....	29
2.1 Material	29
2.1.1 Mouse strains	29
2.1.2 Chemicals and reagents	29
2.1.3 Buffers, solutions and media.....	31
2.1.4 Antibodies for flow cytometry	32
2.1.5 Plastic ware and disposable items.....	34
2.1.6 Commercially available kits.....	35
2.1.7 Laboratory equipment	35

2.1.8	Computer software.....	37
2.2	Methods.....	38
2.2.1	Animals.....	38
2.2.1.1	Generation of floxed reporter mice.....	38
2.2.1.2	ENU (N-ethyl-N-nitrosourea) mutagenesis.....	38
2.2.1.3	Generation of mixed bone marrow chimeric mice.....	39
2.2.2	<i>Toxoplasma gondii</i> mouse infection models.....	40
2.2.2.1	Generating a stock of <i>T. gondii</i> cysts for infections.....	40
2.2.2.2	Determination of <i>T. gondii</i> brain cysts in infected mice.....	41
2.2.2.3	Oral infection model.....	41
2.2.2.4	Intraperitoneal infection model.....	42
2.2.2.5	Acute and chronic <i>T. gondii</i> infection models.....	42
2.2.2.6	Evaluation of <i>T. gondii</i> -induced disease severity in mice.....	43
2.2.3	Immune cell isolation from mouse tissue.....	43
2.2.3.1	Cell number determination.....	45
2.2.4	Histological sections.....	45
2.2.4.1	Wright-Giemsa staining using Diff-Quik.....	45
2.2.4.2	Evaluation of histology sections.....	45
2.2.5	Measurement of cytokine production in sera and supernatants.....	46
2.2.5.1	Enzyme-linked immunosorbent assay (ELISA)-based measurement.....	46
2.2.5.2	AYOXXA LUNARIS™ 12-Plex Cytokine Kit.....	46
2.2.6	<i>In vitro</i> NK cell stimulation.....	46
2.2.7	Flow cytometry.....	47
2.2.7.1	Surface staining and general gating strategy.....	47
2.2.7.2	Intracellular stainings.....	48
2.2.8	Statistical analyses.....	48
3	Results.....	50
3.1	The survival after oral <i>T. gondii</i> infection is higher in C5aR1 ^{-/-} and C5aR2 ^{-/-} mice than in WT mice.....	50
3.2	Potential protective role of C5a receptors in the intestine during <i>T. gondii</i> infections....	52
3.3	Impact of the parasite infection dose on disease development in the oral <i>T. gondii</i> infection model.....	53
3.4	Assessment of C5aR1/2 expression during acute i.p. <i>T. gondii</i> infection using floxed GFP-C5aR1 and floxed tdTomato-C5aR2 mice.....	57
3.5	Functional roles of C5aR2 on NK cells and DCs.....	78

3.5.1	Frequencies and cell numbers of DCs and NK cells of WT, C5aR1 ^{-/-} and C5aR2 ^{-/-} mice in the spleen .	78
3.5.2	The C5a/C5aR2 axis controls IFN- γ production from NK cells after IL-12/IL-18 stimulation.....	79
3.5.3	C5aR2 stimulation results in phosphorylation of p38 mitogen-activated protein kinase.....	80
3.5.4	C5aR2 ^{-/-} NK cells show elevated NKp46 expression compared to WT NK cells	81
3.5.5	tdTomato-C5aR2 ⁺ NK cells express higher numbers of NKp46 receptors than tdTomato-C5aR2 ⁻ NK cells from the spleen and peritoneal cavity.....	83
3.5.6	Increased CD11a and VCAM1 expression in DCs and NK cells from the spleen of C5aR2 ^{-/-} as compared to WT mice	83
3.6	Gab3^{R27C} mice suffer from increased susceptibility and cyst burden during <i>T. gondii</i> infection.....	85
3.6.1	Gab3 ^{R27C} and WT mice show similar cytokine and chemokine profiles in serum	86
3.6.2	Impaired cell differentiation of myeloid cells from Gab3 ^{R27C} mice in mixed BM-chimeric mice.....	88
4	Discussion	90
4.1	C5a receptors are critical for controlling intestinal inflammation during early <i>T. gondii</i> infection.....	90
4.2	Uncoupled co-expression of C5aR1 and C5aR2 as an important immune regulatory mechanism.....	91
4.3	C5aR2 controls NK cell-derived IFN-γ production in response to IL-12/IL-18 stimulation. 96	
4.4	The C5a/C5aR2 axis may control NKp46 expression as one mechanism of NK cell regulation.....	97
4.5	Control of cell-cell interaction between NK cells and DCs as a mechanism of C5aR2-mediated regulation of NK cell activation	98
4.6	Gab3 is crucially important for cell differentiation and influences <i>T. gondii</i> susceptibility ..	99
5	References.....	102
6	APPENDIX.....	120
6.1	Abbreviations	121
6.2	Figures	124
6.3	Tables	133
6.4	List of publications.....	134
6.4.1	Congress contributions	134

7	<i>Acknowledgements</i>	136
8	<i>Curriculum Vitae</i>	138

Summary

Toxoplasma gondii (*T. gondii*) is an obligate intracellular parasite which is able to infect every nucleated cell in humans and animals. It is globally spread, and infections are usually asymptomatic. However, in immunocompromised patients, the infection can cause life-threatening symptoms. Furthermore, primary infections during pregnancy can seriously harm the unborn and result in abortion or death shortly after birth.

In mice, the immune response against *T. gondii* is mainly driven by the recognition of the Toll-like receptor (TLR) 11 and 12 ligand profilin. TLR11 and TLR12 are, besides other cells, expressed on CD8 α^+ dendritic cells (DCs), which produce pro-inflammatory cytokines like IL-12, IL-15 and IL-18 in response to *T. gondii* sensing. These cytokines are necessary to prime other effector cells like natural killer (NK) cells, which are responsible for early production of IFN- γ . Previous results from our institute suggested that C5aR2 $^{-/-}$ NK cells respond with increased IFN- γ production after IL-12 and IL-18 stimulation and that C5aR1 $^{-/-}$ mice suffer from increased susceptibility during *T. gondii* infections.

Based on these data, I hypothesized that regulation of C5aR1 and C5aR2 plays an important role during *T. gondii* infections on different cell types and that regulation of both C5a receptors might be a key feature in controlling the parasite.

To test my hypotheses, I used floxed GFP-C5aR1 and floxed tdTomato-C5aR2 reporter mice which allow to analyze cell-specific C5a receptor expression. I found that C5aR1 and C5aR2 are independently regulated on several immune cell populations like NK cells, macrophages and neutrophils. Importantly, C5aR2 but not C5aR1 was expressed in subpopulations of NK cells in different compartments. Furthermore, I showed that C5aR1 and C5aR2 were independently expressed and regulated in the blood, spleen and lung.

The function of C5aR2 is still enigmatic as both, anti- and pro-inflammatory properties have been reported. To determine potential functions of C5aR2, I focused on NK cell that exclusively expressed C5aR2 but not C5aR1. I found that the lack of C5aR2 on NK cells results in hyperresponsiveness in response to IL-12 / IL-18 stimulation resulting in massive IFN- γ production. Mechanistically, my findings suggest that C5aR2-mediated p38 MAPK phosphorylation and NKp46 expression may account for the suppressive effect of C5aR2 on NK cell activation.

As DC and NK cell interaction is indispensable for the induction of an early immune response upon *T. gondii* infections, I investigated the expression of important cell-cell-interaction molecules like VCAM1 and CD11a on these two cell types. I could show that VCAM1 as well as CD11a expression is altered on NK cells and DCs from C5aR1 $^{-/-}$ and C5aR2 $^{-/-}$ mice compared to WT mice.

In addition to C5aR2, I assessed the role of the growth factor receptor-bound protein 2 (Grb-2) associated binder (Gab) Gab3, another protein highly expressed in NK cells. In the IRTG partner lab, Dr. *Hoebe* identified an ENU-generated germline mutant with a point mutation in the *gab3* gene resulting in an amino acid change from arginine to cysteine at position 27. I found that non-functional Gab3^{R27C} resulted in increased susceptibility to *T. gondii* infection characterized by increased mortality and parasite burden in the brain. Furthermore, the Gab3^{R27C} mutations resulted in impaired cell-differentiation of myeloid cells in the peritoneal cavity, but not in spleen or bone marrow.

My findings show that the complement system and more specifically the anaphylatoxin C5a and its two receptors C5aR1 and C5aR2 play important roles during *T. gondii* infections. Especially my findings of the independent regulation of C5aR1 and C5aR2 on different immune cell population and the unique expression of C5aR2 on NK cells provide new insights into the regulation and activation of the complement system. Furthermore, my results provide new evidence for the important function of Gab3 during *T. gondii* infections, which may result from the impact on cell differentiation.

Zusammenfassung

Toxoplasma gondii (*T. gondii*) ist ein intrazellulärer Parasit, der jede Zellkern-haltige Zelle in Menschen und Tieren befallen kann. Er ist auf der ganzen Welt zu finden und Infektionen verlaufen in der Regel asymptomatisch. In immungeschwächten Patienten kann eine Infektion allerdings zu lebensbedrohlichen Symptomen führen. Außerdem können Primärinfektionen während der Schwangerschaft zu Fehlgeburten oder massiven gesundheitlichen Schädigungen des Ungeborenen, bis hin zum Tod, führen.

In Mäusen erfolgt die Erkennung des Parasiten über die Toll-like-Rezeptoren (TLR) 11 und 12, welche das *T. gondii*-produzierte Protein Profilin erkennen. TLR11 und 12 sind unter anderem auf CD8 α^+ dendritischen Zellen (DCs) exprimiert, welche als Antwort auf die Erkennung des Parasiten pro-inflammatorische Zytokine wie IL-12, IL-15 und IL-18 produzieren. Diese Zytokine sind notwendig um weitere Effektorzellen, wie natürliche Killer (NK) Zellen, zu aktivieren, damit diese IFN- γ produzieren. NK Zellen sind maßgeblich für die Produktion von IFN- γ in der Frühphase der Infektion verantwortlich. Vorherige Ergebnisse aus unserem Institut haben gezeigt, dass C5aR2^{-/-} NK Zellen mit signifikant erhöhter IFN- γ Produktion auf Stimulation mit IL-12 und IL-18 reagieren. Außerdem wurde gezeigt, dass C5aR1^{-/-} Mäuse eine höhere Suszeptibilität während einer *T. gondii* Infektion aufweisen.

Basierend auf diesen Ergebnissen vermute ich, dass die Regulation von C5aR1 und C5aR2 auf verschiedenen Zelltypen während der Infektion eine wichtige Rolle spielt. Außerdem könnte eine Regulation der Expression der beiden Rezeptoren eine wichtige Rolle spielen.

Um meine Hypothesen zu testen, habe ich floxed GFP-C5aR1 und floxed tdTomato-C5aR2 Reporter-mäuse verwendet, welche eine genaue Analyse der Expression der beiden C5a Rezeptoren auf einzelnen Zelltypen erlauben. Ich konnte zeigen, dass beide Rezeptoren in unterschiedlicher Ausprägung exprimiert und außerdem nicht immer im gleichen Maße reguliert werden. So konnte eine unterschiedliche Regulation zum Beispiel auf NK Zellen, Makrophagen und Neutrophilen nachgewiesen werden. Außerdem konnte ich zeigen, dass C5aR2, aber nicht C5aR1, auf Subpopulationen von NK Zellen in verschiedenen Organen exprimiert ist.

Die Funktion von C5aR2 ist immer noch nicht endgültig geklärt, da sowohl pro- als auch anti-inflammatorische Funktionen beschrieben sind. Um potenzielle Funktionen des C5aR2 zu ermitteln, habe ich vermehrt NK Zellen analysiert, da diese exklusiv den C5aR2 exprimieren. Ich konnte zeigen, dass das Fehlen von C5aR2 auf NK Zellen für eine Hypersensibilität nach IL-12 und IL-18 Stimulation sorgt, welche durch eine erhöhten IFN- γ Produktion charakterisiert ist. Mechanistisch deuten meine Ergebnisse darauf hin, dass C5aR2-bedingte p38 MAPK Phosphorylierung und NKp46 Expression für den reduzierten C5aR2-Effekt auf NK Zellen verantwortlich sind.

Da die direkte Interaktion von DCs und NK Zellen für eine Aktivierung der NK Zellen unerlässlich ist, um eine Immunantwort nach einer *T. gondii* Infektion einzuleiten, habe ich mir die Expression von Molekülen für die Zell-Zell-Interaktion, wie VCAM1 und CD11a, auf diesen beiden Zelltypen angesehen. Ich konnte zeigen, dass die Expression von VCAM1 und CD11a auf NK Zellen und DCs von C5aR1^{-/-} und C5aR2^{-/-} Mäusen im Vergleich zu WT Mäusen unterschiedlich ist.

Zusätzlich zu den Untersuchungen am C5aR2, habe ich mir die Funktion vom *growth factor receptor-bound protein 2 (Grb-2) associated binder 3 (Gab 3)* angeguckt, welches ebenfalls stark auf NK Zellen exprimiert ist. Im IRTG-Partnerlabor von Dr. Hoebe wurde eine ENU-generierte Mauslinie erstellt, welche eine Punktmutation im *gab3* Gen aufweist. Diese Mutation sorgt für einen Aminosäureaustausch von Arginin zu Cystein an der 27. Position.

Ich konnte zeigen, dass ein nicht-funktionales Gab3 Protein für eine erhöhte Suszeptibilität während der *T. gondii* Infektion sorgt, welche durch erhöhte Sterblichkeit und Parasitenlasten im Gehirn charakterisiert ist. Außerdem führt die Gab3 Mutation zu einer Beeinträchtigung der Zelldifferenzierung von myeloischen Zellen in der Bauchhöhle, nicht aber in der Milz oder im Knochenmark.

Meine Ergebnisse zeigen, dass das Komplementsystem und vor allem das Anaphylatoxin C5a und die beiden Rezeptoren C5aR1 und C5aR2 wichtige Rollen während der *T. gondii* Infektion spielen. Vor allem meine Ergebnisse zur unterschiedlichen Regulierung der Expression der beiden Rezeptoren auf verschiedenen Zellpopulationen und die spezifische Expression von C5aR2 auf NK Zellen erlaubt neue Rückschlüsse auf die Regulation und Aktivität des Komplementsystems. Außerdem konnte ich neue Beweise für die Wichtigkeit und Funktion von Gab3 während einer *T. gondii* Infektion herausarbeiten, welche möglicherweise auf eine Beeinträchtigung bei der Zelldifferenzierung zurückzuführen sind.

1 INTRODUCTION

1.1 The immune system

1.1.1 Innate and adaptive immunity

To protect the host from pathogens, different defense strategies have developed during evolution. The first defense mechanisms include outer physical barriers like the skin on which anti-microbial peptides are secreted, while the inner defense mechanisms comprise the innate and adaptive immune responses (**Figure 1**). These defense mechanisms protect the body from pathogens and also eliminate damaged host cells and maintain body homeostasis. If pathogens enter the host, immediate innate immune responses prevent uncontrolled spreading of the pathogen throughout the host. After this initial phase, the innate immune system instructs the adaptive immune system to mount pathogen-specific immune response to eliminate the threat. Here, antigen-specific receptors on T- and B-cells recognize specific pathogen structures resulting in the induction of a pathogen-specific immune response subsequently leading to the elimination of the specific pathogen (Murphy and Weaver, 2016).

The **innate immune system** has evolved early in multicellular organisms. It consists of anatomical and chemical barriers as well as cellular and humoral defense mechanisms. Important mechanisms involve phagocytic cells like macrophages or granulocytes, dendritic cells (DCs), mast cells, natural killer (NK) cells, and innate lymphoid cells (ILCs) as well as the complement system. As the complement system and NK cells are of major importance for this thesis, I will describe them in detail in chapter 1.1.2. and 1.3., respectively.

An innate immune response occurs within minutes after recognition of pathogen components known as pathogen-associated molecular patterns (PAMPs) like lipopolysaccharides (LPS), bacterial flagellin or nucleic acids including RNA and DNA. PAMPs have been conserved during evolution, hence making them a perfect target for recognition. Additionally, release of molecules from damaged or dying cells of the host known as damage-associated molecular patterns (DAMPs) like for example ATP, which are normally not found in extracellular compartments, are also recognized and can induce innate immune responses. Cells from the innate immune system express a wide range of pathogen recognition receptors (PRRs) which detect PAMPs and DAMPs and trigger an immune response (Thompson et al., 2011).

DCs play crucial roles in the induction of immune responses and are indispensable for a proper NK cell activation. On the one hand, they are able to detect PAMPs and DAMPs via the expression of many

different TLRs. In response to that, they start to produce pro-inflammatory cytokines like IL-2, IL-12, IL-15 or IL-18 and activate effector cells like NK cells. On the other hand, DCs are potent antigen-presenting cells (APCs) that are able to take up, process and finally present antigens via major histocompatibility complexes (MHC) to cells of the adaptive immune system (Summerfield and McCullough, 2009). Thus, DCs act as a bridge between the innate and adaptive immune system.

In comparison to an innate immune response, the induction of an **adaptive immune response** takes days after the first contact with the pathogen. Furthermore, in contrast to innate immunity, adaptive immune responses are pathogen-specific and can induce the formation of an immunological memory. B lymphocytes (B cells) and T lymphocytes (T cells) are the two major cell types of the adaptive immune response which express distinct types of antigen-specific receptors, the so-called B-cell antigen receptor (BCR) and T-cell antigen receptor (TCR).

After recognition of an antigen by the BCR, the B cell starts to proliferate and differentiate into plasma cells, which are the effector form of B cells. Plasma cells start to produce and secrete antibodies with the same antigen specificity as their BCR and hence produce antibodies which target the antigen that has been recognized before (Murphy and Weaver, 2016). Those antibodies can opsonize pathogens to induce elimination by phagocytes, activate the complement system or neutralize the pathogen.

In contrast to B cells, T cells can only recognize antigens which are presented by an APC. However, when T cells recognize an antigen they also start to proliferate and cytotoxic CD8⁺ T cells are activated, while CD4⁺ helper T cells differentiate into different subsets (T_{H1}, T_{H2}, T_{H17}, T_{reg}). CD8⁺ cytotoxic T cells kill infected host cells, whereas CD4⁺ helper T cells produce cytokines to activate or regulate other cells of the immune system. Regulatory T cells (T_{reg}) protect the host from developing an overwhelming immune response characterized by elevated cytokine levels (Alberts et al., 2002).

Another specialty of the adaptive immune system is the capability of some B and T cells to differentiate into memory cells that confer long-lasting specific immunity. Those memory cells will differentiate into effector cells when the organism is exposed to a specific antigen for the second time and allow very quick elimination of pathogens by faster proliferation and activation compared to the first encounter with the specific antigen.

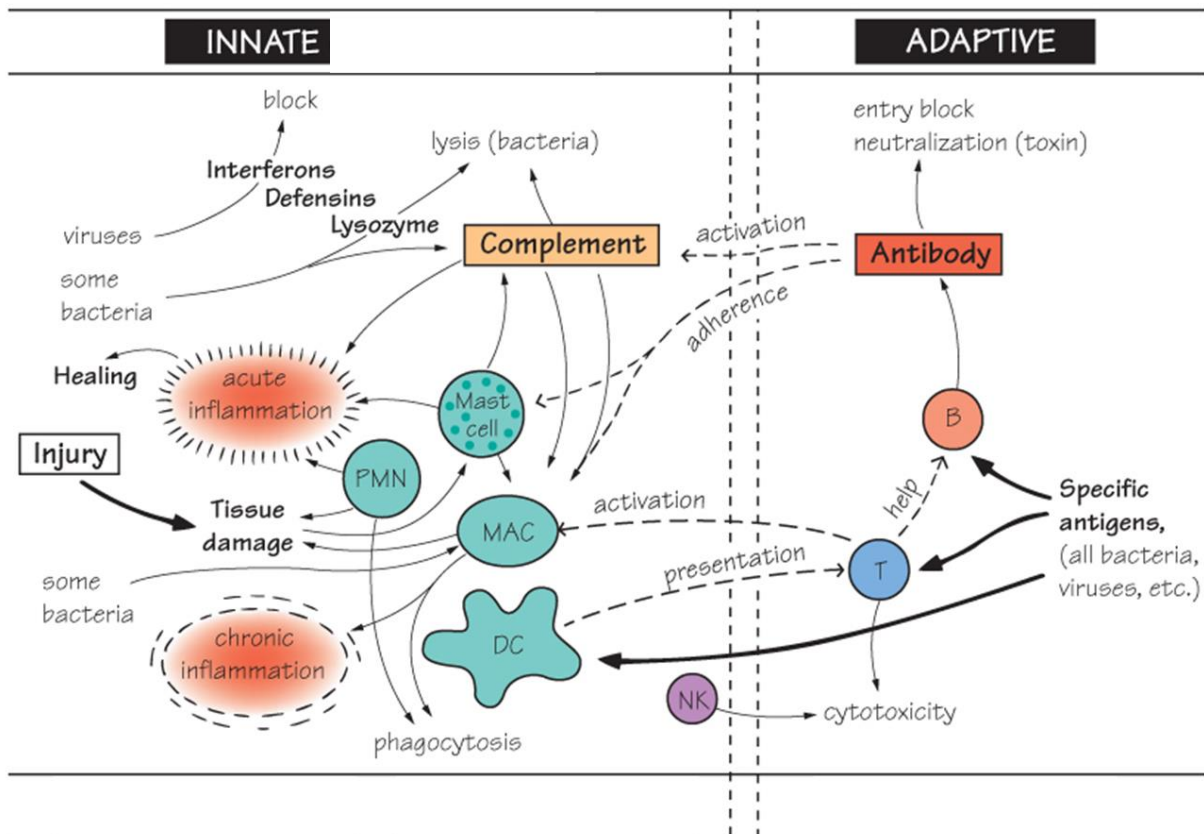


Figure 1: Overview of innate and adaptive immune responses. Shown are major cell types and humoral components of both parts. The fast reacting innate immune system (left) consists of humoral factors (complement) and cell components, that act as a first line defense system. The adaptive immune response (right) is characterized by a slower but individual response and comprises B cells, T cells and antibodies. DCs and NK cells show characteristics of both parts and the complement system is able to regulate cells from the adaptive immune system. From Playfair and Chain, 2012

1.1.2 The complement system

The complement system was first described in the 1890s as a heat-labile protein in serum. Complement proteins appeared early in evolution and it is highly likely that it already played a central role in innate immunity before the evolution of the adaptive immunity. Complement activation can either occur via canonical activation by three different pathways: the classical, lectin and alternative pathway (Fujita et al., 2004; Walport, 2001a, 2001b) or non-canonically by local production or cleavage of complement fragments from immune cells (Bröker et al., 2018; Huber-Lang et al., 2002a). Another non-canonical mechanism serves as a cross-talk between the coagulation and complement cascade and is mediated by thrombin, plasmin, factors Xa/Xia, factor VII-activating protease or kallikrein-related peptidase 14 (Amara et al., 2010; Kanse et al., 2012; Oikonomopoulou et al., 2013). Furthermore, release of specific proteases is one of the strategies known from pathogens like *Salmonella enterica* (Ramu et al., 2007) or *Staphylococcus aureus* (Jusko et al., 2014) to evade complement-mediated killing (Jusko et al., 2012). This can also lead to release of biologically active C3a and C5a peptides (Lambris et al., 2008).

As already mentioned in the previous chapter, the complement system is part of the innate immune system and has the capability of regulating and inducing adaptive immune responses. With its over 50 soluble and membrane bound components, the complement system is a key element in the prevention and control of diseases by opsonizing pathogens and the recruiting of immune cells (Ricklin et al., 2016). Furthermore, the complement system is involved in coagulation processes (Wiegner et al., 2016) and bridges innate and adaptive immunity by its ability to boost the activation of B cells (Rickert, 2005) and induce T cell differentiation (Liszewski et al., 2013).

The traditional view is that the complement-associated plasma proteins are mainly produced in the liver, but recent data suggest that local production from immune cells, like mast cells, macrophages or DCs is more important than initially thought (Cole et al., 1980; Fukuoka et al., 2013; Li et al., 2011). Most of the plasma proteins are enzymes and circulate in inactive forms as proenzymes or zymogens. Complement activation leads to distinct effector pathways like inflammation, phagocytosis, cell migration or membrane attack (Murphy and Weaver, 2016).

1.1.2.1 Activation of the complement system

As described above, **canonical complement activation** can occur after pathogen recognition via three different pathways: the classical, lectin or alternative pathway (**Figure 2**).

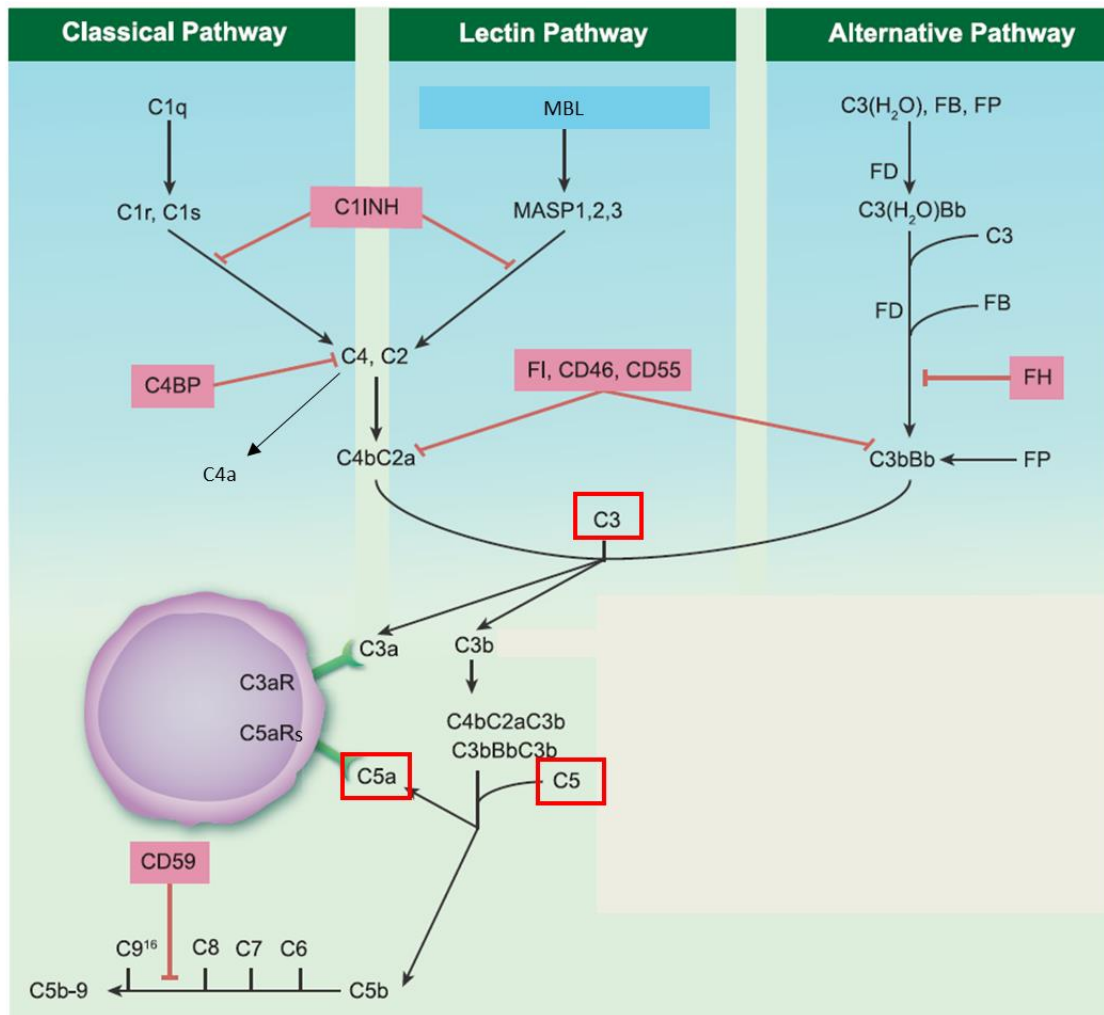


Figure 2: Complement activation and regulation. Complement activation can occur via three different pathways: classical, lectin or alternative pathway. All pathways lead to the cleavage of C3 and C5 via C3 (C4bC2a, C3bBb) or C5 (C4bC2aC3b, C3bBbC3b) convertases. The cleavage products C3a and C5a are important anaphylatoxins inducing cell recruitment or activation. C3b is necessary for opsonization of pathogens. C3b and its further degradation products can bind various complement receptors (CRs). At the end of the complement cascade the membrane attack complex (MAC) (C5b-9) is formed to induce pore formation in the pathogen. MBL=mannose binding lectin; MASP=MBL-associated serine protease; FB=factor B; FP=factor P; FD=factor D; FH=factor H; C1INH=C1 inhibitor; FI=factor I; C4BP=C4 binding protein; CR=complement receptor; Modified from Lubbers et al., 2017.

One important mechanism of classical pathway activation is the formation by antibody-antigen-immune complexes. Those immune complexes can be recognized by C1 which is binding to the Fc part of the antibodies. C1 consists of the hexameric recognition protein C1q and the proenzymes C1r and C1s. Antibodies differ in their potency to activate the complement system via the classical pathway. C1q predominantly binds to IgM and to certain IgG-subclasses. In humans IgG1 and

IgG3 are the most potent IgG-subclasses that activate the complement system, whereas IgG4 lacks that ability and IgG2 just shows minor reactivity (Diebolder et al., 2014). In mice mainly IgG2a/c and IgG2b activate the classical pathway, whereas IgG1 does not activate the complement system via this pathway (Karsten and Köhl, 2012). Other immunoglobulin subtypes do not play a role in the activation of the complement system via the classical pathway. Binding of C1q to immune complexes results in conformational changes in the C1r-C1s-complex and leads to activation of C1r via autocatalytic enzymatic activity. C1r then cleaves C1s to form an active serine protease. Activated C1s then acts on the next two components of the classical pathway, C4 and C2 to generate two small fragments - C4a and C2b - and two large fragments (C4b and C2a) which together form the classical pathway C3 convertase C4bC2a. C4a binds to protease-activated receptor (PAR)1 and 4 (Wang et al., 2017a). The C3 convertase cleaves C3 into C3a and C3b. C3a binds to its receptor C3aR and exerts its properties as an anaphylatoxin, while C3b binds either to the pathogen surface to opsonize it or to the convertase itself to form the C5 convertase C4bC2aC3b. Cleavage of C5 leads to production of C5a and C5b. Like C3a, C5a functions as an anaphylatoxin and chemoattractant which can bind to its two cognate receptors (C5aR1, C5aR2) (Lee et al., 2008). Together with C6, C7, C8 and several molecules of C9, C5b binds to the surface of the pathogen to form the membrane attack complex (MAC) or terminal complement complex (TCC) (Kolev et al., 2014). The MAC induces pore formation within the cell membrane and can directly destroy pathogens.

Activation of the lectin pathway is dependent on mannose binding lectin (MBL) and ficolins. These molecules form complexes with MBL-associated serine proteases (MASP)-1, MASP-2 and MASP-3 and can bind to carbohydrate residues on microbial surfaces or of glycosylated antibodies (Cestari et al., 2013). MASP-2 is then able to cleave C4 and C2 into the two cleaving products each. From here, the lectin pathway follows the same route as the classical pathway.

Surveillance of the alternative pathway is achieved by a low level of spontaneous activation mediated by the hydrolysis of C3 into C3(H₂O). Binding of factor B, which was previously cleaved and activated by factor D, results in the formation of the fluid-phase C3 convertase. This convertase cleaves C3 to form C3a and C3b, which can covalently bind to nearby hydroxyl or amine groups on a cell surface to form a surface-bound C3 convertase (C3bBb). Due to the fact that C3b is both a part of the convertase and the product of the reaction, a positive feedback-loop is formed resulting in opsonization of the surface with C3b which enhances phagocytosis (Du Clos and Mold, 2013). The C3 convertase is stabilized by properdin (factor P) which allows binding of more Bb to form the alternative pathway C5 convertase C3bBbC3b, which is also stabilized by properdin. Together with C6, C7 C8 and C9, C5b forms the MAC which results in pathogen clearance. Additionally, to the described process, it was shown that

the alternative pathway can be activated by activation of pro-factor D through MASP-3 from the lectin pathway (Dobó et al., 2016).

In contrast to the described canonical activation of the complement system via the three pathways, **non-canonical activation** via local production of complement fragments from immune cells becomes more and more important. It is described that several immune cells can produce complement factors upon TLR or Fc gamma receptor (Fc γ R) stimulation (Morgan and Gasque, 1997). Additionally, in human CD4⁺ T cells the lysosomal endopeptidase cathepsin L cleaves C3 and allows C3a to bind its receptor C3aR which is linked to a survival mechanism mediated by mTOR (Liszewski et al., 2013). Furthermore, C5 cleavage in T cells mediates inflammasome activity and induction of T_H1 immune responses (Arbore et al., 2016) and phagocytic cells, in this case rat alveolar macrophages and human blood neutrophils, also produce local C5a, which was chemotactically active, and contribute to increased local complement factor concentrations (Huber-Lang et al., 2002a). Besides alveolar macrophages, also macrophages from the peritoneal cavity are able to produce C5 and cleave it into C5a after TLR2 and IL-10 receptor activation (Bröker et al., 2018). Already in the 1970s it was described that trypsin can cleave C5 to generate C5a (Minta and Man, 1977). Summarized, local complement production is already described for many immune cells like mast cells, neutrophils, monocytes, macrophages, DCs as well as B cells and T cells (Lubbers et al., 2017), but not for NK cells.

Taken together, complement activation occurs by canonical or non-canonical pathways and is not only limited to the well-established classical, lectin and alternative pathways. Also, local production of complement factors and cell-specific activation play important roles in cell recruitment, immune responses and inflammatory conditions.

1.1.2.2 Regulation of the complement system

Even in the absence of pathogens, the complement system is activated spontaneously at low levels. Via the alternative pathway, C3b is generated by spontaneous hydrolysis of C3 and can bind to host cell surfaces. To avoid unwanted and detrimental complement activation and potential damage to host cells, a strong regulation is indispensable. Such regulatory proteins can be soluble or membrane-bound factors and regulate complement activity at different stages including the initiation and the formation of C3 convertase, the amplification and formation of C5 convertase, and the assembly of the MAC (**Figure 2**). Dysregulation can result in disease or pathogen replication when the complement system activation is actively inhibited by pathogens (Wong and Kavanagh, 2018). For example, more than 50% of atypical hemolytic uremic syndrome (aHUS) cases are associated with defective regulation of the alternative pathway resulting in systemic thrombotic microangiopathy (Goodship et al., 2017). One reason are mutations in factor H and consequently impaired decay of the C3 convertase resulting in increased C3 cleavage (Kavanagh et al., 2013). However, also mutations in other regulatory proteins like membrane cofactor protein (MCP/CD46) (Richards et al., 2007), factor B (Goicoechea de Jorge et al., 2007) or C3 (Frémeaux-Bacchi et al., 2008) facilitate the development of aHUS. Other diseases which are associated with dysregulation of complement activation are, among others, C3 glomerulopathy (Master Sankar Raj et al., 2016) and paroxysmal nocturnal hemoglobinuria (PNH) (Risitano, 2013).

1.1.2.3 The anaphylatoxin C5a and its two receptors

Besides the formation of the MAC, complement activation results in the production of the anaphylatoxins C3a and C5a which can bind to their receptors C3aR, C5aR1 or C5aR2. Because of their importance for this thesis, I will outline the role of C5a and its two receptors in detail in this chapter.

C5a consists of 74-79 amino acids and is released upon C5 cleavage (Klos et al., 2013). After its generation, C5a is quickly modified by serum carboxypeptidases N, which removes the C-terminal arginine residue creating C5a des-Arg (Campbell et al., 2002; Gerard and Hugli, 1981). Initially, C5a des-Arg was considered to have a reduced potency to activate cells and therefore the modification from C5a into C5a des-Arg was thought to be a regulatory mechanism (Monk et al., 2007). This view was challenged by the fact that physiological concentrations of C5a des-Arg are able to induce C5aR1, but not C5aR2-dependent cell activation (Reis et al., 2012). Interestingly, C5aR1 binds C5a des-Arg with a 10-100-fold lower affinity as C5a, whereas C5aR2 binds both ligands with nearly equal affinity (Scola et al., 2007).

A strong regulation of C5a is necessary as it is the most potent pro-inflammatory peptide among all complement cleavage fragments and has a broad spectrum of biologic functions (**Table 1**). Initially, C5a was considered as an anaphylaxis-inducing molecule, as it causes muscle contraction and Ca²⁺ influx in smooth muscle cells (Regal et al., 1983; Scheid et al., 1983). However, C5a also works as a strong chemoattractant for neutrophils (Snyderman and Pike, 1984), eosinophils (DiScipio et al., 1999), mast cells (Hartmann et al., 1997), microglia (Yao et al., 1990) as well as monocytes and macrophages (Scola et al., 2007). Furthermore, C5a can modulate cytokine expression from various cell types and reduce neutrophil apoptosis (Perianayagam et al., 2002; Riedemann et al., 2002). C5a also plays a role in the coagulation pathway and contributes to several immunological diseases, like autoimmune bullous disorders (Karsten et al., 2018), sepsis (Yan and Gao, 2012), rheumatoid arthritis (Hornum et al., 2017) or allergic asthma (Köhl et al., 2006).

Table 1: Overview of C5a-mediated effects on immune cells via C5aR1 and C5aR2. Modified from (Lee et al., 2008).

Cell type	Activity
Neutrophils	chemotaxis release of granule enzymes enhanced expression of adhesion molecules oxidative burst phagocytosis delayed apoptosis
Eosinophils	chemotaxis release of granule enzymes
Basophils	histamine release
Mast cells	chemotaxis histamine release
Plasmacytoid dendritic cells	chemotaxis
Macrophages / monocytes	chemotaxis cytokine release
Thymocytes	enhanced apoptosis
Endothelium	vasodilation chemokine release
Hepatocytes	enhanced regeneration
Microglia	chemotaxis

C5a exerts its functions via binding to its two cognate receptors: C5aR1 (CD88) and C5aR2 (former: C5L2). Both receptors are seven-transmembrane receptors and are expressed on a wide range of cells, mainly from the myeloid origin (Dunkelberger et al., 2012; Karsten et al., 2015, 2017; Laumonier et al., 2017).

C5aR1 belongs to the superfamily of G protein-coupled receptors (GPCR) and signal transduction requires the activation of heterotrimeric G proteins (Klos et al., 2009). In general, G proteins are composed of α , β and γ subunits (**Figure 3**). After ligand binding, guanosine diphosphate (GDP), which is bound to the $G\alpha$ subunit, is exchanged for guanosine triphosphate (GTP) and the $G\beta$ and $G\gamma$ subunits dissociate from the $G\alpha$ subunit. That leads to activation of signaling pathways via cyclic adenosine mono-phosphate (cAMP) and calcium mitogen-activated protein (MAP) kinases. Phosphorylation of the cytoplasmic tail of the GPCR by G protein-coupled receptor kinases (GRKs) results in termination of the signaling cascade. Additionally, β -arrestin 1 and 2 are recruited to the cytoplasmic tail, which block G protein binding and promote receptor desensitization followed by receptor internalization (Rajagopal et al., 2010). C5a binding to C5aR1 induces Ca^{2+} influx from intracellular stores and extracellular medium (Monk and Partridge, 1993; Skokowa et al., 2005). Furthermore, stimulation of C5aR1 results in activation of several signaling pathways like phosphatidylinositol 3-kinase (PI-3K), phospholipase D, PKC and MAPK (la Sala et al., 2005; Wrann et al., 2007).

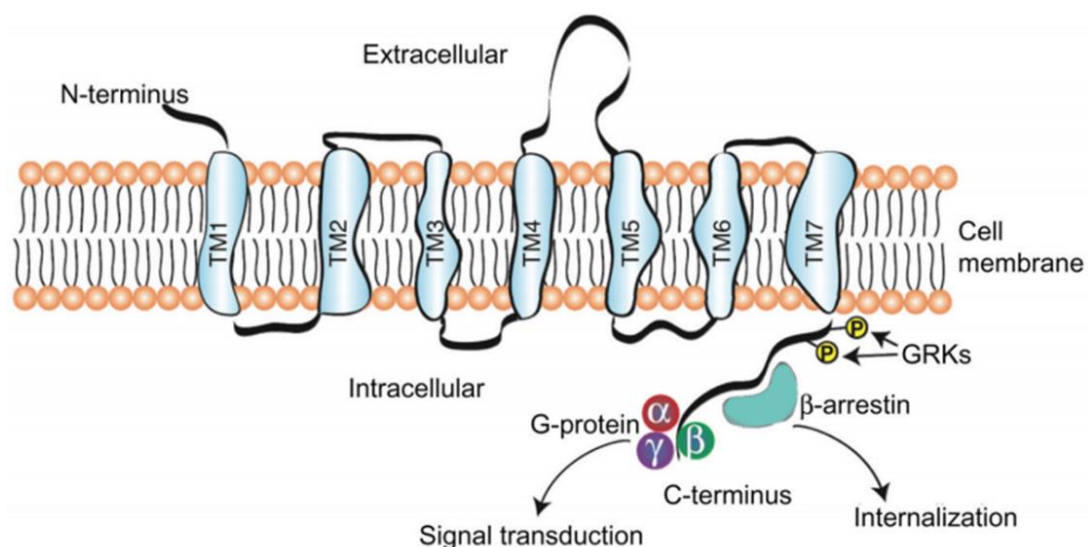


Figure 3: Diagram of a classical model of a seven transmembrane receptor with associated G protein and β -arrestin molecules. From Sarma and Ward, 2012.

C5aR2, the second C5a receptor, is also a seven-transmembrane receptor, but uncoupled from G proteins mainly due to a replacement of an arginine residue in the DRY sequence in the third

transmembrane domain and a change in the NPXXY sequence in the seventh transmembrane domain (He et al., 2001; Ohno et al., 2000; Okinaga et al., 2003). Consequently, the receptor is not able to induce Ca^{2+} influx. Therefore, C5aR2 was initially described as a decoy receptor to control and regulate C5aR1 functions (Scola et al., 2009). In line with that, publications suggest that C5aR2 has anti-inflammatory properties mediated via β -arrestin signaling (Bamberg et al., 2010). However, also pro-inflammatory properties mediated via modulation of C5aR1-induced ERK phosphorylation have been described (Chen et al., 2007; Hsu et al., 2014). Besides the controversial discussion about pro- or anti-inflammatory roles of this receptor, scientists also debate about the cellular location of the receptor. For human granulocytes and peripheral blood monocytes it was shown that C5aR2 is localized predominantly intracellularly (Bamberg et al., 2010). A similar expression was observed for murine neutrophils and macrophages (Karsten et al., 2017).

1.2 IL-12 cytokine family

IL-12 family cytokines include IL-12, IL-23, IL-27 and IL-35 and play important roles on the induction of innate immune responses (de Saint-Vis et al., 1998). Cytokines which belong to this family form heterodimers that consist of an α -chain (p19, p28, p35) and a β -chain (p40 or Ebi3) (**Figure 4**). Pairing of p40 chain with p35 or p19 forms IL-12 and IL-23, respectively, whereas heterodimers of Ebi3 with p28 and p35 result in IL-27 and IL-35. The IL-12 family cytokine receptors consist of heterodimeric structures sharing receptor subunits such as IL-12R β 1 or gp130.

The pro-inflammatory cytokine IL-12 and IL-23 have key roles in the development of the T_H1 and T_H17 subsets of helper T cells. IL-12 is also a crucial pro-stimulatory cytokine for NK cells in the induction of innate immune responses (Ferlazzo et al., 2004). IL-27 is reported to have mainly inhibitory activity and is often generated during the resolution phase of an immune response by APCs. IL-35 is a potent anti-inflammatory cytokine expressed by Treg cells. It controls the development of T_H1 and T_H17 cells and inhibits T_H1 cell proliferation (Vignali and Kuchroo, 2012).

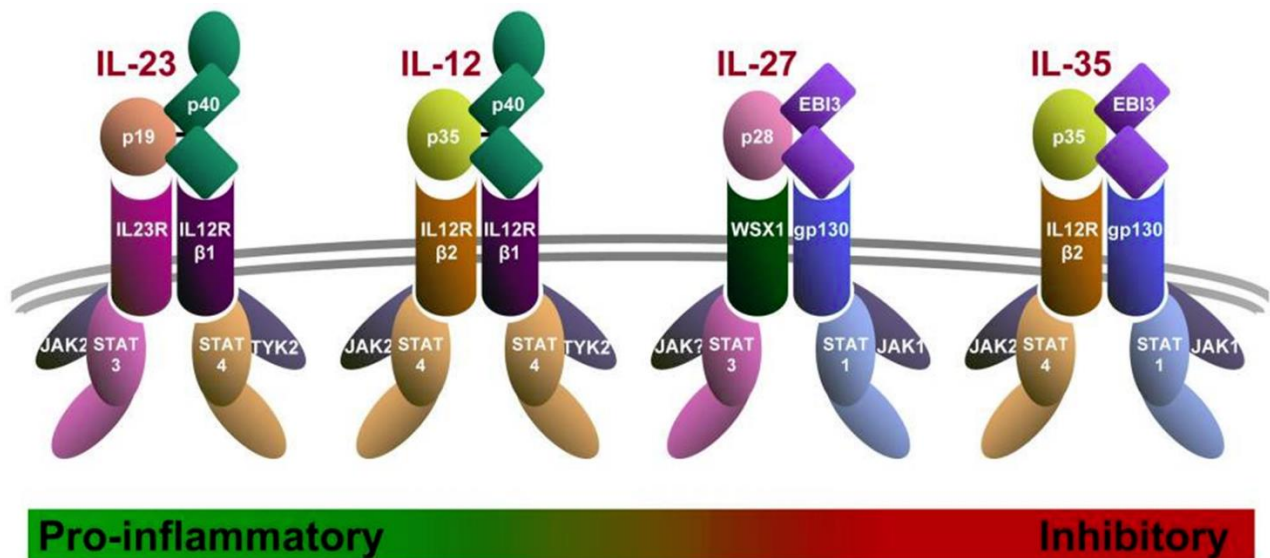


Figure 4: IL-12 cytokine family, receptors and signaling components. The IL-12 family comprises the heterodimeric cytokines IL-12, IL-23, IL-27 and IL-35. They consist of an α -chain (p19, p28, p35) and a β -chain (p40 or Ebi3). These cytokines exert their functions upon binding to heterodimeric receptors and involve distinct JAK-STAT signaling partners. The bottom bar reflects their functional spectrum ranging from pro-inflammatory (IL-23, IL-12) to inhibitory (IL-35). From Vignali and Kuchroo, 2012.

1.3 Natural killer cells: key players during early innate immune responses

NK cells develop in the thymus and liver (Sojka et al., 2014) and belong to the first defense line of the organism against pathogens. Under naïve conditions, NK cells are found mainly in the spleen, but in lower numbers also in blood, liver, lymph nodes, in the uterus during gestation as well as in the peritoneal cavity. During development, NK cells undergo different maturation steps to fulfill effector functions like recognition and killing of virally-infected cells or the production of pro-inflammatory cytokines like IFN- γ (Orr and Lanier, 2010; Vivier et al., 2008). To promote and control their function and development, NK cells rely on cytokines like IL-2, IL-12, IL-15 or IL-18 and on transcription factors like Nfil3 or PU.1 (Colucci et al., 2001; Kamizono et al., 2009; Mandal and Viswanathan, 2015).

1.3.1 Natural killer cell activation and pathogen clearance

As already mentioned above, circulating NK cells require activation by cytokines to allow their recruitment to the site of infection (Fogler et al., 1996). NK cells in the lymph nodes or spleen receive their activation signals via DCs, which form a stimulatory synapse and start to secrete cytokines like IL-2, IL-12, IL-15 and IL-18 to induce NK cell activity (Borg et al., 2004). Furthermore, NK cell activity is controlled by a wide range of receptors, which are expressed on the surface and have inhibitory or

activating properties. Killer immunoglobulin-like receptors (KIR), Ig-like receptors (CD158), the C-type lectin receptor (NKG2A) and leukocyte inhibitory receptors (LIR1, LAIR-1) belong to the inhibitory receptor family. Activating receptors are the natural cytotoxicity receptors (NKp46, NKp44), C-type lectin receptors (NKG2D) and Ig-like receptors (2B4) (Carrillo-Bustamante et al., 2016). The ability of NK cells to respond to a variety of stimuli and to participate in immune responses under different pathological conditions is based on their different expression of inhibitory and activating receptors. Under physiological conditions, NK cells express two to four inhibitory receptors and an array of activation receptors which results in a heterogeneity within the NK cell population (Mandal and Viswanathan, 2015). With these receptors, NK cells are able to regulate cytotoxicity (**Figure 5**). Inhibitory receptors recognize self-MHC class I molecules on the surface of the cell. This signal prevents activation of the NK cell. Tumor cells or virus-infected cells tend to downregulate MHC class I on the surface of the cells to escape recognition by cytotoxic T lymphocytes (CTL) making them a target for NK cells (Malnati et al., 1993). Once the NK cell is activated, the cytotoxic ability is mediated via different pathways: Perforin, a membrane-disrupting protein, and granzymes are secreted by exocytosis. Both substances work together to induce apoptosis of the target cell. The second pathway depends on a caspase-dependent apoptosis. Here, death receptors (e.g. Fas) on target cells are associated with their equivalent ligand (FasL) and tumor necrosis factor-related apoptosis-inducing ligand (TRAIL) on NK cells which results in caspase-dependent apoptosis (Zamai et al., 1998). A third pathway includes the antibody-dependent cellular cytotoxicity (ADCC) as NK cells express the low-affinity Fc γ RIII. Here, Fc γ RIII recognizes antibodies bound to the surface of a target cell which induces the release of cytotoxic factors (Wang et al., 2015). Interestingly, ADCC requires processes of the adaptive immunity as it results from binding of antibodies and therefore emphasizes the role of NK cells in innate and adaptive immune responses.

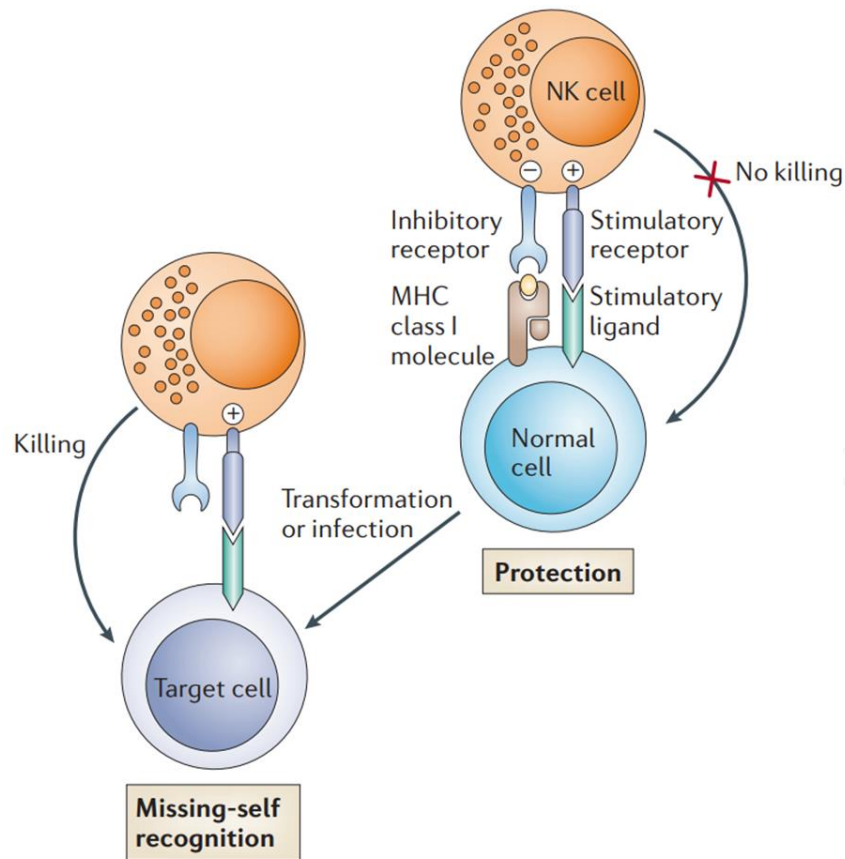


Figure 5: The balance of inhibitory and stimulatory signals received by NK cells. Cells under naïve conditions are protected from killing when stimulatory signals are counter-balanced by inhibitory signals delivered by MHC I. Missing MHC I expression results in activation of the NK cell and killing of the target cell (missing-self recognition). Modified from Raulet and Vance, 2006.

1.3.2 Dendritic cell – mediated NK cell activation via stimulatory synapse formation

DCs are professional APCs and are necessary to induce immune responses by recognizing pathogens via PRRs. Besides their role in activating and regulating adaptive immune responses, they are also involved in the activation of NK cells. Here, soluble and contact-dependent activation by DCs is necessary to induce cytokine production, proliferation and cytotoxicity of NK cells (**Figure 6**). Contact-dependent activation is mediated via the ligation of NKp46, NKp30, NKG2D or 2B with MHC I or IL-15 receptor provided on the DC side. Soluble factors, which mediate NK cell activation include IL-2 (Granucci et al., 2004), IL-12 (Lehmann et al., 2001), IL-15, IL-18 (Srivastava et al., 2013), IFN- α and IFN- β (Swann et al., 2007) produced by DCs. IL-15 has a dual function and can act as a soluble factor after secretion and a contact-dependent factor via presentation through the IL-15 receptor in the stimulatory synapse (Viaud et al., 2009). *Borg et al* showed that a direct cell-cell interaction between DCs and NK cells is necessary to induce IFN- γ production (Borg et al., 2004). Following the activation, NK cells become cytotoxic and secrete granzymes and perforins, start to proliferate or produce high amounts of the pro-inflammatory cytokines TNF- α and IFN- γ . Reciprocally, NK cell-derived IFN- γ is

important to induce DC maturation and polarization of T cells into the T_H1 phenotype (Elssen et al., 2014). Besides specific NK cell receptors, other adhesion molecules like vascular cell adhesion protein 1 (VCAM1) or very late antigen-4 (VLA4) play important roles in mediating NK cell activity via DCs (Fogler et al., 1996).

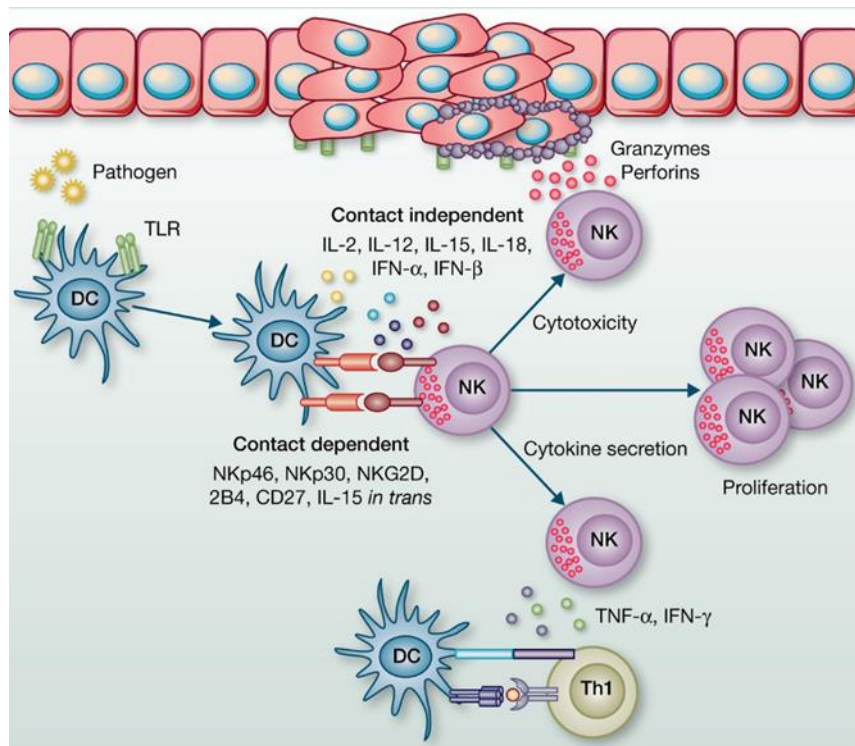


Figure 6: DC-induced NK cell activation. DCs can affect NK cell function by augmentation of cytotoxicity, cytokine secretion (IFN- γ and TNF- α), and proliferation. This depends on contact-dependent (ligation of NKp46, NKp30, NKG2D, 2B4) as well as soluble factors (IL-2, IL-12, IL-15, IL-18, IFN- α , and IFN- β). IFN- γ secretion by NK cells is, in turn, responsible for DC maturation and Th1 polarization, whereas augmentation of NK cell cytotoxicity contributes to tumor cell lysis. From Elssen et al., 2014.

1.4 *Toxoplasma gondii*: an intracellular parasite

1.4.1 Biology and life cycle of *Toxoplasma gondii*

T. gondii is an intracellular parasite, which is able to infect virtually all nucleated cells and therefore, is present in a wide range of hosts. Depending on age and environment, up to 50 % of the human population is infected with *T. gondii* (Flegr et al., 2014). The parasite has a sexual life cycle in the definitive host and a two-staged asexual life cycle in secondary hosts (**Figure 7**). *T. gondii* can be divided into three different strains (I, II, III), which differ in their virulence, ability to cause encephalitis and cytokine induction (Araujo and Slifer, 2003; Haque et al., 1999). For my experiments, I used ME49 type II strain parasites.

Within the definitive host, *T. gondii* undergoes sexual reproduction in the gut. Members of the definitive host family (cats) can be infected by ingesting infected animals like mice. Once taken up, the cyst form of the parasite survives the passage through the stomach and starts to infect epithelial cells of the cat's small intestine (Dubey et al., 2011a). Within these cells the parasite undergoes sexual reproduction that ends up in the production of millions of zygote-containing cysts known as oocysts. After massive reproduction inside the epithelial cell, oocysts are released into the intestinal lumen and are shed in the cat's feces. Due to the sexual replication and as a result of meiosis, many of the generated oocysts contain different genotypes and thus a huge number of genetically distinct parasites can be generated from one single cat. In the environment, oocysts can spread to soil, water, food or anything else potentially contaminated with the feces. Due to its structure, oocysts can survive and remain infectious for many months in cold and dry climates (Dubey et al., 2011b). Humans are infected with parasites by consuming raw meat or contaminated water. Farmed animals like cow, sheep or pigs are infected by consuming contaminated water or food contaminated with cat feces. In immunocompetent humans, symptoms of the infection are flu-like, often the infection is asymptomatic. However, in immunocompromised patients, e.g. HIV patients, the parasite can cause blindness or seriously harm the host, causing life-threatening symptoms like brain or heart damage (Wang et al., 2017b). Furthermore, during pregnancy, a primary *T. gondii* infection can result in serious symptoms up to stillbirth or death of the newborn shortly after birth (Endris et al., 2014).

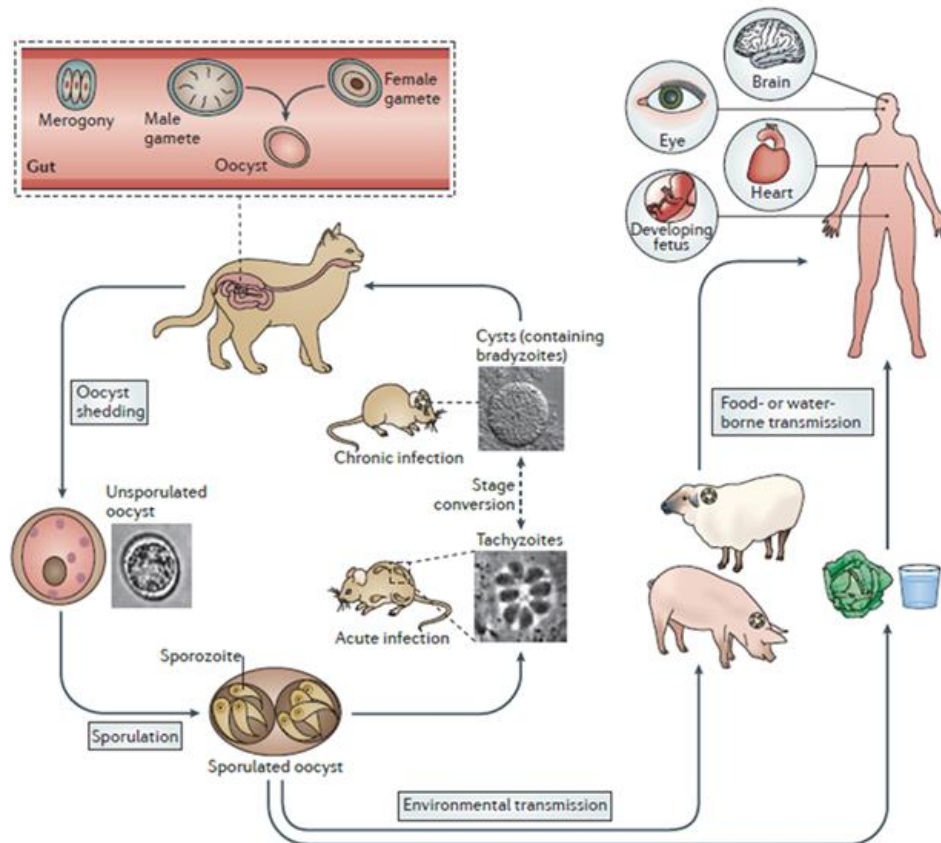


Figure 7: Life cycle of *T. gondii*. Cats are the definitive host, in which sexual replication takes place: male and female gametes are formed within the host cell. Fusion of gametes leads to the formation of diploid oocysts that are shed in cat feces and undergo meiosis in the environment. Oocysts can survive in the environment for long periods and can contaminate food and water, which is consumed by intermediate hosts. In intermediate hosts (here: rodents) asexual replication occurs. Acute infection is characterized by fast replicating tachyzoites that disseminate throughout the body. Activation of the immune system is leading to the differentiation into slow-replicating bradyzoites that are stored in tissue cysts and characterize the chronic infection. Humans become infected by eating undercooked meat from farming animals containing cysts or by consuming cat feces-contaminated water. Although in immunocompetent individuals, infections are mild, immunocompromised humans can develop severe symptoms leading to brain damage or blindness. From Hunter and Sibley, 2012.

1.4.2 The innate immune response against *T. gondii*

Infections with *T. gondii* require a fast, organized and strong immune response to prevent massive replication of the parasite and its spreading throughout the host. Most important and critical for the induction of an innate immune response is the ability of DCs to sense the pathogen via TLRs and to produce the cytokine IL-12 to promote a T_H1 immune response (Tosh et al., 2016) (**Figure 8**). Besides DCs, inflammatory monocytes, neutrophils, macrophages and NK cells play important roles during the infection by producing other pro-inflammatory cytokines, mainly $IFN-\gamma$, and migration to the site of infection (Gazzinelli et al., 1994).

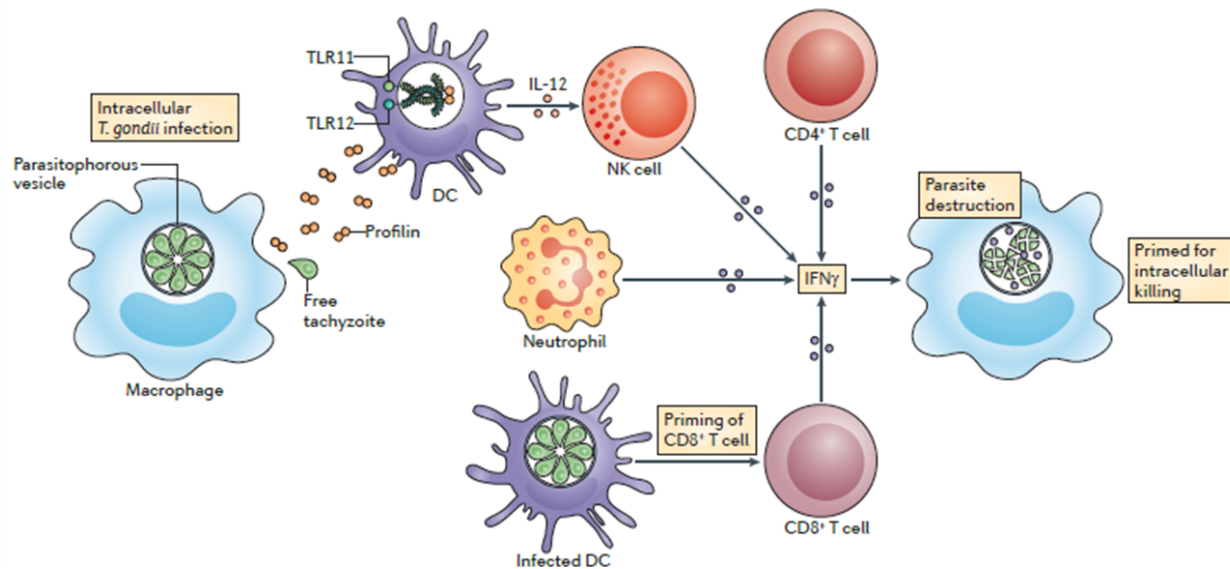


Figure 8: Immune response to *T. gondii* infection. IFN- γ is crucial for survival of the host during *Toxoplasma gondii* infection. Production of this cytokine by NK-cells is dependent on TLR11-mediated recognition of *T. gondii* profilin by DCs. Neutrophils provide an important innate source for IFN- γ ; the mechanisms that regulate neutrophil-derived IFN- γ are not well understood because this IFN- γ is not regulated by TLRs or by IL-12. Macrophages are primed with the IFN- γ to destruct the parasite and limit replication. In later stages of the infection, DCs also prime T cells to produce IFN- γ . From Yarovinsky, 2014.

As already mentioned, TLRs play a key role in sensing the parasite as MyD88-deficient mice are highly susceptible to toxoplasmosis and succumb to death early after an infection (Sukhumavasi et al., 2008). TLRs which are involved in *T. gondii* sensing are TLR 2, 4, 7, 9 and especially 11 and 12 which play a central role (Yarovinsky and Sher, 2006). Quadruple knockout mice for TLRs 3, 7, 9, 11 show complete loss of resistance to *T. gondii* infections emphasizing the important role for an early and well-organized immune response induction (Kim et al., 2008). TLR11 and TLR12 recognize the *T. gondii*-derived protein profilin, a conserved molecule among protozoan parasites, via different ways: the direct interaction of TLR11 with profilin within endolysosomes results in the recruitment of MyD88 and the initiation of downstream immune signaling cascades. Furthermore, TLR11 and TLR12 heterodimerization or TLR12 homodimerization and subsequent profilin detection also results in MyD88 recruitment and induction of DC responsiveness (Koblansky et al., 2013; Raetz et al., 2013; Yarovinsky et al., 2005). Besides TLR11 and TLR12, other TLRs play important roles in detecting *T. gondii*-derived substrates and induce an immune response. TLR2 functions as a sensor for glycosylphosphatidylinositol (GPI) anchors which cover the cell surface of many protozoan parasites (Campos et al., 2004; Krishnegowda et al., 2005). It is expressed on macrophages, where it is responsible for the induction of tumor necrosis factor (TNF) and CC-chemokine ligand 2 (CCL2) production. On epithelial cells TLR2 triggers the production of chemokines during the infection (Debierre-Grockiego et al., 2007; Ju et al., 2009). Besides TLR2, TLR4 can also detect *T. gondii* GPIs *in vitro*. Furthermore, both TLRs can also be activated by *T. gondii*-derived heat shock protein (HSP) 70 (Debierre-Grockiego et al., 2007; Mun et al., 2005). *T. gondii* can also be

detected in a TLR-independent manner via inflammasomes. This intracellular sensor system can cooperate with TLRs in pathogen recognition, but primarily functions to detect microbial ligands in the cytosolic compartment. Here, it is involved in processing of the pro-inflammatory cytokines IL-1 β and IL-18, which are involved in host defense against *T. gondii*. Deficiency in inflammasome-associated intracellular sensor NLRP1 results in increased susceptibility to *T. gondii*, but the exact mechanism how it is involved remains elusive (Ewald et al., 2014).

Finally, *Andrade et al* published that, in case of insufficient MyD88 activation via TLR11 and TLR12, heterodimers of TLR7 and TLR9, which sense *T. gondii*-derived nucleic acids, compensate and induce DC responsiveness (Andrade et al., 2013). That is an interesting observation, as TLR12 is not present in the human genome and therefore the TLR11/12-dependent recognition is central in host defense in mice or rodents and not applicable to the human innate immune system. Similar to mice, data support that a T_H1/T_H17-based immune response and T-cell-derived IFN- γ are critical for parasite control in humans (Meira et al., 2014). Nevertheless, a detailed model of *T. gondii* recognition by the human immune system is still missing. Analyses showed that human TLR5 is evolutionary close to the mouse *trl11* family which suggests that TLR5 in humans mimics murine TLR11 function (Gonzalez et al., 2014).

Like many parasites, *T. gondii* promotes host survival to allow maximum parasite replication and spreading through the body. As already described, *T. gondii* infections result in IL-12-mediated IFN- γ production from innate immune cells and a T_H1 response by CD4⁺ and CD8⁺ T cells. Both is critical for host survival. Blocking of IL-12 or genetically ablating the IL-12 subunits IL-12p35 or IL-12p40 results in increased susceptibility to *T. gondii*, comparable to that of MyD88-deficient mice (Scanga et al., 2002). Injection with soluble tachyzoite antigen (STAg) revealed that splenic **CD8⁺ α DCs** are the main source of IL-12 (Sousa et al., 1997). However, other DC subsets and also macrophages are able to produce IL-12 after priming with IFN- γ (Trinchieri, 2003). Analysis of mice lacking the transcription factor IFN-regulatory factor 8 (IRF8) resulted in blocked CD8⁺ α DC development, lack of early IL-12 production and decreased survival during *T. gondii* infections (Scharton-Kersten et al., 1997a). It is published that IRF8 regulates both IL-12p40 and IL-12p35 expression downstream of TLR-11 and MyD88, which explains the increased susceptibility of IRF8-deficient mice (Raetz et al., 2013). The first cells which respond to TLR-mediated IL-12 production from CD8⁺ α DCs are NK cells, which start to produce IFN- γ and therefore are responsible for the induction of a potent immune response.

Besides DCs, **neutrophils** are an important source for IL-12 as they are able to secrete pre-stored IL-12 upon *T. gondii* detection *in vivo* and *in vitro* (Bliss et al., 1999a, 1999b, 2000). The importance of neutrophils during infections is shown by decreased IL-12 levels and increased parasite replication after neutrophil depletion (Bliss et al., 2001). However, neutrophil depletion using Gr-1, which is a combined antibody of the neutrophil-specific Ly6g and monocyte and neutrophil-expressing Ly6c, also

affects other cells like inflammatory monocytes, due to the fact the both cell types share the same surface marker Ly6c. That complicates interpretation of the obtained data (Dunay et al., 2010). In addition to IL-12 secretion, neutrophils migrate in large numbers to the site of infection and start to produce IFN- γ to support NK cells in limiting parasite spreading, although the amount of IFN- γ is low compared to that produced by NK cells and T cells (Biswas et al., 2017). Moreover, neutrophils are involved in direct parasite killing via phagocytosis, release of reactive oxygen species and the formation of DNA containing extracellular traps (NETs) (Abi Abdallah et al., 2012; Chtanova et al., 2008; Konishi and Nakao, 1992; Nakao and Konishi, 1991). Therefore, it is not surprising that mice which lack the recruitment receptor CXCR2 result in a defect in neutrophil recruitment, suffer from higher parasite levels in the central nervous system (CNS) (Del Rio et al., 2001).

In addition to neutrophils, also impaired migration of **monocytes** due to a CCR2 deficiency leads to increased susceptibility to *T. gondii* infection (Benevides et al., 2008; Dunay et al., 2010; Robben et al., 2005). Monocytes contribute to the control of *T. gondii* in a direct and an indirect manner. They produce IL-1 β and IL-12 after stimulation with the parasite to enhance IFN- γ production and contribute to parasite killing through the production of nitric oxide (NO) and inducible nitric oxide synthase (iNOS) (Dunay and Sibley, 2010; Mordue and Sibley, 2003; Robben et al., 2005). CCR2-deficient mice succumb to death during *T. gondii* infections after 3-4 weeks due to decreased expression of iNOS and increased parasite burden in the CNS (Benevides et al., 2008). Monocytes can develop into monocyte-derived DCs (moDCs) or macrophages. As moDCs they can induce adaptive immune responses (Domínguez and Ardavín, 2010) and as macrophages they migrate to the site of infection and control the infection by pathogen clearance or cytokine production. For a more detailed discussion see the review from (Gordon and Taylor, 2005).

In **macrophages** the fate of *T. gondii* depends on the mechanism of uptake into the cell. If macrophages phagocytose dead or opsonized parasites, the parasite is degraded in lysosomal compartments (Sibley et al., 1985), whereas live parasites that actively invade the cell hide in parasitophorous vacuoles (PV) (Mordue and Sibley, 1997). Macrophages which have been primed with IFN- γ are capable of controlling parasite replication in PVs through upregulation of NO and iNOS (Adams et al., 1990). iNOS^{-/-} mice survive the acute infection phase, but are highly susceptible to toxoplasmic encephalitis (Khan et al., 1997; Scharon-Kersten et al., 1997b). IFN- γ also induces upregulation of 47-48 kDa immune GTPases (IGTP,LRG47, IRG47) which are essential for resistance in the acute and chronic infection and limit parasite growth (Collazo et al., 2001; Taylor et al., 2000). Independent from IFN- γ and NO, TNF- α and CD40/CD40L signaling results in anti-microbial activity and increases survival during the infection (Andrade et al., 2003, 2005). Additionally, activated macrophages contribute to IL-12 production

regulated by TRAF6-dependent phosphorylation of the MAPK family member p38 and ERK1/2 (Mason et al., 2004).

1.4.3 The role of NK cells during *T. gondii* infection

NK cells are an essential and early source for IFN- γ in *T. gondii* infection that compensates for the lack of CD8⁺ T cells (Denkers et al., 1993; Hunter et al., 1994; Johnson et al., 1993). As the NK cell activity peaks early during the acute phase of infection, NK cells do not appear to be significant in the chronic phase (Kang and Suzuki, 2001). Hence, most studies concentrated on early NK cell activity and IFN- γ production mainly regulated via IL-12, which is produced by other innate immune cells (DCs, monocytes, neutrophils; as described earlier) (Gazzinelli et al., 1993; Hunter et al., 1994). NK cells can also be cytotoxic for cells infected with *T. gondii* (Hauser and Tsai, 1986; Subauste et al., 1992). However, it was shown that NK cells become infected with the parasite when lysing infected cells. In consequence, the parasite can disseminate within the NK cell. It was also proposed that infected NK cells show a higher motility that facilitates spreading of the parasite throughout the organism (Ueno et al., 2015).

1.4.4 The adaptive immune response against *T. gondii* infection

Three to five days after the infection, cells from the adaptive immune system start to induce effector mechanisms that help controlling the parasite. Here, B and T cells occupy important functions as mice with deficiencies in B cell, CD4⁺ T cell or CD8⁺ T cell functions survive the acute phase of the infection, but succumb to death during the chronic stage of infection (Johnson and Sayles, 2002; Kang et al., 2000).

B cells contribute to parasite control by the production of specific antibodies. Parasite-specific IgM, IgA, IgE and IgG2 have been isolated from human patients. Detection of specific antibodies of which certain subtypes help to distinguish between freshly (IgM) and chronically (IgG) infected patients (Correa et al., 2007; Remington, 1969; Remington et al., 1968, 2004). Mice lacking B cells develop normal IFN- γ responses, but succumb to infection within 3-4 weeks, suffering from a high parasite burden in the CNS (Kang et al., 2000). As passive transfer of antibodies confers protection to B cell-deficient mice, it is likely that the lack of antibodies is responsible for the increased susceptibility (Johnson and Sayles, 2002).

The importance of **T cells** becomes clear as HIV patients develop severe toxoplasmosis associated with reduced T cell numbers (Israelski and Remington, 1988). The initiation of proper T cell responses requires that naïve CD4⁺ or CD8⁺ T cells encounter APCs bearing cognate *T. gondii* antigens. Additionally, co-stimulatory signals via CD28 and inducible co-stimulator (ICOS) and cytokines like IL-12 are required for T cell activation, which is characterized by proliferation, differentiation and IFN- γ production (Curtsinger et al., 1999, 2003; Harding et al., 1992). Presentation of antigens occurs mainly via DCs, but also B cells and macrophages are capable of presenting antigens to CD4⁺ T cells via MHC class II (Jenkins et al., 2001). Presentation of *T. gondii* antigens requires phagocytosis of the parasite, infected cells, parasitic debris or is achieved through endocytosis of antigens secreted by *T. gondii* itself. Alternatively, antigens are presented on APCs after active infection with the parasite (Koshy et al., 2010).

CD8⁺ T cells are specialized to recognize cells infected with viral, bacterial or parasitic organisms, hence it is not surprising that these cells play an important role in maintaining resistance to *T. gondii* infections. CD8⁺ T cells control infection by production of IFN- γ , CD40/CD40L interactions and through perforin-mediated cytolysis of infected cells (Denkers et al., 1997; Gazzinelli et al., 1992; Reichmann et al., 2000). Depletion of CD8⁺ T cells in mice results in increased susceptibility to toxoplasmosis and mice succumb to death approximately 50 days post infection (p.i.) (Denkers et al., 1997). Additionally, adoptive transfer of CD8⁺ T cells from chronically infected mice or mice vaccinated with an attenuated strain of *T. gondii*, is sufficient to maintain resistance (Gigley et al., 2009; Parker et al., 1991). Some epitopes of *T. gondii* presented on MHC class I alleles can be recognized by CD8⁺ T cells. These include peptides which are conserved across multiple *T. gondii* strains and that are actively secreted by the parasite (Blanchard et al., 2008; Frickel et al., 2008; Wilson et al., 2010).

1.4.5 The role of the complement system during *T. gondii* infections

Assessment of *T. gondii*-specific antibody production to distinguish between freshly and chronically infected patients has already been discovered in 1948 by Sabin and Feldman (Sabin and Feldman, 1948). In 1980, the classical complement pathway was identified as the most important part of the complement system in controlling *T. gondii*, as depletion of alternative pathway complement factors B, D and P did not impair parasite killing (Schreiber and Feldman, 1980). The minor importance of the alternative pathway can be explained with the reduced capacity of C3b to bind to the cellular membrane of tachyzoites and the fast degradation into its inactive form iC3b (Fuhrman and Joiner, 1989). During chronic stage of infection, rupture of brain cysts causes C1q production and activation of the classical complement pathway (Xiao et al., 2016). *In vivo* blocking of complement protein C3 in

mice results in acute susceptibility to toxoplasmosis due to impaired CD4⁺ and CD8⁺ T cell responses (Johnson et al., 1996). Furthermore, C3aR- and C5aR1-double deficiency in mice leads to increased susceptibility due to decreased IL-12 and IFN- γ levels (Strainic et al., 2008). Experiments from Daria Briukhovetska in the Institute for Systemic Inflammation Research (Lübeck, Germany) showed that C5aR1 deficiency leads to increased susceptibility in mice characterized by increased weight loss and mortality rate (Briukhovetska, 2017). Additionally, C5aR1- and C5aR2-deficient mice suffer from increased parasite burdens in the brain 30 days p.i. In both strains altered IL-12 and IFN- γ levels seem to be at least one critical factor for the increased susceptibility emphasizing the importance of complement activation for the immune response to *T. gondii* infection.

1.5 The growth factor receptor-bound protein 2 (Grb-2)-associated binder (Gab) protein family

1.5.1 Role and function in signal transduction

As demonstrated in the previous chapters, the complement system and especially NK cells play crucial and important roles during *T. gondii* infection. For further investigation of the specific NK cell function, I focused on another protein which is highly expressed on NK cells: Gab3.

The growth factor receptor-bound protein 2 (Grb-2) associated binder (Gab) protein family describes three different docking and scaffolding proteins (Gab1, Gab2, Gab3) which contribute to specific signal transduction pathways. Although the overall sequence homology between all three proteins is only 40 %-50 %, they share similar topology. Each protein contains an N-terminal pleckstrin homology (PH) domain, proline-rich motifs and multiple potential tyrosyl and seryl/threonyl phosphorylation sites (Nishida and Hirano, 2003) (**Figure 9**). Although the overall topology is similar, the three Gab proteins are expressed in different cells and expression deficiency has different consequences (**Figure 10**). Gab1 and Gab2 are ubiquitously expressed but are found only in low levels in lymphoid tissues. In contrast, Gab3 is highly expressed in lymphoid tissues. The key mechanism to induce activation of Gab proteins is the phosphorylation of tyrosine residues in response to growth factors or cytokines. Phosphorylation occurs, besides other factors, in response to IL-3, IL-6 and oncoproteins in case of Gab1 and Gab2 and in response to M-CSF in the case of Gab3 (Nishida and Hirano, 2003). Grb-2 is described as an adaptor protein which is involved in signal transduction and cell communication. The protein contains one Src Homology (SH) 2 and two SH3 domains which form complexes with the phosphorylated tyrosine residues from the Gab proteins and therefore allow transport of Grb2 to the membrane to bring it in close proximity to associated receptors (Berry et al., 2002).

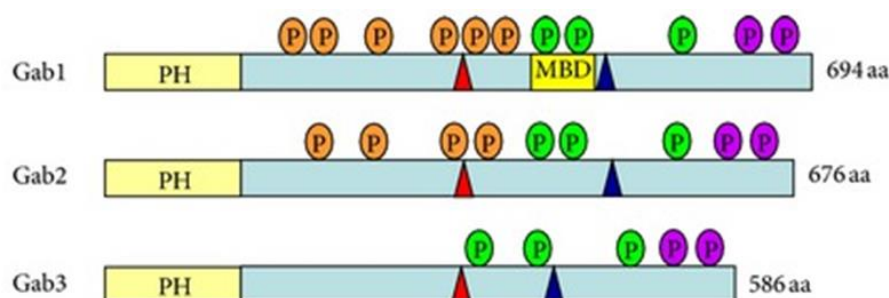


Figure 9: Schematic structures of Gab family docking proteins. Shown are the schematic domain structures of three human Gab proteins (Gab1–3). All Gab proteins consist of a highly conserved N-terminal PH domain that is involved in membrane targeting. The central proline-rich regions mediate the association with SH3 domain-containing adaptor proteins such as Grb2. PH=Pleckstrin homology; P=Proline From Nakaoka and Komuro, 2013.

The downstream signaling partner of all Gab proteins are largely unknown, but experiments with mice lacking either Gab1, Gab2 or Gab3 revealed first hints for the involvement of Gab proteins in several cell signaling pathways. Gab1-deficient embryos die between gestational day 12.5 and 18.5 with multiple defects in the heart, placenta and liver (Itoh et al., 2000). Furthermore, ERK activation in response to epidermal growth factor (EGF), platelet-derived growth factor (PDGF) and hepatocyte growth factor (HGF) in Gab1-deficient primary fibroblasts was strongly reduced. These results indicate that Gab1 acts downstream of receptor tyrosine kinases (RTK), but upstream of ERK. Additionally, *Cai et al* showed that Gab1 promotes Ras/MAPK signaling to enhance epidermal cell proliferation and differentiation (Cai et al., 2002).

In contrast to Gab1-deficient mice, Gab2-deficient mice are viable, generally healthy and have a normal lifespan. The only differences compared to WT mice are decreased mast cells numbers and impaired mast cell activation in the skin and stomach of Gab2-deficient mice (Nishida et al., 2002). The defective activation is due to impaired PI-3 kinase and ERK activation.

The biological function of Gab3 is poorly understood. Mice with targeted disruption of the Gab3 gene have been generated and these mice develop normally, are generally healthy and immunocompetent (Seiffert et al., 2003). Data from the exAC gene database showed no loss of function mutations in humans indicating a role of Gab3 for survival, reproduction or cell differentiation.

Targeted disruption in Gab1, Gab2 and/or Gab3 in double and triple knockouts have not been studied yet but will answer open questions regarding signaling partners and the involvement in cell differentiation and activation.

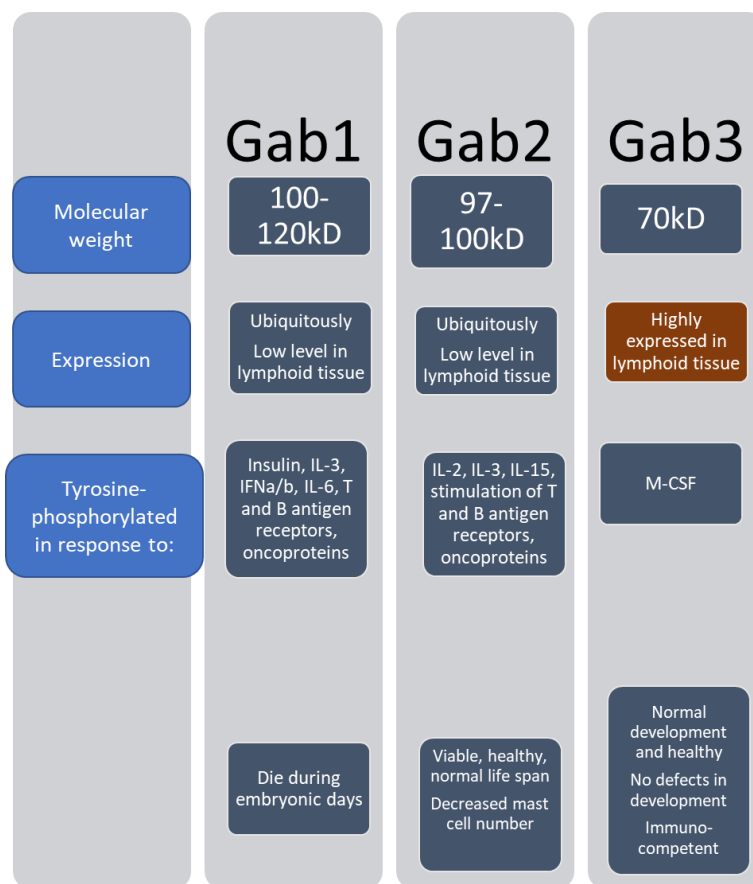


Figure 10: Overview of Gab1, Gab2 and Gab3 regarding molecular weight, expression, tyrosine phosphorylation and consequences of expression deficiency. Reviewed in (Nishida and Hirano, 2003)

1.5.2 PH-domain – associated recruitment of Gab proteins

Recruitment of Gab proteins to activate receptors can be achieved via direct and indirect mechanisms (**Figure 11**). The interaction of Gab1 with c-Met, the receptor for HGF, is described as the only direct recruitment among Gab proteins (Weidner et al., 1996). In all other signaling pathways, the recruitment of Grb2-Gab complexes require additional molecules and is described as an indirect mechanism. One of these indirect mechanisms includes the Gab protein PH domain. This domain can bind to phospholipids and therefore allows recruitment of the Grb2-Gab complex to the receptor. As the PH domain is highly conserved among all three Gab proteins it is likely that all Gab proteins are able to bind to the cell membrane via its PH domain. The role of the PH domain is best understood for EGFR signaling in the context with Gab1 (Rodrigues et al., 2000). Here, Gab1 is initially targeted to Grb2 leading to phosphorylation of tyrosyl residues in the Grb2 protein, activation of PI3K and generation of 3-phosphoinositide lipids. The Gab1 PH domain is then able to bind to these lipids and creates a positive feedback loop allowing more sustained signaling. In general, the PH domain is important and required for several recruitment mechanisms as point mutations in the PH domain result in impaired recruitment of Gab proteins (Schutzman et al., 2001).

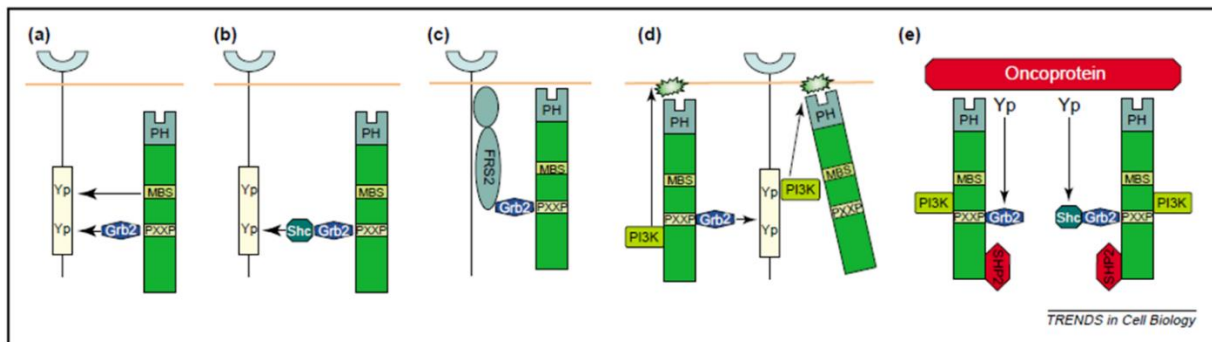


Figure 11: Gab protein recruitment mechanisms. **a)** Recruitment via MBS and Grb2–Gab1 complexes. Shown is a schematic of Gab1 recruitment to the HGF receptor. Gab1 can bind directly to the HGF receptor (HGFR) through its Met-binding sequence (MBS), as well as indirectly, as part of a Grb2–Gab1 complex, to a Grb2 SH2 domain binding site in the HGFR. **b)** Recruitment via Shc–Grb2–Gab2. Gab2 is recruited to IL3/GM-CSF/IL-5 receptor family by means of a Shc–Grb2–Gab2 complex. **c)** Recruitment via another scaffolding adaptor. In FGF receptor signaling, Gab1 is recruited to the receptor complex via Grb2 binding to the scaffolding adaptor FRS2. **d)** Recruitment via Gab family PH domains. In some signaling pathways, binding of the Gab PH domain to appropriate phosphoinositides is required for initial recruitment to receptor complexes or for sustained signaling (e.g. EGFR). **e)** Recruitment of Gab proteins to oncoproteins. Gab proteins are phosphorylated in response to several oncogenic stimuli. Recruitment of Gab2 to Y177 of Bcr–Abl as part of a Grb2–Gab2 complex. Abbreviations: BCR, B-cell receptor; EGFR, epidermal growth factor receptor; GM-CSF, granulocyte–macrophage colony-stimulating factor; IL, interleukin; PH, pleckstrin-homology; PI3K, phosphoinositide 3-kinase; SH2, Src-homology 2; Yp, phosphorytyrosine. From Gu and Neel, 2003.

1.6 Hypothesis and specific aims

Previous experiments have shown that C5aR1^{-/-} mice suffer from increased susceptibility and parasite burden in the brain during *T. gondii* infections. C5aR2^{-/-} mice also showed increased parasite burden in the brain compared to WT mice, but not as distinct as C5aR1^{-/-} mice (Briukhovetska, 2017). It has been shown that C5a is critical for the development of an appropriate CD4⁺ T cell response during *T. gondii* infections (Strainic et al., 2008). However, the underlying mechanisms regarding the signaling via C5aR1 and C5aR2 in DCs and especially in NK cells in the acute phase of the infection remain elusive. Using novel floxed reporter mice for C5aR1 and C5aR2, the Köhl laboratory already identified NK cells as C5aR2, but not C5aR1 expressing cells what makes them a unique cell type to investigate the functions of the still poorly understood C5aR2 during *T. gondii* infections. Besides the unique C5aR2 expression as an extrinsic factor influencing NK cell function, the Hoebe laboratory showed that NK cells are highly expressing Gab3 cells, which is a Grb-2-associated binder protein, the function of which is also poorly understood. Therefore, NK cells are a suitable cell type to investigate and define the role of C5aR2 and Gab3 during early *T. gondii* infections. Besides the undisputed role of NK cells in *T. gondii* infections, the regulation of C5aR1 and C5aR2 expression on other innate and adaptive immune cells in naïve mice and during the early phase of *T. gondii* infection has never been investigated before.

Based on previous data, I hypothesized that C5aR1/C5aR2 expression and regulation on immune cells and especially C5aR2 expression on NK cells play important roles during early *T. gondii* infection. Further, I proposed that potential independent co-expression of both anaphylatoxin receptors may play a key role in controlling the parasite. Finally, as Gab3 is highly expressed on NK cells, I hypothesized that a point mutation in the *gab3* gene results in altered susceptibility toward *T. gondii* infection. To test these hypotheses, I pursued the following specific aims:

1. Define the role of C5aR1 and C5aR2 signaling in DC-dependent and -independent activation of NK cells.
2. Delineate the role of C5aR1 and C5aR2 signaling in NK cell-mediated control of *T. gondii* infection.
3. Define the regulation of C5aR1 and C5aR2 expression on innate and adaptive immune cells during *T. gondii* infection.
4. Define the potential role of Gab3 and C5aR1/2 signaling pathways in NK cells for the induction of *T. gondii*-specific immune responses.

2 MATERIAL AND METHODS

2.1 Material

2.1.1 Mouse strains

Table 2: Mouse Strains. B6 = C57BL/6J, cg = congenic, tg = transgenic, tm = targeted mutation

Strain	Nomenclature	Background	Supplier
GFP-C5aR1 ^{fl/fl}	B6. C5aR1 ^{tm1JKo}	C57BL/6J	Internal breeding
C5aR1 ^{-/-}	B6.129S4-C5aR1 ^{tm1Cge}	C57BL/6J	Internal breeding
TdTomato-C5aR2 ^{fl/fl}	C5aR2 tdTomato ^{fl/fl}	C57BL/6J	Internal breeding
C5aR2 ^{-/-}	B6.Cg-Gpr77 ^{tm1Cge}	C57BL/6J	Internal breeding
Gab3 ^{R27C}	Gab3 ^{R27C}	C57BL/6J	Internal breeding
NMRI	CrI: NMRI (Han)	NMRI	Charles River
Wild Type	B6 JRj	C57BL/6J	Janvier

2.1.2 Chemicals and reagents

Table 3: Chemicals and reagents

Substance	Manufacturer
1-STEP™ Ultra TMB-ELISA Substrate solution	Thermo Scientific Inc., Waltham, USA
Auto-MACS Rinsing solution	Miltenyi Biotec GmbH, Bergisch Gladbach
BD Cytotfix/Cytoperm™ buffer	BD Biosciences Europe, Erembodegem, Belgium
BD Cytotfix™ fixation buffer	BD Biosciences Europe, Erembodegem, Belgium
BD FACS-Flow™ Sheath Fluid	BD Biosciences Europe, Erembodegem, Belgium
Bovine serum albumin (BSA)	Sigma-Aldrich Chemie GmbH, Steinheim
Brefeldin A, 1000x solution	eBioscience, Vienna, Austria
CD11c beads	Miltenyi Biotec GmbH, Bergisch Gladbach
Compensation beads (anti rat/hamster, anti-mouse)	BD Biosciences Europe, Erembodegem, Belgium

Substance	Manufacturer
Dimethyl sulfoxide (DMSO)	Sigma-Aldrich Chemie GmbH, Steinheim
DNase I recombinant, RNase-free	Sigma-Aldrich Chemie GmbH, Steinheim
Dulbecco's phosphate buffered saline (DPBS)	Gibco® by Life Technologies Corporation, Carlsbad, USA
Ethanol, 70 % denaturated	Carl Roth GmbH & Co. KG, Karlsruhe
Ethanol, 96 % denaturated	Carl Roth GmbH & Co. KG, Karlsruhe
Ethanol, absolute	J. T. Baker, Deventer, Netherlands
Ethylenediaminetetraacetic acid (EDTA)	Sigma-Aldrich Chemie GmbH, Steinheim
Fetal calf serum (FCS)	PAA Laboratories GmbH, Pasching, Austria
Formaldehyde solution, 37 %	Sigma-Aldrich Chemie GmbH, Steinheim
HEPES (4-(2-hydroxyethyl)-1-piperazineethanesulfonic acid) buffer solution 1M	Life technologies Corporation, Carlsbad, USA
Isopropanol	Otto Fisher GmbH & Co. KG, Saarbrücken
Ketamine	Sigma-Aldrich Chemie GmbH, Steinheim
L-glutamine (200mM concentrate)	Life technologies Corporation, Carlsbad, USA
Liberase™ TL Research Grade	Sigma-Aldrich Chemie GmbH, Steinheim
MACS BSA stock solution	Miltenyi Biotec GmbH, Bergisch Gladbach
Methanol (CH ₃ OH), 99.8 %	Sigma-Aldrich Chemie GmbH, Steinheim
Paraffin	Sigma-Aldrich Chemie GmbH, Steinheim
Penicillin-Streptomycin, 100x liquid	Gibco® by Life Technologies Corporation, Carlsbad, USA
Potassium bicarbonate (KHCO ₃)	Sigma-Aldrich Chemie GmbH, Steinheim
Potassium carbonate (K ₂ CO ₃)	Sigma-Aldrich Chemie GmbH, Steinheim
Potassium chloride (KCL)	Carl Roth GmbH & Co. KG, Karlsruhe
Potassium dihydrogen phosphate (KH ₂ PO ₄)	Carl Roth GmbH & Co. KG, Karlsruhe
RPMI 1640	Gibco® by Life Technologies Corporation, Carlsbad, USA
Sodium chloride (NaCl)	Carl Roth GmbH & Co. KG, Karlsruhe
Sodium dihydrogen phosphate (NaH ₂ PO ₄)	Carl Roth GmbH & Co. KG, Karlsruhe
Sodium hydrogen phosphate (Na ₂ HPO ₄)	Sigma-Aldrich Chemie GmbH, Steinheim
Sodium pyruvate	Life technologies Corporation, Carlsbad, USA

Substance	Manufacturer
Tris-aminomethane (Tris)	Sigma-Aldrich Chemie GmbH, Steinheim
Tris-HCL	Sigma-Aldrich Chemie GmbH, Steinheim
Trypan blue	Life technologies Corporation, Carlsbad, USA
Trypsin-EDTA 0.5 %, 10x	Life technologies Corporation, Carlsbad, USA
Tween® 20	Sigma-Aldrich Chemie GmbH, Steinheim
Xylazine	Sigma-Aldrich Chemie GmbH, Steinheim

Table 4: Stimulants

Substance	Manufacturer
C5a, human recombinant	Hycult Biotech, Uden, Netherlands
CSF-2 (GM-CSF), murine recombinant	Peprtech Corporation, Rocky Hill, USA
P32 C5aR2-specific agonist	Trent M. Woodruff, University of Queensland, Brisbane, Australia

2.1.3 Buffers, solutions and media

Table 5: Buffers, solutions and media

Buffer/Solution/Medium	Formulation
Complete RPMI medium	RPMI 1640 10 % FCS, heat-inactivated 100 units/ml Penicillin 100 µg/ml Streptomycin 2mM L-Glutamine
Dulbecco's Phosphate-Buffered Saline (DPBS) (self-made)	13.7 mM NaCl 0.27 mM KCl 0.81 mM Na ₂ HPO ₄ 0.15 mM KH ₂ PO ₄ pH 7.2-7.4 <i>Aqua destillata</i>
Diff-Quik solution B	Thiazine dye (blue colour)

Buffer/Solution/Medium	Formulation
	Phosphate buffer
Diff-Quik solution C	Eosin dye (red colour) Phosphate buffer
ELISA wash buffer (self-made)	0.05 % Tween® 20 in DPBS
Flow cytometer buffer, ELISA block buffer	1 % BSA in DPBS
MACS buffer	Auto MACS Rinsing-solution MACS BSA stock solution 1:20
Red blood cell (RBC) lysis buffer	155 mM NH ₄ Cl 10 mM KHCO ₃ 0.1 mM EDTA <i>Aqua destillata</i> pH 7.2, sterile
Tris buffer	500 mM NaCl 20 mM Tris-HCl <i>Aqua destillata</i> pH 7.2

2.1.4 Antibodies for flow cytometry

Table 6: Antibodies. AF = Alexa Fluor®, APC = Allophycocyanin, BV = Brilliant Violet, Cy = Cyanin, FITC = Fluorescein isothiocyanate, PE = Phycoerythrin, PerCP = Peridinin-chlorophyll-protein complex, hamster = Armenian hamster

Target	Dye	Clone	Species	Manufacturer	Concentration (µg/ml)
CD103	PerCP-Cy5.5	E7	hamster	Biologend	0.25
	BV510			Biologend	0.125
CD11b	AF700	M1/70	rat	eBioscience	0.5
	PerCP-Cy5.5			Biologend	1
CD11c	APC	N418	hamster	eBioscience	0.5
	PE			Biologend	1
CD16/32	-	93	rat	eBioscience	10
CD19	eFluor450	eBio1D3	rat	eBioscience	1.25
CD23	PacificBlue	B3B4	rat	Biologend	1.25

Target	Dye	Clone	Species	Manufacturer	Concentration (µg/ml)
CD27	PE	LG-3A10	hamster	BD Biosciences	0.5
CD3	eFluor450	17A2	rat	eBioscience	0.5
CD3e	PerCP-Cy5.5	145-2C11	hamster	BD Biosciences	1.25
CD4	PE-Cy7	RM4-5	rat	eBioscience	0.5
CD4	PE-Cy5	GK1.5	rat	Biolegend	0.5
CD4	BV421	RM4-5	rat	Biolegend	1
CD43	BV421	S7	rat	BD Biosciences	0.5
CD45R	APC	RA3-6B2	rat	eBioscience	1.25
	APC-Cy7			Biolegend	0.5
	PerCP-Cy5.5			Biolegend	1
CD49b	eF450	DX5	rat	eBioscience	0.5
CD5	PerCP	53-7.3	rat	Biolegend	0.5
CD64	BV711	10.1	mouse	BD Biosciences	0.5
CD8	PerCP-Cy5.5	53-6.7	rat	Biolegend	1
	FITC		rat	Biolegend	2.5
	BV510			Biolegend,	0.125
F4/80	BV510	BM8	rat	Biolegend,	0.5
	APC			Biolegend	1
IFN-γ	BV605	XMG1.2	rat	Biolegend	10
	PE			eBioscience	2
IgD	AF700	11-26c.2a	rat	Biolegend	1.25
IgM	PE-Cy7	II/41	rat	eBioscience	0.5
IL-12p40/70	PE	C15.6	rat	BD Biosciences	2
Ly49c/i	FITC	5E6	mouse	BD Biosciences	2.5
Ly49g2	PerCP-eFluor710	4D11	rat	Thermo Fisher	1
Ly6C	PerCP-Cy5.5	HK1.4	rat	eBioscience	0.5
Ly6G	eF450	RB6-8C5	rat	Thermo Fisher	0.5
	FITC	1A8		Biolegend	2.5
MHCII	APC-eFluor780	M5/114.15.2	rat	eBioscience	0.2
	PE-Cy7			Biolegend	0.5

Target	Dye	Clone	Species	Manufacturer	Concentration (µg/ml)
	APC			Miltenyi	3
NK1.1	AF700	PK136	rat	Biologend	1.25
	APC		mouse	Biologend	0.5
NKp46	APC	29A1.4	rat	Biologend	0.5
	eFluor450		rat	Thermo Fisher	0.5
Siglec-F	BV421	E50-2440	rat	BD Biosciences	0.25

2.1.5 Plastic ware and disposable items

Table 7: Plastic ware and disposable items

Material	Manufacturer
BD Microtainer tube	BD Biosciences Europe, Erembodegem, Belgium
Blunt fill needle, 18G	BD Biosciences Europe, Erembodegem, Belgium
Cell strainer 40 µm	BD Biosciences Europe, Erembodegem, Belgium
Cover glass, 20x20 mm, thickness 1	Glaswarenfabrik Karl Hecht GmbH & Co. KG, Sondheim/Rhön
Cover glass, circular, 25 mm, borosilicate glass thickness 1	VWR, international GmbH, Darmstadt
ELISA reservoir, 25 ml	VWR, international GmbH, Darmstadt
Falcon Tube 15 ml, 50 ml	Sarstedt AD & Co., Nümbrecht
Filter tip 10 µl, 100 µl, 1000 µl	Sarstedt AD & Co., Nümbrecht
Lancet	B. Braun Melsungen AG, Melsungen
MACS Separation MS Column	Miltenyi Biotech GmbH, Bergisch Gladbach
Microscope slide, 76x26 mm	Gerhard Menzel GmbH, Braunschweig
Microtiter plate, 6-well	Sarstedt AD & Co., Nümbrecht
Microtiter plate, 96-well, high bind	Corning, Corning, USA
Microtiter plate, 96-well, with lid (F bottom)	Greiner Bio-One GmbH, Frickenhausen
Microtiter plate, 96-well, with lid (U bottom)	Greiner Bio-One GmbH, Frickenhausen
Needle hypodermic, 26G	BD Biosciences Europe, Erembodegem, Belgium
Nitrile powder-free examination gloves	Ansell Healthcare GmbH, Munich

Material	Manufacturer
Pipette 5 ml, 10 ml, 25 ml	Greiner Bio-One GmbH, Frickenhausen
Pipette tips 10 µl, 100 µl, 1000 µl	Sarstedt AD & Co., Nümbrecht
Reaction tube 0.5 ml, 1.5 ml, 2.0 ml (low-binding)	Sarstedt AD & Co., Nümbrecht
Reaction tube 0.5 ml, 1.5 ml, 2.0 ml, 5.0 ml	Eppendorf AG, Hamburg
Single use cannula 21G, blunt	B. Braun Melsungen AG, Melsungen
Spatula	VWR International GmbH, Darmstadt
Syringe 1 ml, 5 ml, 10 ml, Luer-Lok™	BD Biosciences Europe, Erembodegem, Belgium
Syringe 5 ml, 10 ml	BD Biosciences Europe, Erembodegem, Belgium
Syringe, 1 ml	B. Braun Melsungen AG, Melsungen
Tube 5 ml, 75x12 mm, unsterile for flow cytometry	Sarstedt AD & Co., Nümbrecht
Weighing dish	Greiner Bio-One GmbH, Frickenhausen

2.1.6 Commercially available kits

Table 8: Commercially available kits

Kit	Manufacturer
AYOXXA LUNARIS Multiplex 12-plex	Ayoxxa Biosystems GmbH, Cologne
Fixable Viability Dye eFluor 780	eBioscience, Vienna, Austria
LEGENDplex Mouse Inflammation Panel	Biolegend Europe, London, UK
Mouse IFN-gamma DuoSet® ELISA	R&D Systems, Minneapolis, USA
Mouse IL12/IL-23p40 DuoSet® ELISA	R&D Systems, Minneapolis, USA
Mouse IL-12p70 DuoSet® ELISA	R&D Systems, Minneapolis, USA

2.1.7 Laboratory equipment

Table 9: Laboratory equipment

Equipment	Manufacturer
Biological safety cabinets	Nuaire Inc., Plymouth, USA
Cell sorter FACS ARIAIII	Beckton Dickinson GmbH, Heidelberg

Equipment	Manufacturer
Centrifuge 5424	Eppendorf AG, Hamburg
Centrifuge 5424R	Eppendorf AG, Hamburg
Centrifuge 5810R	Eppendorf AG, Hamburg
Centrifuge Rotofix 32A	Hettich Lab Technology, Tuttlingen
Chemical hood	Waldner Laboreinrichtungen GmbH & Co KG, Wangen
Confocal microscope FluoView1000	Olympus, Hamburg
Dissecting scissors	WPI Deutschland GmbH, Berlin
ELISA reader Fluostar Omega 0415	BMG Labtech GmbH, Ortenberg
ELISA washer Nunc-Immuno™ wash 12	Thermo Fisher Scientific Inc., Waltham, USA
Flow cytometer BD LSRII	Beckton Dickinson GmbH, Heidelberg
Forceps	WPI Deutschland GmbH, Berlin
Fridge, 4°C and -20°C combined	Liebherr International GmbH, Biberach an der Riß
Ice machine AF-10	Scotsman, Milan, Italy
MACS Magnetic Cell Separator	Miltenyi Biotech GmbH, Bergisch Gladbach
Microscope BA310 LED	Motic, Wetzlar
Microscope camera Leica EC3	Leica Mikrosystem Vertrieb GmbH, Wetzlar
Microscope camera Moticom	Motic, Wetzlar
Microscope Fluoview FS	Leica Mikrosystem Vertrieb GmbH, Wetzlar
Microscope Leica DM IL LED	Leica Mikrosystem Vertrieb GmbH, Wetzlar
Multichannel pipette Biohit M300	Sartorius Biohit Liquid Handling Oy, Helsinki, Finland
Neubauer counting chamber, improved	VWR International GmbH, Darmstadt
pH-Meter Seven Easy PH S20-K	Mettler Toledo, Schwerzenbach, Switzerland
Pipetboy pipette controller	Integra Biosciences AG, Zizers, Switzerland
Pipette (0.1-2.5 µl, 0.5-10 µl, 10-100 µl, 20-200 µl, 100-1000 µl)	Eppendorf AG, Hamburg
Precision balance EMB 1000-2	Kern & Sohn, Balingen
Precision balance LC6200S	Sartorius AG, Göttingen
Pump, VacuGene	Pharmacia, Belgium
Pure water system Nanopure Diamond D11931	Thermo Fisher Scientific GmbH, Bremen
Shaker Polymax 1040	Heidolph Instruments GmbH & Co. KG, Schwabach

Equipment	Manufacturer
Suction system Vacusafe 158310	Integra Biosciences GmbH, Fernwald
Table centrifuge	Carl Roth GmbH & Co. KG, Karlsruhe
Tablet Acer Iconia Tab	Acer, Xizhi, New Taipei, Taiwan
Thermomixer 5436	Eppendorf, Hamburg
Ultra-low temperature freezer, -80°C	SANYO Electrics Co., Japan
Vortex-Genie 2	Scientific Industries Inc., New York, USA
Water bath	GFL, Burgwedel

2.1.8 Computer software

Table 10: Computer Software

Software	Developer
Adobe Acrobat Reader DC	Adobe Systems Inc., San Jose, USA
BD FACSDiva V8.0	BD Biosciences, San Jose, USA
FlowJO X	FlowJo, LLD, Ashland, USA
FluoView FV1000 2.0b	Olympus, Hamburg
GraphPad Prism 7	Graph Pad Software Inc., LaJolla, USA
Imaris 7.2.3	Bitplane AG, Zurich, Switzerland
Leica Aquire 1.0	Leica Microsystems CMS GmbH, Wetzlar
Microsoft Office 365	Microsoft Corporation, Redmond, USA
MARS – Data Analysis Software 2.30 R2	BMG Labtech GmbH, Ortenberg
Omega 1.30	BMG Labtech GmbH, Ortenberg

2.2 Methods

2.2.1 Animals

WT C57BL/6J and NMRI mice were purchased from JANVIER. C5aR1^{-/-}, C5aR2^{-/-}, floxed GFP-C5aR1 and floxed tdTomato-C5aR2 mice on the C57BL/6J background were bred and maintained in an SPF animal facility of the University of Lübeck. Gab3^{R27C} mice on the C57BL/6J background were bred and maintained in an SPF animal facility of the CCHMC in Cincinnati, USA. All animal experiments were conducted according to protocols (number 39(36-3/15) and 39_2017-03-02) approved by the ethical committee (Ministerium für Energiewende, Landwirtschaft, Umwelt, Natur und Digitalisierung, Kiel, Germany). Animals used were male or female and between 8 and 12 weeks old.

2.2.1.1 Generation of floxed reporter mice

The Köhl laboratory (Lübeck, Germany) generated two floxed reporter mice to track C5aR1 or C5aR2 expression. These strains allow to track C5aR1 and C5aR2 expression without the need of antibodies and to generate cell- or tissue-specific C5aR1 or C5aR2 knockouts.

Floxed GFP-C5aR1 reporter mice were generated as described in Karsten et al. 2015 (Karsten et al., 2015). Floxed td-Tomato-C5aR2 reporter mice were generated as described in Karsten et al. 2017 (Karsten et al., 2017).

2.2.1.2 ENU (N-ethyl-N-nitrosourea) mutagenesis

ENU-mutation experiments were conducted at Cincinnati Children's Hospital Medical Center (CCHMC) in the laboratory of Kasper Hoebe.

N-ethyl-N-nitrosourea (ENU) is reported to be the most potent germline mutagen in mice (Russell et al., 1979). At optimal concentrations (100 mg/kg) it causes one new mutation per gene in every 700 gametes. ENU primarily induces point mutations through alkylation of nucleic acids resulting in mispairing and base-pair substitutions during the next DNA replication round. The most frequently induced mutations are AT to TA transversions and AT to GC transitions (Popp et al., 1983) that primarily lead to missense mutations (64 % missense, 26 % splicing errors, 10 % non-sense mutations) (Salinger and Justice, 2008). As high doses of ENU are toxic, application protocols need to be precise to allow mutations and avoid toxicity. Besides its toxicity, ENU is carcinogenic and can lead to various types of tumors in treated mice (Keller et al., 2016). When used as a mutagen, it induces mutations in male

spermatogonial stem cells. Mutations in female germ cells and post-spermatogonial stem cells are one magnitude below that of male stem cell spermatogonia.

To initiate mutations, 5-6 weeks old C57BL/6 male mice were anesthetized with isoflurane. ENU was injected i.p. in three weekly doses (100 mg/kg body weight).

After the last dose, mice were separated for 12 weeks to allow recovery of fertility. Then, treated males were bred with untreated C57BL/6 female mice to generate G1 offspring. These animals were either used for phenotypic screening or to produce G2 offspring to allow backcrossing (**Figure 12**).

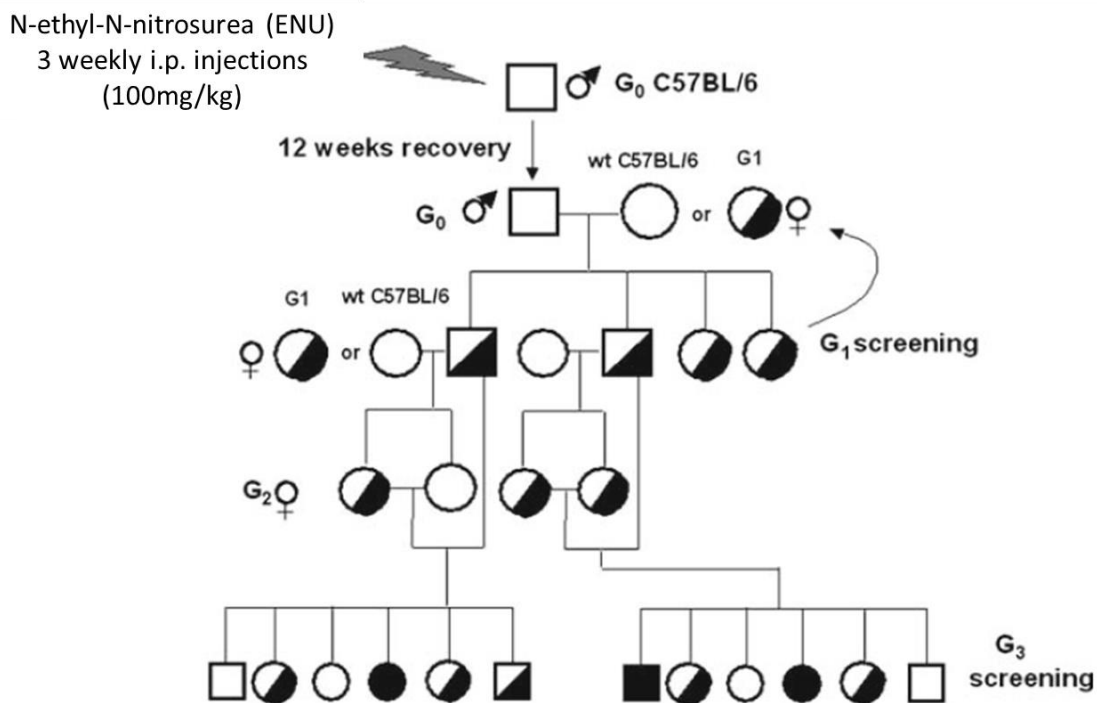


Figure 12: ENU treatment of C57BL/6 mice. Each G₁ male is bred with 2 G₂ females. Subsequently from each G₂ female 3 G₃ offspring are tested in recessive screens. From Hoebe, 2009.

2.2.1.3 Generation of mixed bone marrow chimeric mice

Mixed bone marrow (BM) chimeric mice experiments were conducted at Cincinnati Children's Hospital Medical Center (CCHMC) in the laboratory of Kasper Hoebe.

BM chimeric mice were generated by lethally irradiating mice and replacing the BM and all BM-derived cells. Such mice are a perfect tool to study the contribution of various immune cell types in the course of an immune response with respect to their hematopoietic origin (Holl, 2013).

The common leukocyte antigen CD45 is often used in generating mixed BM chimeric mice, because it is expressed by most hematopoietic cells and therefore allows to distinguish between cells from different donors and the host in mixed BM mice (Shen et al., 1985). Recipient mice (here: CD45.1⁺ WT,

CD45.2⁺ WT) were irradiated with a first dose of 700 rad followed by a second dose of 475 rad 3 h later. The next day, BM cells from donor mice (here: CD45.1⁺ WT, CD45.2⁺ Gab3^{R27C}) were harvested and diluted to 5x10⁶ cells/100 µl in PBS. The BM of donors was mixed 1:1 and transferred intravenously (i.v.) into the irradiated recipients the same day. On day 29 post transplantation, recipients were euthanized and cells from different compartments were isolated and analyzed by flow cytometry with respect to CD45.1 and CD45.2 expression (**Figure 13**).

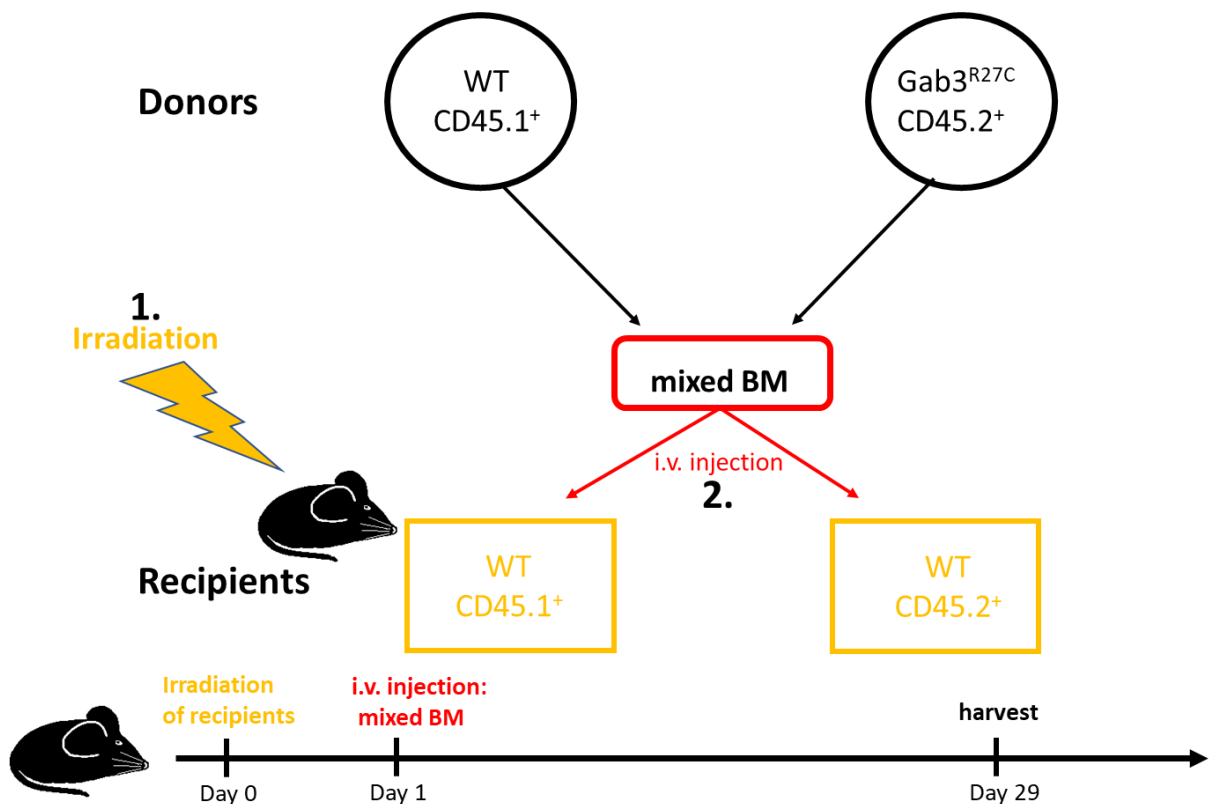


Figure 13: Generation of mixed BM chimeric mice. Mixed BM were created by combining BM cells from two different donors: CD45.1⁺ WT mice and CD45.2⁺ Gab3^{R27C} mice. Mixed BM cells were then i.v. injected into two different recipients (CD45.1⁺ WT mice and CD45.2⁺ WT mice) which had been UV-irradiated before to deplete immune cells. After 29 days of recovery, recipient mice were euthanized to analyze cell composition in different compartments.

2.2.2 *Toxoplasma gondii* mouse infection models

2.2.2.1 Generating a stock of *T. gondii* cysts for infections

To ensure generation of a homogeneous stock of *T. gondii* ME49 cysts, we used NMRI mice and infected them i.p. with 10 cysts of *T. gondii* ME49 (provided by D. Schlüter, Institute for Medical Microbiology and Hospital Hygiene, University Magdeburg). NMRI mice do not develop acute toxoplasmosis and serve as the perfect vehicle to generate cyst stocks (Lu et al., 2005). Expansion of the cyst stock was achieved by i.p. infection of NMRI or WT C57BL/6J mice with 10 cysts harvested from long-time infected NMRI mice. After at least 4 months, cysts from brains of C57BL/6J or NMRI

mice were used for the intraperitoneal (i.p.) infection model (see below). After the first experiments, I noticed that the harvested cysts from infected WT C57BL/6J mice lack homogeneity regarding cyst size and infectivity and therefore I decided to use cysts from long-time infected NMRI mice only.

2.2.2.2 Determination of *T. gondii* brain cysts in infected mice

T. gondii cysts were harvested from brains of NMRI or C57BL/6 mice which were infected at least for 4 months. For this purpose, mice were euthanized with CO₂ followed by cervical dislocation, before wetting the head with 70 % ethanol and removing the skin using scissors. The skull was opened with scissors and the brain was removed. The brain was then placed in a 5 ml reaction tube filled with 1 ml ice-cold and sterile DPBS. To homogenize the tissue, it was repeatedly pumped through a 5 ml luer lock syringe which was connected to different needles (18G, 21G, 26G; 5-10 times each needle). To determine the tissue cyst count, 20 µl of the brain suspension was placed on a microscope slide, covered with a 20x20 mm coverslip and cysts were counted using a phase-contrast microscope with a 40-fold magnification (**Figure 14**). Cysts were counted on the entire slight to calculate the total number of cysts in the brain suspension using the following formula:

$$cyst\ count_{total} = \left(\frac{Volumen_{total}}{20\mu l} \right) * cyst\ count_{20\mu l}$$

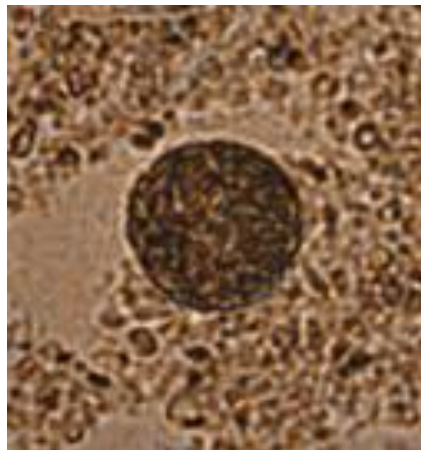


Figure 14: *T. gondii* cyst in brain suspension at 40-fold magnification under a phase contrast microscope.

2.2.2.3 Oral infection model

T. gondii cysts were harvested from NMRI or C57BL/6 mice, the cyst numbers were determined as described in 2.2.2.2. and the brain solution was diluted with DPBS. Mice were infected by oral gavage

with 1-10 cysts in 0.2 ml DPBS. The gavage needle was connected to a 1 ml syringe containing the brain cyst solution. The needle was then placed through the mouth in the esophagus into the stomach where 0.2 ml of the solution was injected. Afterwards, mice were observed for at least 15 min to exclude the development of any discomfort in response to life-threatening rupture of the stomach or esophagus. If any suspicious behavior, like apathy, bleeding from mouth or nose or any other criteria mentioned in 2.2.2.6, was observed, the mice were immediately euthanized as described in 2.2.2.2.

2.2.2.4 Intraperitoneal infection model

For i.p. injections of *T. gondii* cysts, brain cysts from NMRI or C57BL/6 mice were harvested and the cyst load was determined as described above. Brain cysts were diluted to 250 cysts/ml, of which 200 μ l were injected directly into the peritoneal cavity using a 27G needle connected to a 1 ml syringe.

2.2.2.5 Acute and chronic *T. gondii* infection models

After infecting mice orally or i.p., survival, the disease score and changes in relative and absolute weight were determined daily. Leukocyte distribution was analyzed using flow cytometry between days 1 and 7 p.i. in spleen, lung, blood and peritoneal cavity. In some experiments, mice were sacrificed after 30 days p.i. to determine the brain cyst count. Serum and peritoneal lavage supernatants were used to measure cytokine levels (**Figure 15**).

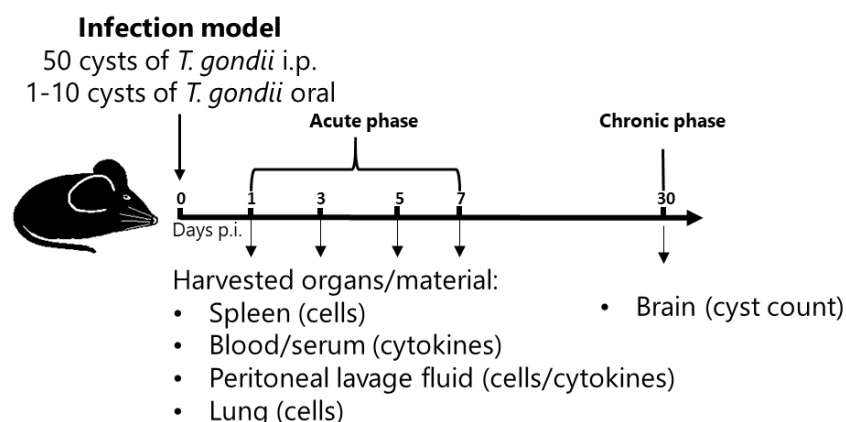


Figure 15: *T. gondii* infection models. Mice were infected with either 10 cysts i.p. or 1-10 cysts orally. The immune reaction was analyzed during the acute phase of the infection between days 1 and 7 p.i. in spleen, blood, peritoneal cavity and lung or during the chronic phase 30 days p.i. in the brain.

2.2.2.6 Evaluation of *T. gondii*-induced disease severity in mice

After infection, the health status of infected mice was controlled daily. In case that any termination criteria were reached, mice were anesthetized and euthanized by inhalation of CO₂ followed by cervical dislocation. Termination criteria were defined as follows:

1. Weight loss of more than 20 % of the initial weight (before infection). Relative weight was calculated using the following formula:

$$\text{relative weight, \%} = \frac{\text{current weight, g}}{\text{initial weight, g}} \times 100\%$$

2. Disease score \geq 4.

Disease scores were defined by the animal protection ordinance (*Tierschutz-Versuchstierordnung*) as followed:

- **Score 1:** coat, appetite, gait, posture is normal. Mouse is alert and responds normally to external stimuli (escape behavior, reactivity).
- **Score 2:** Mouse is active, but moves slower than normal, back slightly humped, fur starts to become dull
- **Score 3:** Score 2 plus tilted head, ataxia and delayed righting reflex
- **Score 4:** Mouse is quiet, alert and responsive, but shows a strongly curved back, coarse fur, reacts with movement only to external stimuli
- **Score 5:** Mouse no longer responds to stimuli and is apathetic, lays on the side.

2.2.3 Immune cell isolation from mouse tissue

Cell isolation from peritoneal cavity

For cell isolation from peritoneal cavity, mice were anesthetized with CO₂ and euthanized by cervical dislocation. A small incision was made in the outer skin of the peritoneum followed by pulling back the skin. One ml (to determine cytokine concentrations) or 5 ml (to analyze immune cell composition) of ice-cold DPBS was injected in the peritoneal cavity using a 26G needle and the abdomen was gently massaged to detach peritoneal cells. Then, the injected DPBS was removed from the cavity, transferred into a 15 ml Falcon tube and stored on ice. To isolate the cells, the Falcon tube was centrifuged for 5 min at 500 g, 4°C. The supernatant was either discarded or in case of a 1 ml lavage kept for cytokine analysis. The cell pellet was used for further analysis.

Cell isolation from spleen and lymph nodes

After euthanizing the mice as described above, the spleen or inguinal lymph nodes were removed and transferred into a 1.5 ml reaction tube filled with ice-cold DPBS and stored on ice. Using a plunger, spleens or lymph nodes were passed through a nylon cell strainer (40 μm pore size) which was placed on a 50 ml Falcon tube to obtain a single cell suspension. The cell suspension was washed with DPBS once, centrifuged at 400 g, 5 min, 4°C and treated with RBC lysis buffer (3 ml, 4 min, RT). To stop lysis, 37 ml of DPBS were added, before the cell suspension was centrifuged for 5 min at 400 g, 4°C again. The cell pellet was used for analysis, the supernatant was discarded.

Cell isolation from lung

After euthanizing the mice as described above, lungs were removed and transferred to a nylon cell strainer (40 μm pore size), which was placed in a 6-well-plate filled with pure RPMI medium and lungs were mechanically chopped with scissors. To obtain single cell suspensions, the lungs were digested with Liberase TL (0.25 mg/ml)/DNase I (0.5 mg/ml) solution in RPMI for 45 min at 37°C, 5 % CO₂ (shaking). Then, the cell strainer was placed on a 50 ml Falcon tube and cells were passed through the strainer using a plunger from a 5 ml syringe. The cell strainer was washed with 10 ml RPMI twice to collect all cells. After 10 min centrifugation at 350 g, 4°C the supernatant was discarded, and the cell pellet was resuspended in 3 ml RBC lysis buffer. After 3 min incubation time, the Falcon tube was filled up with DPBS to a final volume of 30 ml. After another centrifugation step (350 g, 10 min, 4°C) the supernatant was discarded, and the cell pellet was used for further analysis.

Cell isolation from blood and collecting of serum

Blood was collected from the submandibular vein. After pricking the vein with a lancet, drops of blood were collected in a 1.5 ml reaction tube containing 10 μl of 0.5 M EDTA.

In acute infection phase experiments, blood was collected by cardiac puncture. For this purpose, the mice were anesthetized by injecting 50 μl of a Ketamine/Xylazine solution (10 ml 10 % Ketamine, 3.12 ml 2 % Xylazine) i.p. The heart was punctured using a 26G needle and blood was collected into a 1 ml syringe and transferred into a 1.5 ml collection tube containing 10 μl of 0.5 M EDTA.

To remove erythrocytes, blood was treated twice with 10 ml RBC lysis buffer for 10 min followed each by a centrifugation step for 5 min at 450 g. The supernatant was discarded, and the cell pellet was used for further analysis.

To obtain serum, blood samples were transferred to BD microtainer SST blood collection tubes and centrifuged for 2 min at 10000 g. Serum was transferred to 0.5 ml collection tubes and stored at -20°C for further analysis.

2.2.3.1 Cell number determination

To determine the cell number of different cell suspensions, cell pellets were dissolved in PBS+1 % BSA and mixed 1:1 with trypan blue to stain dead cells. Ten µl of this mixture were used in an improved Neubauer chamber under the microscope to count living cells. The cell number was calculated using the following formula:

$$cell\ count\ x10^4 = \frac{cells\ counted\ x\ dilution\ factor\ x\ vol.\ in\ ml}{\#\ of\ counted\ squares}$$

2.2.4 Histological sections

2.2.4.1 Wright-Giemsa staining using Diff-Quik

Histology sections of the ileum and jejunum of infected WT, C5aR1^{-/-} and C5aR2^{-/-} mice were fixed with methanol (10 sec.), then dipped 5 times in solution C containing thiazine dye, followed by 5 dips in solution B containing eosin dye. After each staining process, the remaining staining-solution was washed-off with water and sections were air-dried before use.

2.2.4.2 Evaluation of histology sections

To analyze and evaluate histology sections from the intestine of infected mice, Dr. Sebastian Jendrek (Department of Internal Medicine, University of Lübeck) and Prof. Dr. Christian Sina (Institute for Nutritional Medicine, University of Lübeck) provided their expertise. They scored all sections according to *Erben et al* (Erben et al., 2014) evaluating tissue destruction (score 0-3) and inflammatory cell infiltration (score 0-3). Each score ranges from 0 (no damage or cell infiltration) to 3 (massive damage and cell infiltration) and the sum of both scores (max. score 6) allows a precise evaluation of the severity of the infection. The scoring was blinded as Dr. Jendrek and Prof. Dr. Sina did not know which section came from which mice.

2.2.5 Measurement of cytokine production in sera and supernatants

2.2.5.1 Enzyme-linked immunosorbent assay (ELISA)-based measurement

Enzyme-linked immunosorbent assay (ELISA) was used to determine the cytokine concentrations of IFN- γ (detection limit: 30 pg/ml), IL-12p40 (detection limit: 39 pg/ml) and IL-12p70 (detection limit: 39 pg/ml) in serum and peritoneal lavage supernatants. Furthermore, cytokine production from *in vitro* cell culture supernatants was analyzed. R&D DuoSet ELISA-Kits were used according to the manufacturers' recommendations. The reaction volume was reduced to 50 μ l without loss of sensitivity and reproducibility.

2.2.5.2 AYOXXA LUNARIS™ 12-Plex Cytokine Kit

The LUNARIS™ multiplex system from AYOXXA (AYOXXA Biosystems GmbH, Cologne, Germany) was used to measure cytokines from serum and peritoneal lavage supernatants. The following cytokines were measured simultaneously: IL-1 β , IL-2, IL-4, IL-5, IL-6, IL-10, IL-12p70, IL-13, IL-17A, IFN- γ , TNF α , GM-CSF. The multiplex system which determines cytokine concentrations from only 3 μ l per sample, is a protein assay format, based on antibody-coated beads immobilized on a solid surface. Every well on a LUNARIS™ BioChip has a unique biomarker-specific antibody-bead distribution which is saved in a chip-specific datafile. The reaction principle follows a classical sandwich ELISA and all antibodies are tagged with a fluorophore to analyze cytokine production via the mean fluorescence intensity (MFI). The LUNARIS™ BioChip was analyzed using the AYOXXA LUNARIS™ Reader.

2.2.6 *In vitro* NK cell stimulation

Stimulation with IL-12 and IL-18

Splenic NK cells were purified using either the MoFlo Legacy or FACS ARIA III cell sorter. Prior to the cell sorting, the splenic cells were stained with CD3 ϵ , NKp46 or NK1.1 to identify NK cells as NK1.1⁺ CD3⁻ or NK1.1⁺ NKp46⁺ cells (**Figure 16**).

After sorting, 1x10⁵ NK cells were cultured in a 6-well plate in 200 μ l medium and stimulated with 10 ng/ml IL-12 and 10 ng/ml IL-18 for 24 h. In some experiments, NK cells were also stimulated with 100 μ M of the C5aR2-specific agonist P32. After 24h, the supernatant was collected, and IFN- γ production was measured by ELISA.

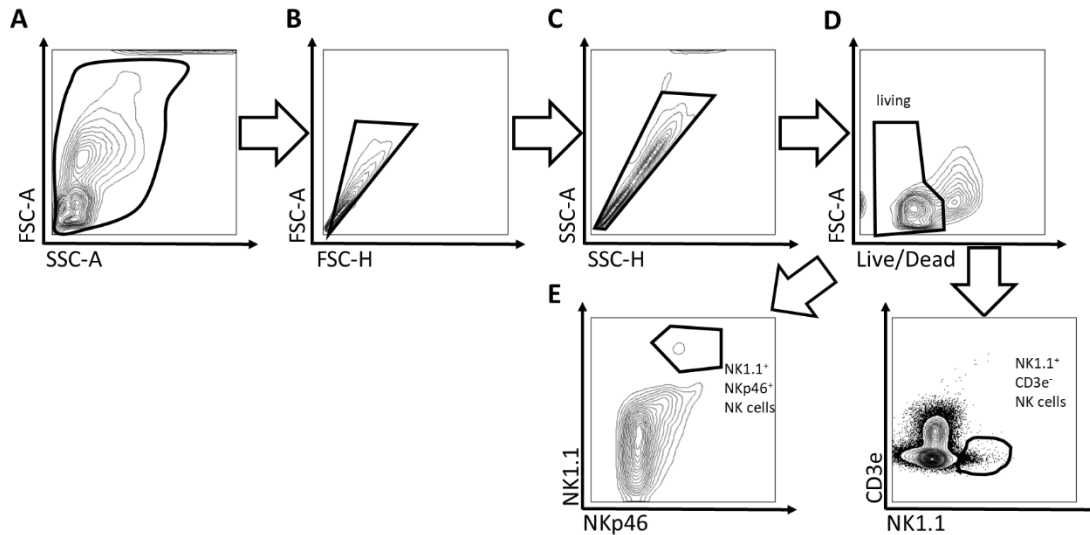


Figure 16: Gating strategy for sorting NK cells from the spleen depicted as dot plots. A) Excluding cell debris. B) + C) excluding cell doublets. D) Gating on living cells. E) Gating on NK cells as NK1.1⁺ NKp46⁺ cells (left) or NK1.1⁺ CD3e⁻ cells (right).

Stimulation with C5a

NK cells were purified and cultured as described before and 12.5nM C5a was used for the stimulation. The stimulation was stopped by the addition of 200µl 2 % PFA after 1 min, 2 min, 3 min, 5 min, 10 min and 30 min. The NK cells were then used for intracellular staining and analysis of MAP-kinase phosphorylation.

2.2.7 Flow cytometry

2.2.7.1 Surface staining and general gating strategy

Identification and phenotypical analysis of different immune cells from distinct organs was achieved by flow cytometry. Before staining with specific antibodies, Fc-block (CD16/CD32) was used to block Fcγ receptors preventing unspecific binding of antibodies. Fc block was used at 10 µg/ml for 15 min at 4°C. Master mixes were prepared with specific antibodies from **Table 6** using the indicated concentrations. After Fc block incubation, cells were washed with 1 ml of PBS+1 %BSA and centrifuged at 500 g, 5 min, 4°C before the cell pellet was resuspended in 300 µl of master mix solution and incubated for 15 min at 4°C again. Following another washing step with 1 ml of PBS+1 %BSA, the cell pellet was resuspended in BD Cytofix™ buffer and incubated for 10 min at 4°C. After another washing step with 1 ml PBS+1 %BSA and centrifugation at 500 g, 4°C the cell pellet was resuspended in 350 µl PBS+1 %BSA and analyzed on the BD LSRII cell analyzer or BD FACS ARIAIII cell sorter. For reliable results, I recorded up to 2x10⁶ cells per sample. To exclude small particles and cell debris, the FSC

threshold was set to 10,000-15,000. Furthermore, FSC-A/SSC-A, FSC-A/FSC-H and SSC-A/SSC-H gating was used to exclude cell debris and cell doublets (**Figure 17**).

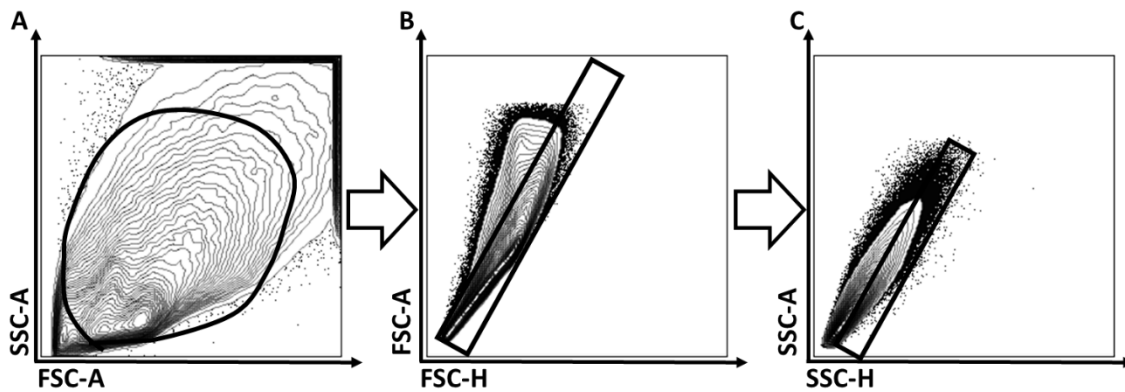


Figure 17: Gating strategy depicted as dot plots. **A)** Gate setting to exclude small particles and cell debris. Gating for single cells to exclude cell doublets using **B)** FSC-A and FSC-H and **C)** SSC-A and SSC-H.

2.2.7.2 Intracellular stainings

Intracellular staining for different phosphorylated MAP kinases required fixation and permeabilization with paraformaldehyde (PFA) and methanol. Cells were stained for surface markers before stimulation as described above. After stimulation (1 min, 2 min, 3 min, 5 min, 10 min, 30 min) 200 μ l 2 % PFA was added to 2×10^5 cells in 100 μ l. Cells were transferred to 1.5 ml reaction tubes containing 1 ml 2 % PFA to fix the cells. After 10 min incubation at room temperature, pelleting of cells was achieved by centrifugation at 500 g, 5 min, 4°C. After carefully removing the supernatant, the cell pellet was resuspended in 1 ml pre-cooled (-20°C) 100 % methanol and vortexed to initiate permeabilization. After 20 min of incubation on ice and centrifugation at 500 g, 5 min, 4°C, cells were resuspended in 100 μ l PBS+1 %BSA and stained with the respective antibodies for intracellular targets (45 min, 4°C) (**Table 6**). Finally, after washing cells with PBS+1 %BSA, cells were resuspended in 300 μ l PBS+1 %BSA and analyzed on the BD LSRII flow cytometer.

2.2.8 Statistical analyses

Statistical analyses were performed using GraphPad Prism 7 (GraphPad Software, La Jolla, USA). The presented data show the individual values and the mean \pm standard error of the mean (SEM). Two group comparisons were performed with unpaired *students t-test* (if not mentioned otherwise) and multiple group comparisons were performed with *one-way ANOVA* (analysis of variance) with Tukey multiple comparison test. Multiple comparisons with more than one independent variable were performed using *two-way ANOVA* with Sidak multiple comparison test. To compare survival curves of

two groups log-rank (Mantel-Cox) test was used. P-values ≤ 0.05 were considered as statistically significant (* $p \leq 0.05$; ** $p < 0.01$; *** $p < 0.001$; **** $p < 0.0001$).

3 RESULTS

3.1 The survival after oral *T. gondii* infection is higher in C5aR1^{-/-} and C5aR2^{-/-} mice than in WT mice

Due to the life cycle of the parasite, oral infection of mice with *T. gondii* cysts is the natural way how mice become infected with the parasite (Dubey, 1998) and 10 cysts have been considered to be an appropriate amount of cysts according to the literature (Dias et al., 2014; Liesenfeld, 2002) as well as personal communication with Prof. Schlüter (Institute for Medical Microbiology, Magdeburg).

To investigate whether C5aR1^{-/-} and C5aR2^{-/-} mice develop different disease severities in comparison to WT mice, I infected these strains with 10 cysts *T. gondii* orally.

To evaluate the disease progression, I weighed and scored the mice every day. Mice that fulfilled one of the termination criteria (weight loss $\geq 20\%$, disease score ≥ 4) were sacrificed.

I observed that WT mice were more susceptible compared to C5aR1^{-/-} and C5aR2^{-/-} regarding weight loss, disease score and survival (**Figure 18**). However, also C5aR1^{-/-} and C5aR2^{-/-} mice developed severe inflammation characteristics and were sacrificed due to weight loss of more than 20 % at latest on day 20 p.i.

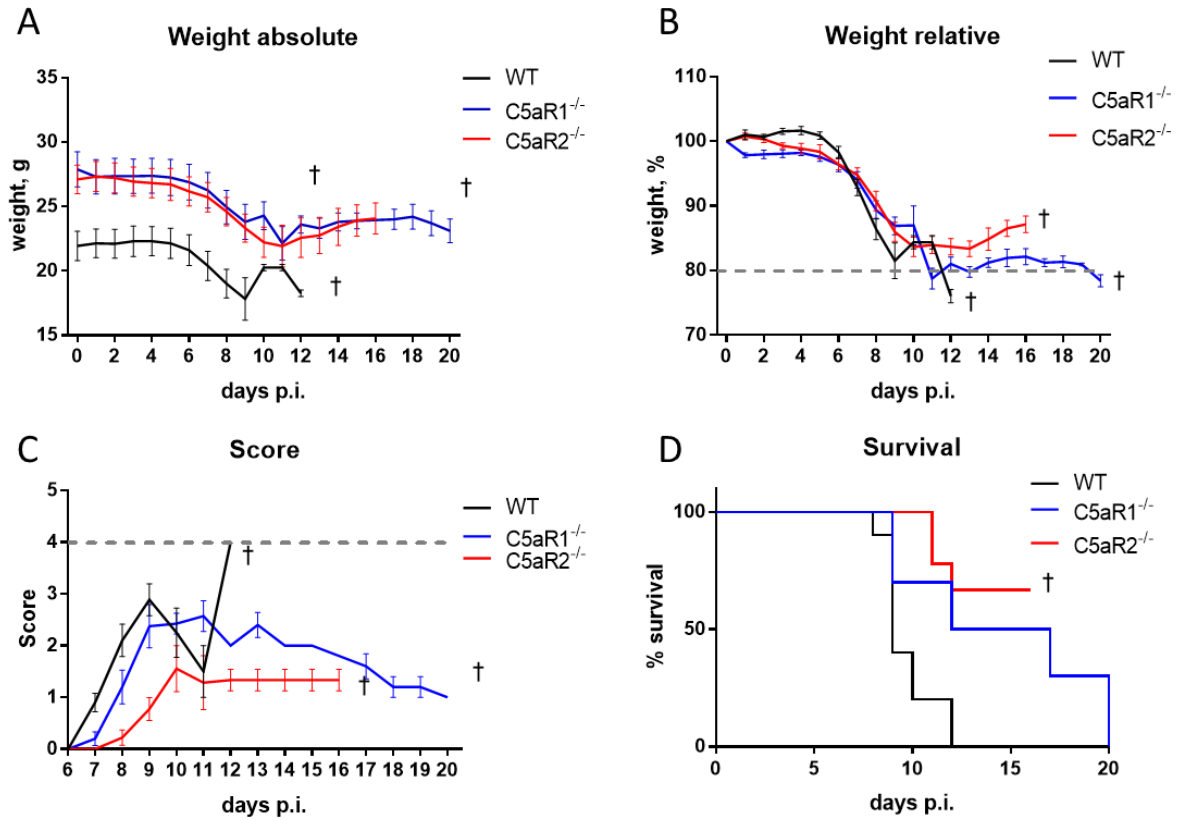


Figure 18: The development of weight loss, disease score and survival after oral *T. gondii* infection with 10 cysts is more dominant in WT than in C5aR1^{-/-} or C5aR2^{-/-} mice. Changes in **(A)** absolute and **(B)** relative weight during 20 days after p.i. with 10 *T. gondii* cysts. Groups indicated with † had to be sacrificed due to weight loss of more than 20 % of initial weight. **(C)** Disease score during infection. **(D)** Survival. n=10/group for all graphs; Values show the mean ± SEM (A-C). Statistical analyses were determined by ANOVA (A-C) or Log-rank (Mantel Cox) test (D). Groups indicated with † had to be sacrificed due to weight loss of more than 20 % of initial weight (dashed line in (B)) or disease score of ≥4 (dashed line in (C)) or died during the experiment.

3.2 Potential protective role of C5a receptors in the intestine during *T. gondii* infections

To evaluate whether C5aR1 or C5aR2 control the immune response after *T. gondii* infection and cell infiltration into the intestine, I infected WT, C5aR1^{-/-} and C5aR2^{-/-} mice orally with 10 cysts and after 7 days I analyzed tissue destruction and cell infiltration into the jejunum and ileum.

The qualitative evaluation was performed in collaboration with Dr. Sebastian Jendrek (Department of Internal Medicine, University of Lübeck) and Prof. Dr. Christian Sina (Institute for Nutritional Medicine, University of Lübeck) who analyzed all tissue samples according to Erben et al. (Erben et al., 2014) and scored them for inflammatory cell infiltration and tissue damage. Both scores can range from 0 (no tissue destruction or cell infiltration) to 3 (massive tissue destruction and cell infiltration) resulting in a total score ranging from 0 to 6.

The scoring results from the ileum clearly indicated that C5aR2^{-/-} mice are protected from developing severe inflammation during the early phase of *T. gondii* infection (**Figure 19**). The score of C5aR2^{-/-} (1.3) was much lower than the score of C5aR1^{-/-} (3.6) or WT (4) mice.

In jejunum sections, WT and C5aR2^{-/-} mice showed an average score of 1.6 and 2, respectively and were protected from developing severe inflammation, whereas C5aR1^{-/-} mice showed a higher score reaching an average of 4.3, confirming the observed tissue destruction and massive cell infiltration (**Figure 19**).

The restriction in C5aR1^{-/-} and C5aR2^{-/-} mice resulting in only a small sample size did not allow a conclusive statistical evaluation of the data. In future experiments it will be important to increase the number of mice to obtain more robust results.

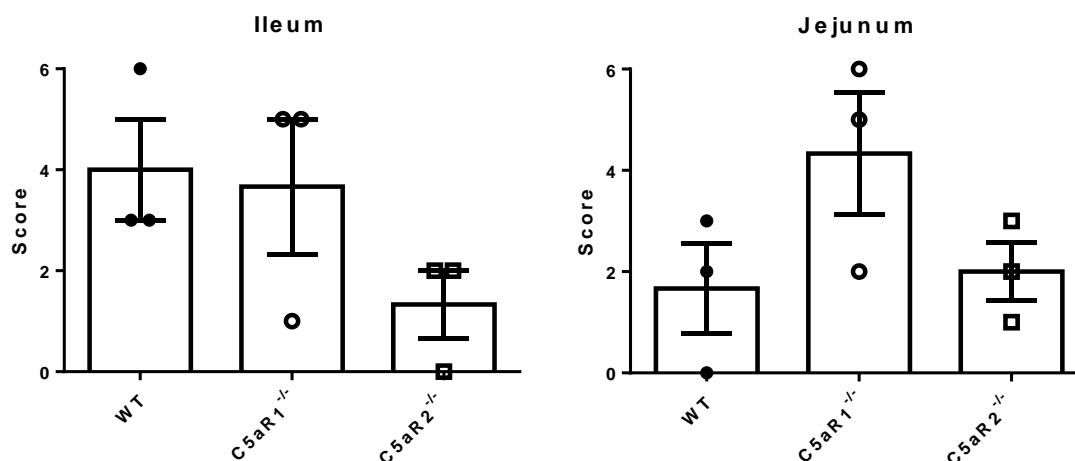


Figure 19: Inflammatory cell infiltration and tissue damage score in WT, C5aR1^{-/-} and C5aR2^{-/-} mice after seven days of oral *T. gondii* infection. Scoring results from paraffin-embedded tissue sections of the ileum (left) and jejunum (right) from orally infected WT, C5aR1^{-/-} and C5aR2^{-/-} mice 7 days p.i. Scoring includes tissue destruction and cell infiltration. Statistical analyses were determined by ANOVA. Values show the mean \pm SEM. n=3/group

3.3 Impact of the parasite infection dose on disease development in the oral *T. gondii* infection model

My previous results showed that the oral infection with 10 cysts resulted in a high mortality as evidenced by the fulfillment of termination criteria such as massive weight loss in all treatment groups (**Figure 18**). In light of this finding, I decided to evaluate the impact of a lower number of cysts on disease development. I conducted a titration experiment with different numbers of cysts and specifically infected them with 1, 3, 5, 7, and 10 cysts. Uninfected WT mice were used as a control. To evaluate the disease progression, I weighed the mice and determined their disease scores every day.

All infected mice started to lose weight after day four p.i. (**Figure 20A**). All mice infected with ≥ 3 cysts reached the threshold of 20 % weight loss and had to be sacrificed before the end of the 15-day experiment (**Figure 20B**). In line with the reduced weight, mice showed strong disease symptoms as indicated by their disease scores (**Figure 20C**). Here, comparable with weight loss, mice infected with higher numbers of *T. gondii* cysts developed a more severe disease score. Mice infected with 10 cysts already showed first symptoms 7 days p.i., whereas mice infected with 3, 5 and 7 cysts started to develop symptoms between days 8 and 9. Mice infected with a minimum of one cyst showed first disease signs between days 10 and 15 and lost a maximum of 15 % of their initial weight. Mice infected with one cyst were able to recover after the initial infection phase with the exception of one mouse, while all mice infected with ≥ 3 cysts died (**Figure 20D**).

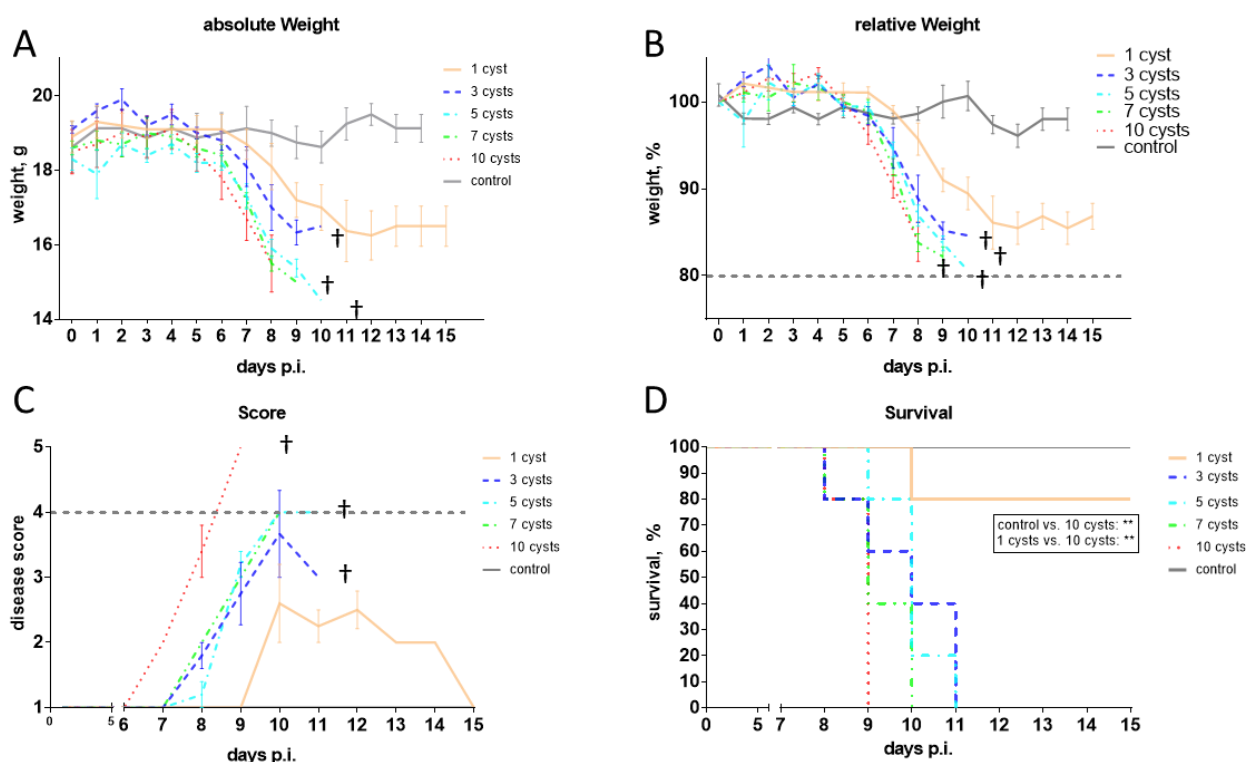


Figure 20: Impact of parasite infection dose on disease development in oral *T. gondii* infection. Oral infection of WT mice with 1, 3, 5, 7, 10 *T. gondii* cysts. Absolute (A) and relative weight (B) over 15 days p.i. (C) Disease score during infection. Groups indicated with † had to be sacrificed due to weight loss of more than 20 % of initial weight or died during the experiment. (D) Animal survival; n=5/group for all graphs. Values show the mean \pm SEM (A-C). Statistical analyses were determined by ANOVA (A-C) and by Log-rank (Mantel Cox) test (D). Groups indicated with † had to be sacrificed due to termination criteria weight loss of more than 20 % of initial weight (dashed line in B) or disease score of ≥ 4 (dashed line in C) or died during the experiment.

IL12-p40 and IFN- γ production during infection

As already described in the introduction, IL-12 and IFN- γ play important roles for the induction of an immune response after *T. gondii* infection (1.4.2). DCs are able to recognize *T. gondii*-derived proteins and start to produce IL-12 and other pro-inflammatory cytokines. IL-12, besides others, is necessary to activate NK cells following the production of IFN- γ to limit the parasite spreading throughout the host. Therefore, I measured serum-levels of IL-12p40 and IFN- γ on day 5 and day 7 p.i. as an indicator for the early immune response.

The results show that IL-12p40 levels raised with increasing parasite load from 2000 pg/ml (1 cyst) up to 6000 pg/ml (10 cysts) and revealed significant differences between the infection with 1 cyst and 10 cysts 5 days p.i. (Figure 21A). IFN- γ levels followed the same trend and showed significant differences, but the concentrations were lower and ranged from 1000 pg/ml (1 cyst) up to 3000 pg/ml

(10 cysts) (**Figure 21B**). Interestingly, analyses from day 7 showed different results, as the IL-12p40 production increased from 6000 pg/ml (1 cyst) up to 10000 pg/ml (5 cysts) and slightly dropped to 8000 pg/ml after the infection with 7 or 10 cysts (**Figure 21C**). On the other hand, the IFN- γ production significantly increased up to 6000 pg/ml (3-10 cysts) compared to 3000 pg/ml (1 cyst) on day 7 p.i. (**Figure 21D**).

The comparison of IL-12p40 and IFN- γ production between day 5 and 7 showed that IL-12p40 levels ranged from 2000 pg/ml (1 cyst) up to 6000 pg/ml (10 cysts) 5 days p.i. (**Figure 22A**). Furthermore, IL-12p40 levels significantly increased between day 5 and 7 in all groups, except for mice infected with 10 cysts, which reached their plateau already after 5 days.

IFN- γ levels significantly increased between day 5 and day 7 after infection in all groups (**Figure 22B**). Interestingly, one cyst was enough to induce a strong IFN- γ response ranging from 1000 pg/ml after 5 days p.i. to 3000 pg/ml after seven days p.i. Noticeable, IFN- γ levels reached a plateau at around 6000 pg/ml after infection with 3 or more cysts 5 days p.i.

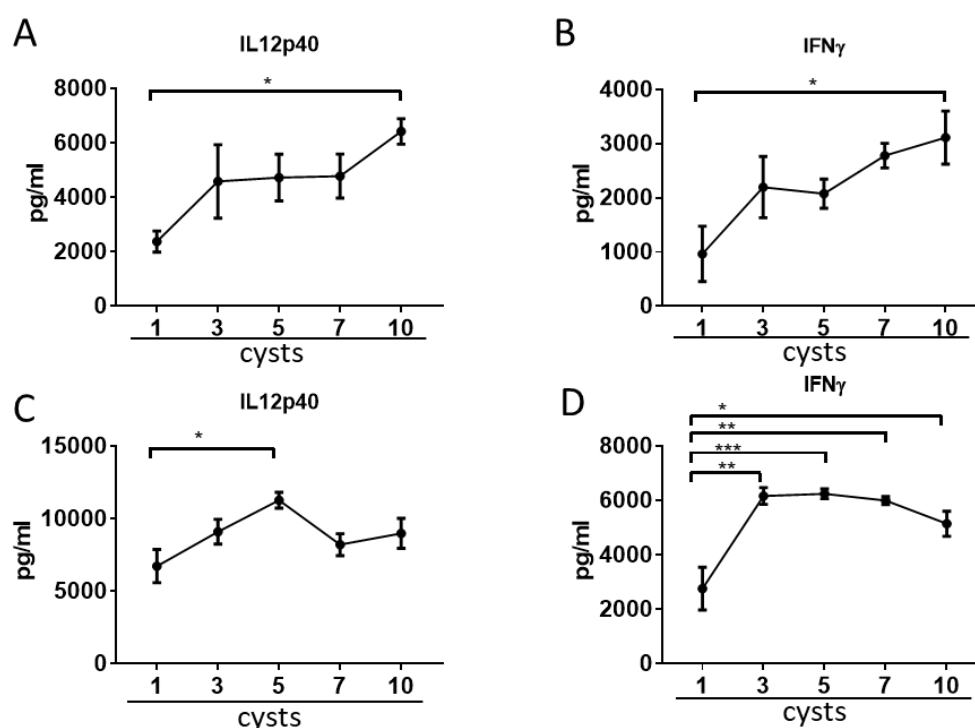


Figure 21: Impact of parasite infection dose on IL-12p40 and IFN- γ production on day 5 (**A, B**) and day 7 (**C, D**) p.i. to compare the cytokine production relative to the parasite infection dose. IL-12p40 (**A**) and IFN- γ (**B**) production significantly increases after the infection with 1 cyst and 10 cysts 5 days p.i. IL-12p40 production (**C**) significantly increases after infection with 5 cysts compared to 1 cyst 7 days p.i., whereas the IFN- γ production (**D**) significantly increases after infection with 3, 5, 7 and 10 cysts compared to the infection with 1 cyst. Cytokine concentrations from uninfected mice were below the detection limit and are not shown. Values show the mean \pm SEM; n=5/group for all graphs. *p<0.05; **p<0.01; ***p<0.001 (ANOVA).

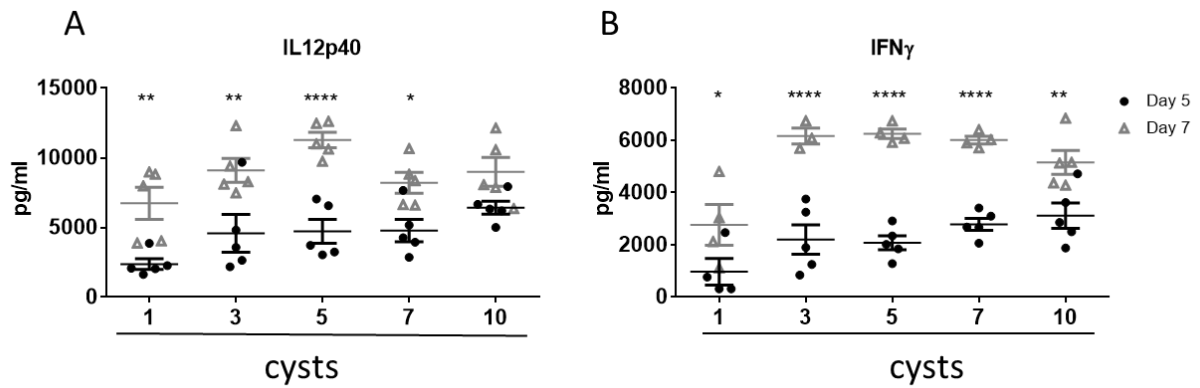


Figure 22: Impact of parasite infection dose on IL-12p40 and IFN- γ production to compare the difference between day 5 and day 7 p.i. Serum cytokine levels for **(A)** IL-12p40 and **(B)** IFN- γ in response to infection using 1, 3, 5, 7, 10 cysts on day 5 and 7 p.i. Values show the mean \pm SEM. n=5/group; asterisks indicate significance between day 5 and day 7; *p<0.05; **p<0.01; ***p<0.001; ****p<0.0001 (ANOVA).

In summary, the results from the oral infection model show that already one cyst is enough to induce a strong immune response characterized by massive weight loss, a high disease score and high IL12p40 and IFN- γ levels 5 and 7 days p.i. Although the oral infection is the natural route of infection with the parasite, my results indicate that this model has a high variability. The reliable administration of only one cyst is technically difficult.

3.4 Assessment of C5aR1/2 expression during acute i.p. *T. gondii* infection using floxed GFP-C5aR1 and floxed tdTomato-C5aR2 mice

The results from the oral infection experiments revealed that infection with already one cyst induced a strong infection characterized by weight loss, the development of a disease score and solid IL-12p40 and IFN- γ levels. Due to the high variability of parasites within one cyst and the difficult preparation and precise application of only one cyst, I decided to use the i.p. infection model to obtain more reliable results. Previous experiments from Daria Briukhovetska (Briukhovetska, 2017) revealed that C5aR1^{-/-} mice suffered from increased susceptibility during i.p. *T. gondii* infections characterized by increased cyst burden in the brain 30 days p.i. as well as increased mortality. Mainly responsible for the altered susceptibility were decreased systemic IL-12 and IFN- γ levels in C5aR1^{-/-} mice in the early phase of the infection.

Recently the Koehl laboratory generated floxed GFP-C5aR1 and floxed tdTomato-C5aR2 knock-in mice to analyze and evaluate the expression of complement receptors C5aR1 and C5aR2, respectively. The mice were already used to characterize C5aR1 and C5aR2 expression in different immune cells isolated from different organs under steady state conditions (Karsten et al., 2015, 2017). My data obtained with the oral infection model and the previous data from Daria Briukhovetska (Briukhovetska, 2017) showed that C5aR1 and C5aR2 exert important roles during *T. gondii* infection. Here, I aimed to use floxed GFP-C5aR1 and floxed tdTomato-C5aR2 mice to evaluate the expression of both receptors under steady state conditions and seven days after i.p. infection with *T. gondii*.

Expression and regulation of C5aR1 on immune cells under steady state and infectious conditions

To define the background signal caused by autofluorescent cells, I used WT mice as controls (**Figure 23A, left panel**). Samples from uninfected and infected GFP-C5aR1^{fl/fl} reporter mice showed for all tissues a clear and distinct GFP-C5aR1 expression. The immune cell population was pre-gated as described in chapter 2.2.7. The comparison of uninfected and infected reporter mice showed that significantly more cells express GFP-C5aR1 in the peritoneal cavity, spleen and lung under infectious conditions (**Figure 23B**). The comparison of uninfected and infected reporter mice in blood showed no significant differences in cell numbers or the frequency of C5aR1⁺ cells (**Figure 23B**). In the peritoneal cavity, GFP-C5aR1 expressing cells significantly increased from 1×10^5 cells (6 %) under steady state conditions to 2.5×10^5 cells (15 %) under infectious conditions. Cells in the spleen also significantly increased GFP-C5aR1 expression under infectious conditions from 1×10^6 cells (2 %) up to 3×10^6 cells (4 %). In the lung, immune cells expressing GFP-C5aR1 increased from 1×10^6 cells (5 %) under steady

state conditions up to 3×10^6 cells (13 %) under infectious conditions (**Figure 23B**). The significant changes in C5aR1 expression were also reflected by the relative increase in C5aR1⁺ cells (**Figure 23C**).

Taken together, these results showed that more cells in the peritoneal cavity, spleen and lung expressed GFP-C5aR1 during an acute *T. gondii* infection. Furthermore, steady state levels of GFP-C5aR1 expression in the blood, peritoneal cavity and lung were comparable in all tissues (3-6 % of all cells were GFP-C5aR1⁺). Under infectious conditions, cells expressing GFP-C5aR1 increased to a different extent.

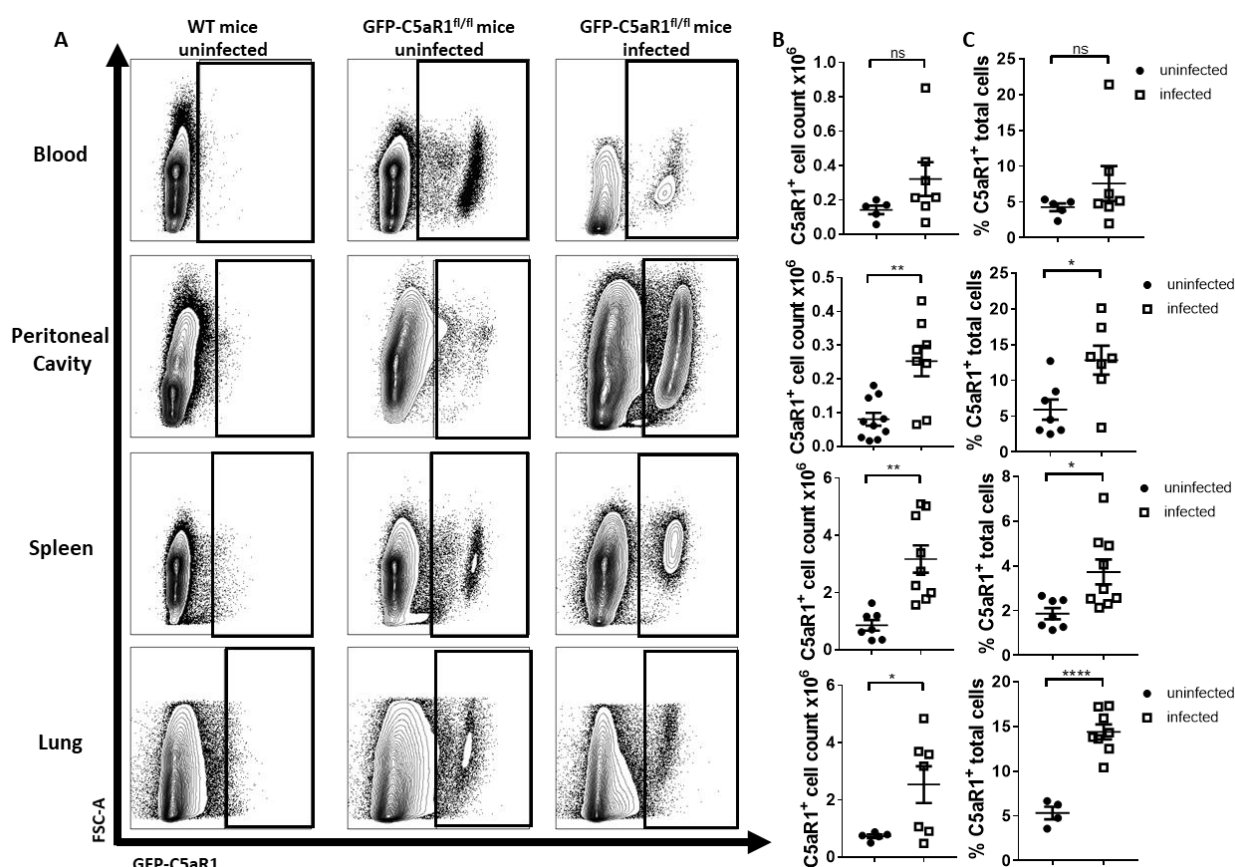


Figure 23: The number and the frequency of GFP-C5aR1⁺ mice is increased in the peritoneal cavity, spleen and lung, but not in blood seven days after peritoneal *T. gondii* infection. GFP-C5aR1^{fl/fl} mice were infected i.p. with 50 *T. gondii* cysts and sacrificed on day 7 p.i. Uninfected WT mice served as controls. **(A)** Flow cytometric analysis of the GFP-C5aR1 signal in cells from blood, peritoneal cavity, spleen and lung. Dot plots depict the GFP-C5aR1 signal in WT, uninfected GFP-C5aR1^{fl/fl} and infected GFP-C5aR1^{fl/fl} mice. **(B)** Cell counts of GFP-C5aR1 positive cells in blood, peritoneal cavity, spleen and lung. **(C)** Graphs show the percentage of GFP-C5aR1 positive cells in blood, peritoneal cavity, spleen and lung. Values show the mean \pm SEM; n = 5-10. Results are from three independent experiments. Statistical differences between groups were assessed by student t test. *p<0.05, **p<0.01, ****p<0.0001

Expression and regulation of C5aR2 on immune cells under steady state and infectious conditions

In addition to C5aR1, C5a is able to bind to C5aR2. In comparison to C5aR1, our knowledge regarding C5aR2 expression and function is less profound. To reduce the gap, I used tdTomato-C5aR2^{fl/fl} mice to analyze the expression of C5aR2 in different tissues under steady state conditions and after peritoneal *T. gondii* infection.

For tdTomato-C5aR2^{fl/fl} reporter mice, I used the same experimental design to define and analyze tdTomato-C5aR2 expressing cells and regulation of this receptor as for GFP-C5aR1. Comparable with the results obtained with GFP-C5aR1^{fl/fl} mice, cells from tdTomato-C5aR2^{fl/fl} mice showed a distinct tdTomato-C5aR2⁺ population in all analyzed compartments under steady state and infectious conditions (**Figure 24A**). Comparing blood cells from uninfected and infected reporter mice revealed that the cell number significantly increased from 0.5×10^6 (10 %) to 1.5×10^6 (40 %) cells (**Figure 24B+C**). In the peritoneal cavity around 2.5×10^5 cells (13 %) showed tdTomato-C5aR2 expression under steady state and infectious conditions. Spleen cells significantly increased tdTomato-C5aR2 expression from 1×10^7 (10 %) to 1.8×10^7 (20 %). The number of tdTomato C5aR2-expressing cells in the lung did not change after infection and was around 1.2×10^6 cells (5 %) (**Figure 24B+C**).

Interestingly, the number of tdTomato-C5aR2⁺ cells in the spleen under steady state and infectious conditions was 10-times higher than the number of GFP-C5aR1⁺ cells.

These results show that more cells in the blood and spleen express tdTomato-C5aR2 in response to i.p. *T. gondii* infection. The cells in the peritoneal cavity and lung did not change their tdTomato-C5aR2 expression pattern under infectious conditions.

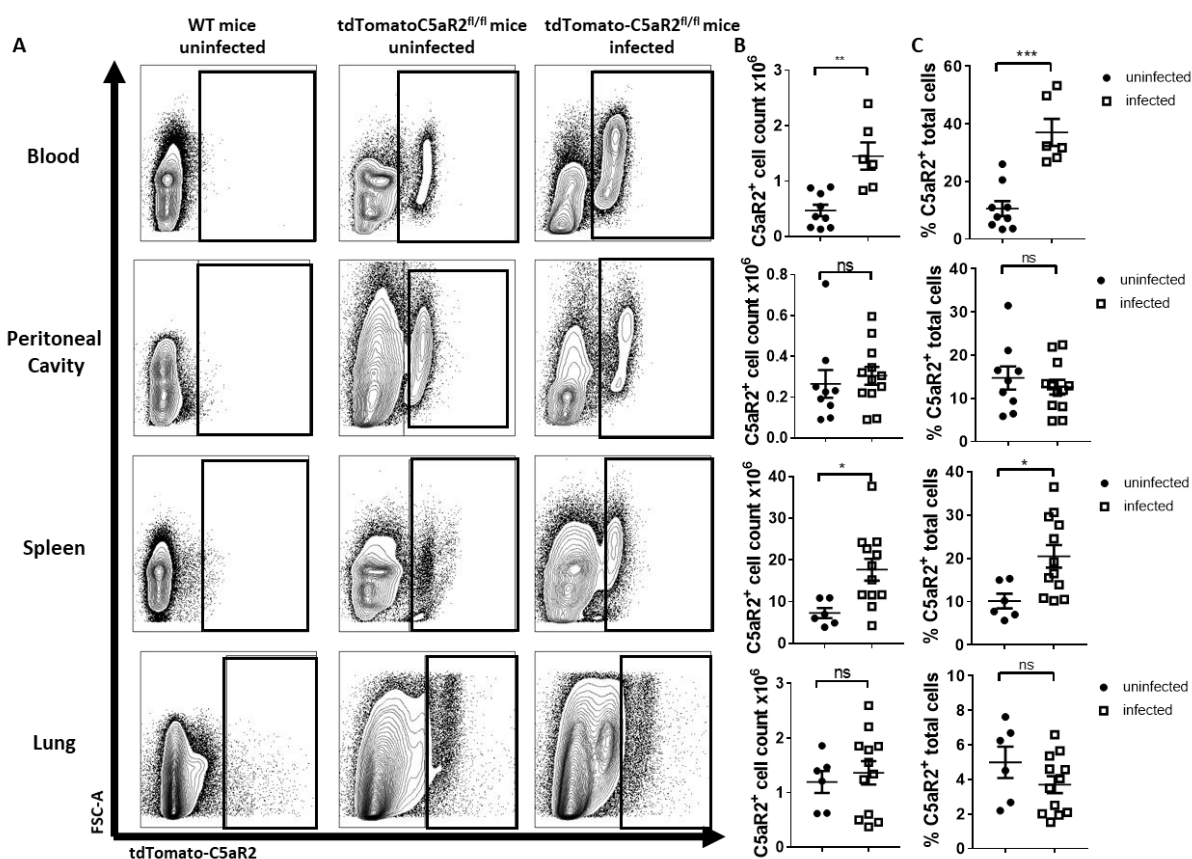


Figure 24: The number and frequency of td-Tomato-C5aR2⁺ cells increased in the blood and the spleen, but not in the peritoneal cavity and the lung after peritoneal *T. gondii* infection. Td-Tomato-C5aR2^{fl/fl} mice infected i.p. with 50 *T. gondii* cysts and sacrificed on day 7 p.i. Uninfected WT mice served as controls. **(A)** Flow cytometric analysis of the tdTomato-C5aR2 signal in cells from blood, peritoneal cavity, spleen and lung. Dot plots depict the tdTomato-C5aR2 signal in WT, uninfected tdTomato-C5aR2^{fl/fl} and infected tdTomato-C5aR2^{fl/fl} mice. **(B)** Cell counts of tdTomato-C5aR2-positive cells in blood, peritoneal cavity, spleen and lung. **(C)** Frequency of tdTomato-C5aR2-positive cells in blood, peritoneal cavity, spleen and lung as measured by flow cytometry. Values show the mean \pm SEM; n = 5-10. Results are from three independent experiments. Statistical differences between groups were assessed by students t-test; *p<0.05, **p<0.01, ***p<0.001

GFP-C5aR1 and tdTomato-C5aR2 are not always regulated in a similar manner in blood, spleen and lung

Since the discovery of C5aR2 in 2000, several reports have shown that C5aR2 is co-expressed and co-regulated with C5aR1 (Bamberg et al., 2010; Gerard et al., 2005). Further, it has been shown that C5aR2 can function independent of C5aR1, or even counter-act C5aR1 signaling (Huber-Lang et al., 2005; Xu et al., 2016). Therefore, and after analyzing the two receptors independently from each other (**Figure 23** and **Figure 24**), I aimed to analyze the regulation of both receptors in relation to each other.

Using the two reporter mice, I found that C5aR1 and C5aR2 are differentially expressed during *T. gondii* infection. In blood, a higher frequency of cells expressed tdTomato-C5aR2 under infectious conditions, while no change in GFP-C5aR1 expression was detectable (**Figure 25A**). This trend is also reflected by cell numbers (**Figure 26A**). In the peritoneal cavity, the frequencies (**Figure 25B**) and numbers (**Figure**

26B) of GFP-C5aR1⁺ and tdTomato-C5aR2⁺ cells were similar under infectious conditions. In contrast, I found a higher frequency of cells expressing tdTomato-C5aR2 under steady state conditions. The results from the spleen showed that a higher frequency (**Figure 25C**) and a higher number of cells (**Figure 26C**) expressed tdTomato-C5aR2 under steady state conditions. Even more cells expressed tdTomato-C5aR2 under infectious conditions. Frequencies from lung cells showed significant differences between GFP-C5aR1⁺ and tdTomato-C5aR2⁺ cells, as the frequency for GFP-C5aR1⁺ cells was 3-times higher under infectious conditions (**Figure 25D**) than that of tdTomato-C5aR2⁺ cells. I found a similar trend regarding the cell numbers (**Figure 26D**).

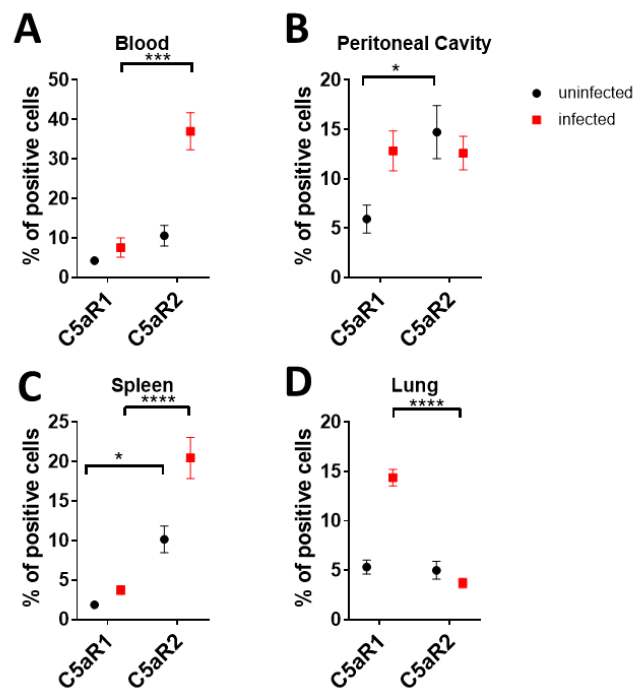


Figure 25: Frequency of GFP-C5aR1 and tdTomato-C5aR2-expressing cells in different tissues under steady state conditions and infectious conditions are regulated differently. Frequencies of C5aR1-GFP⁺ and C5aR2-tdTomato⁺ cells in **(A)** blood, **(B)** peritoneal cavity, **(C)** spleen and **(D)** lung in samples from uninfected (black) or infected (red) mice. Values show the mean \pm SEM. n=5-11. Results are from three independent experiments. Statistical differences between groups were assessed by ANOVA. ***p<0.001; ****p<0.0001.

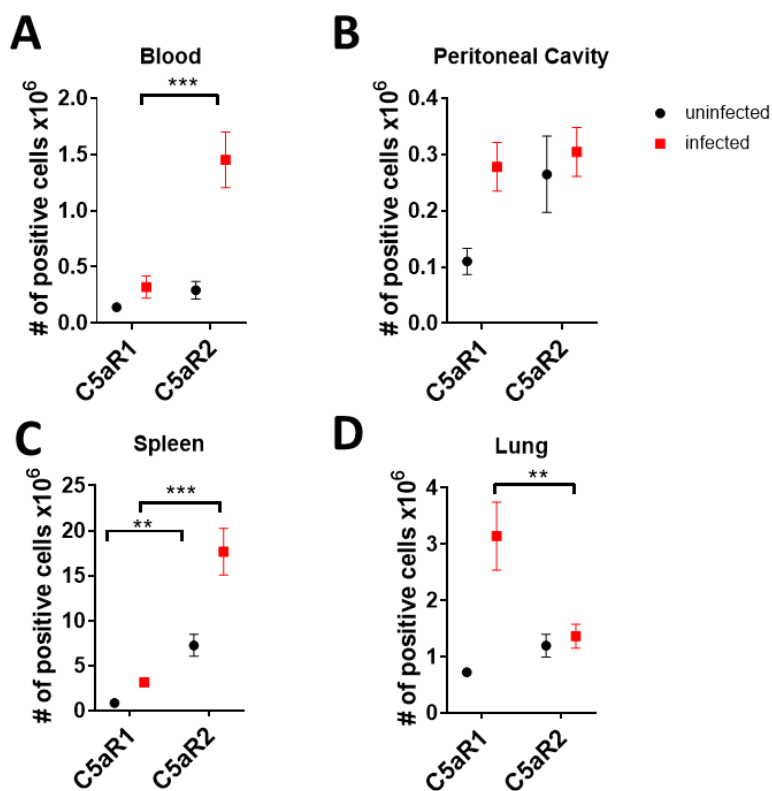


Figure 26: Cell numbers of GFP-C5aR1 and tdTomato-C5aR2-expressing cells in different tissues under steady state conditions and infectious conditions also regulated differently. Cell numbers of C5aR1-GFP⁺ and C5aR2-tdTomato⁺ cells in (A) blood, (B) peritoneal cavity, (C) spleen and (D) lung in samples from uninfected (black) or infected (red) mice. Values show the mean \pm SEM. n=5-11. Results are from three independent experiments. Statistical differences between groups were assessed by ANOVA. ***p<0.001;

In the next set of experiments, I determined the expression of C5aR1 and C5aR2 in different immune cells including NK cells, neutrophils, inflammatory monocytes, cDCs and eosinophils using flow cytometry.

Regulation of C5aR1 and C5aR2 expression on natural killer cells

NK cells are one of the most important innate immune cell population during early *T. gondii* infections. As the main producer of IFN- γ , NK cells play a crucial role in controlling the spreading of the parasite by activation of other innate immune cells (Denkers et al., 1993). IFN- γ production from NK cells is dependent on DC-derived cytokines like IL-12, IL-15 or IL-18 (Une et al., 2003). Additionally, NK cells

regulate the immune response during *T. gondii* infection by producing anti-inflammatory cytokines like IL-10 (Gigley, 2016).

For flow cytometric analysis, NK cells were identified as NK1.1⁺ NKp46⁺ cells (**Figure 27A**). Under naïve conditions, the blood, spleen and lung are the tissues with the highest frequency of NK cells with around 3 % of total cells, followed by the peritoneal cavity with around 1 % of total cells (**Figure 27B**). Most NK cells reside in the spleen ($\sim 20 \times 10^5$ cells), followed by the lung (4×10^5 cells), the blood (1×10^5 cells) and the peritoneal cavity (0.2×10^5 cells) (**Figure 27C**). Under infectious conditions NK cell frequencies dropped in blood, spleen and lung and increased in the peritoneal cavity, which is the first compartment to encounter the parasite during the infection (**Figure 27B**). Similar to the cell frequencies, cell numbers decreased in the peritoneal cavity and the spleen. In contrast, I observed no drop of cell numbers in blood and lung (**Figure 27C**). As shown in **Figure 27D+E**, NK cells did not express GFP-C5aR1 in any of the examined organs. In contrast, NK cells showed a clear and comparable signal of tdTomato-C5aR2 expression under steady state and infectious conditions (**Figure 27D+F**). In the blood, around 2 % of cells from non-infected and 5 % from infected mice and in the lung around 2 % cells from non-infected and 3% of infected mice were tdTomato-C5aR2⁺. Twelve percent of naïve NK cells in the peritoneal cavity were tdTomato-C5aR2⁺ and around 10 % of NK cells under infectious conditions. Thus, the peritoneal cavity was the compartment with the highest frequency of tdTomato-C5aR2⁺ NK cells. NK cells from the spleen also expressed tdTomato-C5aR2. Here, 7 % of cells from non-infected and around 10 % of cells from infected mice were tdTomato-C5aR2⁺. The frequencies for tdTomato-C5aR2-expressing NK cells did not change between steady state and infectious conditions in all tissues. Interestingly, the total number of NK cells, which express tdTomato-C5aR2 in the spleen, dropped significantly under infectious conditions (**Figure 27H**).

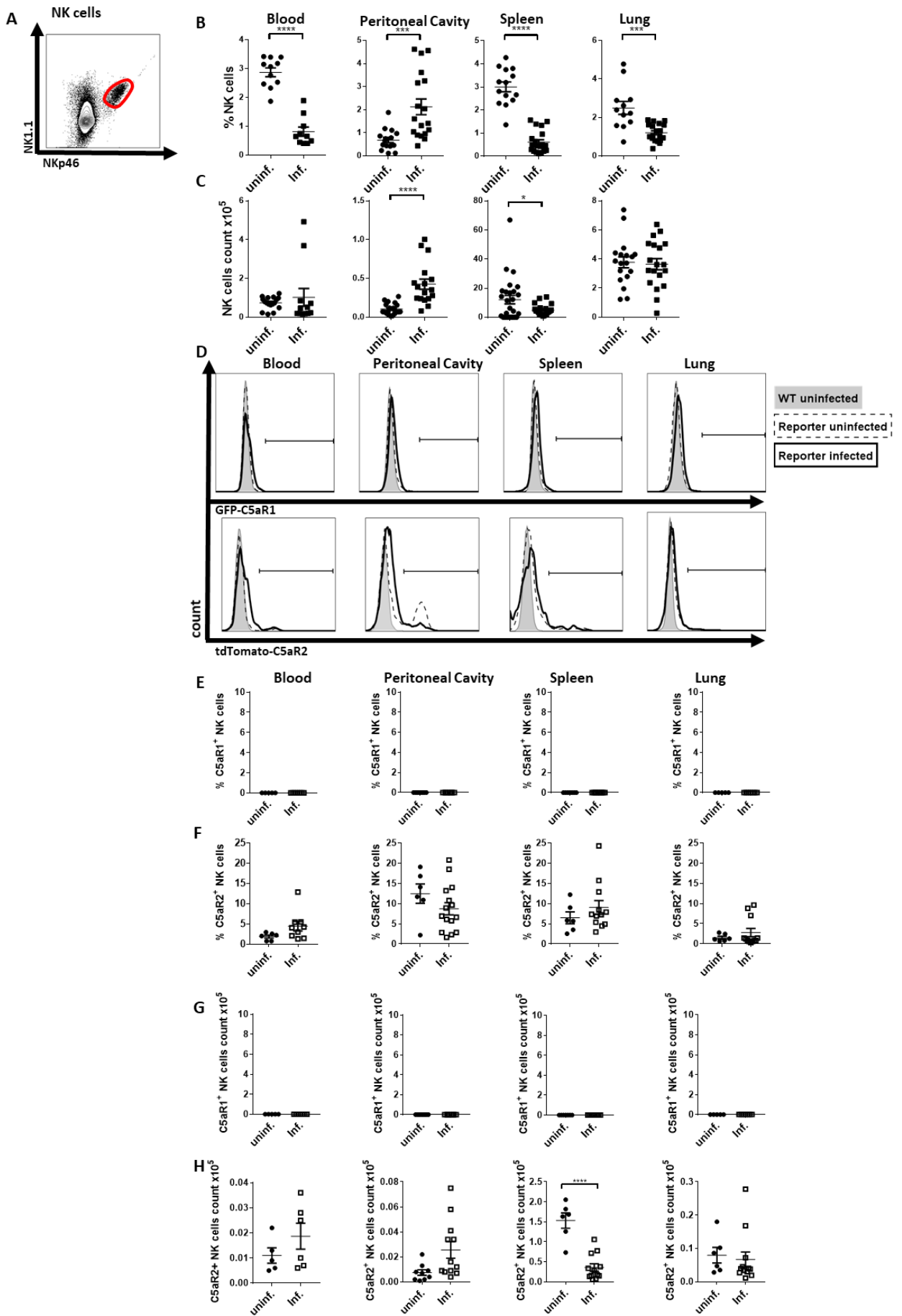


Figure 27: NK cells from blood, peritoneal cavity, spleen and lung express tdTomato-C5aR2, but not GFP-C5aR1 under steady state conditions and seven days after i.p. infection with *T. gondii*. **(A)** NK cells were identified as NK1.1⁺NKp46⁺ cells. Depicted is the dot plot from an uninfected spleen sample. Frequencies **(B)** and cell counts **(C)** of NK cells in non-infected and infected reporter mice shown as percentage of living cells. **(D)** Flow cytometric analysis of GFP-C5aR1 (upper histograms) and tdTomato-C5aR2 (lower histograms) expression in NK cells from blood, peritoneal cavity, spleen and lung of non-infected WT mice (gray histograms), non-infected (dashed line) and infected (solid line) C5aR1/2 reporter mice. **(E-F)** Frequencies of GFP-C5aR1⁺ and tdTomato-C5aR2⁺ NK cells in blood, peritoneal cavity, spleen and lung under steady state conditions and upon i.p. infection with *T. gondii*. **(G-H)** cell counts of GFP-C5aR1⁺ and tdTomato-C5aR2⁺ NK cells in blood, peritoneal cavity, spleen and lung under steady state conditions and upon i.p. infection with *T. gondii*. Values show the mean \pm SEM; n = 5-14. Results are from three independent experiments. Statistical differences between groups were assessed by student t test. ***p<0.001; ****p<0.0001

Regulation of C5aR1 and C5aR2 expression on macrophages

Macrophages are not only able to phagocytose dead parasites, but can also be infected by living parasites, which can actively invade immune cells (Mordue and Sibley, 1997; Sibley et al., 1985). For flow cytometric analysis, macrophages were identified by expression of the macrophage surface marker F4/80 (Dos Anjos Cassado, 2017) (**Figure 28A**). Under naïve conditions, macrophages were a major cell population in the peritoneal cavity with around 30 % of all cells, while only 4 % in the spleen and 2 % in the lung were identified as macrophages (**Figure 28B**). I found that the spleen was the compartment with the highest number of macrophages (30×10^5) under naïve conditions, followed the peritoneal cavity (4×10^5) and the spleen ($1,5 \times 10^5$) (**Figure 28C**). Under infectious conditions, the frequencies significantly dropped in the peritoneal cavity and lung, while the frequency in the spleen significantly increased (**Figure 28B**). Interestingly, the cell numbers only increased in the spleen, but did not significantly change in the peritoneal cavity or lung during *T. gondii* infection. As visible in the histograms, macrophages from different compartments expressed both C5aRs with different intensities under steady state and infectious conditions (**Figure 28D**).

Between 40 to 80 % of macrophages in the peritoneal cavity, spleen and lung expressed GFP-C5aR1 and tdTomato-C5aR2 under steady state conditions. (**Figure 28G+H**). The histograms showed that, in contrast to the homogeneous expression levels in the spleen, macrophages in the peritoneal cavity and the lung expressed GFP-C5aR1 in a heterogenous manner under steady state conditions (**Figure 28D**). Furthermore, only a slight change in expression occurred after infection. Around 80 % of naïve and 65 % of peritoneal macrophages under infectious conditions were GFP-C5aR1⁺ (**Figure 28G**). The high variance of data and low cell frequency under steady state conditions may also be responsible for the reduced GFP-C5aR1 expression results.

Interestingly, cell numbers for GFP-C5aR1-expressing macrophages dropped significantly (**Figure 28I**). In the spleen, nearly all naïve macrophages expressed GFP-C5aR1, but the frequencies and cell numbers of GFP-C5aR1⁺ cells significantly dropped under infectious conditions (**Figure 28I**). In the lung, the frequency of GFP-C5aR1 expressing macrophages increased from 40 % in uninfected to 55 % in

macrophages from infected mice. In contrast, I observed no change in the number of GFP-C5aR1⁺ cells (**Figure 28I**). Interestingly, the expression of GFP-C5aR1 on macrophages from lung but not from the peritoneal cavity or spleen significantly decreased during *T. gondii* infection (**Figure 28E**).

Furthermore, the overall frequencies and the number of tdTomato-C5aR2-expressing macrophages decreased in spleen and peritoneal cavity. In contrast, frequencies were unchanged whereas cell numbers of tdTomato-C5aR2⁺ macrophages were significantly reduced in the lung (**Figure 28H+J**). The reduced frequencies and numbers of tdTomato-C5aR2⁺ macrophages in the peritoneal cavity and spleen were associated with a significant downregulation of tdTomato-C5aR2 on macrophages found in the two compartments (**Figure 28F**).

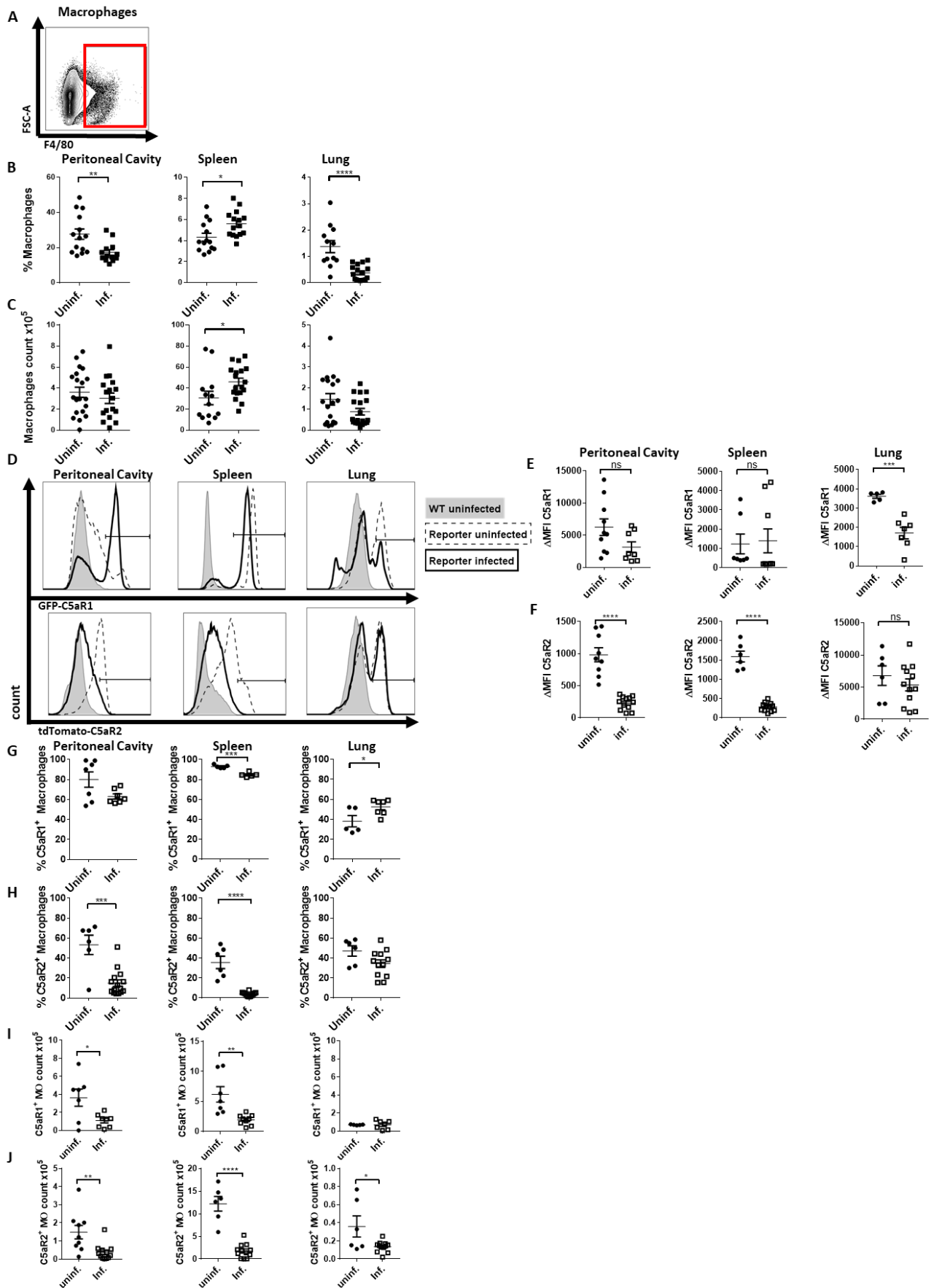


Figure 28: Regulation of GFP-C5aR1 and tdTomato-C5aR2 expression in macrophages is different in the peritoneal cavity, spleen and lung under steady state conditions and seven days after i.p. infection with *T. gondii*. **(A)** Macrophages were identified as F4/80⁺ cells. Depicted is the dot plot from an uninfected spleen sample. Frequencies **(B)** and cell counts **(C)** of F4/80⁺ macrophages in non-infected and infected reporter mice shown as percentage of living cells. **(D)** Flow cytometric analysis of GFP-C5aR1 (upper histograms) and tdTomato-C5aR2 (lower histograms) expression in macrophages from peritoneal cavity, spleen and lung from non-infected WT mice (grey histograms), non-infected (dashed line) and infected (solid line) C5aR1/2 reporter mice. **(E+F)** Δ MFI values for GFP-C5aR1 and tdTomato-C5aR2 expression in macrophages from the peritoneal cavity, spleen and lung under steady state conditions and upon i.p. infection with *T. gondii*. **(G+H)** Frequencies of GFP-C5aR1⁺ and tdTomato-C5aR2⁺ macrophages in peritoneal cavity, spleen and lung under steady state conditions and upon i.p. infection with *T. gondii*. **(I+J)** cell counts of GFP-C5aR1⁺ and tdTomato-C5aR2⁺ macrophages in peritoneal cavity, spleen and lung under steady state conditions and upon i.p. infection with *T. gondii*. Values show the mean \pm SEM; n = 5-14. Results are from three independent experiments. Statistical differences between groups were assessed by student t test. *p<0.05; **p<0.01; ***p<0.001; ****p<0.0001

Regulation of C5aR1 and C5aR2 expression on neutrophils

For flow cytometric analysis, neutrophils were identified as Ly6g⁺ SSC-A^{high} cells (**Figure 29A**). Comparison of neutrophil frequencies showed that less than 10 % of the cells in the blood, spleen or lung were neutrophils under steady state conditions (**Figure 29B**). Neutrophils are normally stored in the bone-marrow and start migrating to the site of infection after activation or recognition of chemoattractants like C5a (Swamydas and Lionakis, 2013). In the peritoneal cavity, no neutrophils could be detected under steady state conditions. Under infectious conditions, around 40 % of the cells in the blood, 15 % of cells in the spleen and lung and 10 % of cells in the peritoneal cavity were neutrophils. This increase in frequencies is associated with an increase in the neutrophil cell count (**Figure 29C**). I found the highest number of neutrophils (around 100×10^5 cells) in the spleen, followed by the lung (40×10^5), the blood (20×10^5) and the peritoneal cavity (3×10^5). As shown in the histograms, neutrophils expressed both C5a receptors under steady state and infectious conditions (**Figure 29D**). Between 80 % and 90 % of neutrophils expressed GFP-C5aR1 in the blood, spleen and lung under steady state conditions (**Figure 29G**). No expression could be determined for neutrophils in the peritoneal cavity due to the absence of neutrophils under steady state conditions. Under infectious conditions between 75 % and 85 % of neutrophils in all compartments expressed GFP-C5aR1. The GFP-C5aR1 expression was significantly reduced in neutrophils located in the blood or the lung but not in neutrophils located in the spleen (**Figure 29E**). The numbers of GFP-C5aR1⁺ neutrophils in the spleen significantly increased (**Figure 29I**). In the blood 95 % of neutrophils expressed tdTomato-C5aR2, while only 60 % to 65 % expressed the receptor in the spleen and lung under steady state conditions (**Figure 29H**). During infection, the expression in the blood dropped to 70 %, while no change was observed in the spleen and lung. In the peritoneal cavity, around 60 % expressed tdTomato-C5aR2 under infectious conditions. From the MFI it was visible, that the tdTomato-C5aR2 expression on neutrophils in the blood and lung, but not in spleen decreased upon infection (**Figure 29F**). Similarly, the frequency of tdTomato-C5aR2 significantly decreased in the blood following infection, while I found no change in

the other compartments. The cell number of tdTomato-C5aR2⁺ neutrophils increased in all compartments (**Figure 29J**).

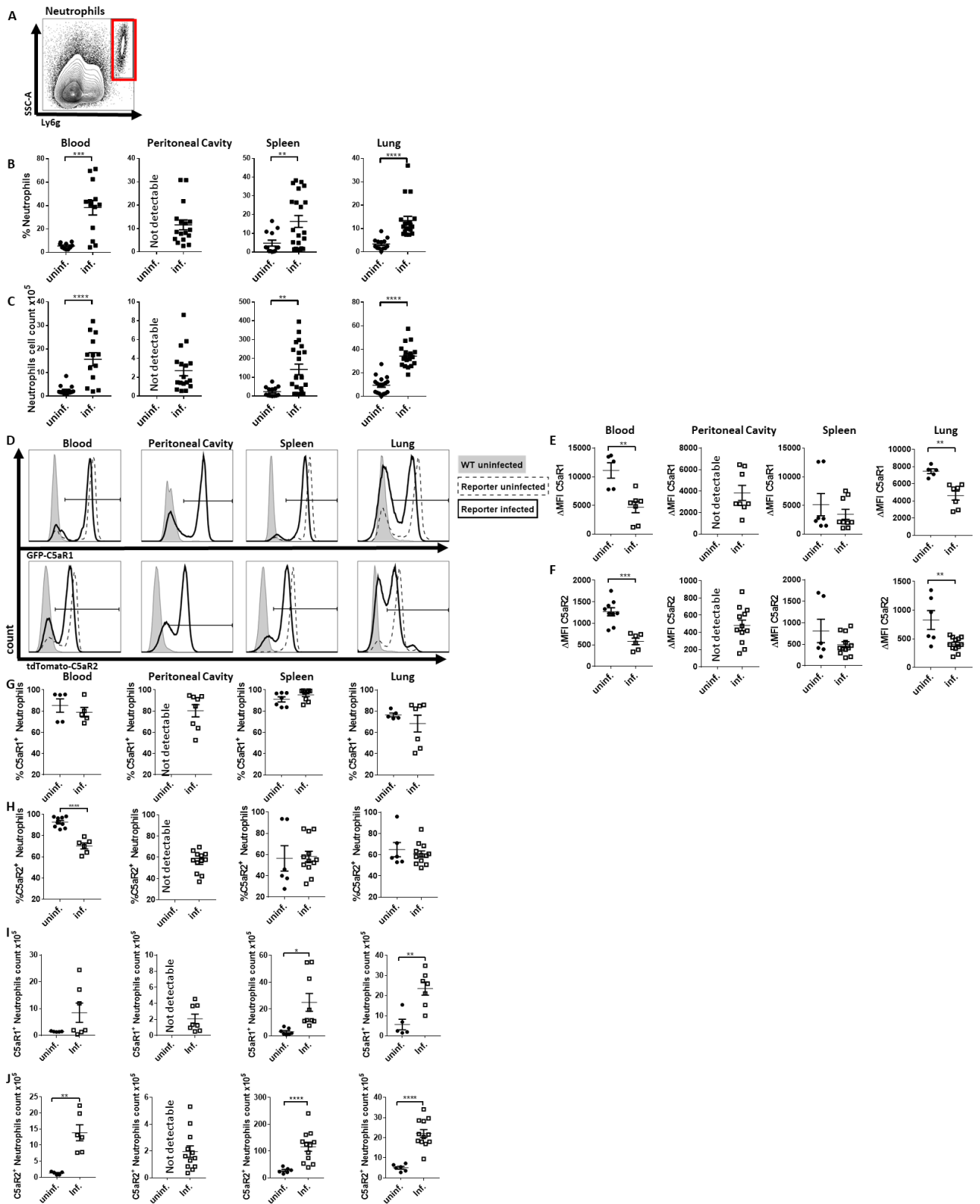


Figure 29: Regulation of GFP-C5aR1 and tdTomato-C5aR2 expression in neutrophils from the blood, peritoneal cavity, spleen and lung under steady state conditions and seven days after i.p. infection with *T. gondii*. (A) Neutrophils were identified as Ly6g⁺ SSC-A^{high} cells. Depicted is the dot plot from an uninfected spleen sample. Frequencies (B) and cell counts (C) of neutrophils in non-infected and infected reporter mice shown as percentage of living cells. (D) GFP-C5aR1 (upper histograms) and tdTomato-C5aR2 (lower histograms) expression in neutrophils from blood, peritoneal cavity, spleen and lung of non-infected WT mice (grey histogram), non-infected (dashed line) and infected (solid line) C5aR1/2 reporter mice. (E+F) \square MFI values for GFP-C5aR1 and tdTomato-C5aR2 in neutrophils from the blood, peritoneal cavity, spleen and lung under steady state conditions and upon i.p. infection with *T. gondii*. (G+H) Frequencies of GFP-C5aR1⁺ and tdTomato-C5aR2⁺ neutrophils in blood, peritoneal cavity, spleen and lung under steady state and upon i.p. infection with *T. gondii*. (I+J) Cell counts of GFP-C5aR1⁺ and tdTomato-C5aR2⁺ neutrophils in blood, peritoneal cavity, spleen and lung under steady state conditions and upon i.p. infection with *T. gondii*. Values show the mean \pm SEM; n = 5-14. Results are from three independent experiments. Statistical differences between groups were assessed by student t test. p<0.05; **p<0.01; ***p<0.001; ****p<0.0001

Regulation of C5aR1 and C5aR2 expression on inflammatory monocytes

During *T. gondii* infections, inflammatory monocytes are recruited to the site of infection through a mechanism that involves the TLR11 and TLR12 ligand profilin (Neal and Knoll, 2014). Mice deficient in inflammatory monocytes or with impaired ability to recruit such cells succumb to death during *T. gondii* infections due to an uncontrolled pro-inflammatory response (Dunay et al., 2010). For flow cytometric analysis, inflammatory monocytes were defined as Ly6G⁻ Ly6C^{high} cells (**Figure 30A**). Under naïve conditions around 10 % of the cells in the blood and spleen and less than 5 % in the peritoneal cavity were inflammatory monocytes (**Figure 30B**). The only significant increase to 25 % during *T. gondii* infection occurred in the peritoneal cavity. The number of GFP-C5aR1⁺ monocytes significantly increased under infectious conditions in the peritoneal cavity and the spleen (**Figure 30C**). Investigating GFP-C5aR1 and tdTomato-C5aR2 expression revealed at best minor expression for GFP-C5aR1, but a solid expression of tdTomato-C5aR2 in the spleen under both conditions. Further, tdTomato-C5aR2 was expressed on a small population of blood monocytes under steady state conditions which was absent following infection (**Figure 30D+F**). A clear increase in frequencies of GFP-C5aR1⁺ and tdTomato-C5aR2⁺ inflammatory monocytes under infectious conditions was detectable in the peritoneal cavity but not in the blood or spleen (**Figure 30E+F**). In contrast, the cell numbers of GFP-C5aR1⁺ or tdTomato-C5aR2⁺ monocytes in the different compartments did not change upon infection (**Figure 30H+I**). Interestingly, up to 20 % of inflammatory monocytes expressed tdTomato-C5aR2 during infection, but only 7 % expressed GFP-C5aR1. The frequency of tdTomato-C5aR2⁺ inflammatory monocytes in the spleen was around 20 %-25 % and did not change in response to infection. Interestingly, the number of tdTomato-C5aR2⁺ inflammatory monocytes increased significantly which was in line with the increased number of total inflammatory monocytes in the spleen (**Figure 30C+I**).

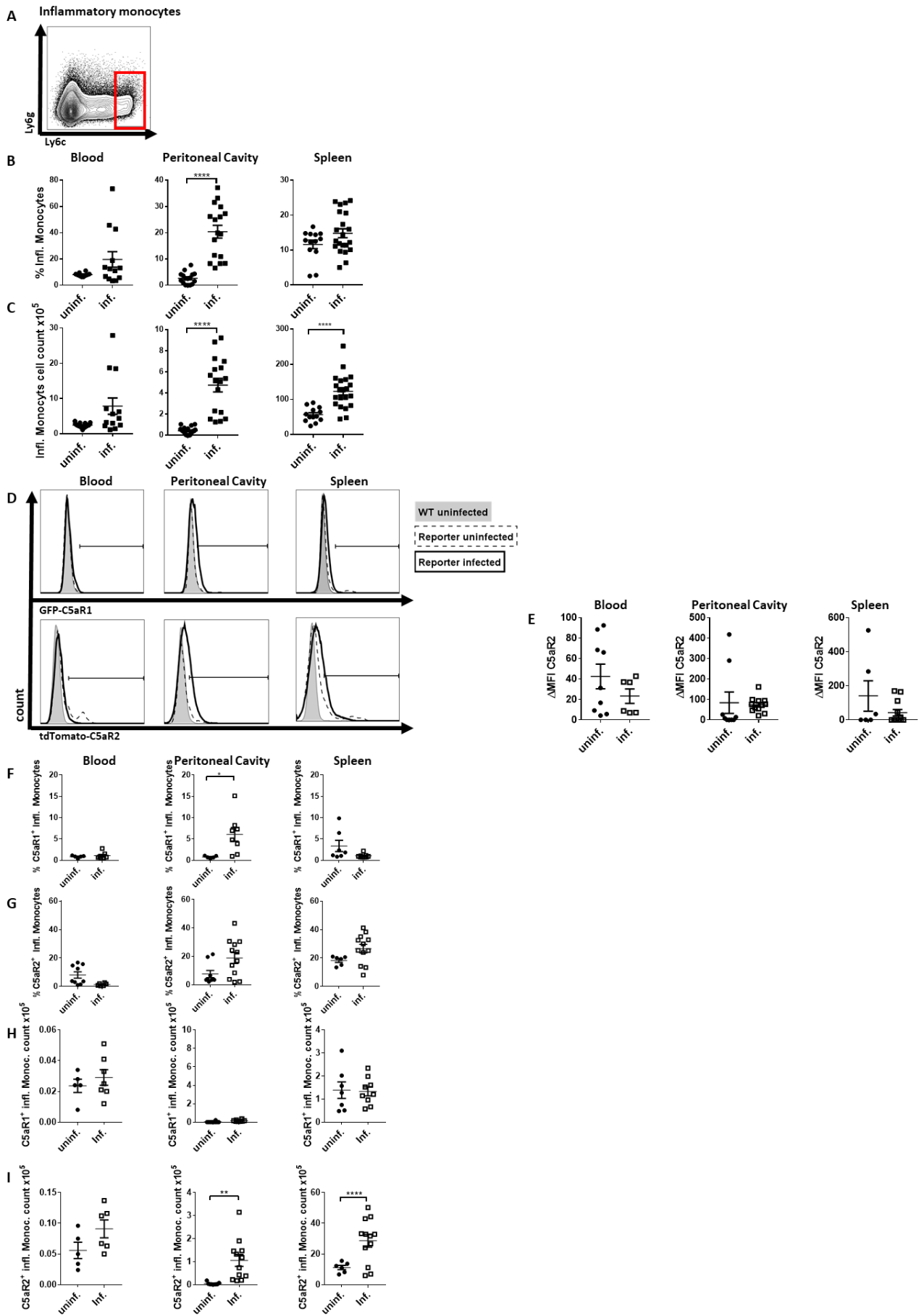


Figure 30: Regulation of GFP-C5aR1 and tdTomato-C5aR2 expression in inflammatory monocytes from the blood, peritoneal cavity and spleen under steady state conditions and seven days after i.p. infection with *T. gondii*. **(A)** Inflammatory monocytes were identified as Ly6g⁺ Ly6c⁺ cells. Depicted is the dot plot from an uninfected spleen sample. Frequencies **(B)** and cell counts **(C)** of inflammatory monocytes in non-infected and infected reporter mice as percentage of living cells. **(D)** Flow cytometric analysis of GFP-C5aR1 (upper histograms) and tdTomato-C5aR2 (lower histograms) expression in inflammatory monocytes from blood, peritoneal cavity and spleen of non-infected WT mice (grey histogram), non-infected (dashed line) and infected (solid line) C5aR1/2 reporter mice. **(E)** Δ MFI values for tdTomato-C5aR2 in inflammatory monocytes from the blood, peritoneal cavity and spleen under steady state conditions and upon i.p. infection with *T. gondii*. **(F+G)** Frequencies of GFP-C5aR1⁺ and tdTomato-C5aR2⁺ inflammatory monocytes in blood, peritoneal cavity and spleen under steady state conditions and upon i.p. infection with *T. gondii*. **(H+I)** Cell counts of GFP-C5aR1⁺ and tdTomato-C5aR2⁺ inflammatory monocytes in blood, peritoneal cavity and spleen under steady state conditions and upon i.p. infection with *T. gondii*. Values show the mean \pm SEM; n = 5-14. Results are from three independent experiments. Statistical differences between groups were assessed by student t test. p<0.05; **p<0.01; ***p<0.001; ****p<0.0001

Regulation of C5aR1 and C5aR2 expression on conventional dendritic cells

During *T. gondii* infections, DCs play important roles, as they are the main producers of IL-12 and therefore responsible for the activation of other immune cells and especially NK cells during the early phase of the infection (Liu et al., 2006).

For flow cytometric analysis, DCs were identified as MHCII^{hi} CD11c⁺ cells (**Figure 31A**). Under naïve conditions, around 1.5 % of cells in the blood, peritoneal cavity and spleen were identified as DCs (**Figure 31B**). Under infectious conditions the frequency and the number of DCs significantly increased in the peritoneal cavity and spleen (**Figure 31B+C**). As shown in the histograms, DCs expressed GFP-C5aR1, but not tdTomato-C5aR2 (**Figure 31D**). The GFP-C5aR1 expression in DCs from the blood, peritoneum or spleen from uninfected and infected mice was similar (**Figure 31E**). The frequencies and numbers of GFP-C5aR1⁺ DCs in the peritoneum (50 %, 1x10⁵ cells) and spleen (10 %, 3x10⁵ cells) increased significantly upon infection (**Figure 31F+G**).

DCs showed no expression of tdTomato-C5aR2 in the different compartments under steady state conditions (**Figure 31D**). Under infectious conditions the expression of tdTomato-C5aR2 increased, at best, minor. The number of tdTomato-C5aR2⁺ DC in the blood and the spleen but not in the peritoneal cavity increased significantly. The significant increase in tdTomato-C5aR2⁺ blood DC numbers was associated with a significant increase in the frequency of tdTomato-C5aR2⁺ blood DCs whereas the frequency of tdTomato-C5aR2⁺ spleen DCs did not change upon infection (**Figure 31G+I**).

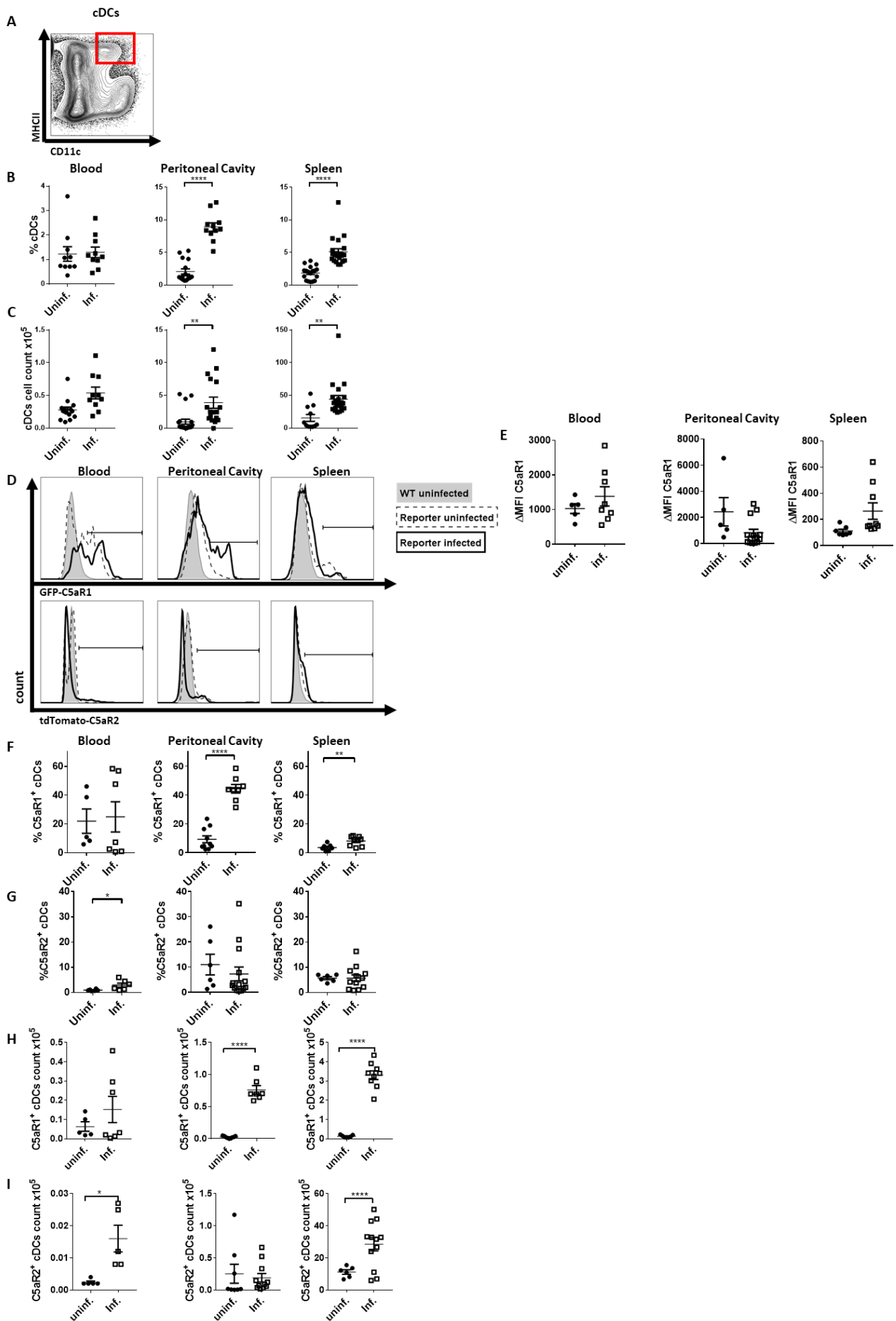


Figure 31: Regulation of GFP-C5aR1 and tdTomato-C5aR2 expression in cDCs from the blood, peritoneal cavity and spleen under steady state conditions and seven days after i.p. infection with *T. gondii*. **(A)** cDCs were identified as MHCI⁺ CD11C⁺ cells. Depicted is the dot plot from an uninfected spleen sample. Frequencies **(B)** and cell counts **(C)** of cDCs in non-infected and infected reporter mice shown as percentage of living cells. **(D)** Flow cytometric analysis of GFP-C5aR1 (upper histograms) and tdTomato-C5aR2 (lower histograms) expression in cDCs from blood, peritoneal cavity and spleen of non-infected WT mice (grey histogram), non-infected (dashed line) and infected (solid line) C5aR1/2 reporter mice. **(E)** Δ MFI values for GFP-C5aR1 in cDCs from the blood, peritoneal cavity and spleen under steady state conditions and upon i.p. infection with *T. gondii*. **(F+G)** Frequencies of GFP-C5aR1⁺ and tdTomato-C5aR2⁺ cDCs in blood, peritoneal cavity and spleen under steady state conditions and upon i.p. infection with *T. gondii*. **(H+I)** Cell counts of GFP-C5aR1⁺ and tdTomato-C5aR2⁺ cDCs in blood, peritoneal cavity and spleen under steady state conditions and upon i.p. infection with *T. gondii*. Values show the mean \pm SEM; n = 5-14. Results are from three independent experiments. Statistical differences between groups were assessed by student t test. p<0.05; **p<0.01; ***p<0.001; ****p<0.0001

Regulation of C5aR1 and C5aR2 expression on eosinophils

Previous findings suggest that eosinophils control *T. gondii* infections mainly in the lung (Fenoy et al., 2009). Therefore, I only analyzed GFP-C5aR1 and tdTomato-C5aR2 expression on eosinophils from the lung.

For flow cytometric analysis, eosinophils in the lung were defined as Siglec-F⁺ CD11c⁻ cells (**Figure 32A**). The frequencies of eosinophils in the lung were low under steady state conditions and further decreased under infectious conditions (**Figure 32B**). The number of lung eosinophils did not change upon infection (**Figure 32C**).

As shown in **Figure 32D**, eosinophils expressed both C5a receptors under both conditions. The expression intensity was similar on eosinophils from non-infected and infected mice as shown by the MFI (**Figure 32E+F**). The comparison of the frequencies and cell numbers of GFP-C5aR1⁺ or tdTomato-C5aR2⁺ eosinophils in the pulmonary compartment showed no differences between steady state or infectious conditions (**Figure 32G-J**).

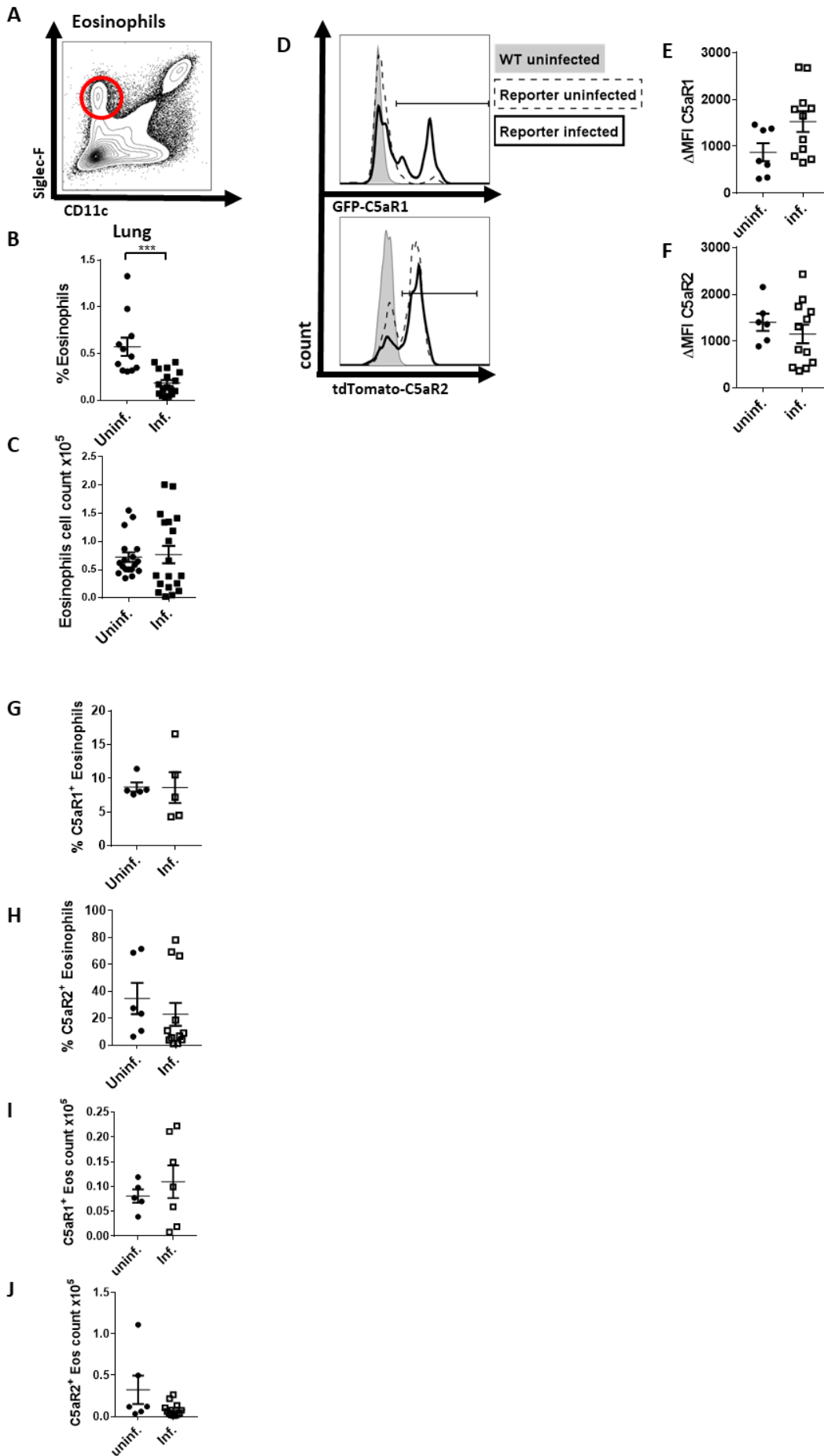


Figure 32: Regulation of GFP-C5aR1 and tdTomato-C5aR2 expression in eosinophils from the lung C5aR1 under steady state conditions and seven days after i.p. infection with *T. gondii*. **(A)** eosinophils were identified as Siglec-F⁺ CD11c⁻ cells. Depicted is the dot plot from an uninfected lung sample. Frequencies **(B)** and cell counts **(C)** of eosinophils in non-infected and infected reporter mice as percentage of living cells. **(D)** Flow cytometric analysis of GFP-C5aR1 (upper histograms) and tdTomato-C5aR2 (lower histograms) expression in eosinophils from the lung of non-infected WT mice (grey histogram), non-infected (dashed line) and infected (solid line) C5aR1/2 reporter mice. **(E+F)** Δ MFI values for GFP-C5aR1 and tdTomato-C5aR2 in eosinophils from the lung under steady state conditions and upon i.p. infection with *T. gondii*. **(G+H)** Frequencies of GFP-C5aR1⁺ and tdTomato-C5aR2⁺ eosinophils in the lung under steady state conditions and upon i.p. infection with *T. gondii*. **(I+J)** Cell counts of GFP-C5aR1⁺ and tdTomato-C5aR2⁺ eosinophils in the lung under steady state conditions and upon i.p. infection with *T. gondii*. Values show the mean \pm SEM; n = 5-14. Results are from three independent experiments. Statistical differences between groups were assessed by student t test. ***p<0.001

3.5 Functional roles of C5aR2 on NK cells and DCs

3.5.1 Frequencies and cell numbers of DCs and NK cells of WT, C5aR1^{-/-} and C5aR2^{-/-} mice in the spleen

The results obtained from the reporter mice showed that NK cells express tdTomato-C5aR2, but not GFP-C5aR1. The exclusive expression of C5aR2 in NK cells makes them a suitable cell population to investigate the function and potential consequences of the absence of C5aR2.

Splenic DCs are important and indispensable for activation of NK cells. The formation of a stimulatory synapse between DCs and NK cells with cell-cell contact is the basis for a strong NK cell-driven immune response (Borg et al., 2004). In response to stimulatory synapse formation, DCs produce IL-12, IL-15 and IL-18 and deliver these cytokines directly to the NK cells subsequently leading to IFN- γ production.

To determine whether WT, C5aR1^{-/-} and C5aR2^{-/-} DCs or NK cell numbers and frequencies differ in the spleen, I performed flow cytometric analyses. Interestingly, the frequency of cDCs in C5aR2^{-/-} was significantly lower compared to WT mice (**Figure 33A**). Further, the number of cDCs in C5aR2^{-/-} mice was, in trend, lower than in WT mice. Also, the frequencies of NK cells were reduced in C5aR1^{-/-} and C5aR2^{-/-} mice compared to WT mice. This reduction was not reflected by the cell counts (**Figure 33B**), which might be due to the small sample size.

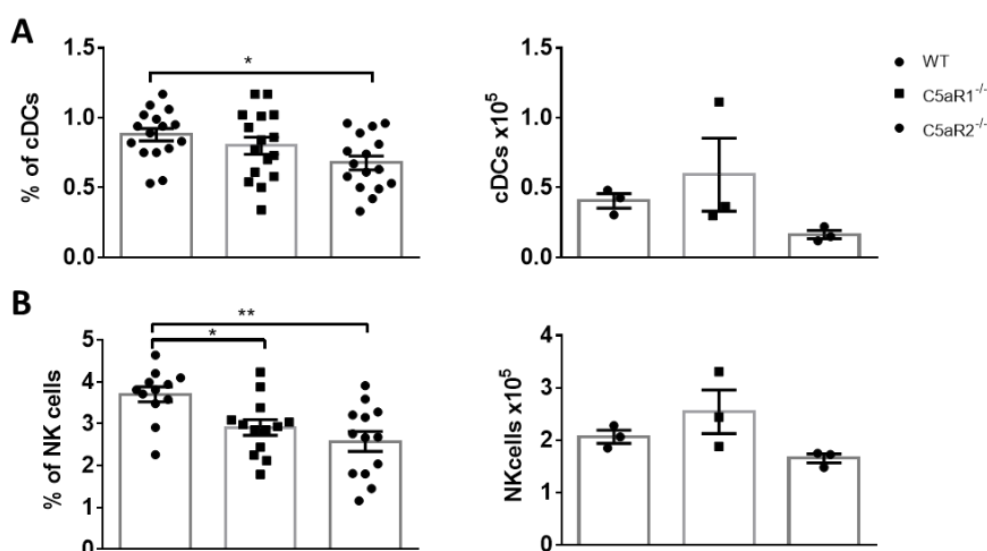


Figure 33: Impact of C5aR1 or C5aR2 deficiency on the relative and absolute cell numbers of cDCs and NK cells in the spleen. **(A)** cDC and **(B)** NK cell frequencies (left) and cell numbers (right) in the spleen of WT, C5aR1^{-/-} and C5aR2^{-/-} mice. Values show the mean \pm SEM. n=3-15. *p<0.05; **p<0.01. Statistical differences between WT, C5aR1^{-/-} and C5aR2^{-/-} were determined by ANOVA.

3.5.2 The C5a/C5aR2 axis controls IFN- γ production from NK cells after IL-12/IL-18 stimulation

To test whether C5aR2 regulates IFN- γ production from NK cells, I purified NK cells from WT and C5aR2^{-/-} mice via FACS and stimulated them with or without IL-12 and IL-18 for 20h at 37°C and 5 % CO₂. After 24h, I collected the supernatant from the NK cell cultures and measured IFN- γ by ELISA. In some experiments, I pre-stimulated the purified NK cells with the specific C5aR2 agonist P32 30 minutes before IL-12/IL-18 stimulation. P32 (Crocker et al., 2016) was kindly provided by Trent Woodruff (The University of Queensland, Australia).

Stimulation of WT NK cells with IL-12 and IL-18 resulted in strong production of IFN- γ (**Figure 34A**). Strikingly, purified NK cells from C5aR2^{-/-} mice produced significantly higher amounts of IFN- γ than NK cells from WT mice under the same stimulatory conditions, suggesting that C5aR2 controls IL12/18-driven IFN- γ production from NK cells. To test whether the C5aR2 is directly involved in the regulation of the production of IFN- γ , I pre-stimulated purified NK cells with the C5aR2-specific agonist P32. The IFN- γ production from NK cells pre-stimulated with the agonist P32 was significantly reduced compared to samples stimulated only with IL-12 and IL-18 (**Figure 34B**). This effect was not visible in C5aR2^{-/-} NK cells.

Taken together, the results suggest a novel and important regulatory function for C5aR2 in NK cells, as specific C5aR2 activation suppresses IL-12/IL-18-driven IFN- γ production in NK cells.

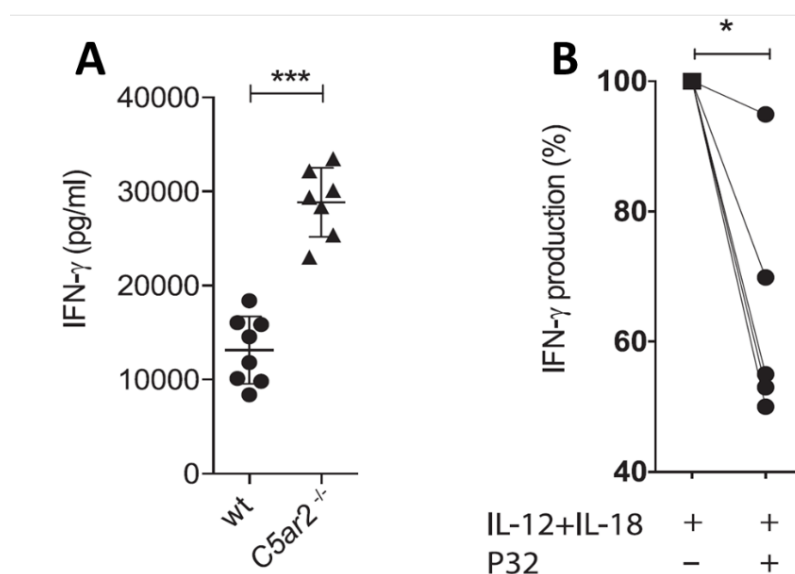


Figure 34: C5aR2 controls IFN- γ produced by NK cells. **(A)** IFN- γ production from sorted splenic NK cells of WT and C5aR2^{-/-} mice 24 h after stimulation with IL-12/IL-18. **(B)** IFN- γ production from sorted WT splenic NK cells 24 h after stimulation with IL-12/IL-18 in the presence or the absence of the C5aR2 agonist P32. Shown is the relative decrease in IL-12/IL-18-mediated IFN- γ production in response to C5aR2 stimulation by the C5aR2 agonist P32. Values show the mean \pm SEM. n=5-7 *p<0.05; ***p<0.001. Data were analyzed using unpaired student t-test (A) or paired student t-test (B).

3.5.3 C5aR2 stimulation results in phosphorylation of p38 mitogen-activated protein kinase

After unveiling the novel role for C5aR2 in controlling the IFN- γ production from NK cells, I aimed to identify intracellular pathways which are involved in the C5aR2 signaling and might mechanistically explain the reduced IFN- γ production after activation of C5aR2. It is well known that p38 is critically involved in IFN- γ production by stabilizing IFN- γ mRNA through IL-18-dependent activation of p38 MAPK (Mavropoulos et al., 2005). Therefore, with the help of Caroline Hennig (undergraduate student at the Institute for Systemic Inflammation Research), we started to investigate p38 phosphorylation levels in WT and C5aR2^{-/-} NK cells after time-dependent C5a stimulation and analyzed the samples via flow cytometry. In WT NK cells, p38 phosphorylation showed a relative increase of around 8 % 2 min after C5a stimulation. The p38 levels dropped below the initial level during the next 8 min (**Figure 35B**). No change in p38 phosphorylation was observed using C5aR2^{-/-} NK cells after C5a stimulation (**Figure 35C**).

Taken together, the results show that p38 MAPK is involved in C5aR2 signaling in response to C5a signaling.

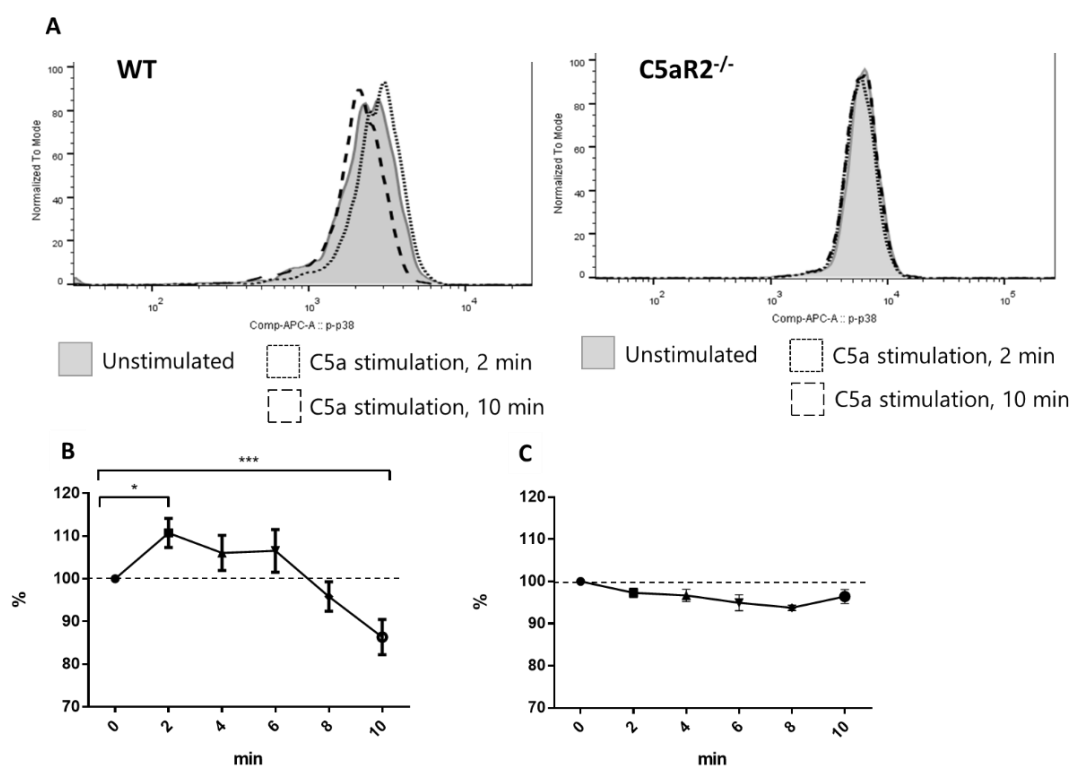


Figure 35: Stimulation of NK cells with C5a results in reduced phosphorylation levels of p38 in WT NK cells within 10 min. **(A)** Histogram data from WT NK cells (left) and C5aR2^{-/-} NK cells (right) unstimulated (grey histograms), after 2 min C5a stimulation (dashed lines) and after 10 min C5a stimulation (bold dashed lines). Relative change of phosphorylated p38 in unstimulated or C5a-stimulated purified NK cells from **(B)** WT or **(C)** C5aR2^{-/-} mice. Values show the mean \pm SEM. n=6; *p<0.05; ***p<0.001 (ANOVA)

3.5.4 C5aR2^{-/-} NK cells show elevated NKp46 expression compared to WT NK cells

To test whether the absence of C5aR2 expression on NK cells influences the expression of other cell surface receptors, I investigated the expression of the NK cell receptors NK1.1 and NKp46. An important function of NKp46 is to recognize the hemagglutinin proteins of influenza viruses (Draghi et al., 2007) or poxviruses (Jarahian et al., 2011). Furthermore, it can recognize self and tumor ligands, although the identity of these ligands remains mostly unknown (Glasner et al., 2017). Additionally, it has been reported, that the absence of NKp46 on NK cells results in increased IFN- γ production when co-cultured with YAC1 cells (Narni-Mancinelli et al., 2012). Furthermore, NKp46 deficiency leads to significantly increased susceptibility to murine cytomegalovirus infections. The same group also published, that NKp46 is a receptor for complement factor P (properdin). However, binding of properdin to NKp46 leads to activation of different genetic programs and does not induce classical NK cell activation. mRNA sequencing revealed that stimulation of NK cells with anti-NKp46 monoclonal antibodies results in upregulation of *Ifn- γ* and *Ccl3* transcripts, which was not observed after stimulation with properdin (Narni-Mancinelli et al., 2017).

As shown in section 3.5.2, C5aR2^{-/-} NK cells produce significantly more IFN- γ after stimulation with IL-12/IL-18 (**Figure 34**). To investigate whether the increased production is associated with altered NKp46 expression, I prepared single cell suspensions from spleen and peritoneal lavage fluid of WT, C5aR1^{-/-} and C5aR2^{-/-} mice and analyzed NKp46 and NK1.1 expression on NK cells using flow cytometry.

Results from the experiments showed that - compared to WT cells - NKp46 expression is significantly upregulated on NK cells in the spleen and peritoneal cavity of C5aR2^{-/-}, but not of C5aR1^{-/-} mice (**Figure 36**). The expression level for NK1.1 was similar in all three mouse strains (data not shown).

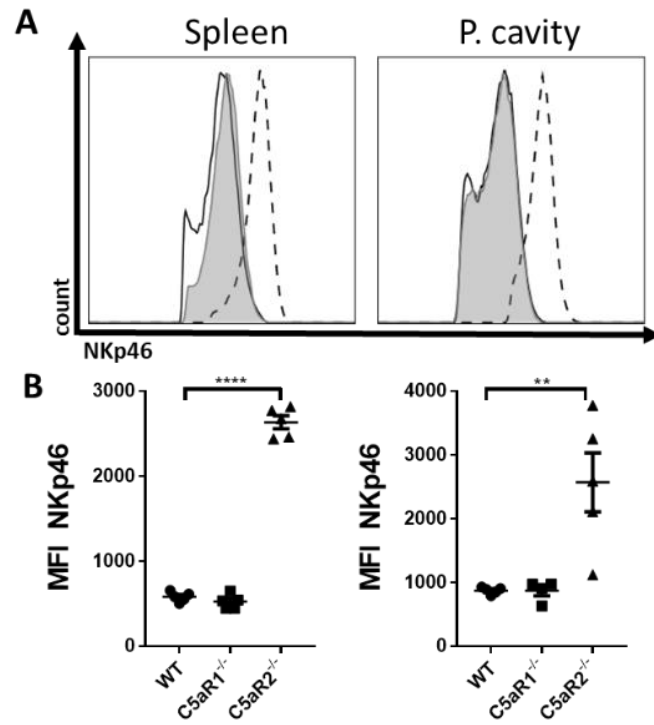


Figure 36: NKp46 expression levels in NK cells from spleen and peritoneal cavity of WT, C5aR1^{-/-} and C5aR2^{-/-} mice. **(A)** NKp46 expression in NK cells from the spleen (left) and peritoneal cavity (right) of WT (grey histograms), C5aR1^{-/-} (solid line) and C5aR2^{-/-} mice (dashed line). **(B)** Shown is the NKp46 expression as mean fluorescence intensity (MFI) on NK cells from WT, C5aR1^{-/-} and C5aR2^{-/-} mice in the spleen (left) and peritoneal cavity (right). Values show the mean \pm SEM. n=5. **p<0.01, ****p<0.0001 (ANOVA)

3.5.5 tdTomato-C5aR2⁺ NK cells express higher numbers of NKp46 receptors than tdTomato-C5aR2⁻ NK cells from the spleen and peritoneal cavity.

To further investigate whether C5aR2 is involved in NKp46 expression, I used the tdTomato-C5aR2 reporter mice and checked whether I can link NKp46 expression to C5aR2 expression. Interestingly, I found higher NKp46 expression in tdTomato-C5aR2⁺ NK cells as compared to tdTomato-C5aR2⁻ NK cells in the spleen (**Figure 37C**) and peritoneal cavity (**Figure 37B**), but not in the blood (**Figure 37A**).

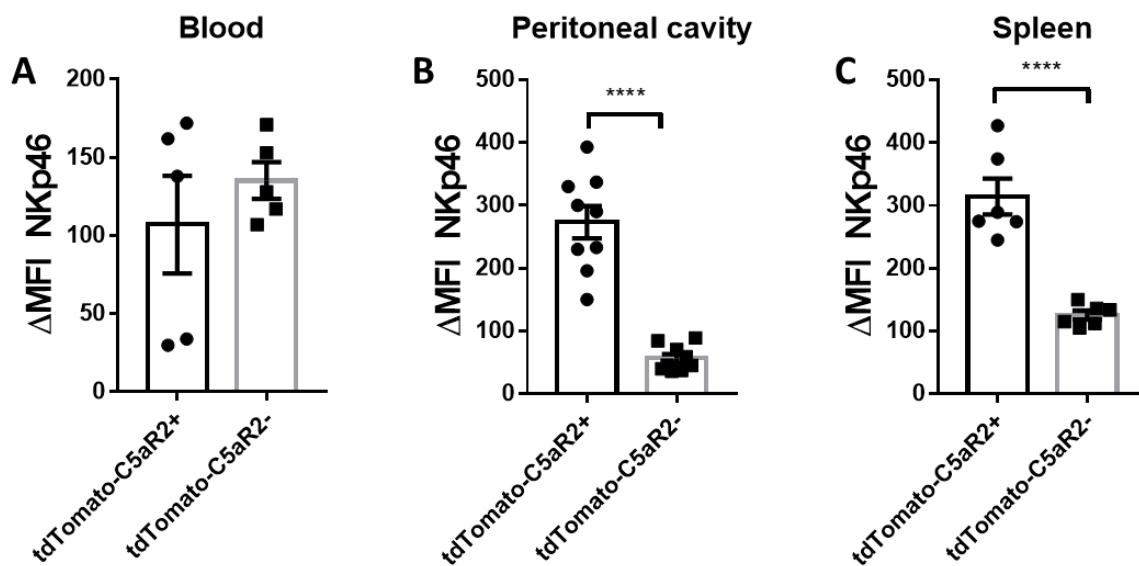


Figure 37: NKp46 expression is higher in tdTomato-C5aR2⁺ NK cells than in tdTomato-C5aR2⁻ NK cells from spleen and peritoneal cavity, but not in the blood. Shown is the Δ MFI of NKp46 expression on tdTomato-C5aR2⁺ and tdTomato-C5aR2⁻ NK cells in (A) blood, (B) peritoneal cavity and (C) spleen. Δ MFI = $MFI_{tdTomato-C5aR2} - MFI_{WT}$; Values show the mean \pm SEM. n=5-9. ****p<0.0001 (unpaired student t test)

3.5.6 Increased CD11a and VCAM1 expression in DCs and NK cells from the spleen of C5aR2^{-/-} as compared to WT mice

To establish a stable stimulatory synapse between NK cells and DCs, the expression of co-stimulatory molecules is of major importance. Besides other co-stimulatory molecules, the binding partner VCAM1 and VLA4 as well as LFA-1 and ICAM1 play important roles in this process. VLA4 is expressed on the surface of NK cells and, after NK cell activation, it can bind VCAM1. Besides VCAM1 binding, it is important to drive NK cell infiltration to the site of infection where they can promote inflammatory responses (Gan et al., 2012; Lin and Castro, 1998). VCAM1 is expressed on lymphocytes, monocytes

and eosinophils. It mediates the adhesion of those cells to the vascular endothelium and also functions as a co-stimulatory molecule for stimulatory synapses by binding to VLA4 (Cook-Mills, 2002). LFA-1 is composed of two subunits, CD18 and CD11a and binds ICAM1 (Choi et al., 2008), among other ligands.

To investigate whether NK cells and DCs from WT, C5aR1^{-/-} and C5aR2^{-/-} mice differ in the expression of VCAM1 and VLA4, I analyzed those molecules via flow cytometry together with Lilit Grigoryan (RISE student).

Splenic DCs showed an increased expression for VCAM1 in C5aR2^{-/-} mice when compared to WT DCs, which was associated with a higher frequency of VCAM⁺ DCs in C5aR2^{-/-} mice as compared with WT mice (**Figure 38A, B**). Furthermore, CD11a expression was increased on C5aR1^{-/-} but not on C5aR2^{-/-} DCs when compared to WT DCs (**Figure 38A**). The increased expression of CD11a in DCs from C5aR1^{-/-} was associated with an increased frequency of CD11a⁺ DCs in C5aR1^{-/-} mice as compared with WT mice. Of note, the frequency of CD11a⁺ DCs was also higher in C5aR2^{-/-} mice (Figure 38B).

In NK cells I observed only minor regulatory differences in VCAM1 and CD11a expression. The expression of VCAM1 was significantly upregulated on C5aR2^{-/-} NK cells when compared to NK cells from WT mice (**Figure 38C**). CD11a expression was similar in NK cells from all mouse strains. The cell frequencies did not show any difference for VCAM1 and CD11a when comparing NK cells from the three strains (**Figure 38D**).

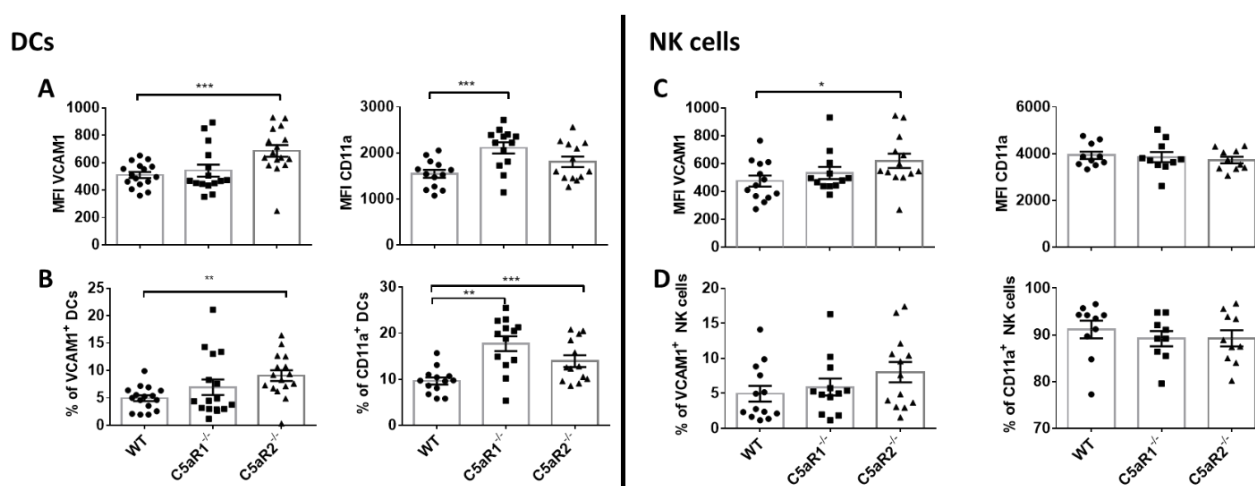


Figure 38: VCAM1 and CD11a expression in DCs and NK cells and frequencies of VCAM1⁺ or CD11a⁺ DCs or NK cells in WT, C5aR1^{-/-} and C5aR2^{-/-} mice. Shown is the MFI (**A, C**) or frequency (**B, D**) of DCs (**A, B**) or NK cells (**C, D**). Values show the mean \pm SEM. $n \geq 13-16$; * $p < 0.05$; ** $p < 0.01$; *** $p < 0.001$ (ANOVA)

3.6 $Gab3^{R27C}$ mice suffer from increased susceptibility and cyst burden during *T. gondii* infection

In addition to the important role of C5aR2 for NK cell function during *T. gondii* infections, I focused on another molecule called Gab3, which was found to be highly expressed on NK cells and therefore potentially exerts important roles in controlling *T. gondii* infection.

Gab3 belongs to the Grb-2-associated binder (Gab) protein family and works as a docking and scaffolding protein. In contrast to Gab1 and Gab2, relatively little is known about the function and possible intracellular interaction partners of Gab3. Interestingly, the Hoebe lab in Cincinnati found that NK cells express Gab3. The Hoebe lab induced a point mutation in the *gab3* gene by ENU mutagenesis. Using this mouse strain allowed me to investigate whether the mutation affects the ability of the innate and adaptive immune system to control *T. gondii* infections in the acute and chronic phase.

I infected female $Gab3^{R27C}$ and WT mice with 50 cysts of *T. gondii* ME49 i.p. I recorded the weight and health condition daily for 30 days. Relative weight loss was comparable between the two groups. Both strains lost up to 15 % of their initial weight during the acute phase of the infection until day 12 (**Figure 39A**). After initial recovery between day 12 and 16 p.i. all mice started losing weight until day 22 p.i. At the end of the experiment both groups ended up with 85 % of the initial weight. Although WT and $Gab3^{R27C}$ mice did not differ in weight loss, $Gab3^{R27C}$ were more susceptible to infection as shown by lower survival rates between days 22 and 30 p.i. (**Figure 39C**). Interestingly, both mouse strains behaved similar in the acute phase of the infection, but $Gab3^{R27C}$ mice showed increased susceptibility from day 22 p.i. when the survival rate dropped to 33 % at the end of the experiment. In addition to the increased susceptibility, $Gab3^{R27C}$ mice suffered from significantly more brain cysts 30 days p.i. as compared to WT mice (**Figure 39C**). The number of *T. gondii* cysts found in the brain of surviving $Gab3^{R27C}$ mice almost doubled as compared to WT mice. Besides the weight, I also recorded the overall health score daily during the experiment, but no change or difference in the general health condition was observed (data not shown).

The decreased survival (**Figure 39C**) and the elevated parasite burden in the brain (**Figure 39D**) showed that Gab3 is crucially involved in the control of the parasite.

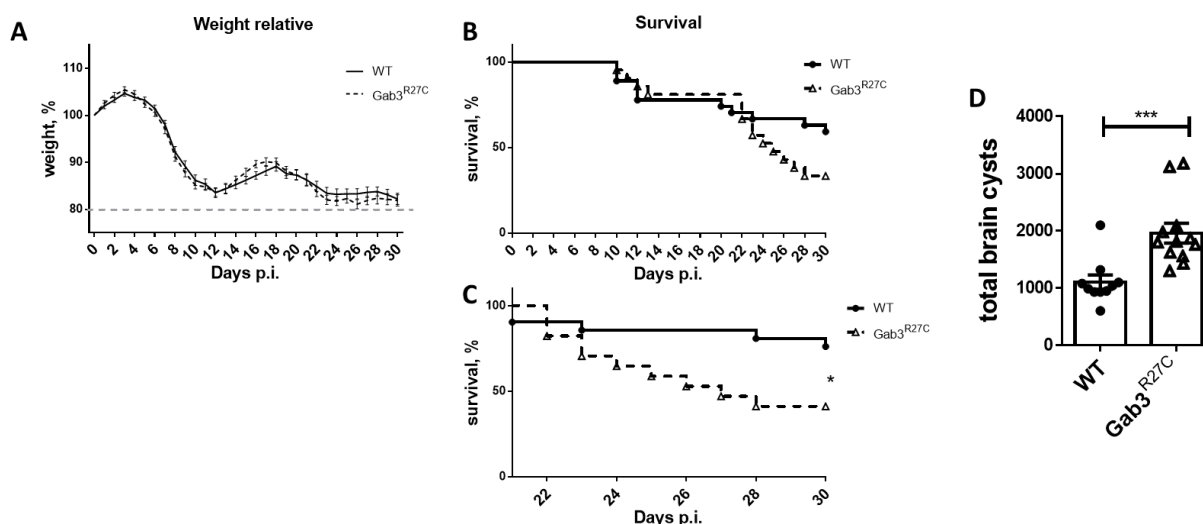


Figure 39: *Gab3^{R27C}* mice showed increased susceptibility and higher cyst counts in the brain during *T. gondii* infections. **(A)** Relative weight loss. **(B)** Survival of WT and *Gab3^{R27C}* mice during first 30 days after infection. **(C)** Survival of WT and *Gab3^{R27C}* mice between day 22 and day 30 after infection. **(D)** *Gab3^{R27C}* mice show significantly increased parasite burden in the brain 30 days p.i. The data are from three independent experiments; values show the mean \pm SEM. $n=10-15$; Data were analyzed by ANOVA (A), by Log-rank (Mantel-Cox) (B+C) and by unpaired student t-test (D). * $p \leq 0.05$ *** $p < 0.001$

3.6.1 *Gab3^{R27C}* and WT mice show similar cytokine and chemokine profiles in serum

For the induction of an appropriate immune response during *T. gondii* infections, the production of pro-inflammatory cytokines, mainly IFN- γ , TNF- α or IL-12, is indispensable. Here, DCs are mainly responsible for the production of IL-12, IL-15 or IL-18, which is necessary for an appropriate activation of NK cells. After activation, NK cells produce IFN- γ , which is important to limit parasite spreading. Without an appropriate production of IL-12 or IFN- γ , the parasite would infect multiple cells of the host and irreversibly damage the tissue. However, to balance the immune response and to prevent an overwhelming pro-inflammatory response, the production of anti-inflammatory cytokines, e.g. IL-10, is of equal importance (Dogruman-Al et al., 2011). To investigate whether the increased susceptibility and parasite brain cyst count in *Gab3^{R27C}* mice was related to altered serum cytokine levels, I collected blood samples from WT and *Gab3^{R27C}* mice on days 1, 3, 5 and 7 p.i., isolated the serum and performed a multiplex analysis with the Bio-Plex[®] multiplex system (Bio-Rad Laboratories GmbH, Munich). The multiplex analysis showed that WT and *Gab3^{R27C}* mice only differ slightly in their serum cytokine profile (**Figure 40**). I measured higher IL-12p70 levels in *Gab3^{R27C}* mice on day 5 p.i. However, the overall concentration of IL-12p70 was still very low with 0.5 ng/ml up to 1.0 ng/ml (**Figure 40**). The kinetics for all other cytokines and the chemokine MCP-1 were comparable between WT and *Gab3^{R27C}* mice. The IFN- γ , TNF- α and IL-6 levels significantly increased until day 7 p.i., while MCP-1 already reached the

highest concentration 3 days p.i. Interestingly, the anti-inflammatory cytokine IL-10 also significantly increased during the first 7 days p.i.

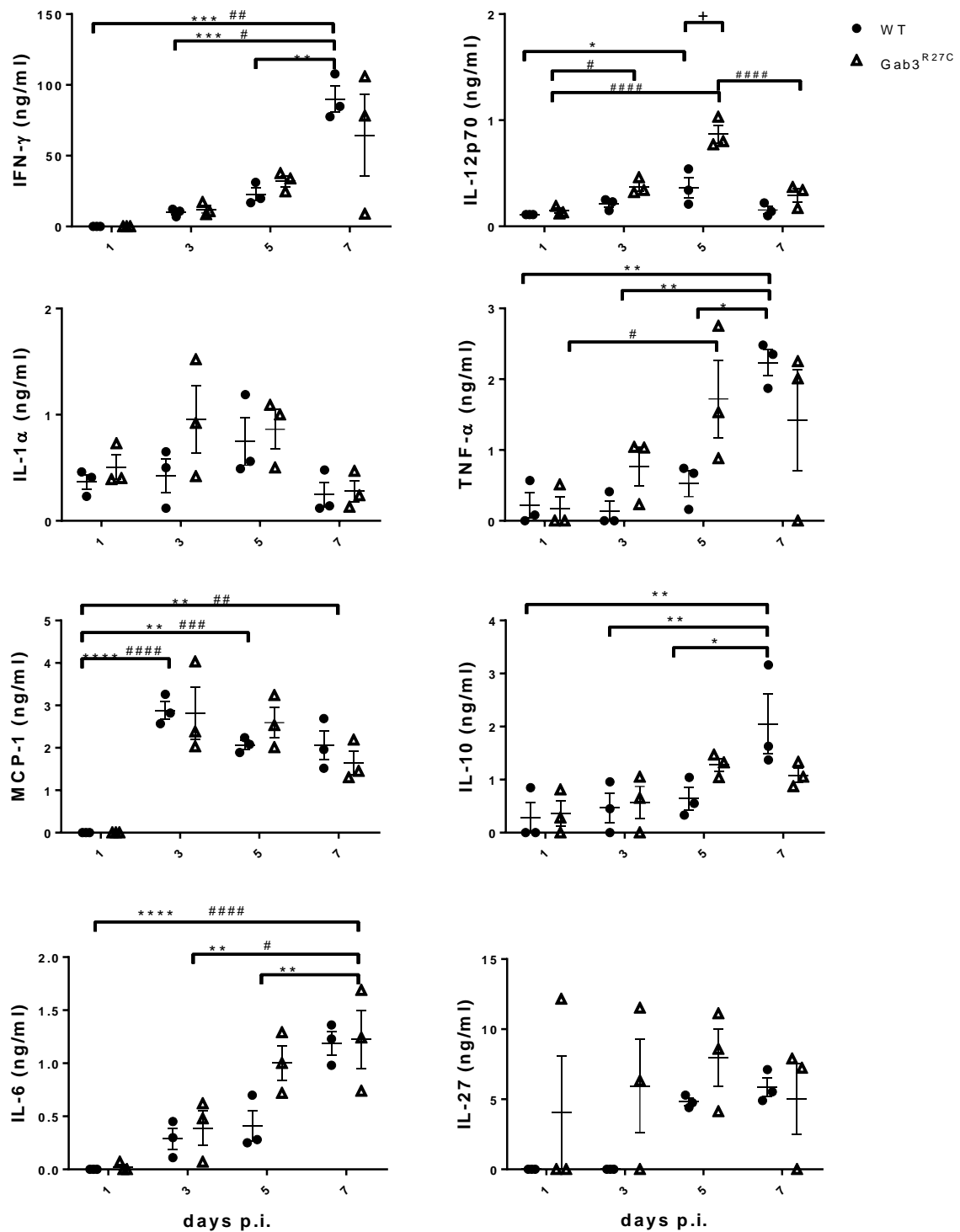


Figure 40: Cytokine and chemokine levels from WT and Gab3^{R27C} mice in serum were comparable between day 1 and day 7 p.i. with 50 cysts of *T. gondii* i.p. Cytokine levels were analyzed using Bio-Plex[®] multiplex system (Bio-Rad Laboratories GmbH, Munich). Values show the mean \pm SEM. n=3; * indicates significant differences during the observation period within the WT group, # indicates significant differences during the observation period within the Gab3^{R27C} group, + indicates differences during the observation period between the WT and Gab3^{R27C} group; # *p<0.05; **p<0.01; ***p<0.001 ****p<0.0001. Data were analyzed by ANOVA.

3.6.2 Impaired cell differentiation of myeloid cells from $Gab3^{R27C}$ mice in mixed BM-chimeric mice

After figuring out that the cytokine and chemokine profiles are comparable for most of the analyzed cytokines and chemokine and therefore could not be the explanation for the different survival after the *T. gondii* infection, I investigated the ability of cells from $Gab3^{R27C}$ mice to differentiate compared to WT mice. For this purpose, I performed a mixed BM-chimeric experiment. I collected BM cells from $CD45.1^+$ WT mice and $CD45.2^+$ $Gab3^{R27C}$ mice, mixed them in a 1:1 ratio and injected the mixed BM-cells *i.v.* into $CD45.1^+$ and $CD45.2^+$ WT recipients, that had been irradiated by 700 rad before. Thirty days after the cell transfer, mice were sacrificed and the cell composition in the peritoneal cavity was analyzed using flow cytometry. With the help of CD45.1 and CD45.2 markers it was possible to distinguish cells originating from $CD45.1^+$ WT or $CD45.2^+$ $Gab3^{R27C}$ BM-cells.

A comparison of total lymphocytes isolated from the peritoneal cavity revealed a shift towards $CD45.1^+$ WT cells in both recipients (**Figure 41A**). The percentage of $CD45.1^+$ cells was 86 % and 73 % in $CD45.1^+$ and $CD45.2^+$ recipients, respectively. Additionally, I analyzed single cell types in both recipients to evaluate if only specific cell lineages were affected by the impaired cell differentiation.

Results from $CD45.1^+$ WT recipients uncovered that all analyzed cell types mainly differentiated from $CD45.1^+$ WT donors and only a minor fraction from $CD45.2^+$ $Gab3^{R27C}$ donors (**Figure 41B, left**). In line with that, analysis of $CD45.2^+$ WT recipients showed the same results, as most of the cells are $CD45.1^+$ and therefore originated from WT BM cells (**Figure 41B, right**). Interestingly, $CD4^+$ and $CD8^+$ T cells mainly differentiated from $CD45.2^+$ $Gab3^{R27C}$ donors.

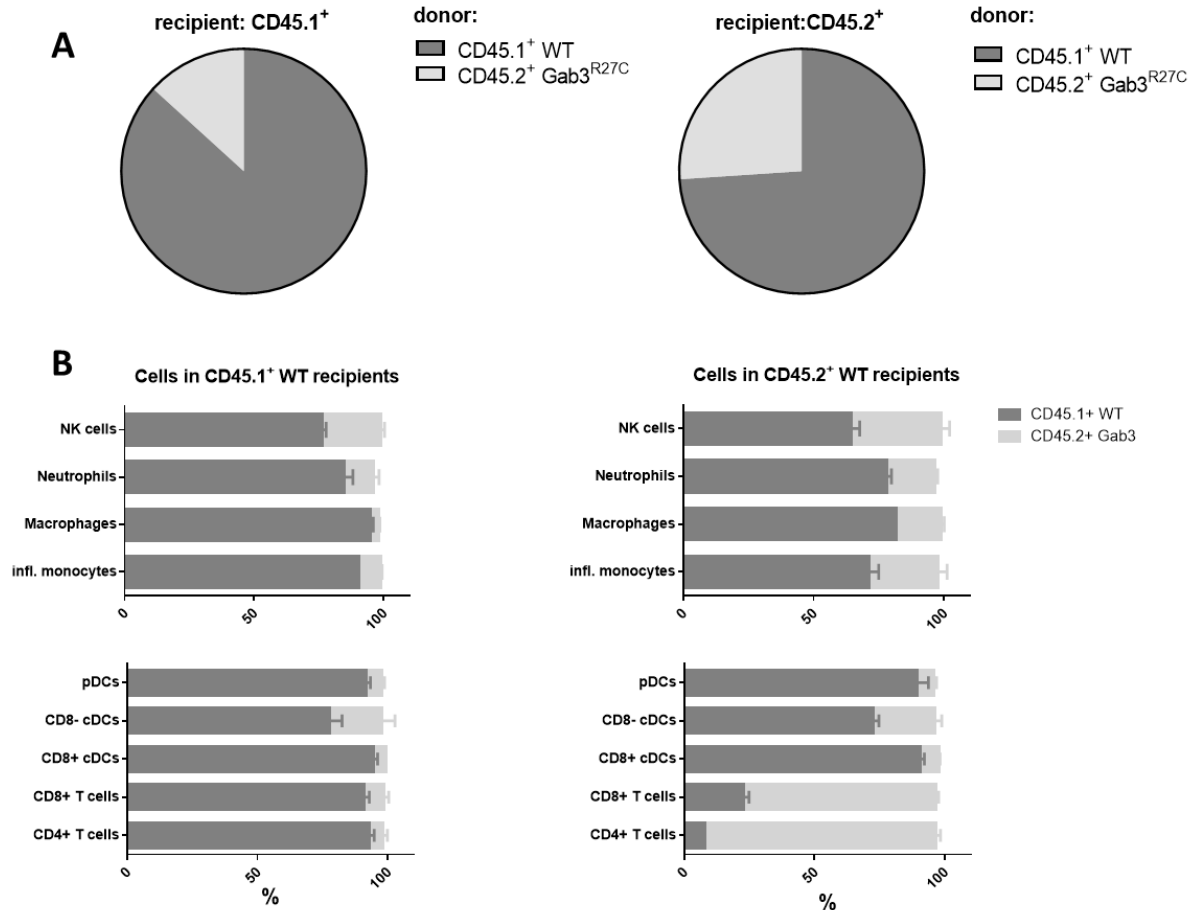


Figure 41: Immune cells predominantly differentiate from CD45.1⁺ WT donors. Results obtained with mixed BM chimeric mice using WT CD45.1⁺ and CD45.2⁺ recipients and WT (CD45.1⁺) as well as Gab3^{R27C} (CD45.2⁺) donors. The graphs depict immune cells differentiated either from WT or Gab3^{R27C} cells in the peritoneal cavity 30 days after transfer. **(A)** Cell frequencies of CD45.1⁺ WT and CD45.2⁺ Gab3^{R27C} cells. **(B)** Frequencies of myeloid and lymphoid cell populations in the peritoneal cavity that differentiated from either CD45.1⁺ WT or CD45.2⁺ Gab3^{R27C} donor cells in CD45.1⁺ (left) and CD45.2⁺ (right) WT recipients. Values in B show the mean \pm SEM. n=4

4 DISCUSSION

4.1 C5a receptors are critical for controlling intestinal inflammation during early *T. gondii* infection

By infecting WT mice with 1, 3, 5, 7 or 10 cysts orally, I showed that infection with only 1 cyst is sufficient to induce a massive inflammation characterized by weight loss, increase of disease scores and mortality. Additionally, higher systemic IFN- γ and IL-12 levels after 5 and 7 days p.i. were observed. Interestingly, oral infection of C5aR2^{-/-} mice with 10 cysts did not result in massive tissue inflammation in the gut as cell infiltration into the intestine was significantly lower than in WT and C5aR1^{-/-} mice. C5aR2 was discovered in the year 2000 and initially described as a decoy receptor for C5a (Ohno et al., 2000). As already mentioned, different publications suggest an anti-inflammatory role for C5aR2 during lung injury (Gerard et al., 2005) and in contrast to that, pro-inflammatory roles as C5aR2 is involved in ERK1/2 or p38 MAPK phosphorylation mediated via β -arrestin recruitment in human monocyte-derived macrophages (HMDMs) (Croker et al., 2014). The importance of C5aR2 is emphasized by *in vivo* experiments showing that β -arrestin 2 knockout mice show decreased survival and increased release of pro-inflammatory cytokines during sepsis-induced inflammation (Fan et al., 2010). Additionally, C5aR2 is involved in neutrophil mobilization as specific stimulation of C5aR2 inhibits neutrophil migration in WT, but not in C5aR2^{-/-} mice (Croker et al., 2016). In summary, it was already shown that C5aR2 has both, pro- and anti-inflammatory properties, depending on the cell type, tissue and signaling pathway. Interestingly, in a dextran sulfate sodium (DSS)- induced mouse model of acute ulcerative colitis (UC), C5aR2^{-/-} mice are less susceptible characterized by reduced weight loss and a lower disease score in comparison to WT mice (Hsu et al., 2014). As a result of the massive destruction of tissue and crypt architecture in WT and C5aR1^{-/-} mice it is likely that these mice do not only suffer from intestinal inflammation caused by the parasite, but also from sepsis caused by breaking up the barrier and leaking of bacteria and other pro-inflammatory mediators into the blood stream. It has been shown that a combined blockade of C5aR1 and C5aR2 during sepsis is necessary to improve the survival of mice (Rittirsch et al., 2008), again underlining the functional role of C5aR2. These results are in line with my observations and indicate that C5aR2 plays an important role in mediating C5a-induced inflammation during acute *T. gondii* infections in the intestine. However, the exact mechanism how C5aR2 regulates C5a-mediated signaling during acute *T. gondii* infections remains elusive. It is possible that C5aR2 forms dimers with C5aR1 as already described previously to regulate the pro-inflammatory signaling through C5aR1 and induce the production of anti-inflammatory cytokines like IL-10 (Hsu et al., 2014). The potential lack of anti-inflammatory cytokines in C5aR1^{-/-} mice would explain the severe inflammation induced by both, elevated levels of

pro-inflammatory cytokines like IFN- γ due to the missing control of C5aR1-mediated cytokine production and the lack of anti-inflammatory cytokines like IL-10. On the other hand, lack of C5aR2 would also result in missing interaction of C5aR1 and C5aR2 and should result in the same cytokine production, if the interaction of C5aR1 and C5aR2 is the key mechanism here. However, C5aR2^{-/-} mice are protected from developing severe inflammation in the gut which indicates that missing C5aR2 results in a better controlled immune response regarding production of pro- and anti-inflammatory cytokines. A potential explanation might be the missing transfer of intracellularly expressed C5aR2 to the surface of the cell to counterbalance C5aR1-mediated pro-inflammatory immune responses, but not due to missing C5aR1-C5aR2 interaction at a first step. Another potential crosstalk partner for C5aR2 could involve TLRs, as it was already described that C5aR1 can form dimers with TLR4 in which C5a negatively regulates TLR4-induced immune responses (Hawlich et al., 2005). As C5aR1 and C5aR2 are structurally similar, it is possible that also C5aR2 forms dimers with different TLRs to control pro- and anti-inflammatory immune responses. In this case, my results indicate that missing interaction of C5aR2 and TLRs results in a better controlled immune response with potentially lower levels of pro-inflammatory cytokines.

Taken together, I hypothesize that C5aR2 has significant roles in regulation of *T. gondii*-induced inflammation in the intestine and it seems unlikely that C5aR2 only acts as a decoy receptor for C5a, because the obtained results regarding the development of inflammation in the gut of WT, C5aR1^{-/-} and C5aR2^{-/-} mice are too diverse. Further experiments unveiling better insights into locally produced cytokines and complement activation, would help to better understand the role of C5aR2 in the induction of *T. gondii*-dependent inflammation in the intestine.

4.2 Uncoupled co-expression of C5aR1 and C5aR2 as an important immune regulatory mechanism

The institute for systemic inflammation research recently published the expression pattern of C5aR1 and C5aR2 on innate and adaptive immune cells under naïve conditions. With the help of floxed GFP-C5aR1 and floxed tdTomato-C5aR2 reporter mice it was possible to reliably determine the expression pattern of both C5a receptors (Karsten et al., 2015, 2017). To follow this up, I investigated the regulation of C5aR1 and C5aR2 expression during early *T. gondii* infection. So far, nothing is published regarding a potential uncoupled co-expression of C5aR1 and C5aR2 under specific inflammatory conditions. I could show that during early *T. gondii* infections this specific regulation of C5aR1 and C5aR2 might play an important role. Previous experiments from our institute showed that C5aR1^{-/-} mice suffered from increased susceptibility and parasite burden in the brain and C5aR2^{-/-} mice

also showed increased parasite burden 30 days p.i. (Briukhovetska, 2017). Together with my results showing that C5aR2^{-/-} mice are protected from developing severe inflammation in the gut, the available results emphasize the importance of both C5aRs and their potential cross-talk. Analyzing C5aR1 and C5aR2 expression in the blood showed that significantly more cells express C5aR2 under infectious conditions. Interestingly, cells expressing C5aR1 did not change. In the spleen more cells express C5aR1 and C5aR2 during the infection. Interestingly, under steady state conditions more cells express C5aR2 compared to C5aR1. In the lung it was the other way around, as C5aR1 was expressed on more immune cells under infectious conditions compared to C5aR2. However, the C5a receptor expression on immune cells in the peritoneal cavity did not change during *T. gondii* infection at all, but under steady state condition more cells expressed C5aR2. As the peritoneal cavity is the first tissue which encountered the parasite in the i.p. infection model, no regulation of the expression of both receptors on immune cells in the peritoneal cavity might indicate that C5aR1 and C5aR2 are not crucially involved in cell activation, what is unlikely in light of several publications (Crocker et al., 2014; Denk et al., 2017), or the parasites infiltrated and killed cells before they were able to respond to the infection. Although, no regulation on total immune cells was detectable, single cell populations showed regulatory differences. Macrophages, which are highly positive for C5aR1 and C5aR2 expression under naïve conditions, show the same regulation in the spleen and peritoneal cavity as less cells are C5aR2⁺ under infectious conditions. Interestingly, the expression results indicate the C5aR2, but not C5aR1 is downregulated on macrophages. Furthermore, the cell frequency for macrophages in the peritoneal cavity drops significantly under infectious conditions, indicating that macrophages which remain inside the peritoneal cavity downregulate C5aR2, while those who migrate to other tissues keep high C5aR2 expression levels. This regulation suggests that downregulation of C5aR2 is necessary to activate macrophages, as C5aR2 acts to counter-balance C5aR1-mediated cell activation (Bamberg et al., 2010). In the presence of C5a, a downregulation of C5aR2 would result in higher potency of C5a to bind to its pro-inflammatory receptor C5aR1 and activate the cells as the counter-balancing via C5aR2 is missing. The reduction in macrophage frequency in the peritoneal cavity is surprising as those cells play an important role during early *T. gondii* infections by phagocytosing free parasites, but they also get actively infected by tachyzoites. The fate of the macrophage depends on priming with IFN- γ after the infection with *T. gondii*, but before the parasite enters the cell (Nathan et al., 1983). If macrophages are primed with IFN- γ , they are able to induce effector mechanisms like upregulation of iNOS and NO which leads to parasite killing. However, if IFN- γ is missing because neutrophils or NK cells, which are responsible for early IFN- γ production, are already infected with the parasite, lack activation or migration to the site of infection, the parasite can reproduce within the macrophage and spread throughout the organism. For NK cells it was already shown that infected NK cells develop a hypermobility after infection with *T. gondii* facilitating parasite spreading throughout the body (Ueno

et al., 2015). It is possible that also infected macrophages tend to migrate out of the peritoneal cavity to facilitate parasite spreading. Another possibility is that insufficient IFN- γ levels inhibit macrophage activation and therefore, *T. gondii* actively infects macrophages and kills them after intracellular tachyzoite reproduction.

As an early IFN- γ producer, neutrophils are of main importance in controlling the infection. Unfortunately, it was not able to analyze the C5aRs regulation on neutrophils under naïve conditions in the peritoneal cavity, because neutrophils are absent under steady state conditions. However, compared to other analyzed tissues and the fact that neutrophils, like macrophages, are highly expressing C5aRs cells (Dunkelberger et al., 2012; Karsten et al., 2015, 2017) and the fact the C5a is a strong chemoattractant for neutrophils and enhances phagocytosis and release of granule enzymes (Goldstein and Weissmann, 1974; Mollnes et al., 2002), it seems that less cells express C5aR2 under infectious conditions, whereas C5aR1 expression remains stable. Hence, the expression of C5aR2 on neutrophils is comparable to the expression on macrophages. The importance of neutrophil-derived IFN- γ during *T. gondii* infections is shown by Hunter et al. (Hunter et al., 1994) who published that NK cell and T cell-deficient mice suffer from increased susceptibility during *T. gondii* infections, but are not as susceptible as IFN- γ deficient mice, due to the fact that IFN- γ produced by neutrophils compensates the lack of NK cell- and T cell-derived IFN- γ . The frequency of neutrophils expressing C5aR2 and the expression intensity is downregulated under infectious conditions in the blood. Therefore, it seems that neutrophils which migrate into the blood downregulate C5aR2. Downregulation of C5aR2 allows more C5a to bind to C5aR1 and that could alter the migration behavior of neutrophils and increase migration to the sites of infection. On the other hand, publications showed that high doses of C5a can lead to nonspecific chemotactic migration and neutrophil dysfunction when bound to C5aR1 (Huber-Lang et al., 2002b). Therefore, maintaining high expression levels of C5aR2 could be necessary to prevent neutrophil dysfunction and counter-balance C5aR1-mediated neutrophil migration and activation. Based on my results I hypothesize that downregulation of C5aR2 facilitates neutrophil activation and migration as well as it improves parasite killing or phagocytosis what is necessary to limit parasite spreading and the development of systemic inflammation. Consequently, C5aR2^{-/-} mice would survive *T. gondii* infections significantly better than C5aR1^{-/-} mice. Unfortunately, we could not observe such a prominent difference between these two KO mice as both strains showed similar survival (Briukhovetska, 2017). Although these results limit the assumed anti-inflammatory role of the C5aR2, it is still tempting to speculate that the receptor is important to maintain cells inactive under naïve conditions. For a better understanding, further experiments are necessary to investigate whether local cytokine production is altered in cells from WT and C5aR2^{-/-} mice. Furthermore,

migration experiments with uninfected and infected neutrophils or macrophages will help to understand if *T. gondii* actively influences mobility.

Besides neutrophils, eosinophils belong to the group of granulocytes. However, they show significantly reduced expression intensity for both receptors compared to neutrophils. They are known to be important in fighting parasites and have important roles during allergic asthma (Gleich and Loegering, 1984; Weller, 1994). After recruitment to the site of infection they start to produce pro-inflammatory cytokines like IL-2, IL-4, IL-5 and IL-12 besides others (Kita, 1996). In the induction phase of allergic asthma, eosinophil and neutrophil influx as well as production of pro-inflammatory cytokines are the main reasons for establishing a maladaptive immune response (Verstraelen et al., 2008). Therefore, it is surprising that *T. gondii* infections lead to significant reduction of the eosinophil population in the lung. It is tempting to speculate that eosinophils are either phagocytosing free tachyzoites or are actively infected by the parasite. In both cases the parasite would replicate inside of the eosinophil and that results in killing of the cell. As the lung is one of the first organs where *T. gondii* aims to migrate into, the observed reduction and nearly complete loss of eosinophil population demonstrates the severity of the infection. Regarding C5aR1 and C5aR2 expression in eosinophils, no change between non-infectious and infectious conditions was observed. Eosinophils express both receptors at moderate levels with slightly increased expression levels for C5aR2. It is important to notice, that the eosinophil population is nearly absent under infectious conditions what exacerbates the flow cytometric analysis and reduces the validity of the obtained data regarding the expression of C5aR1 and C5aR2. However, as no regulation was detected, C5a receptors seem to have just minor roles in regulating eosinophil activation and migration. Interestingly, Fenoy et al (Fenoy et al., 2009) showed that *T. gondii* infections protect BALB/c mice from the development of allergic airway inflammation by blocking eosinophil and neutrophil migration to the lung. Due to the missing eosinophils and neutrophils, the establishment of a maladaptive immune response is unlikely. Although, *T. gondii* infections do not block eosinophil migration into the lung, it seems that the infection leads to increased eosinophil death and therefore to diminished frequencies in the lung, what has the same effect as blocking the migration and preventing the induction of a maladaptive immune response. On the other hand, missing neutrophils and eosinophils in the lung also results in reduced pro-inflammatory cytokines and consequently facilitates spreading and reproduction of parasites like *T. gondii*.

Besides the described high-expressing C5aR1 and C5aR2 cells, low-expressing inflammatory monocytes were detected. In contrast to the described high-expressing C5aR1 and C5aR2 cells, these cells only show minor regulatory mechanisms. The cell frequency of C5aR1 and C5aR2 expressing cells is upregulated after infection in the peritoneal cavity. They are known to be recruited to the site of infection following profilin detection via TLR11 in mice (Neal and Knoll, 2014), what is also reflected by

increased frequencies in the peritoneal cavity. Furthermore, they produce iNOS and TNF- α as essential mediators for controlling parasite spreading (Dunay et al., 2008; Mordue and Sibley, 2003). Consequently, depletion of inflammatory monocytes leads to increased susceptibility and mice succumb to death early during the acute phase of the infection (Dunay et al., 2010). However, only little is known about the role of anaphylatoxins for regulation and activation of inflammatory monocytes. That is not surprising as my results indicate that inflammatory monocytes at best show minor C5aR1 or C5aR2 expression in all investigated organs. Although inflammatory monocytes do not express or regulate C5a receptors as distinct as neutrophils or macrophages, their role during *T. gondii* infections is undisputed. In contrast to macrophages and neutrophils, which downregulate C5aRs under infectious conditions, cells expressing C5aR1 or C5aR2 on DCs either do not change or increase, as visible for C5aR1 in the peritoneal cavity and spleen and C5aR2 in the blood. Interestingly, the expression intensity did not change. DCs in general and especially cDCs play an indispensable role during *T. gondii* infections as they are the main source for IL-12 after recognizing profilin via TLR11 and TLR12 in mice (Plattner et al., 2008). IL-12 is necessary to activate other effector cells to induce a potent immune response and limit parasite growth and spreading. Additionally, DCs are known to be important in regulating T_H1 and T_H17 differentiation. Furthermore, it has previously been shown that exposure to LPS and C5a resulted in enhanced production of cytokines, indicating synergism between TLRs and C5aR1 (Riedemann et al., 2002, 2004). Another synergism between TLRs and C5a receptors was shown by a negative regulation of TLR4- and CD40-induced synthesis of IL-12 family cytokines from inflammatory macrophages via C5a (Hawlich et al., 2005). Additionally, it is published that TLR modulates C5a-induced responses by negatively modulating C5aR2 to reduce the counter-balancing effect and increase pro-inflammatory responses (Raby et al., 2011). The published results are in line with my results as cDCs massively upregulate C5aR1 expression in the peritoneal cavity and spleen under infectious conditions which could lead to increased TLR- and C5a-mediated activation and cytokine production. Additionally, the assumed anti-inflammatory role of C5aR2 is reduced, because increased expression of C5aR1 results in higher potential for C5a to bind to its pro-inflammatory receptor. The fact that cDCs in the peritoneal cavity show the most distinct difference in C5aR1 expression comparing steady state and infectious conditions is due to the i.p. infection model which results in the encounter of immune cells with the parasite in this compartment first.

To obtain more detailed information about the function of C5aR1 and C5aR2 on single cell populations during early *T. gondii* infections, it will be necessary to generate cell-specific C5aR1 or C5aR2 knockouts using the Cre/lox system. With this opportunity it will be possible to investigate the impact of C5aR1 and C5aR2 on individual immune responses regarding parasite susceptibility and cytokine production *in vivo* and to draw precise conclusions about the role of both receptors.

4.3 C5aR2 controls NK cell-derived IFN- γ production in response to IL-12/IL-18 stimulation

One of the key result of the C5aR1- and C5aR2-expression studies is that NK cells and B cells express C5aR2 but not C5aR1 (Karsten et al., 2015, 2017). This unique expression pattern makes them a suitable cell type to directly investigate C5aR2 functions and downstream signaling events. Furthermore, the data show that only a subpopulation of NK cells expresses C5aR2. The expression pattern was confirmed using PCR, GFP-C5aR1 and tdTomato-C5aR2 reporter mice. Functionally I was able to show that C5aR2^{-/-} NK cells produce significantly more IFN- γ after IL-12 and IL-18 stimulation than WT NK cells. In line with this observation, pre-stimulation of WT NK cells with the specific C5aR2 agonist P32 (Crocker et al., 2016) resulted in reduced IFN- γ production. Thus, C5aR2 on NK cells negatively regulated IFN- γ production in NK cells upon cytokine stimulation demonstrating a crucial and novel regulatory function for the C5a/C5aR2-axis in IL-12/IL-18-driven production of IFN- γ . As IFN- γ is an important cytokine to control infections, it is not surprising that some *T. gondii* strains developed mechanisms to block IFN- γ production from effector cells by increasing the association of STAT1 with DNA (Rosowski et al., 2014). As the *in vitro* results indicate a regulatory function for C5aR2, I aimed to identify intracellular signaling pathways of C5aR2 and stimulated NK cells with C5a and stained for phosphorylated p38 MAPK, which is a signaling pathway downstream of IL-12 and IL-18 (Zhang and Kaplan, 2000). Experiments showed that C5a stimulation in WT NK cells results in phosphorylation of p38 after 2 min and desensitization after 10 min after stimulation. This effect was C5aR2-specific, since stimulation of C5aR2^{-/-} NK cells did not result in any change in p38 phosphorylation. These results indicate that C5aR2 is involved in the regulation of p38 phosphorylation as it can counter-balance phosphorylation of p38 upon IL-12 or IL-18 stimulation to prevent an overwhelming cytokine storm (**Figure 42**). Considering the fact that complement factors like C5a can also be produced locally during inflammation by various cell types (Bröker et al., 2018; Huber-Lang et al., 2002a; Lubbers et al., 2017), the unique expression of C5aR2 on NK cells becomes even more important. Locally produced C5a can regulate NK cell activation by binding to the anti-inflammatory C5aR2 to prevent NK cells from excessive activation resulting in the massive production of pro-inflammatory cytokines what could harm the host. As it is important during an inflammatory response to keep the balance between an adequate inflammatory response that limits parasite growth or spreading and prevention of overproduction of pro-inflammatory cytokines that would harm the host, C5aR2-controlled NK cell activation seems to play an important role in this process of local inflammation. In future experiments it will be necessary to identify other downstream signaling pathways of C5aR2 to better understand, how C5aR2 controls NK cell activation. Additionally, stimulating NK cells with IL-12/IL-18 in the

presence or absence of C5a could help to understand how C5aR2 signaling influences IFN- γ production *in vitro*.

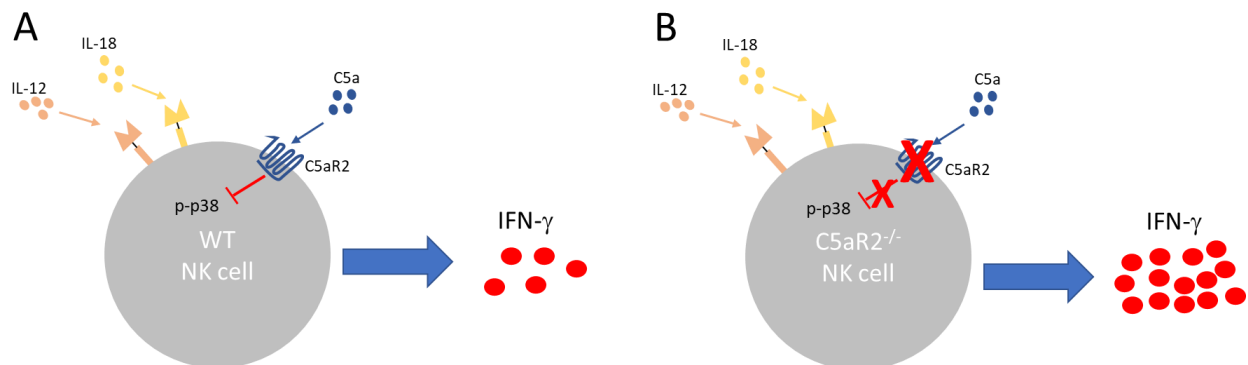


Figure 42: C5aR2 stimulation leads to blockade of p38 phosphorylation. Schematic figure illustrating the function of C5aR2 on (A) WT and (B) C5aR2^{-/-} NK cells. C5a stimulation of C5aR2 results in decreased phosphorylation of p38 MAPK and consequently in reduced IFN- γ production after IL-12/18 stimulation in WT NK cells. C5aR2^{-/-} NK cells lack this regulatory mechanism and are hyperresponsive to IL-12/18 stimulation and produce more IFN- γ .

4.4 The C5a/C5aR2 axis may control NKp46 expression as one mechanism of NK cell regulation

NKp46 is known as an activating receptor on NK cells and able to recognize self and tumor ligands (Glasner et al., 2017). The absence of the receptor results in increased IFN- γ production in the presence of YAC1 cells (Narni-Mancinelli et al., 2012). The same group also published, that NKp46 is a receptor for complement factor P (properdin) (Narni-Mancinelli et al., 2017). Interestingly, binding of factor P to NKp46 leads to activation of different genetic programs and does not induce classical NK cell activation. Additionally, it was shown that NKp46 is involved in the expression of TNF-related apoptosis inducing ligand (TRAIL), which is important for anti-tumor, anti-viral and immunoregulatory functions (Sheppard et al., 2018). Interestingly, NKp46 is the only cytotoxicity receptor, which is shared by primates and rodents, emphasizing an essential role during evolution (Kruse et al., 2014). Therefore, I investigated the expression of NKp46 on NK cells of WT, C5aR1^{-/-} and C5aR2^{-/-} mice. My experiments showed that C5aR2^{-/-} NK cells from the spleen and peritoneal cavity express significantly higher levels of NKp46 as compared to NK cells from WT or C5aR1^{-/-} mice. Further, I found that C5aR2⁺ NK cells from reporter mice in the spleen and peritoneal cavity have a higher NKp46 expression compared to C5aR2⁻ NK cells. I expected reverse results regarding the expression of NKp46 on C5aR2⁺ NK cells, as NKp46 is significantly higher expressed on C5aR2^{-/-} NK cells, but it still allows to speculate about the NKp46 function in connection with C5aR2 on NK cells. *In vitro* results showed that the lack of C5aR2

on NK cells resulted in increased production of IFN- γ after IL-12/18 stimulation, suggesting an anti-inflammatory role for C5aR2 on NK cells. Since NKp46 is described as an activating receptor, I expected regulation of C5aR2 and NKp46 in the same manner to control NK cell activity and prevent excessive activation which could result in host tissue damage. In this case, C5aR2 would counter-balance NKp46-dependent NK cell activation. Using the tdTomato-C5aR2 reporter mice, I showed that C5aR2⁻ NK cells express less NKp46 than WT cells, supporting the view that NKp46-mediated NK cell activation is controlled via C5aR2 and lower NKp46 expression requires lower C5aR2 expression. Interestingly, on C5aR2^{-/-} NK cells the expression is not regulated in the same manner. Here, lack of C5aR2 results in massively increased NKp46 expression levels. If NKp46 and C5aR2 expression is linked, these results explain the increased IFN- γ production from C5aR2^{-/-} NK cells, as increased NKp46 expression results in enhanced NK cell activation, which cannot be counter-regulated due to the lack of suppressive C5aR2. Additionally, it was shown that NKp46 ligand complement factor P can bind to tumor cell lines and potentially work as a NK cell activator (Kemper et al., 2010), which would further increase NKp46-mediated NK cell activation. Taken together, NK cells from C5aR2^{-/-} mice might exert an increased cytotoxicity and/or IFN- γ production as the anti-inflammatory C5aR2 is missing and simultaneously, the activating receptor NKp46 is overexpressed. Another reason for the overexpressed NKp46 might be genomic changes resulting from the knockout of the *c5ar2* gene in C5aR2^{-/-} mice, as interference of genomic equipment not only affects the targeted gene *c5ar2* but can also have an influence on closely located or structurally related genes.

4.5 Control of cell-cell interaction between NK cells and DCs as a mechanism of C5aR2-mediated regulation of NK cell activation

Besides the direct regulation of NK cells by receptors like C5aR2, NK cells need further signals, mediated via other immune cells like DCs, to become fully activated. To achieve that, NK cells need priming by various factors like IL-12, IL-15 or IL-18 which are mainly produced by DCs or macrophages (Chaix et al., 2008; Guia et al., 2008; Lucas et al., 2007). *Borg et al.* (Borg et al., 2004) showed that activation of NK cells via DCs requires the formation of a stimulatory synapse resulting in a direct cell-cell-contact between NK cells and DCs. Furthermore, they showed that DC-derived IL-12 and IL-18 is directly released into the synapse to allow rapid NK cell activation and that IL-15 is presented to the NK cells via the IL-15R. Besides directed cytokine release, cell adhesion molecules like VCAM-1 and LFA-1 play an important role in stabilizing the stimulatory synapse. In experiments investigating splenic DC and NK cell frequencies, total cell numbers and VCAM1 and CD11a expression, I found differences between WT, C5aR1^{-/-} and C5aR2^{-/-} which might explain altered NK cell responsiveness to cytokines, as

C5aR2^{-/-} cells express higher levels of interaction molecules and therefore might respond to cytokines in a more sensitive way. I observed that total splenic DC numbers in C5aR2^{-/-} mice were reduced compared to WT mice. Furthermore, C5aR2^{-/-} DCs expressed higher levels of VCAM1 and more DCs were positive for CD11a when compared to WT DCs. For C5aR2^{-/-} NK cells, significant differences for cell frequencies, but not for total cell numbers were observed. Furthermore, C5aR2^{-/-} NK cells expressed higher levels of VCAM1 as compared to WT NK cells. The increased expression of VCAM1 could result in a lowered threshold for NK cell activation and might explain the hyperresponsiveness of C5aR2^{-/-} NK cells in stimulation experiments and the increased IFN- γ production in *in vitro* experiments. Interestingly, I did not find systemic differences for IFN- γ between WT and C5aR2^{-/-} mice, which might be explained by the reduced numbers of DCs and NK cells in C5aR2^{-/-} mice as cells from C5aR2^{-/-} mice have a lower threshold for activation due to increased expression of important adhesion molecules, but reduced cell numbers. One reason for the same amount of measured IFN- γ might be that the increased production of IFN- γ by each cell was overlaid by the reduced cell numbers. Furthermore, the reduced DC numbers could result in less effective NK cell activation due to missing interaction partner. However, as the relative number of both populations was reduced, the ratio between DCs and NK cells remains the same. Increased expression of co-stimulatory adhesion molecules could work as a compensation mechanism and allow potent NK cell activation by DCs, as formation of the stimulatory synapse is facilitated by increased expression of co-stimulatory adhesion molecules.

4.6 Gab3 is crucially important for cell differentiation and influences *T. gondii* susceptibility

In addition to unique expression pattern for C5aR2 on NK cells, I uncovered high expression of Gab3 while I was in the IRTG partner laboratory of Dr. Hoebe at the CCHMC. Gab3 belongs to the scaffolding protein family of Grb-2 associated proteins together with Gab1 and Gab2. They contribute to specific signal transduction pathways and all three molecules share a similar topology. However, relatively little is known about the function, interaction partners and the role of Gab3 as reflected in the low number of publications dealing with Gab3. It is known that Gab3 deficient mice develop normal and are generally healthy and immunocompetent, suggesting that Gab3 functions can be compensated under steady state conditions (Seiffert et al., 2003). In contrast to Gab1 and Gab2, Gab3 is highly expressed in the lymphoid tissue. Furthermore, experiments from the *Hoebe* lab revealed a strong expression on NK cells, mast cells and CD8⁺ T cells (unpublished data). To investigate the function of Gab3, the Hoebe lab generated an ENU-mutated germline mouse strain with a missense mutation in the pleckstrin

homology (PH) domain of Gab3 (Gab3^{R27C}). As NK cells are crucially involved during early *T. gondii* infections, I chose this model to further investigate the role and function of Gab3. I.p. infection with 50 *T. gondii* cysts showed that Gab3^{R27C} mice suffered from increased susceptibility to the infection and elevated parasite burden after 30 days p.i. compared to WT mice. Interestingly, no substantial differences in disease-associated systemic cytokine levels were observed during the first seven days p.i. However, all measured cytokines showed only very low concentrations ranging from 0 ng/ml to 10 ng/ml, except for IFN- γ which was present in higher concentrations. These results indicate that the Gab3 protein is not involved in the regulation of cytokine production and therefore it is unlikely that Gab3 is associated in pathways downstream of TLRs, the IL-12-family or IFN- γ receptors. Interestingly, experiments investigating the cell composition in the peritoneal cavity of Gab3^{R27C} mice showed that under steady state conditions cell frequencies of NK cells, neutrophils and macrophages were reduced compared to WT mice. Additionally, mixed BM-chimeric mice experiments revealed impaired ability of BM cells from Gab3^{R27C} to differentiate into innate and adaptive immune cells in the peritoneal cavity, but not in the spleen. The slight heterogeneity in CD45.1⁺ and CD45.2⁺ WT donors, as well as the shift towards Gab^{R27C}-differentiated T cells might be explained by insufficient irradiation at the beginning of the experiment, which resulted in increased CD45.2⁺ cells already before i.v. injection of the mixed BM. Especially the reduced macrophage population and the impaired differentiation ability of macrophages in the context of *T. gondii* infections seems to be a major reason for the increased susceptibility of Gab3^{R27C} mice. Although macrophages represent the major cell population in the peritoneal cavity with up to 35 % of all cells, I could not detect differences in disease-associated systemic cytokine levels on different days p.i. This might be explained by the local impaired differentiation ability of Gab3^{R27C} cells, which is limited to the peritoneal cavity. Therefore, potential lack of cytokines produced in the peritoneal cavity are compensated or overlaid by unaffected cells in the spleen or blood. However, macrophages are one of the first cell populations which interact with *T. gondii* after i.p. infections and play an important role in limiting the reproduction and spreading of the parasite (Masek and Hunter, 2013). This massive and significant reduction in the macrophage population may result in less effector cells, local cytokines or phagocytosis during the early state of infection and facilitate parasite spreading throughout the organism. Hence, it is tempting to speculate that reduced macrophages numbers and impaired cell differentiation results in delayed or insufficient activation or migration into the peritoneal cavity early after i.p. infection (**Figure 43**). Additionally, also the local reduction of neutrophil and NK cell numbers in the peritoneal cavity can contribute to increased susceptibility as the lack of local produced cytokines, mainly IFN- γ (Johnson et al., 1993), facilitates *T. gondii* reproduction and spreading throughout the body. For a better understanding how Gab3 influences cell activation or migration, further experiments to identify potential downstream

target proteins of Gab3 need to be done. Additionally, measurement of local produced cytokines in the peritoneal cavity would help to understand the role of Gab3.

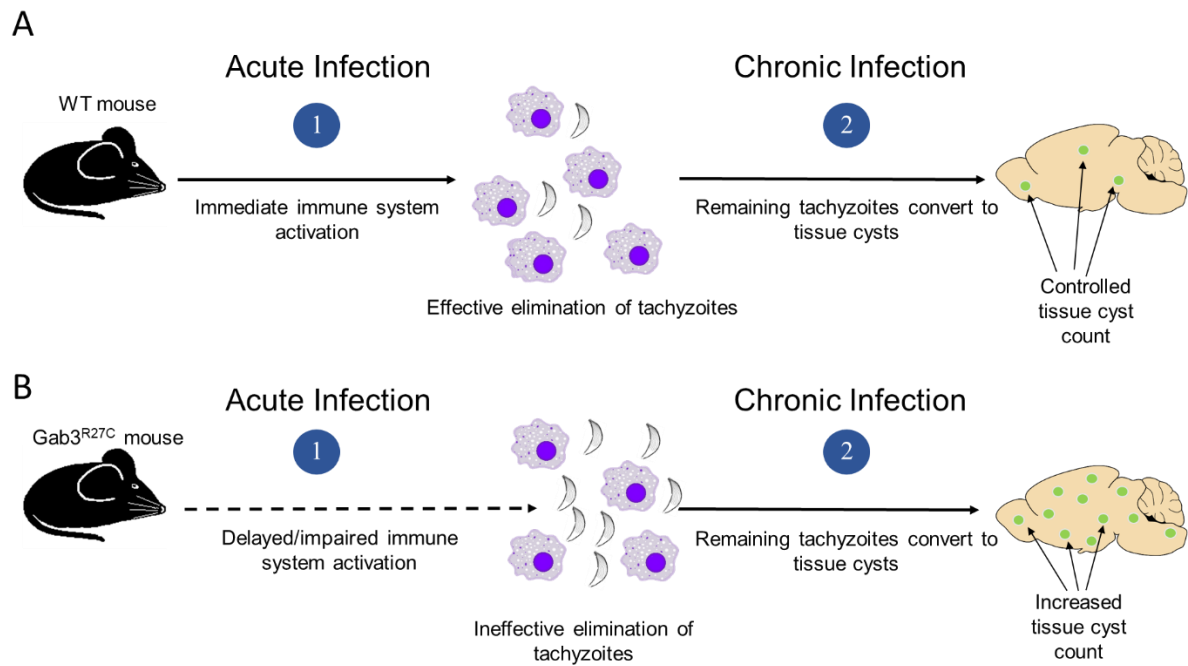


Figure 43: Schematic figure showing the impact of the Gab3 mutation Gab3^{R27C} during the acute and chronic phase of *T. gondii* infection. **(A)** In the WT mice immediate innate immune cell activation drives effective elimination of tachyzoites. The development of an appropriate adaptive immune response converts the remaining tachyzoites into tissue cysts residing preferentially in the brain. **(B)** In the Gab3^{R27C} mice, a delayed or impaired innate immune response results in ineffective elimination of tachyzoites in the acute phase of the infection which leads to increased tissue cyst production that cannot be efficiently controlled by the adaptive immune system.

5 REFERENCES

- Abi Abdallah, D.S., Lin, C., Ball, C.J., King, M.R., Duhamel, G.E., and Denkers, E.Y. (2012). *Toxoplasma gondii* triggers release of human and mouse neutrophil extracellular traps. *Infect. Immun.* *80*, 768–777.
- Adams, L.B., Hibbs, J.B., Taintor, R.R., and Krahenbuhl, J.L. (1990). Microbiostatic effect of murine-activated macrophages for *Toxoplasma gondii*. Role for synthesis of inorganic nitrogen oxides from L-arginine. *J. Immunol. Baltim. Md 1950* *144*, 2725–2729.
- Alberts, B., Johnson, A., Lewis, J., Raff, M., Roberts, K., and Walter, P. (2002). *The Adaptive Immune System*. Mol. Biol. Cell 4th Ed.
- Amara, U., Flierl, M.A., Rittirsch, D., Klos, A., Chen, H., Acker, B., Brückner, U.B., Nilsson, B., Gebhard, F., Lambris, J.D., et al. (2010). Molecular intercommunication between the complement and coagulation systems. *J. Immunol. Baltim. Md 1950* *185*, 5628–5636.
- Andrade, R.M., Wessendarp, M., and Subauste, C.S. (2003). CD154 activates macrophage antimicrobial activity in the absence of IFN-gamma through a TNF-alpha-dependent mechanism. *J. Immunol. Baltim. Md 1950* *171*, 6750–6756.
- Andrade, R.M., Portillo, J.-A.C., Wessendarp, M., and Subauste, C.S. (2005). CD40 signaling in macrophages induces activity against an intracellular pathogen independently of gamma interferon and reactive nitrogen intermediates. *Infect. Immun.* *73*, 3115–3123.
- Andrade, W.A., Souza, M. do C., Ramos-Martinez, E., Nagpal, K., Dutra, M.S., Melo, M.B., Bartholomeu, D.C., Ghosh, S., Golenbock, D.T., and Gazzinelli, R.T. (2013). Combined action of nucleic acid-sensing Toll-like receptors and TLR11/TLR12 heterodimers imparts resistance to *Toxoplasma gondii* in mice. *Cell Host Microbe* *13*, 42–53.
- Araujo, F.G., and Slifer, T. (2003). Different Strains of *Toxoplasma gondii* Induce Different Cytokine Responses in CBA/Ca Mice. *Infect. Immun.* *71*, 4171–4174.
- Arbore, G., West, E.E., Spolski, R., Robertson, A.A.B., Klos, A., Rheinheimer, C., Dutow, P., Woodruff, T.M., Yu, Z.X., O’Neill, L.A., et al. (2016). T helper 1 immunity requires complement-driven NLRP3 inflammasome activity in CD4⁺ T cells. *Science* *352*, aad1210.
- Bamberg, C.E., Mackay, C.R., Lee, H., Zahra, D., Jackson, J., Lim, Y.S., Whitfeld, P.L., Craig, S., Corsini, E., Lu, B., et al. (2010). The C5a Receptor (C5aR) C5L2 Is a Modulator of C5aR-mediated Signal Transduction. *J. Biol. Chem.* *285*, 7633–7644.
- Benevides, L., Milanezi, C.M., Yamauchi, L.M., Benjamim, C.F., Silva, J.S., and Silva, N.M. (2008). CCR2 receptor is essential to activate microbicidal mechanisms to control *Toxoplasma gondii* infection in the central nervous system. *Am. J. Pathol.* *173*, 741–751.
- Berry, D.M., Nash, P., Liu, S.K.-W., Pawson, T., and McGlade, C.J. (2002). A High-Affinity Arg-X-X-Lys SH3 Binding Motif Confers Specificity for the Interaction between Gads and SLP-76 in T Cell Signaling. *Curr. Biol.* *12*, 1336–1341.
- Biswas, A., French, T., Düsedau, H.P., Mueller, N., Riek-Burchardt, M., Dudeck, A., Bank, U., Schüler, T., and Dunay, I.R. (2017). Behavior of Neutrophil Granulocytes during *Toxoplasma gondii* Infection in the Central Nervous System. *Front. Cell. Infect. Microbiol.* *7*.

- Blanchard, N., Gonzalez, F., Schaeffer, M., Joncker, N.T., Cheng, T., Shastri, A.J., Robey, E.A., and Shastri, N. (2008). Immunodominant, protective response to the parasite *Toxoplasma gondii* requires antigen processing in the endoplasmic reticulum. *Nat. Immunol.* *9*, 937–944.
- Bliss, S.K., Marshall, A.J., Zhang, Y., and Denkers, E.Y. (1999a). Human polymorphonuclear leukocytes produce IL-12, TNF-alpha, and the chemokines macrophage-inflammatory protein-1 alpha and -1 beta in response to *Toxoplasma gondii* antigens. *J. Immunol. Baltim. Md 1950* *162*, 7369–7375.
- Bliss, S.K., Zhang, Y., and Denkers, E.Y. (1999b). Murine neutrophil stimulation by *Toxoplasma gondii* antigen drives high level production of IFN-gamma-independent IL-12. *J. Immunol. Baltim. Md 1950* *163*, 2081–2088.
- Bliss, S.K., Butcher, B.A., and Denkers, E.Y. (2000). Rapid recruitment of neutrophils containing prestored IL-12 during microbial infection. *J. Immunol. Baltim. Md 1950* *165*, 4515–4521.
- Bliss, S.K., Gavrilescu, L.C., Alcaraz, A., and Denkers, E.Y. (2001). Neutrophil Depletion during *Toxoplasma gondii* Infection Leads to Impaired Immunity and Lethal Systemic Pathology. *Infect. Immun.* *69*, 4898–4905.
- Borg, C., Jalil, A., Laderach, D., Maruyama, K., Wakasugi, H., Charrier, S., Ryffel, B., Cambi, A., Figdor, C., Vainchenker, W., et al. (2004). NK cell activation by dendritic cells (DCs) requires the formation of a synapse leading to IL-12 polarization in DCs. *Blood* *104*, 3267–3275.
- Briukhovetska, D. (2017). The roles of C5a receptor 1 and chemokine receptor 5 in *Toxoplasma gondii* infection.
- Bröker, K., Figge, J., Magnusen, A.F., Manz, R.A., Köhl, J., and Karsten, C.M. (2018). A Novel Role for C5a in B-1 Cell Homeostasis. *Front. Immunol.* *9*.
- Cai, T., Nishida, K., Hirano, T., and Khavari, P.A. (2002). Gab1 and SHP-2 promote Ras/MAPK regulation of epidermal growth and differentiation. *J. Cell Biol.* *159*, 103–112.
- Campbell, W.D., Lazoura, E., Okada, N., and Okada, H. (2002). Inactivation of C3a and C5a octapeptides by carboxypeptidase R and carboxypeptidase N. *Microbiol. Immunol.* *46*, 131–134.
- Campos, M.A., Closel, M., Valente, E.P., Cardoso, J.E., Akira, S., Alvarez-Leite, J.I., Ropert, C., and Gazzinelli, R.T. (2004). Impaired production of proinflammatory cytokines and host resistance to acute infection with *Trypanosoma cruzi* in mice lacking functional myeloid differentiation factor 88. *J. Immunol. Baltim. Md 1950* *172*, 1711–1718.
- Carrillo-Bustamante, P., Keşmir, C., and de Boer, R.J. (2016). The evolution of natural killer cell receptors. *Immunogenetics* *68*, 3–18.
- Cestari, I., Evans-Osses, I., Schlapbach, L.J., de Messias-Reason, I., and Ramirez, M.I. (2013). Mechanisms of complement lectin pathway activation and resistance by trypanosomatid parasites. *Mol. Immunol.* *53*, 328–334.
- Chaix, J., Tessmer, M.S., Hoebe, K., Fuséri, N., Ryffel, B., Dalod, M., Alexopoulou, L., Beutler, B., Brossay, L., Vivier, E., et al. (2008). Cutting edge: Priming of NK cells by IL-18. *J. Immunol. Baltim. Md 1950* *181*, 1627–1631.
- Chen, N.-J., Mirtsos, C., Suh, D., Lu, Y.-C., Lin, W.-J., McKerlie, C., Lee, T., Baribault, H., Tian, H., and Yeh, W.-C. (2007). C5L2 is critical for the biological activities of the anaphylatoxins C5a and C3a. *Nature* *446*, 203–207.

- Choi, E.Y., Orlova, V.V., Fagerholm, S.C., Nurmi, S.M., Zhang, L., Ballantyne, C.M., Gahmberg, C.G., and Chavakis, T. (2008). Regulation of LFA-1–dependent inflammatory cell recruitment by Cbl-b and 14-3-3 proteins. *Blood* *111*, 3607–3614.
- Chtanova, T., Schaeffer, M., Han, S.-J., van Dooren, G.G., Nollmann, M., Herzmark, P., Chan, S.W., Satija, H., Camfield, K., Aaron, H., et al. (2008). Dynamics of neutrophil migration in lymph nodes during infection. *Immunity* *29*, 487–496.
- Cole, F.S., Matthews, W.J., Marino, J.T., Gash, D.J., and Colten, H.R. (1980). Control of complement synthesis and secretion in bronchoalveolar and peritoneal macrophages. *J. Immunol. Baltim. Md 1950* *125*, 1120–1124.
- Collazo, C.M., Yap, G.S., Sempowski, G.D., Lusby, K.C., Tessarollo, L., Vande Woude, G.F., Sher, A., and Taylor, G.A. (2001). Inactivation of LRG-47 and IRG-47 reveals a family of interferon gamma-inducible genes with essential, pathogen-specific roles in resistance to infection. *J. Exp. Med.* *194*, 181–188.
- Colucci, F., Samson, S.I., DeKoter, R.P., Lantz, O., Singh, H., and Di Santo, J.P. (2001). Differential requirement for the transcription factor PU.1 in the generation of natural killer cells versus B and T cells. *Blood* *97*, 2625–2632.
- Cook-Mills, J.M. (2002). VCAM-1 signals during lymphocyte migration: role of reactive oxygen species. *Mol. Immunol.* *39*, 499–508.
- Correa, D., Cañedo-Solares, I., Ortiz-Alegría, L.B., Caballero-Ortega, H., and Rico-Torres, C.P. (2007). Congenital and acquired toxoplasmosis: diversity and role of antibodies in different compartments of the host. *Parasite Immunol.* *29*, 651–660.
- Croker, D.E., Halai, R., Kaeslin, G., Wende, E., Fehlhaber, B., Klos, A., Monk, P.N., and Cooper, M.A. (2014). C5a2 can modulate ERK1/2 signaling in macrophages via heteromer formation with C5a1 and β -arrestin recruitment. *Immunol. Cell Biol.* *92*, 631–639.
- Croker, D.E., Monk, P.N., Halai, R., Kaeslin, G., Schofield, Z., Wu, M.C., Clark, R.J., Blaskovich, M.A., Morikis, D., Floudas, C.A., et al. (2016). Discovery of functionally selective C5aR2 ligands: novel modulators of C5a signalling. *Immunol. Cell Biol.* *94*, 787–795.
- Curtsinger, J.M., Schmidt, C.S., Mondino, A., Lins, D.C., Kedl, R.M., Jenkins, M.K., and Mescher, M.F. (1999). Inflammatory cytokines provide a third signal for activation of naive CD4+ and CD8+ T cells. *J. Immunol. Baltim. Md 1950* *162*, 3256–3262.
- Curtsinger, J.M., Johnson, C.M., and Mescher, M.F. (2003). CD8 T cell clonal expansion and development of effector function require prolonged exposure to antigen, costimulation, and signal 3 cytokine. *J. Immunol. Baltim. Md 1950* *171*, 5165–5171.
- Debierre-Grockiego, F., Campos, M.A., Azzouz, N., Schmidt, J., Bieker, U., Resende, M.G., Mansur, D.S., Weingart, R., Schmidt, R.R., Golenbock, D.T., et al. (2007). Activation of TLR2 and TLR4 by glycosylphosphatidylinositols derived from *Toxoplasma gondii*. *J. Immunol. Baltim. Md 1950* *179*, 1129–1137.
- Del Rio, L., Bennouna, S., Salinas, J., and Denkers, E.Y. (2001). CXCR2 deficiency confers impaired neutrophil recruitment and increased susceptibility during *Toxoplasma gondii* infection. *J. Immunol. Baltim. Md 1950* *167*, 6503–6509.

- Denk, S., Taylor, R.P., Wiegner, R., Cook, E.M., Lindorfer, M.A., Pfeiffer, K., Paschke, S., Eiseler, T., Weiss, M., Barth, E., et al. (2017). Complement C5a-induced changes in neutrophil morphology during inflammation. *Scand. J. Immunol.* *86*, 143–155.
- Denkers, E.Y., Gazzinelli, R.T., Martin, D., and Sher, A. (1993). Emergence of NK1.1+ cells as effectors of IFN-gamma dependent immunity to *Toxoplasma gondii* in MHC class I-deficient mice. *J. Exp. Med.* *178*, 1465–1472.
- Denkers, E.Y., Yap, G., Schariton-Kersten, T., Charest, H., Butcher, B.A., Caspar, P., Heiny, S., and Sher, A. (1997). Perforin-mediated cytolysis plays a limited role in host resistance to *Toxoplasma gondii*. *J. Immunol. Baltim. Md 1950* *159*, 1903–1908.
- Dias, R.R.F., de Carvalho, E.C.Q., Leite, C.C. da S., Tedesco, R.C., Calabrese, K. da S., Silva, A.C., DaMatta, R.A., and de Fatima Sarro-Silva, M. (2014). *Toxoplasma gondii* Oral Infection Induces Intestinal Inflammation and Retinochoroiditis in Mice Genetically Selected for Immune Oral Tolerance Resistance. *PLoS ONE* *9*.
- Diebolder, C.A., Beurskens, F.J., de Jong, R.N., Koning, R.I., Strumane, K., Lindorfer, M.A., Voorhorst, M., Ugurlar, D., Rosati, S., Heck, A.J.R., et al. (2014). Complement Is Activated by IgG Hexamers Assembled at the Cell Surface. *Science* *343*, 1260–1263.
- DiScipio, R.G., Daffern, P.J., Jagels, M.A., Broide, D.H., and Sriramarao, P. (1999). A comparison of C3a and C5a-mediated stable adhesion of rolling eosinophils in postcapillary venules and transendothelial migration in vitro and in vivo. *J. Immunol. Baltim. Md 1950* *162*, 1127–1136.
- Dobó, J., Pál, G., Cervenak, L., and Gál, P. (2016). The emerging roles of mannose-binding lectin-associated serine proteases (MASPs) in the lectin pathway of complement and beyond. *Immunol. Rev.* *274*, 98–111.
- Dogruman-Al, F., Fidan, I., Celebi, B., Yesilyurt, E., Erdal, B., Babur, C., and Kustimur, S. (2011). Cytokine profile in murine toxoplasmosis. *Asian Pac. J. Trop. Med.* *4*, 16–19.
- Domínguez, P.M., and Ardavín, C. (2010). Differentiation and function of mouse monocyte-derived dendritic cells in steady state and inflammation. *Immunol. Rev.* *234*, 90–104.
- Dos Anjos Cassado, A. (2017). F4/80 as a Major Macrophage Marker: The Case of the Peritoneum and Spleen. *Results Probl. Cell Differ.* *62*, 161–179.
- Draghi, M., Pashine, A., Sanjanwala, B., Gendzekhadze, K., Cantoni, C., Cosman, D., Moretta, A., Valiante, N.M., and Parham, P. (2007). Nkp46 and NKG2D recognition of infected dendritic cells is necessary for NK cell activation in the human response to influenza infection. *J. Immunol. Baltim. Md 1950* *178*, 2688–2698.
- Du Clos, T.W., and Mold, C. (2013). 20 - Complement in host deficiencies and diseases. In *Clinical Immunology (Fourth Edition)*, R.R. Rich, T.A. Fleisher, W.T. Shearer, H.W. Schroeder, A.J. Frew, and C.M. Weyand, eds. (London: Content Repository Only!), pp. 252–269.
- Dubey, J.P. (1998). Advances in the life cycle of *Toxoplasma gondii*. *Int. J. Parasitol.* *28*, 1019–1024.
- Dubey, J.P., Velmurugan, G.V., Rajendran, C., Yabsley, M.J., Thomas, N.J., Beckmen, K.B., Sinnott, D., Ruid, D., Hart, J., Fair, P.A., et al. (2011a). Genetic characterisation of *Toxoplasma gondii* in wildlife from North America revealed widespread and high prevalence of the fourth clonal type. *Int. J. Parasitol.* *41*, 1139–1147.

- Dubey, J.P., Ferreira, L.R., Martins, J., and Jones, J.L. (2011b). Sporulation and Survival of *Toxoplasma gondii* Oocysts in Different Types of Commercial Cat Litter. *J. Parasitol.* *97*, 751–754.
- Dunay, I.R., and Sibley, L.D. (2010). Monocytes mediate mucosal immunity to *Toxoplasma gondii*. *Curr. Opin. Immunol.* *22*, 461–466.
- Dunay, I.R., DaMatta, R.A., Fux, B., Presti, R., Greco, S., Colonna, M., and Sibley, L.D. (2008). Gr1+ Inflammatory Monocytes Are Required for Mucosal Resistance to the Pathogen *Toxoplasma gondii*. *Immunity* *29*, 306–317.
- Dunay, I.R., Fuchs, A., and Sibley, L.D. (2010). Inflammatory monocytes but not neutrophils are necessary to control infection with *Toxoplasma gondii* in mice. *Infect. Immun.* *78*, 1564–1570.
- Dunkelberger, J., Zhou, L., Miwa, T., and Song, W.-C. (2012). C5aR expression in a novel GFP reporter gene knock-in mouse: implications for the mechanism of action of C5aR signaling in T cell immunity. *J. Immunol. Baltim. Md 1950* *188*, 4032–4042.
- Elssen, C.H.M.J.V., Oth, T., Germeraad, W.T.V., Bos, G.M.J., and Vanderlocht, J. (2014). Natural Killer Cells: The Secret Weapon in Dendritic Cell Vaccination Strategies. *Clin. Cancer Res.* *20*, 1095–1103.
- Endris, M., Belyhun, Y., Moges, F., Adefiris, M., Tekeste, Z., Mulu, A., and Kassu, A. (2014). Seroprevalence and Associated Risk Factors of *Toxoplasma gondii* in Pregnant Women Attending in Northwest Ethiopia. *Iran. J. Parasitol.* *9*, 407–414.
- Erben, U., Loddenkemper, C., Doerfel, K., Spieckermann, S., Haller, D., Heimesaat, M.M., Zeitz, M., Siegmund, B., and Kühn, A.A. (2014). A guide to histomorphological evaluation of intestinal inflammation in mouse models. *Int. J. Clin. Exp. Pathol.* *7*, 4557–4576.
- Ewald, S.E., Chavarria-Smith, J., and Boothroyd, J.C. (2014). NLRP1 Is an Inflammasome Sensor for *Toxoplasma gondii*. *Infect. Immun.* *82*, 460–468.
- Fan, H., Bitto, A., Zingarelli, B., Luttrell, L.M., Borg, K., Halushka, P.V., and Cook, J.A. (2010). Beta-arrestin 2 negatively regulates sepsis-induced inflammation. *Immunology* *130*, 344–351.
- Fenoy, I., Giovannoni, M., Batalla, E., Martin, V., Frank, F.M., Piazzon, I., and Goldman, A. (2009). *Toxoplasma gondii* infection blocks the development of allergic airway inflammation in BALB/c mice. *Clin. Exp. Immunol.* *155*, 275–284.
- Ferlazzo, G., Pack, M., Thomas, D., Paludan, C., Schmid, D., Strowig, T., Bougras, G., Muller, W.A., Moretta, L., and Münz, C. (2004). Distinct roles of IL-12 and IL-15 in human natural killer cell activation by dendritic cells from secondary lymphoid organs. *Proc. Natl. Acad. Sci. U. S. A.* *101*, 16606–16611.
- Flegr, J., Prandota, J., Sovičková, M., and Israili, Z.H. (2014). Toxoplasmosis – A Global Threat. Correlation of Latent Toxoplasmosis with Specific Disease Burden in a Set of 88 Countries. *PLoS ONE* *9*.
- Fogler, W.E., Volker, K., McCormick, K.L., Watanabe, M., Ortaldo, J.R., and Wiltrot, R.H. (1996). NK cell infiltration into lung, liver, and subcutaneous B16 melanoma is mediated by VCAM-1/VLA-4 interaction. *J. Immunol.* *156*, 4707–4714.
- Frémeaux-Bacchi, V., Miller, E.C., Liszewski, M.K., Strain, L., Blouin, J., Brown, A.L., Moghal, N., Kaplan, B.S., Weiss, R.A., Lhotka, K., et al. (2008). Mutations in complement C3 predispose to development of atypical hemolytic uremic syndrome. *Blood* *112*, 4948–4952.

- Frickel, E.-M., Sahoo, N., Hopp, J., Gubbels, M.-J., Craver, M.P.J., Knoll, L.J., Ploegh, H.L., and Grotenbreg, G.M. (2008). Parasite stage-specific recognition of endogenous *Toxoplasma gondii*-derived CD8+ T cell epitopes. *J. Infect. Dis.* *198*, 1625–1633.
- Fuhrman, S.A., and Joiner, K.A. (1989). *Toxoplasma gondii*: mechanism of resistance to complement-mediated killing. *J. Immunol. Baltim. Md 1950* *142*, 940–947.
- Fujita, T., Matsushita, M., and Endo, Y. (2004). The lectin-complement pathway--its role in innate immunity and evolution. *Immunol. Rev.* *198*, 185–202.
- Fukuoka, Y., Hite, M.R., Dellinger, A.L., and Schwartz, L.B. (2013). Human skin mast cells express complement factors C3 and C5. *J. Immunol. Baltim. Md 1950* *191*, 1827–1834.
- Gan, Y., Liu, R., Wu, W., Darin, O., Bompreszi, R., and Shi, F.-D. (2012). Antibody to $\alpha 4$ Integrin Suppresses Natural Killer Cells Infiltration in Central Nervous System in Experimental Autoimmune Encephalomyelitis. *J. Neuroimmunol.* *247*, 9–15.
- Gazzinelli, R., Xu, Y., Hieny, S., Cheever, A., and Sher, A. (1992). Simultaneous depletion of CD4+ and CD8+ T lymphocytes is required to reactivate chronic infection with *Toxoplasma gondii*. *J. Immunol. Baltim. Md 1950* *149*, 175–180.
- Gazzinelli, R.T., Hieny, S., Wynn, T.A., Wolf, S., and Sher, A. (1993). Interleukin 12 is required for the T-lymphocyte-independent induction of interferon gamma by an intracellular parasite and induces resistance in T-cell-deficient hosts. *Proc. Natl. Acad. Sci. U. S. A.* *90*, 6115–6119.
- Gazzinelli, R.T., Wysocka, M., Hayashi, S., Denkers, E.Y., Hieny, S., Caspar, P., Trinchieri, G., and Sher, A. (1994). Parasite-induced IL-12 stimulates early IFN-gamma synthesis and resistance during acute infection with *Toxoplasma gondii*. *J. Immunol. Baltim. Md 1950* *153*, 2533–2543.
- Gerard, C., and Hugli, T.E. (1981). Identification of classical anaphylatoxin as the des-Arg form of the C5a molecule: Evidence of a modulator role for the oligosaccharide unit in human des-Arg74-C5a. *Proc. Natl. Acad. Sci.* *78*, 1833–1837.
- Gerard, N.P., Lu, B., Liu, P., Craig, S., Fujiwara, Y., Okinaga, S., and Gerard, C. (2005). An Anti-inflammatory Function for the Complement Anaphylatoxin C5a-binding Protein, C5L2. *J. Biol. Chem.* *280*, 39677–39680.
- Gigley, J.P. (2016). The Diverse Role of NK Cells in Immunity to *Toxoplasma gondii* Infection. *PLOS Pathog.* *12*, e1005396.
- Gigley, J.P., Fox, B.A., and Bzik, D.J. (2009). Cell-mediated immunity to *Toxoplasma gondii* develops primarily by local Th1 host immune responses in the absence of parasite replication. *J. Immunol. Baltim. Md 1950* *182*, 1069–1078.
- Glasner, A., Isaacson, B., and Mandelboim, O. (2017). Expression and function of NKp46 W32R: the human homologous protein of mouse NKp46 W32R (Noé). *Sci. Rep.* *7*, 40944.
- Gleich, G.J., and Loegering, D.A. (1984). Immunobiology of Eosinophils. *Annu. Rev. Immunol.* *2*, 429–459.
- Goicoechea de Jorge, E., Harris, C.L., Esparza-Gordillo, J., Carreras, L., Arranz, E.A., Garrido, C.A., López-Trascasa, M., Sánchez-Corral, P., Morgan, B.P., and Rodríguez de Córdoba, S. (2007). Gain-of-function mutations in complement factor B are associated with atypical hemolytic uremic syndrome. *Proc. Natl. Acad. Sci. U. S. A.* *104*, 240–245.

- Goldstein, I.M., and Weissmann, G. (1974). Generation of C5-derived lysosomal enzyme-releasing activity (C5a) by lysates of leukocyte lysosomes. *J. Immunol. Baltim. Md 1950* *113*, 1583–1588.
- Gonzalez, R.M.S., Shehata, H., O’Connell, M.J., Yang, Y., Moreno-Fernandez, M.E., Chougnet, C.A., and Aliberti, J. (2014). *Toxoplasma gondii*-derived profilin triggers Human TLR5-dependent cytokine production. *J. Innate Immun.* *6*, 685–694.
- Goodship, T.H.J., Cook, H.T., Fakhouri, F., Fervenza, F.C., Frémeaux-Bacchi, V., Kavanagh, D., Nester, C.M., Noris, M., Pickering, M.C., Rodríguez de Córdoba, S., et al. (2017). Atypical hemolytic uremic syndrome and C3 glomerulopathy: conclusions from a “Kidney Disease: Improving Global Outcomes” (KDIGO) Controversies Conference. *Kidney Int.* *91*, 539–551.
- Gordon, S., and Taylor, P.R. (2005). Monocyte and macrophage heterogeneity. *Nat. Rev. Immunol.* *5*, 953–964.
- Granucci, F., Zanoni, I., Pavelka, N., Dommelen, S.L.H. van, Andoniou, C.E., Belardelli, F., Esposti, M.A.D., and Ricciardi-Castagnoli, P. (2004). A Contribution of Mouse Dendritic Cell–Derived IL-2 for NK Cell Activation. *J. Exp. Med.* *200*, 287–295.
- Gu, H., and Neel, B.G. (2003). The ‘Gab’ in signal transduction. *Trends Cell Biol.* *13*, 122–130.
- Guia, S., Cognet, C., de Beaucoudrey, L., Tessmer, M.S., Jouanguy, E., Berger, C., Filipe-Santos, O., Feinberg, J., Camcioglu, Y., Levy, J., et al. (2008). A role for interleukin-12/23 in the maturation of human natural killer and CD56+ T cells in vivo. *Blood* *111*, 5008–5016.
- Haque, S., Hanna, S., Gharbi, S., Franck, J., Dumon, H., and Haque, A. (1999). Infection of mice by a *Toxoplasma gondii* isolate from an AIDS patient: virulence and activation of hosts’ immune responses are independent of parasite genotype. *Parasite Immunol.* *21*, 649–657.
- Harding, F.A., McArthur, J.G., Gross, J.A., Raulet, D.H., and Allison, J.P. (1992). CD28-mediated signalling co-stimulates murine T cells and prevents induction of anergy in T-cell clones. *Nature* *356*, 607–609.
- Hartmann, K., Henz, B.M., Krüger-Krasagakes, S., Köhl, J., Burger, R., Guhl, S., Haase, I., Lippert, U., and Zuberbier, T. (1997). C3a and C5a stimulate chemotaxis of human mast cells. *Blood* *89*, 2863–2870.
- Hauser, W.E., and Tsai, V. (1986). Acute toxoplasma infection of mice induces spleen NK cells that are cytotoxic for *T. gondii* in vitro. *J. Immunol. Baltim. Md 1950* *136*, 313–319.
- Hawlich, H., Belkaid, Y., Baelder, R., Hildeman, D., Gerard, C., and Köhl, J. (2005). C5a negatively regulates toll-like receptor 4-induced immune responses. *Immunity* *22*, 415–426.
- He, R., Browning, D.D., and Ye, R.D. (2001). Differential roles of the NPXXY motif in formyl peptide receptor signaling. *J. Immunol. Baltim. Md 1950* *166*, 4099–4105.
- Hoebe, K. (2009). Genetic dissection of Toll-like receptor signaling using ENU mutagenesis. *Methods Mol. Biol. Clifton NJ* *517*, 239–251.
- Holl, E.K. (2013). Generation of Bone Marrow and Fetal Liver Chimeric Mice. *Methods Mol. Biol. Clifton NJ* *1032*, 315–321.
- Hornum, L., Hansen, A.J., Tornehave, D., Fjording, M.S., Colmenero, P., Wätjen, I.F., Sjøe Nielsen, N.H., Bliddal, H., and Bartels, E.M. (2017). C5a and C5aR are elevated in joints of rheumatoid and psoriatic arthritis patients, and C5aR blockade attenuates leukocyte migration to synovial fluid. *PLoS ONE* *12*.

- Hsu, W.-C., Yang, F.-C., Lin, C.-H., Hsieh, S.-L., and Chen, N.-J. (2014). C5L2 is required for C5a-triggered receptor internalization and ERK signaling. *Cell. Signal.* *26*, 1409–1419.
- Huber-Lang, M., Younkin, E.M., Sarma, J.V., Riedemann, N., McGuire, S.R., Lu, K.T., Kunkel, R., Younger, J.G., Zetoune, F.S., and Ward, P.A. (2002a). Generation of C5a by Phagocytic Cells. *Am. J. Pathol.* *161*, 1849–1859.
- Huber-Lang, M., Sarma, J.V., Rittirsch, D., Schreiber, H., Weiss, M., Flierl, M., Younkin, E., Schneider, M., Suger-Wiedeck, H., Gebhard, F., et al. (2005). Changes in the Novel Orphan, C5a Receptor (C5L2), during Experimental Sepsis and Sepsis in Humans. *J. Immunol.* *174*, 1104–1110.
- Huber-Lang, M.S., Younkin, E.M., Sarma, J.V., McGuire, S.R., Lu, K.T., Guo, R.F., Padgaonkar, V.A., Curnutte, J.T., Erickson, R., and Ward, P.A. (2002b). Complement-Induced Impairment of Innate Immunity During Sepsis. *J. Immunol.* *169*, 3223–3231.
- Hunter, C.A., and Sibley, L.D. (2012). Modulation of innate immunity by *Toxoplasma gondii* virulence effectors. *Nat. Rev. Microbiol.* *10*, 766–778.
- Hunter, C.A., Subauste, C.S., Van Cleave, V.H., and Remington, J.S. (1994). Production of gamma interferon by natural killer cells from *Toxoplasma gondii*-infected SCID mice: regulation by interleukin-10, interleukin-12, and tumor necrosis factor alpha. *Infect. Immun.* *62*, 2818–2824.
- Israelski, D.M., and Remington, J.S. (1988). Toxoplasmic encephalitis in patients with AIDS. *Infect. Dis. Clin. North Am.* *2*, 429–445.
- Itoh, M., Yoshida, Y., Nishida, K., Narimatsu, M., Hibi, M., and Hirano, T. (2000). Role of Gab1 in heart, placenta, and skin development and growth factor- and cytokine-induced extracellular signal-regulated kinase mitogen-activated protein kinase activation. *Mol. Cell. Biol.* *20*, 3695–3704.
- Jarahian, M., Fiedler, M., Cohnen, A., Djandji, D., Hämmerling, G.J., Gati, C., Cerwenka, A., Turner, P.C., Moyer, R.W., Watzl, C., et al. (2011). Modulation of NKp30- and NKp46-mediated natural killer cell responses by poxviral hemagglutinin. *PLoS Pathog.* *7*, e1002195.
- Jenkins, M.K., Khoruts, A., Ingulli, E., Mueller, D.L., McSorley, S.J., Reinhardt, R.L., Itano, A., and Pape, K.A. (2001). In vivo activation of antigen-specific CD4 T cells. *Annu. Rev. Immunol.* *19*, 23–45.
- Johnson, L.L., and Sayles, P.C. (2002). Deficient humoral responses underlie susceptibility to *Toxoplasma gondii* in CD4-deficient mice. *Infect. Immun.* *70*, 185–191.
- Johnson, L.L., VanderVegt, F.P., and Havell, E.A. (1993). Gamma interferon-dependent temporary resistance to acute *Toxoplasma gondii* infection independent of CD4+ or CD8+ lymphocytes. *Infect. Immun.* *61*, 5174–5180.
- Johnson, L.L., Gibson, G.W., and Sayles, P.C. (1996). CR3-dependent resistance to acute *Toxoplasma gondii* infection in mice. *Infect. Immun.* *64*, 1998–2003.
- Ju, C.-H., Chockalingam, A., and Leifer, C.A. (2009). Early response of mucosal epithelial cells during *Toxoplasma gondii* infection. *J. Immunol. Baltim. Md 1950* *183*, 7420–7427.
- Jusko, M., Potempa, J., Karim, A.Y., Ksiazek, M., Riesbeck, K., Garred, P., Eick, S., and Blom, A.M. (2012). A metalloproteinase karilysin present in the majority of *Tannerella forsythia* isolates inhibits all pathways of the complement system. *J. Immunol. Baltim. Md 1950* *188*, 2338–2349.

- Jusko, M., Potempa, J., Kantyka, T., Bielecka, E., Miller, H.K., Kalinska, M., Dubin, G., Garred, P., Shaw, L.N., and Blom, A.M. (2014). Staphylococcal proteases aid in evasion of the human complement system. *J. Innate Immun.* *6*, 31–46.
- Kamizono, S., Duncan, G.S., Seidel, M.G., Morimoto, A., Hamada, K., Grosveld, G., Akashi, K., Lind, E.F., Haight, J.P., Ohashi, P.S., et al. (2009). Nfil3/E4bp4 is required for the development and maturation of NK cells in vivo. *J. Exp. Med.* *206*, 2977–2986.
- Kang, H., and Suzuki, Y. (2001). Requirement of non-T cells that produce gamma interferon for prevention of reactivation of *Toxoplasma gondii* infection in the brain. *Infect. Immun.* *69*, 2920–2927.
- Kang, H., Remington, J.S., and Suzuki, Y. (2000). Decreased resistance of B cell-deficient mice to infection with *Toxoplasma gondii* despite unimpaired expression of IFN-gamma, TNF-alpha, and inducible nitric oxide synthase. *J. Immunol. Baltim. Md 1950* *164*, 2629–2634.
- Kanse, S.M., Gallenmueller, A., Zeerleder, S., Stephan, F., Rannou, O., Denk, S., Etscheid, M., Lochnit, G., Krueger, M., and Huber-Lang, M. (2012). Factor VII-activating protease is activated in multiple trauma patients and generates anaphylatoxin C5a. *J. Immunol. Baltim. Md 1950* *188*, 2858–2865.
- Karsten, C.M., and Köhl, J. (2012). The immunoglobulin, IgG Fc receptor and complement triangle in autoimmune diseases. *Immunobiology* *217*, 1067–1079.
- Karsten, C.M., Laumonier, Y., Eurich, B., Ender, F., Bröker, K., Roy, S., Czabanska, A., Vollbrandt, T., Figge, J., and Köhl, J. (2015). Monitoring and cell-specific deletion of C5aR1 using a novel floxed GFP-C5aR1 reporter knock-in mouse. *J. Immunol. Baltim. Md 1950* *194*, 1841–1855.
- Karsten, C.M., Wiese, A.V., Mey, F., Figge, J., Woodruff, T.M., Reuter, T., Scurtu, O., Kordowski, A., Almeida, L.N., Briukhovetska, D., et al. (2017). Monitoring C5aR2 Expression Using a Floxed tdTomato-C5aR2 Knock-In Mouse. *J. Immunol. Baltim. Md 1950* *199*, 3234–3248.
- Karsten, C.M., Beckmann, T., Holtsche, M.M., Tillmann, J., Tofern, S., Schulze, F.S., Heppe, E.N., Ludwig, R.J., Zillikens, D., König, I.R., et al. (2018). Tissue Destruction in Bullous Pemphigoid Can Be Complement Independent and May Be Mitigated by C5aR2. *Front. Immunol.* *9*, 488.
- Kavanagh, D., Goodship, T.H., and Richards, A. (2013). Atypical hemolytic uremic syndrome. *Semin. Nephrol.* *33*, 508–530.
- Keller, R.R., Gestl, S.A., Lu, A.Q., Hoke, A., Feith, D.J., and Gunther, E.J. (2016). Carcinogen-specific mutations in preferred Ras-Raf pathway oncogenes directed by strand bias. *Carcinogenesis* *37*, 810–816.
- Kemper, C., Atkinson, J.P., and Hourcade, D.E. (2010). Properdin: emerging roles of a pattern-recognition molecule. *Annu. Rev. Immunol.* *28*, 131–155.
- Khan, I.A., Schwartzman, J.D., Matsuura, T., and Kasper, L.H. (1997). A dichotomous role for nitric oxide during acute *Toxoplasma gondii* infection in mice. *Proc. Natl. Acad. Sci. U. S. A.* *94*, 13955–13960.
- Kim, Y.-M., Brinkmann, M.M., Paquet, M.-E., and Ploegh, H.L. (2008). UNC93B1 delivers nucleotide-sensing toll-like receptors to endolysosomes. *Nature* *452*, 234–238.
- Kita, H. (1996). The eosinophil: A cytokine-producing cell? *J. Allergy Clin. Immunol.* *97*, 889–892.
- Klos, A., Tenner, A.J., Johswich, K.-O., Ager, R.R., Reis, E.S., and Köhl, J. (2009). The role of the anaphylatoxins in health and disease. *Mol. Immunol.* *46*, 2753–2766.

- Klos, A., Wende, E., Wareham, K.J., and Monk, P.N. (2013). International Union of Basic and Clinical Pharmacology. [corrected]. LXXXVII. Complement peptide C5a, C4a, and C3a receptors. *Pharmacol. Rev.* *65*, 500–543.
- Koblansky, A.A., Jankovic, D., Oh, H., Hieny, S., Sungnak, W., Mathur, R., Hayden, M.S., Akira, S., Sher, A., and Ghosh, S. (2013). Recognition of profilin by Toll-like receptor 12 is critical for host resistance to *Toxoplasma gondii*. *Immunity* *38*, 119–130.
- Köhl, J., Baelder, R., Lewkowich, I.P., Pandey, M.K., Hawlisch, H., Wang, L., Best, J., Herman, N.S., Sproles, A.A., Zwirner, J., et al. (2006). A regulatory role for the C5a anaphylatoxin in type 2 immunity in asthma. *J. Clin. Invest.* *116*, 783–796.
- Kolev, M., Le Friec, G., and Kemper, C. (2014). Complement--tapping into new sites and effector systems. *Nat. Rev. Immunol.* *14*, 811–820.
- Konishi, E., and Nakao, M. (1992). Naturally occurring immunoglobulin M antibodies: enhancement of phagocytic and microbicidal activities of human neutrophils against *Toxoplasma gondii*. *Parasitology* *104* (Pt 3), 427–432.
- Koshy, A.A., Fouts, A.E., Lodoen, M.B., Alkan, O., Blau, H.M., and Boothroyd, J.C. (2010). *Toxoplasma* secreting Cre recombinase for analysis of host-parasite interactions. *Nat. Methods* *7*, 307–309.
- Krishnegowda, G., Hajjar, A.M., Zhu, J., Douglass, E.J., Uematsu, S., Akira, S., Woods, A.S., and Gowda, D.C. (2005). Induction of proinflammatory responses in macrophages by the glycosylphosphatidylinositols of *Plasmodium falciparum*: cell signaling receptors, glycosylphosphatidylinositol (GPI) structural requirement, and regulation of GPI activity. *J. Biol. Chem.* *280*, 8606–8616.
- Kruse, P.H., Matta, J., Ugolini, S., and Vivier, E. (2014). Natural cytotoxicity receptors and their ligands. *Immunol. Cell Biol.* *92*, 221–229.
- Lambris, J.D., Ricklin, D., and Geisbrecht, B.V. (2008). Complement evasion by human pathogens. *Nat. Rev. Microbiol.* *6*, 132.
- Laumonnier, Y., Karsten, C.M., and Köhl, J. (2017). Novel insights into the expression pattern of anaphylatoxin receptors in mice and men. *Mol. Immunol.* *89*, 44–58.
- Lee, H., Whitfeld, P.L., and Mackay, C.R. (2008). Receptors for complement C5a. The importance of C5aR and the enigmatic role of C5L2. *Immunol. Cell Biol.* *86*, 153–160.
- Lehmann, C., Zeis, M., and Uharek, L. (2001). Activation of natural killer cells with interleukin 2 (IL-2) and IL-12 increases perforin binding and subsequent lysis of tumour cells. *Br. J. Haematol.* *114*, 660–665.
- Li, K., Fazekasova, H., Wang, N., Sagoo, P., Peng, Q., Khamri, W., Gomes, C., Sacks, S.H., Lombardi, G., and Zhou, W. (2011). Expression of complement components, receptors and regulators by human dendritic cells. *Mol. Immunol.* *48*, 1121–1127.
- Liesenfeld, O. (2002). Oral infection of C57BL/6 mice with *Toxoplasma gondii*: a new model of inflammatory bowel disease? *J. Infect. Dis.* *185 Suppl 1*, S96-101.
- Lin, K.C., and Castro, A.C. (1998). Very late antigen 4 (VLA4) antagonists as anti-inflammatory agents. *Curr. Opin. Chem. Biol.* *2*, 453–457.

- Liszewski, M.K., Kolev, M., Le Friec, G., Leung, M., Bertram, P.G., Fara, A.F., Subias, M., Pickering, M.C., Drouet, C., Meri, S., et al. (2013). Intracellular complement activation sustains T cell homeostasis and mediates effector differentiation. *Immunity* 39, 1143–1157.
- Liu, C.-H., Fan, Y., Dias, A., Esper, L., Corn, R.A., Bafica, A., Machado, F.S., and Aliberti, J. (2006). Cutting edge: dendritic cells are essential for in vivo IL-12 production and development of resistance against *Toxoplasma gondii* infection in mice. *J. Immunol. Baltim. Md 1950* 177, 31–35.
- Lu, F., Huang, S., Hu, M.S., and Kasper, L.H. (2005). Experimental ocular toxoplasmosis in genetically susceptible and resistant mice. *Infect. Immun.* 73, 5160–5165.
- Lubbers, R., van Essen, M.F., van Kooten, C., and Trouw, L.A. (2017). Production of complement components by cells of the immune system. *Clin. Exp. Immunol.* 188, 183–194.
- Lucas, M., Schachterle, W., Oberle, K., Aichele, P., and Diefenbach, A. (2007). Dendritic cells prime natural killer cells by trans-presenting interleukin 15. *Immunity* 26, 503–517.
- Malnati, M.S., Lusso, P., Ciccone, E., Moretta, A., Moretta, L., and Long, E.O. (1993). Recognition of virus-infected cells by natural killer cell clones is controlled by polymorphic target cell elements. *J. Exp. Med.* 178, 961–969.
- Mandal, A., and Viswanathan, C. (2015). Natural killer cells: In health and disease. *Hematol. Oncol. Stem Cell Ther.* 8, 47–55.
- Masek, K.S., and Hunter, C.A. (2013). Pro-Inflammatory Responses in Macrophages during *Toxoplasma gondii* Infection (Landes Bioscience).
- Mason, N.J., Fiore, J., Kobayashi, T., Masek, K.S., Choi, Y., and Hunter, C.A. (2004). TRAF6-dependent mitogen-activated protein kinase activation differentially regulates the production of interleukin-12 by macrophages in response to *Toxoplasma gondii*. *Infect. Immun.* 72, 5662–5667.
- Master Sankar Raj, V., Gordillo, R., and Chand, D.H. (2016). Overview of C3 Glomerulopathy. *Front. Pediatr.* 4.
- Mavropoulos, A., Sully, G., Cope, A.P., and Clark, A.R. (2005). Stabilization of IFN-gamma mRNA by MAPK p38 in IL-12- and IL-18-stimulated human NK cells. *Blood* 105, 282–288.
- Meira, C.S., Pereira-Chiocola, V.L., Vidal, J.E., de Mattos, C.C.B., Motoie, G., Costa-Silva, T.A., Gava, R., Frederico, F.B., de Mattos, L.C., and *Toxoplasma* Groups (2014). Cerebral and ocular toxoplasmosis related with IFN- γ , TNF- α , and IL-10 levels. *Front. Microbiol.* 5, 492.
- Minta, J.O., and Man, D.P. (1977). Cleavage of human C5 by trypsin: characterization of the digestion products by gel electrophoresis. *J. Immunol. Baltim. Md 1950* 119, 1597–1602.
- Mollnes, T.E., Brekke, O.-L., Fung, M., Fure, H., Christiansen, D., Bergseth, G., Videm, V., Lappegård, K.T., Köhl, J., and Lambris, J.D. (2002). Essential role of the C5a receptor in E coli-induced oxidative burst and phagocytosis revealed by a novel lepirudin-based human whole blood model of inflammation. *Blood* 100, 1869–1877.
- Monk, P.N., and Partridge, L.J. (1993). Characterization of a complement-fragment-C5a-stimulated calcium-influx mechanism in U937 monocytic cells. *Biochem. J.* 295, 679–684.
- Monk, P.N., Scola, A.-M., Madala, P., and Fairlie, D.P. (2007). Function, structure and therapeutic potential of complement C5a receptors. *Br. J. Pharmacol.* 152, 429–448.

- Mordue, D.G., and Sibley, L.D. (1997). Intracellular fate of vacuoles containing *Toxoplasma gondii* is determined at the time of formation and depends on the mechanism of entry. *J. Immunol. Baltim. Md 1950* *159*, 4452–4459.
- Mordue, D.G., and Sibley, L.D. (2003). A novel population of Gr-1+ activated macrophages induced during acute toxoplasmosis. *J. Leukoc. Biol.* *74*, 1015–1025.
- Morgan, B.P., and Gasque, P. (1997). Extrahepatic complement biosynthesis: where, when and why? *Clin. Exp. Immunol.* *107*, 1–7.
- Mun, H.-S., Aosai, F., Norose, K., Piao, L.-X., Fang, H., Akira, S., and Yano, A. (2005). Toll-Like Receptor 4 Mediates Tolerance in Macrophages Stimulated with *Toxoplasma gondii*-Derived Heat Shock Protein 70. *Infect. Immun.* *73*, 4634–4642.
- Murphy, K., and Weaver, C. (2016). *Janeway's Immunobiology*, 9th edition (Garland Science).
- Nakao, M., and Konishi, E. (1991). Proliferation of *Toxoplasma gondii* in human neutrophils in vitro. *Parasitology* *103 Pt 1*, 23–27.
- Nakaoka, Y., and Komuro, I. (2013). Gab Docking Proteins in Cardiovascular Disease, Cancer, and Inflammation. *Int. J. Inflamm.* *2013*.
- Narni-Mancinelli, E., Jaeger, B.N., Bernat, C., Fenis, A., Kung, S., De Gassart, A., Mahmood, S., Gut, M., Heath, S.C., Estellé, J., et al. (2012). Tuning of natural killer cell reactivity by NKp46 and Helios calibrates T cell responses. *Science* *335*, 344–348.
- Narni-Mancinelli, E., Gauthier, L., Baratin, M., Guia, S., Fenis, A., Deghmane, A.-E., Rossi, B., Fourquet, P., Escalière, B., Kerdiles, Y.M., et al. (2017). Complement factor P is a ligand for the natural killer cell-activating receptor NKp46. *Sci. Immunol.* *2*.
- Nathan, C.F., Murray, H.W., Wiebe, M.E., and Rubin, B.Y. (1983). Identification of interferon-gamma as the lymphokine that activates human macrophage oxidative metabolism and antimicrobial activity. *J. Exp. Med.* *158*, 670–689.
- Neal, L.M., and Knoll, L.J. (2014). *Toxoplasma gondii* Profilin Promotes Recruitment of Ly6Chi CCR2+ Inflammatory Monocytes That Can Confer Resistance to Bacterial Infection. *PLOS Pathog.* *10*, e1004203.
- Nishida, K., and Hirano, T. (2003). The role of Gab family scaffolding adapter proteins in the signal transduction of cytokine and growth factor receptors. *Cancer Sci.* *94*, 1029–1033.
- Nishida, K., Wang, L., Morii, E., Park, S.J., Narimatsu, M., Itoh, S., Yamasaki, S., Fujishima, M., Ishihara, K., Hibi, M., et al. (2002). Requirement of Gab2 for mast cell development and KitL/c-Kit signaling. *Blood* *99*, 1866–1869.
- Ohno, M., Hirata, T., Enomoto, M., Araki, T., Ishimaru, H., and Takahashi, T.A. (2000). A putative chemoattractant receptor, C5L2, is expressed in granulocyte and immature dendritic cells, but not in mature dendritic cells. *Mol. Immunol.* *37*, 407–412.
- Oikonomopoulou, K., DeAngelis, R.A., Chen, H., Diamandis, E.P., Hollenberg, M.D., Ricklin, D., and Lambris, J.D. (2013). Induction of complement C3a receptor responses by kallikrein-related peptidase 14. *J. Immunol. Baltim. Md 1950* *191*, 3858–3866.

- Okinaga, S., Slattery, D., Humbles, A., Zsengeller, Z., Morteau, O., Kinrade, M.B., Brodbeck, R.M., Krause, J.E., Choe, H.-R., Gerard, N.P., et al. (2003). C5L2, a non-signaling C5A binding protein. *Biochemistry* 42, 9406–9415.
- Orr, M.T., and Lanier, L.L. (2010). Natural killer cell education and tolerance. *Cell* 142, 847–856.
- Parker, S.J., Roberts, C.W., and Alexander, J. (1991). CD8+ T cells are the major lymphocyte subpopulation involved in the protective immune response to *Toxoplasma gondii* in mice. *Clin. Exp. Immunol.* 84, 207–212.
- Perianayagam, M.C., Balakrishnan, V.S., King, A.J., Pereira, B.J.G., and Jaber, B.L. (2002). C5a delays apoptosis of human neutrophils by a phosphatidylinositol 3-kinase-signaling pathway. *Kidney Int.* 61, 456–463.
- Plattner, F., Yarovinsky, F., Romero, S., Didry, D., Carlier, M.-F., Sher, A., and Soldati-Favre, D. (2008). *Toxoplasma* profilin is essential for host cell invasion and TLR11-dependent induction of an interleukin-12 response. *Cell Host Microbe* 3, 77–87.
- Playfair, J.H.L., and Chain, B.M. (2012). *Immunology at a Glance*, 10th Edition.
- Popp, R.A., Bailiff, E.G., Skow, L.C., Johnson, F.M., and Lewis, S.E. (1983). Analysis of a mouse alpha-globin gene mutation induced by ethylnitrosourea. *Genetics* 105, 157–167.
- Raby, A.-C., Holst, B., Davies, J., Colmont, C., Laumonnier, Y., Coles, B., Shah, S., Hall, J., Topley, N., Köhl, J., et al. (2011). TLR activation enhances C5a-induced pro-inflammatory responses by negatively modulating the second C5a receptor, C5L2. *Eur. J. Immunol.* 41, 2741–2752.
- Raetz, M., Kibardin, A., Sturge, C.R., Pifer, R., Li, H., Burstein, E., Ozato, K., Larin, S., and Yarovinsky, F. (2013). Cooperation of TLR2 and TLR11 in the IRF8-dependent IL-12 response to *Toxoplasma gondii* profilin. *J. Immunol. Baltim. Md 1950* 191, 4818–4827.
- Rajagopal, S., Rajagopal, K., and Lefkowitz, R.J. (2010). Teaching old receptors new tricks: biasing seven-transmembrane receptors. *Nat. Rev. Drug Discov.* 9, 373–386.
- Ramu, P., Tanskanen, R., Holmberg, M., Lähteenmäki, K., Korhonen, T.K., and Meri, S. (2007). The surface protease PgtE of *Salmonella enterica* affects complement activity by proteolytically cleaving C3b, C4b and C5. *FEBS Lett.* 581, 1716–1720.
- Raulet, D.H., and Vance, R.E. (2006). Self-tolerance of natural killer cells. *Nat. Rev. Immunol.* 6, 520–531.
- Regal, J.F., Hardy, T.M., Casey, F.B., and Chakrin, L.W. (1983). Effects of C5a on guinea pig lung: histamine release and mechanism of contraction. *Immunopharmacology* 5, 315–327.
- Reichmann, G., Walker, W., Villegas, E.N., Craig, L., Cai, G., Alexander, J., and Hunter, C.A. (2000). The CD40/CD40 ligand interaction is required for resistance to toxoplasmic encephalitis. *Infect. Immun.* 68, 1312–1318.
- Reis, E.S., Chen, H., Sfyroera, G., Monk, P.N., Köhl, J., Ricklin, D., and Lambris, J.D. (2012). C5a receptor-dependent cell activation by physiological concentrations of desarginated C5a: insights from a novel label-free cellular assay. *J. Immunol. Baltim. Md 1950* 189, 4797–4805.
- Remington, J.S. (1969). The present status of the IgM fluorescent antibody technique in the diagnosis of congenital toxoplasmosis. *J. Pediatr.* 75, 1116–1124.

- Remington, J.S., Miller, M.J., and Brownlee, I. (1968). IgM antibodies in acute toxoplasmosis. II. Prevalence and significance in acquired cases. *J. Lab. Clin. Med.* *71*, 855–866.
- Remington, J.S., Thulliez, P., and Montoya, J.G. (2004). Recent developments for diagnosis of toxoplasmosis. *J. Clin. Microbiol.* *42*, 941–945.
- Richards, A., Kathryn Liszewski, M., Kavanagh, D., Fang, C.J., Moulton, E., Fremeaux-Bacchi, V., Remuzzi, G., Noris, M., Goodship, T.H.J., and Atkinson, J.P. (2007). Implications of the initial mutations in membrane cofactor protein (MCP; CD46) leading to atypical hemolytic uremic syndrome. *Mol. Immunol.* *44*, 111–122.
- Rickert, R.C. (2005). Regulation of B lymphocyte activation by complement C3 and the B cell coreceptor complex. *Curr. Opin. Immunol.* *17*, 237–243.
- Ricklin, D., Reis, E.S., and Lambris, J.D. (2016). Complement in disease: a defence system turning offensive. *Nat. Rev. Nephrol.* *12*, 383–401.
- Riedemann, N.C., Guo, R.-F., Sarma, V.J., Laudes, I.J., Huber-Lang, M., Warner, R.L., Albrecht, E.A., Speyer, C.L., and Ward, P.A. (2002). Expression and Function of the C5a Receptor in Rat Alveolar Epithelial Cells. *J. Immunol.* *168*, 1919–1925.
- Riedemann, N.C., Guo, R.-F., Hollmann, T.J., Gao, H., Neff, T.A., Reuben, J.S., Speyer, C.L., Sarma, J.V., Wetsel, R.A., Zetoune, F.S., et al. (2004). Regulatory role of C5a in LPS-induced IL-6 production by neutrophils during sepsis. *FASEB J. Off. Publ. Fed. Am. Soc. Exp. Biol.* *18*, 370–372.
- Risitano, A.M. (2013). Paroxysmal nocturnal hemoglobinuria and the complement system: recent insights and novel anticomplement strategies. *Adv. Exp. Med. Biol.* *735*, 155–172.
- Rittirsch, D., Flierl, M.A., Nadeau, B.A., Day, D.E., Huber-Lang, M., Mackay, C.R., Zetoune, F.S., Gerard, N.P., Cianflone, K., Köhl, J., et al. (2008). Functional roles for C5a receptors in sepsis. *Nat. Med.* *14*, 551–557.
- Robben, P.M., LaRegina, M., Kuziel, W.A., and Sibley, L.D. (2005). Recruitment of Gr-1+ monocytes is essential for control of acute toxoplasmosis. *J. Exp. Med.* *201*, 1761–1769.
- Rodrigues, G.A., Falasca, M., Zhang, Z., Ong, S.H., and Schlessinger, J. (2000). A novel positive feedback loop mediated by the docking protein Gab1 and phosphatidylinositol 3-kinase in epidermal growth factor receptor signaling. *Mol. Cell. Biol.* *20*, 1448–1459.
- Rosowski, E.E., Nguyen, Q.P., Camejo, A., Spooner, E., and Saeij, J.P.J. (2014). *Toxoplasma gondii* Inhibits Gamma Interferon (IFN- γ)- and IFN- β -Induced Host Cell STAT1 Transcriptional Activity by Increasing the Association of STAT1 with DNA. *Infect. Immun.* *82*, 706–719.
- Russell, W.L., Kelly, E.M., Hunsicker, P.R., Bangham, J.W., Maddux, S.C., and Phipps, E.L. (1979). Specific-locus test shows ethylnitrosourea to be the most potent mutagen in the mouse. *Proc. Natl. Acad. Sci.* *76*, 5818–5819.
- Sabin, A.B., and Feldman, H.A. (1948). Dyes as Microchemical Indicators of a New Immunity Phenomenon Affecting a Protozoon Parasite (*Toxoplasma*). *Science* *108*, 660–663.
- de Saint-Vis, B., Fugier-Vivier, I., Massacrier, C., Gaillard, C., Vanbervliet, B., Ait-Yahia, S., Banchereau, J., Liu, Y.J., Lebecque, S., and Caux, C. (1998). The cytokine profile expressed by human dendritic cells is dependent on cell subtype and mode of activation. *J. Immunol. Baltim. Md 1950* *160*, 1666–1676.

- la Sala, A., Gadina, M., and Kelsall, B.L. (2005). G(i)-protein-dependent inhibition of IL-12 production is mediated by activation of the phosphatidylinositol 3-kinase-protein 3 kinase B/Akt pathway and JNK. *J. Immunol. Baltim. Md 1950* *175*, 2994–2999.
- Salinger, A.P., and Justice, M.J. (2008). Mouse Mutagenesis Using N-Ethyl-N-Nitrosourea (ENU). *Cold Spring Harb. Protoc.* *2008*, pdb.prot4985.
- Sarma, J.V., and Ward, P.A. (2012). New developments in C5a receptor signaling. *Cell Health Cytoskelet.* *4*, 73–82.
- Scanga, C.A., Aliberti, J., Jankovic, D., Tilloy, F., Bennouna, S., Denkers, E.Y., Medzhitov, R., and Sher, A. (2002). Cutting edge: MyD88 is required for resistance to *Toxoplasma gondii* infection and regulates parasite-induced IL-12 production by dendritic cells. *J. Immunol. Baltim. Md 1950* *168*, 5997–6001.
- Scharton-Kersten, T., Contursi, C., Masumi, A., Sher, A., and Ozato, K. (1997a). Interferon consensus sequence binding protein-deficient mice display impaired resistance to intracellular infection due to a primary defect in interleukin 12 p40 induction. *J. Exp. Med.* *186*, 1523–1534.
- Scharton-Kersten, T.M., Yap, G., Magram, J., and Sher, A. (1997b). Inducible nitric oxide is essential for host control of persistent but not acute infection with the intracellular pathogen *Toxoplasma gondii*. *J. Exp. Med.* *185*, 1261–1273.
- Scheid, C.R., Webster, R.O., Henson, P.M., and Findlay, S.R. (1983). Direct effect of complement factor C5a on the contractile state of isolated smooth muscle cells. *J. Immunol. Baltim. Md 1950* *130*, 1997–1999.
- Schreiber, R.D., and Feldman, H.A. (1980). Identification of the activator system for antibody to *Toxoplasma* as the classical complement pathway. *J. Infect. Dis.* *141*, 366–369.
- Schutzman, J.L., Borland, C.Z., Newman, J.C., Robinson, M.K., Kokel, M., and Stern, M.J. (2001). The *Caenorhabditis elegans* EGL-15 signaling pathway implicates a DOS-like multisubstrate adaptor protein in fibroblast growth factor signal transduction. *Mol. Cell. Biol.* *21*, 8104–8116.
- Scola, A.-M., Higginbottom, A., Partridge, L.J., Reid, R.C., Woodruff, T., Taylor, S.M., Fairlie, D.P., and Monk, P.N. (2007). The role of the N-terminal domain of the complement fragment receptor C5L2 in ligand binding. *J. Biol. Chem.* *282*, 3664–3671.
- Scola, A.-M., Johswich, K.-O., Morgan, B.P., Klos, A., and Monk, P.N. (2009). The human complement fragment receptor, C5L2, is a recycling decoy receptor. *Mol. Immunol.* *46*, 1149–1162.
- Seiffert, M., Custodio, J.M., Wolf, I., Harkey, M., Liu, Y., Blattman, J.N., Greenberg, P.D., and Rohrschneider, L.R. (2003). *Gab3*-deficient mice exhibit normal development and hematopoiesis and are immunocompetent. *Mol. Cell. Biol.* *23*, 2415–2424.
- Shen, F.W., Saga, Y., Litman, G., Freeman, G., Tung, J.S., Cantor, H., and Boyse, E.A. (1985). Cloning of *Ly-5* cDNA. *Proc. Natl. Acad. Sci. U. S. A.* *82*, 7360–7363.
- Sheppard, S., Schuster, I.S., Andoniou, C.E., Cocita, C., Adejumo, T., Kung, S.K.P., Sun, J.C., Degli-Esposti, M.A., and Guerra, N. (2018). The Murine Natural Cytotoxic Receptor NKp46/NCR1 Controls TRAIL Protein Expression in NK Cells and ILC1s. *Cell Rep.* *22*, 3385–3392.
- Sibley, L.D., Weidner, E., and Krahenbuhl, J.L. (1985). Phagosome acidification blocked by intracellular *Toxoplasma gondii*. *Nature* *315*, 416–419.

- Skokowa, J., Ali, S.R., Felda, O., Kumar, V., Konrad, S., Shushakova, N., Schmidt, R.E., Piekorz, R.P., Nürnberg, B., Spicher, K., et al. (2005). Macrophages induce the inflammatory response in the pulmonary Arthus reaction through G alpha i2 activation that controls C5aR and Fc receptor cooperation. *J. Immunol. Baltim. Md 1950* *174*, 3041–3050.
- Snyderman, R., and Pike, M.C. (1984). Chemoattractant receptors on phagocytic cells. *Annu. Rev. Immunol.* *2*, 257–281.
- Sojka, D.K., Tian, Z., and Yokoyama, W.M. (2014). Tissue-resident natural killer cells and their potential diversity. *Semin. Immunol.* *26*, 127–131.
- Sousa, C.R. e, Hieny, S., Schariton-Kersten, T., Jankovic, D., Charest, H., Germain, R.N., and Sher, A. (1997). In Vivo Microbial Stimulation Induces Rapid CD40 Ligand-independent Production of Interleukin 12 by Dendritic Cells and their Redistribution to T Cell Areas. *J. Exp. Med.* *186*, 1819–1829.
- Srivastava, S., Pelloso, D., Feng, H., Voiles, L., Lewis, D., Haskova, Z., Whitacre, M., Trulli, S., Chen, Y.-J., Toso, J., et al. (2013). Effects of interleukin-18 on natural killer cells: costimulation of activation through Fc receptors for immunoglobulin. *Cancer Immunol. Immunother. CII* *62*, 1073–1082.
- Strainic, M.G., Liu, J., Huang, D., An, F., Lalli, P.N., Muqim, N., Shapiro, V.S., Dubyak, G.R., Heeger, P.S., and Medof, M.E. (2008). Locally Produced Complement Fragments C5a and C3a Provide Both Costimulatory and Survival Signals to Naive CD4+ T Cells. *Immunity* *28*, 425–435.
- Subauste, C.S., Dawson, L., and Remington, J.S. (1992). Human lymphokine-activated killer cells are cytotoxic against cells infected with *Toxoplasma gondii*. *J. Exp. Med.* *176*, 1511–1519.
- Sukhumavasi, W., Egan, C.E., Warren, A.L., Taylor, G.A., Fox, B.A., Bzik, D.J., and Denkers, E.Y. (2008). Toll-Like Receptor Adaptor MyD88 is Essential for Pathogen Control During Oral *Toxoplasma gondii* Infection but not Adaptive Immunity Induced by a Vaccine Strain of the Parasite. *J. Immunol. Baltim. Md 1950* *181*, 3464–3473.
- Summerfield, A., and McCullough, K.C. (2009). Dendritic Cells in Innate and Adaptive Immune Responses against Influenza Virus. *Viruses* *1*, 1022–1034.
- Swamydas, M., and Lionakis, M.S. (2013). Isolation, Purification and Labeling of Mouse Bone Marrow Neutrophils for Functional Studies and Adoptive Transfer Experiments. *J. Vis. Exp. JoVE*.
- Swann, J.B., Hayakawa, Y., Zerafa, N., Sheehan, K.C.F., Scott, B., Schreiber, R.D., Hertzog, P., and Smyth, M.J. (2007). Type I IFN Contributes to NK Cell Homeostasis, Activation, and Antitumor Function. *J. Immunol.* *178*, 7540–7549.
- Taylor, G.A., Collazo, C.M., Yap, G.S., Nguyen, K., Gregorio, T.A., Taylor, L.S., Eagleson, B., Secret, L., Southon, E.A., Reid, S.W., et al. (2000). Pathogen-specific loss of host resistance in mice lacking the IFN-gamma-inducible gene IGTP. *Proc. Natl. Acad. Sci. U. S. A.* *97*, 751–755.
- Thompson, M.R., Kaminski, J.J., Kurt-Jones, E.A., and Fitzgerald, K.A. (2011). Pattern Recognition Receptors and the Innate Immune Response to Viral Infection. *Viruses* *3*, 920–940.
- Tosh, K.W., Mittereder, L., Bonne-Annee, S., Hieny, S., Nutman, T.B., Singer, S.M., Sher, A., and Jankovic, D. (2016). The IL-12 response of primary human DC and monocytes to *Toxoplasma gondii* is stimulated by phagocytosis of live parasites rather than host cell invasion. *J. Immunol. Baltim. Md 1950* *196*, 345–356.

- Trinchieri, G. (2003). Interleukin-12 and the regulation of innate resistance and adaptive immunity. *Nat. Rev. Immunol.* *3*, 133–146.
- Ueno, N., Lodoen, M.B., Hickey, G.L., Robey, E.A., and Coombes, J.L. (2015). *Toxoplasma gondii*-infected natural killer cells display a hypermotility phenotype in vivo. *Immunol. Cell Biol.* *93*, 508–513.
- Une, C., Andersson, J., and Orn, A. (2003). Role of IFN- α / β and IL-12 in the activation of natural killer cells and interferon- γ production during experimental infection with *Trypanosoma cruzi*. *Clin. Exp. Immunol.* *134*, 195–201.
- Verstraelen, S., Bloemen, K., Nelissen, I., Witters, H., Schoeters, G., and Van Den Heuvel, R. (2008). Cell types involved in allergic asthma and their use in in vitro models to assess respiratory sensitization. *Toxicol. Vitro Int. J. Publ. Assoc. BIBRA* *22*, 1419–1431.
- Viaud, S., Terme, M., Flament, C., Taieb, J., André, F., Novault, S., Escudier, B., Robert, C., Caillat-Zucman, S., Tursz, T., et al. (2009). Dendritic cell-derived exosomes promote natural killer cell activation and proliferation: a role for NKG2D ligands and IL-15 α . *PLoS One* *4*, e4942.
- Vignali, D.A.A., and Kuchroo, V.K. (2012). IL-12 family cytokines: immunological playmakers. *Nat. Immunol.* *13*, 722–728.
- Vivier, E., Tomasello, E., Baratin, M., Walzer, T., and Ugolini, S. (2008). Functions of natural killer cells. *Nat. Immunol.* *9*, 503–510.
- Walport, M.J. (2001a). Complement. First of two parts. *N. Engl. J. Med.* *344*, 1058–1066.
- Walport, M.J. (2001b). Complement. Second of two parts. *N. Engl. J. Med.* *344*, 1140–1144.
- Wang, H., Ricklin, D., and Lambris, J.D. (2017a). Complement-activation fragment C4a mediates effector functions by binding as untethered agonist to protease-activated receptors 1 and 4. *Proc. Natl. Acad. Sci. U. S. A.* *114*, 10948–10953.
- Wang, W., Erbe, A.K., Hank, J.A., Morris, Z.S., and Sondel, P.M. (2015). NK Cell-Mediated Antibody-Dependent Cellular Cytotoxicity in Cancer Immunotherapy. *Front. Immunol.* *6*.
- Wang, Z.-D., Liu, H.-H., Ma, Z.-X., Ma, H.-Y., Li, Z.-Y., Yang, Z.-B., Zhu, X.-Q., Xu, B., Wei, F., and Liu, Q. (2017b). *Toxoplasma gondii* Infection in Immunocompromised Patients: A Systematic Review and Meta-Analysis. *Front. Microbiol.* *8*.
- Weidner, K.M., Di Cesare, S., Sachs, M., Brinkmann, V., Behrens, J., and Birchmeier, W. (1996). Interaction between Gab1 and the c-Met receptor tyrosine kinase is responsible for epithelial morphogenesis. *Nature* *384*, 173–176.
- Weller, P.F. (1994). Eosinophils: structure and functions. *Curr. Opin. Immunol.* *6*, 85–90.
- Wiegner, R., Chakraborty, S., and Huber-Lang, M. (2016). Complement-coagulation crosstalk on cellular and artificial surfaces. *Immunobiology* *221*, 1073–1079.
- Wilson, D.C., Grotenbreg, G.M., Liu, K., Zhao, Y., Frickel, E.-M., Gubbels, M.-J., Ploegh, H.L., and Yap, G.S. (2010). Differential regulation of effector- and central-memory responses to *Toxoplasma gondii* Infection by IL-12 revealed by tracking of Tgd057-specific CD8⁺ T cells. *PLoS Pathog.* *6*, e1000815.
- Wong, E.K.S., and Kavanagh, D. (2018). Diseases of complement dysregulation—an overview. *Semin. Immunopathol.* *40*, 49–64.

- Wrann, C.D., Tabriz, N.A., Barkhausen, T., Klos, A., van Griensven, M., Pape, H.C., Kendoff, D.O., Guo, R., Ward, P.A., Krettek, C., et al. (2007). The phosphatidylinositol 3-kinase signaling pathway exerts protective effects during sepsis by controlling C5a-mediated activation of innate immune functions. *J. Immunol. Baltim. Md 1950* *178*, 5940–5948.
- Xiao, J., Li, Y., Gressitt, K.L., He, H., Kannan, G., Schultz, T.L., Svezhova, N., Carruthers, V.B., Pletnikov, M.V., Yolken, R.H., et al. (2016). Cerebral complement C1q activation in chronic *Toxoplasma* infection. *Brain. Behav. Immun.*
- Xu, R., Lin, F., Bao, C., Huang, H., Ji, C., Wang, S., Jin, L., Sun, L., Li, K., Zhang, Z., et al. (2016). Complement 5a receptor-mediated neutrophil dysfunction is associated with a poor outcome in sepsis. *Cell. Mol. Immunol.* *13*, 103–109.
- Yan, C., and Gao, H. (2012). New insights for C5a and C5a receptors in sepsis. *Front. Immunol.* *3*.
- Yao, J., Harvath, L., Gilbert, D.L., and Colton, C.A. (1990). Chemotaxis by a CNS macrophage, the microglia. *J. Neurosci. Res.* *27*, 36–42.
- Yarovinsky, F. (2014). Innate immunity to *Toxoplasma gondii* infection. *Nat. Rev. Immunol.* *14*, 109–121.
- Yarovinsky, F., and Sher, A. (2006). Toll-like receptor recognition of *Toxoplasma gondii*. *Int. J. Parasitol.* *36*, 255–259.
- Yarovinsky, F., Zhang, D., Andersen, J.F., Bannenberg, G.L., Serhan, C.N., Hayden, M.S., Hieny, S., Sutterwala, F.S., Flavell, R.A., Ghosh, S., et al. (2005). TLR11 activation of dendritic cells by a protozoan profilin-like protein. *Science* *308*, 1626–1629.
- Zamai, L., Ahmad, M., Bennett, I.M., Azzoni, L., Alnemri, E.S., and Perussia, B. (1998). Natural Killer (NK) Cell-mediated Cytotoxicity: Differential Use of TRAIL and Fas Ligand by Immature and Mature Primary Human NK Cells. *J. Exp. Med.* *188*, 2375–2380.
- Zhang, S., and Kaplan, M.H. (2000). The p38 mitogen-activated protein kinase is required for IL-12-induced IFN-gamma expression. *J. Immunol. Baltim. Md 1950* *165*, 1374–1380.

6 APPENDIX

6.1 Abbreviations

Abbreviation	Explanation
KO	Knock-out
°C	Degree Celsius
%	Percent
AF	Alexa Fluor®
APC	Allophycocyanin
APC	Antigen-presenting cell
BMDC	Bone marrow derived DC
BSA	Bovine serum albumin
C5aR1	C5a receptor 1
C5aR2	C5a receptor 2
CD	Cluster of differentiation
cDC	Conventional DC
CFSE	Carboxyfluorescein succinimidyl ester
DAMP	Danger associated molecular pattern
DC	Dendritic cell
EDTA	Ethylenediaminetetraacetate
ELISA	Enzyme-linked immunosorbent assay
Et al	At alii
FACS	Fluorescence activated cell sorting
FITC	Fluorescein isothiocyanate
FSC	Forward scatter
g	Gram (unit)

Abbreviation	Explanation
μl	Microliter
ENU	N-ethyl-N-nitrosourea
Flx	Floxed (flanked by LoxP)
g	Gravity
GAB	Grb2-associated binder family
GFP	Green fluorescent protein
GM-CSF	Granulocyte-macrophage colony-stimulating factor
GPCR	G-protein coupled receptor
h	Hour
Hi	High
i.e.	In example
i.p.	Intraperitoneal
Int	Intermediate
IVC	Individually ventilated cage
Lo	Low
LPS	Lipopolysaccharide
MACS	Magnetic associated cell sorting
mg	Milligram
MHC	Major histocompatibility complex
min	Minute
ml	Milliliter
moDC	Monocyte-derived DC
MyD88	Myeloid differentiation primary response gene 88

Abbreviation	Explanation
NK	Natural killer
PAMP	Pathogen-associated molecular pattern
PBS	Phosphate buffered saline
PCR	Polymerase chain reaction
PE	Phycoerythrin
PerCP	Peridinin chlorophyll
Rec	Recombinant
Rpm	Rounds per minute
RT	Room temperature
SD	Standard deviation
SEM	Standard error of the mean
SSC	Side scatter
STAg	Soluble toxoplasma antigen
<i>T. gondii</i>	<i>Toxoplasma gondii</i>
Td-Tomato	Tandem-Tomato
TLR	Toll-like receptor
TM	Trademark
TNF	Tumor necrosis factor
USA	United States of America
WT	Wild type

6.2 Figures

Figure 1: Overview of innate and adaptive immune responses. Shown are major cell types and humoral components of both parts. The fast reacting innate immune system (left) consists of humoral factors (complement) and cell components, that act as a first line defense system. The adaptive immune response (right) is characterized by a slower but individual response and comprises B cells, T cells and antibodies. DCs and NK cells show characteristics of both parts and the complement system is able to regulate cells from the adaptive immune system. From Playfair and Chain, 2012.....3

Figure 2: Complement activation and regulation. Complement activation can occur via three different pathways: classical, lectin or alternative pathway. All pathways lead to the cleavage of C3 and C5 via C3 (C4bC2a, C3bBb) or C5 (C4bC2aC3b, C3bBbC3b) convertases. The cleavage products C3a and C5a are important anaphylatoxins inducing cell recruitment or activation. C3b is necessary for opsonization of pathogens. C3b and its further degradation products can bind various complement receptors (CRs). At the end of the complement cascade the membrane attack complex (MAC) (C5b-9) is formed to induce pore formation in the pathogen. MBL=mannose binding lectin; MASP=MBL-associated serine protease; FB=factor B; FP=factor P; FD=factor D; FH=factor H; C1INH=C1 inhibitor; FI=factor I; C4BP=C4 binding protein; CR=complement receptor; Modified from Lubbers et al., 2017.5

Figure 3: Diagram of a classical model of a seven transmembrane receptor with associated G protein and β -arrestin molecules. From Sarma and Ward, 2012.10

Figure 4: IL-12 cytokine family, receptors and signaling components. The IL-12 family comprises the heterodimeric cytokines IL-12, IL-23, IL-27 and IL-35. They consist of an α -chain (p19, p28, p35) and a β -chain (p40 or Ebi3). These cytokines exert their functions upon binding to heterodimeric receptors and involve distinct JAK-STAT signaling partners. The bottom bar reflects their functional spectrum ranging from pro-inflammatory (IL-23, IL-12) to inhibitory (IL-35). From Vignali and Kuchroo, 2012. .12

Figure 5: The balance of inhibitory and stimulatory signals received by NK cells. Cells under naïve conditions are protected from killing when stimulatory signals are counter-balanced by inhibitory signals delivered by MHC I. Missing MHC I expression results in activation of the NK cell and killing of the target cell (missing-self recognition). Modified from Raulet and Vance, 2006.14

Figure 6: DC-induced NK cell activation. DCs can affect NK cell function by augmentation of cytotoxicity, cytokine secretion (IFN- γ and TNF- α), and proliferation. This depends on contact-dependent (ligation of Nkp46, Nkp30, NKG2D, 2B4) as well as soluble factors (IL-2, IL-12, IL-15, IL-18, IFN- α , and IFN- β). IFN- γ secretion by NK cells is, in turn, responsible for DC maturation and Th1 polarization, whereas augmentation of NK cell cytotoxicity contributes to tumor cell lysis. From Elssen et al., 2014.....15

Figure 7: Life cycle of *T. gondii*. Cats are the definitive host, in which sexual replication takes place: male and female gametes are formed within the host cell. Fusion of gametes leads to the formation of diploid oocysts that are shed in cat feces and undergo meiosis in the environment. Oocysts can survive

in the environment for long periods and can contaminate food and water, which is consumed by intermediate hosts. In intermediate hosts (here: rodents) asexual replication occurs. Acute infection is characterized by fast replicating tachyzoites that disseminate throughout the body. Activation of the immune system is leading to the differentiation into slow-replicating bradyzoites that are stored in tissue cysts and characterize the chronic infection. Humans become infected by eating undercooked meat from farming animals containing cysts or by consuming cat feces-contaminated water. Although in immunocompetent individuals, infections are mild, immunocompromised humans can develop severe symptoms leading to brain damage or blindness. From Hunter and Sibley, 2012.....17

Figure 8: Immune response to *T. gondii* infection. IFN- γ is crucial for survival of the host during *Toxoplasma gondii* infection. Production of this cytokine by NK-cells is dependent on TLR11-mediated recognition of *T. gondii* profilin by DCs. Neutrophils provide an important innate source for IFN- γ ; the mechanisms that regulate neutrophil-derived IFN- γ are not well understood because this IFN- γ is not regulated by TLRs or by IL-12. Macrophages are primed with the IFN- γ to destruct the parasite and limit replication. In later stages of the infection, DCs also prime T cells to produce IFN- γ . From Yarovinsky, 2014.18

Figure 9: Schematic structures of Gab family docking proteins. Shown are the schematic domain structures of three human Gab proteins (Gab1–3). All Gab proteins consist of a highly conserved N-terminal PH domain that is involved in membrane targeting. The central proline-rich regions mediate the association with SH3 domain-containing adaptor proteins such as Grb2. PH=Pleckstrin homology; P=Proline From Nakaoka and Komuro, 2013.....24

Figure 10: Overview of Gab1, Gab2 and Gab3 regarding molecular weight, expression, tyrosine phosphorylation and consequences of expression deficiency. Reviewed in (Nishida and Hirano, 2003)26

Figure 11: Gab protein recruitment mechanisms. **a)** Recruitment via MBS and Grb2–Gab1 complexes. Shown is a schematic of Gab1 recruitment to the HGF receptor. Gab1 can bind directly to the HGF receptor (HGFR) through its Met-binding sequence (MBS), as well as indirectly, as part of a Grb2–Gab1 complex, to a Grb2 SH2 domain binding site in the HGFR. **b)** Recruitment via Shc–Grb2–Gab2. Gab2 is recruited to IL3/GM-CSF/IL-5 receptor family by means of a Shc–Grb2–Gab2 complex. **c)** Recruitment via another scaffolding adaptor. In FGF receptor signaling, Gab1 is recruited to the receptor complex via Grb2 binding to the scaffolding adaptor FRS2. **d)** Recruitment via Gab family PH domains. In some signaling pathways, binding of the Gab PH domain to appropriate phosphoinositides is required for initial recruitment to receptor complexes or for sustained signaling (e.g. EGFR). **e)** Recruitment of Gab proteins to oncoproteins. Gab proteins are phosphorylated in response to several oncogenic stimuli. Recruitment of Gab2 to Y177 of Bcr–Abl as part of a Grb2–Gab2 complex. Abbreviations: BCR, B-cell receptor; EGFR, epidermal growth factor receptor; GM-CSF, granulocyte–macrophage

colony-stimulating factor; IL, interleukin; PH, pleckstrin-homology; PI3K, phosphoinositide 3-kinase; SH2, Src-homology 2; Yp, phosphotyrosine. From Gu and Neel, 2003.	27
Figure 12: ENU treatment of C57BL/6 mice. Each G1 male is bred with 2 G2 females. Subsequently from each G2 female 3 G3 offspring are tested in recessive screens. From Hoebe, 2009.	39
Figure 13: Generation of mixed BM chimeric mice. Mixed BM were created by combining BM cells from two different donors: CD45.1 ⁺ WT mice and CD45.2 ⁺ Gab3 ^{R27C} mice. Mixed BM cells were then i.v. injected into two different recipients (CD45.1 ⁺ WT mice and CD45.2 ⁺ WT mice) which had been UV-irradiated before to deplete immune cells. After 29 days of recovery, recipient mice were euthanized to analyze cell composition in different compartments.	40
Figure 14: <i>T. gondii</i> cyst in brain suspension at 40-fold magnification under a phase contrast microscope.	41
Figure 15: <i>T. gondii</i> infection models. Mice were infected with either 10 cysts i.p. or 1-10 cysts orally. The immune reaction was analyzed during the acute phase of the infection between days 1 and 7 p.i. in spleen, blood, peritoneal cavity and lung or during the chronic phase 30 days p.i. in the brain.	42
Figure 16: Gating strategy for sorting NK cells from the spleen depicted as dot plots. A) Excluding cell debris. B) + C) excluding cell doublets. D) Gating on living cells. E) Gating on NK cells as NK1.1 ⁺ NKp46 ⁺ cells (left) or NK1.1 ⁺ CDe3 ⁻ cells (right).	47
Figure 17: Gating strategy depicted as dot plots. A) Gate setting to exclude small particles and cell debris. Gating for single cells to exclude cell doublets using B) FSC-A and FSC-H and C) SSC-A and SSC-H.	48
Figure 18: The development of weight loss, disease score and survival after oral <i>T. gondii</i> infection with 10 cysts is more dominant in WT than in C5aR1 ^{-/-} or C5aR2 ^{-/-} mice. Changes in (A) absolute and (B) relative weight during 20 days after p.i. with 10 <i>T. gondii</i> cysts. Groups indicated with † had to be sacrificed due to weight loss of more than 20 % of initial weight. (C) Disease score during infection. (D) Survival. n=10/group for all graphs; Values show the mean ± SEM (A-C). Statistical analyses were determined by ANOVA (A-C) or Log-rank (Mantel Cox) test (D). Groups indicated with † had to be sacrificed due to weight loss of more than 20 % of initial weight (dashed line in (B)) or disease score of ≥4 (dashed line in (C)) or died during the experiment.	51
Figure 19: Inflammatory cell infiltration and tissue damage score in WT, C5aR1 ^{-/-} and C5aR2 ^{-/-} mice after seven days of oral <i>T. gondii</i> infection. Scoring results from paraffin-embedded tissue sections of the ileum (left) and jejunum (right) from orally infected WT, C5aR1 ^{-/-} and C5aR2 ^{-/-} mice 7 days p.i. Scoring includes tissue destruction and cell infiltration. Statistical analyses were determined by ANOVA. Values show the mean ± SEM. n=3/group.	53
Figure 20: Impact of parasite infection dose on disease development in oral <i>T. gondii</i> infection. Oral infection of WT mice with 1, 3, 5, 7, 10 <i>T. gondii</i> cysts. Absolute (A) and relative weight (B) over 15 days	

p.i. **(C)** Disease score during infection. Groups indicated with † had to be sacrificed due to weight loss of more than 20 % of initial weight or died during the experiment. **(D)** Animal survival; n=5/group for all graphs. Values show the mean ± SEM (A-C). Statistical analyses were determined by ANOVA (A-C) and by Log-rank (Mantel Cox) test (D). Groups indicated with † had to be sacrificed due to termination criteria weight loss of more than 20 % of initial weight (dashed line in B) or disease score of ≥4 (dashed line in C) or died during the experiment.54

Figure 21: Impact of parasite infection dose on IL-12p40 and IFN- γ production on day 5 **(A, B)** and day 7 **(C, D)** p.i. to compare the cytokine production relative to the parasite infection dose. IL-12p40 **(A)** and IFN- γ **(B)** production significantly increases after the infection with 1 cyst and 10 cysts 5 days p.i. IL-12p40 production **(C)** significantly increases after infection with 5 cysts compared to 1 cyst 7 days p.i., whereas the IFN- γ production **(D)** significantly increases after infection with 3, 5, 7 and 10 cysts compared to the infection with 1 cyst. Cytokine concentrations from uninfected mice were below the detection limit and are not shown. Values show the mean ± SEM; n=5/group for all graphs. *p<0.05; **p<0.01; ***p<0.001 (ANOVA).55

Figure 22: Impact of parasite infection dose on IL-12p40 and IFN- γ production to compare the difference between day 5 and day 7 p.i. Serum cytokine levels for **(A)** IL-12p40 and **(B)** IFN- γ in response to infection using 1, 3, 5, 7, 10 cysts on day 5 and 7 p.i. Values show the mean ± SEM. n=5/group; asterisks indicate significance between day 5 and day 7; *p<0.05; **p<0.01; ***p<0.001; ****p<0.0001 (ANOVA).56

Figure 23: The number and the frequency of GFP-C5aR1⁺ mice is increased in the peritoneal cavity, spleen and lung, but not in blood seven days after peritoneal *T. gondii* infection. GFP-C5aR1^{fl/fl} mice were infected i.p. with 50 *T. gondii* cysts and sacrificed on day 7 p.i. Uninfected WT mice served as controls. **(A)** Flow cytometric analysis of the GFP-C5aR1 signal in cells from blood, peritoneal cavity, spleen and lung. Dot plots depict the GFP-C5aR1 signal in WT, uninfected GFP-C5aR1^{fl/fl} and infected GFP-C5aR1^{fl/fl} mice. **(B)** Cell counts of GFP-C5aR1 positive cells in blood, peritoneal cavity, spleen and lung. **(C)** Graphs show the percentage of GFP-C5aR1 positive cells in blood, peritoneal cavity, spleen and lung. Values show the mean ± SEM; n = 5-10. Results are from three independent experiments. Statistical differences between groups were assessed by student t test. *p<0.05, **p<0.01, ***p<0.000158

Figure 24: The number and frequency of td-Tomato-C5aR2⁺ cells increased in the blood and the spleen, but not in the peritoneal cavity and the lung after peritoneal *T. gondii* infection. Td-Tomato-C5aR2^{fl/fl} mice infected i.p. with 50 *T. gondii* cysts and sacrificed on day 7 p.i. Uninfected WT mice served as controls. **(A)** Flow cytometric analysis of the tdTomato-C5aR2 signal in cells from blood, peritoneal cavity, spleen and lung. Dot plots depict the tdTomato-C5aR2 signal in WT, uninfected tdTomato-C5aR2^{fl/fl} and infected tdTomato-C5aR2^{fl/fl} mice. **(B)** Cell counts of tdTomato-C5aR2-positive

cells in blood, peritoneal cavity, spleen and lung. **(C)** Frequency of tdTomato-C5aR2-positive cells in blood, peritoneal cavity, spleen and lung as measured by flow cytometry. Values show the mean \pm SEM; n = 5-10. Results are from three independent experiments. Statistical differences between groups were assessed by students t-test; *p<0.05, **p<0.01, ***p<0.00160

Figure 25: Frequency of GFP-C5aR1 and tdTomato-C5aR2-expressing cells in different tissues under steady state conditions and infectious conditions are regulated differently. Frequencies of C5aR1-GFP⁺ and C5aR2-tdTomato⁺ cells in **(A)** blood, **(B)** peritoneal cavity, **(C)** spleen and **(D)** lung in samples from uninfected (black) or infected (red) mice. Values show the mean \pm SEM. n=5-11. Results are from three independent experiments. Statistical differences between groups were assessed by ANOVA. ***p<0.001; ****p<0.0001.....61

Figure 26: Cell numbers of GFP-C5aR1 and tdTomato-C5aR2-expressing cells in different tissues under steady state conditions and infectious conditions also regulated differently. Cell numbers of C5aR1-GFP⁺ and C5aR2-tdTomato⁺ cells in **(A)** blood, **(B)** peritoneal cavity, **(C)** spleen and **(D)** lung in samples from uninfected (black) or infected (red) mice. Values show the mean \pm SEM. n=5-11. Results are from three independent experiments. Statistical differences between groups were assessed by ANOVA. ***p<0.001;.....62

Figure 27: NK cells from blood, peritoneal cavity, spleen and lung express tdTomato-C5aR2, but not GFP-C5aR1 under steady state conditions and seven days after i.p. infection with *T. gondii*. **(A)** NK cells were identified as NK1.1⁺NKp46⁺ cells. Depicted is the dot plot from an uninfected spleen sample. Frequencies **(B)** and cell counts **(C)** of NK cells in non-infected and infected reporter mice shown as percentage of living cells. **(D)** Flow cytometric analysis of GFP-C5aR1 (upper histograms) and tdTomato-C5aR2 (lower histograms) expression in NK cells from blood, peritoneal cavity, spleen and lung of non-infected WT mice (gray histograms), non-infected (dashed line) and infected (solid line) C5aR1/2 reporter mice. **(E+F)** Frequencies of GFP-C5aR1⁺ and tdTomato-C5aR2⁺ NK cells in blood, peritoneal cavity, spleen and lung under steady state conditions and upon i.p. infection with *T. gondii*. **(G+H)** cell counts of GFP-C5aR1⁺ and tdTomato-C5aR2⁺ NK cells in blood, peritoneal cavity, spleen and lung under steady state conditions and upon i.p. infection with *T. gondii*. Values show the mean \pm SEM; n = 5-14. Results are from three independent experiments. Statistical differences between groups were assessed by student t test. ***p<0.001; ****p<0.0001.....65

Figure 28: Regulation of GFP-C5aR1 and tdTomato-C5aR2 expression in macrophages is different in the peritoneal cavity, spleen and lung under steady state conditions and seven days after i.p. infection with *T. gondii*. **(A)** Macrophages were identified as F4/80⁺ cells. Depicted is the dot plot from an uninfected spleen sample. Frequencies **(B)** and cell counts **(C)** of F4/80⁺ macrophages in non-infected and infected reporter mice shown as percentage of living cells. **(D)** Flow cytometric analysis of GFP-C5aR1 (upper histograms) and tdTomato-C5aR2 (lower histograms) expression in macrophages from peritoneal

cavity, spleen and lung from non-infected WT mice (grey histograms), non-infected (dashed line) and infected (solid line) C5aR1/2 reporter mice. **(E+F)** Δ MFI values for GFP-C5aR1 and tdTomato-C5aR2 expression in macrophages from the peritoneal cavity, spleen and lung under steady state conditions and upon i.p. infection with *T. gondii*. **(G+H)** Frequencies of GFP-C5aR1⁺ and tdTomato-C5aR2⁺ macrophages in peritoneal cavity, spleen and lung under steady state conditions and upon i.p. infection with *T. gondii*. **(I+J)** cell counts of GFP-C5aR1⁺ and tdTomato-C5aR2⁺ macrophages in peritoneal cavity, spleen and lung under steady state conditions and upon i.p. infection with *T. gondii*. Values show the mean \pm SEM; n = 5-14. Results are from three independent experiments. Statistical differences between groups were assessed by student t test. *p<0.05; **p<0.01; ***p<0.001; ****p<0.0001 ...68

Figure 29: Regulation of GFP-C5aR1 and tdTomato-C5aR2 expression in neutrophils from the blood, peritoneal cavity, spleen and lung under steady state conditions and seven days after i.p. infection with *T. gondii*. (A) Neutrophils were identified as Ly6g⁺ SSC-A^{high} cells. Depicted is the dot plot from an uninfected spleen sample. Frequencies (B) and cell counts (C) of neutrophils in non-infected and infected reporter mice shown as percentage of living cells. (D) GFP-C5aR1 (upper histograms) and tdTomato-C5aR2 (lower histograms) expression in neutrophils from blood, peritoneal cavity, spleen and lung of non-infected WT mice (grey histogram), non-infected (dashed line) and infected (solid line) C5aR1/2 reporter mice. (E+F) Δ MFI values for GFP-C5aR1 and tdTomato-C5aR2 in neutrophils from the blood, peritoneal cavity, spleen and lung under steady state conditions and upon i.p. infection with *T. gondii*. (G+H) Frequencies of GFP-C5aR1⁺ and tdTomato-C5aR2⁺ neutrophils in blood, peritoneal cavity, spleen and lung under steady state and upon i.p. infection with *T. gondii*. (I+J) Cell counts of GFP-C5aR1⁺ and tdTomato-C5aR2⁺ neutrophils in blood, peritoneal cavity, spleen and lung under steady state conditions and upon i.p. infection with *T. gondii*. Values show the mean \pm SEM; n = 5-14. Results are from three independent experiments. Statistical differences between groups were assessed by student t test. p<0.05; **p<0.01; ***p<0.001; ****p<0.000171

Figure 30: Regulation of GFP-C5aR1 and tdTomato-C5aR2 expression in inflammatory monocytes from the blood, peritoneal cavity and spleen under steady state conditions and seven days after i.p. infection with *T. gondii*. (A) Inflammatory monocytes were identified as Ly6g⁺ Ly6c⁺ cells. Depicted is the dot plot from an uninfected spleen sample. Frequencies (B) and cell counts (C) of inflammatory monocytes in non-infected and infected reporter mice as percentage of living cells. (D) Flow cytometric analysis of GFP-C5aR1 (upper histograms) and tdTomato-C5aR2 (lower histograms) expression in inflammatory monocytes from blood, peritoneal cavity and spleen of non-infected WT mice (grey histogram), non-infected (dashed line) and infected (solid line) C5aR1/2 reporter mice. (E) Δ MFI values for tdTomato-C5aR2 in inflammatory monocytes from the blood, peritoneal cavity and spleen under steady state conditions and upon i.p. infection with *T. gondii*. (F+G) Frequencies of GFP-C5aR1⁺ and tdTomato-C5aR2⁺ inflammatory monocytes in blood, peritoneal cavity and spleen under steady state conditions

and upon i.p. infection with *T. gondii*. **(H+I)** Cell counts of GFP-C5aR1⁺ and tdTomato-C5aR2⁺ inflammatory monocytes in blood, peritoneal cavity and spleen under steady state conditions and upon i.p. infection with *T. gondii*. Values show the mean \pm SEM; n = 5-14. Results are from three independent experiments. Statistical differences between groups were assessed by student t test. p<0.05; **p<0.01; ***p<0.001; ****p<0.000173

Figure 31: Regulation of GFP-C5aR1 and tdTomato-C5aR2 expression in cDCs from the blood, peritoneal cavity and spleen under steady state conditions and seven days after i.p. infection with *T. gondii*. **(A)** cDCs were identified as MHCII⁺ CD11c⁺ cells. Depicted is the dot plot from an uninfected spleen sample. Frequencies **(B)** and cell counts **(C)** of cDCs in non-infected and infected reporter mice shown as percentage of living cells. **(D)** Flow cytometric analysis of GFP-C5aR1 (upper histograms) and tdTomato-C5aR2 (lower histograms) expression in cDCs from blood, peritoneal cavity and spleen of non-infected WT mice (grey histogram), non-infected (dashed line) and infected (solid line) C5aR1/2 reporter mice. **(E)** Δ MFI values for GFP-C5aR1 in cDCs from the blood, peritoneal cavity and spleen under steady state conditions and upon i.p. infection with *T. gondii*. **(F+G)** Frequencies of GFP-C5aR1⁺ and tdTomato-C5aR2⁺ cDCs in blood, peritoneal cavity and spleen under steady state conditions and upon i.p. infection with *T. gondii*. **(H+I)** Cell counts of GFP-C5aR1⁺ and tdTomato-C5aR2⁺ cDCs in blood, peritoneal cavity and spleen under steady state conditions and upon i.p. infection with *T. gondii*. Values show the mean \pm SEM; n = 5-14. Results are from three independent experiments. Statistical differences between groups were assessed by student t test. p<0.05; **p<0.01; ***p<0.001; ****p<0.000175

Figure 32: Regulation of GFP-C5aR1 and tdTomato-C5aR2 expression in eosinophils from the lung C5aR1 under steady state conditions and seven days after i.p. infection with *T. gondii*. **(A)** eosinophils were identified as Siglec-F⁺ CD11c⁻ cells. Depicted is the dot plot from an uninfected lung sample. Frequencies **(B)** and cell counts **(C)** of eosinophils in non-infected and infected reporter mice as percentage of living cells. **(D)** Flow cytometric analysis of GFP-C5aR1 (upper histograms) and tdTomato-C5aR2 (lower histograms) expression in eosinophils from the lung of non-infected WT mice (grey histogram), non-infected (dashed line) and infected (solid line) C5aR1/2 reporter mice. **(E+F)** Δ MFI values for GFP-C5aR1 and tdTomato-C5aR2 in eosinophils from the lung under steady state conditions and upon i.p. infection with *T. gondii*. **(G+H)** Frequencies of GFP-C5aR1⁺ and tdTomato-C5aR2⁺ eosinophils in the lung under steady state conditions and upon i.p. infection with *T. gondii*. **(I+J)** Cell counts of GFP-C5aR1⁺ and tdTomato-C5aR2⁺ eosinophils in the lung under steady state conditions and upon i.p. infection with *T. gondii*. Values show the mean \pm SEM; n = 5-14. Results are from three independent experiments. Statistical differences between groups were assessed by student t test. ***p<0.00177

Figure 33: Impact of C5aR1 or C5aR2 deficiency on the relative and absolute cell numbers of cDCs and NK cells in the spleen. **(A)** cDC and **(B)** NK cell frequencies (left) and cell numbers (right) in the spleen of WT, C5aR1^{-/-} and C5aR2^{-/-} mice. Values show the mean \pm SEM. n=3-15. *p<0.05; **p<0.01. Statistical differences between WT, C5aR1^{-/-} and C5aR2^{-/-} were determined by ANOVA. 78

Figure 34: C5aR2 controls IFN- γ produced by NK cells. **(A)** IFN- γ production from sorted splenic NK cells of WT and C5aR2^{-/-} mice 24 h after stimulation with IL-12/IL-18. **(B)** IFN- γ production from sorted WT splenic NK cells 24 h after stimulation with IL-12/IL-18 in the presence or the absence of the C5aR2 agonist P32. Shown is the relative decrease in IL-12/IL-18-mediated IFN- γ production in response to C5aR2 stimulation by the C5aR2 agonist P32. Values show the mean \pm SEM. n=5-7 *p<0.05; ***p<0.001. Data were analyzed using unpaired student t-test (A) or paired student t-test (B)..... 79

Figure 35: Stimulation of NK cells with C5a results in reduced phosphorylation levels of p38 in WT NK cells within 10 min. **(A)** Histogram data from WT NK cells (left) and C5aR2^{-/-} NK cells (right) unstimulated (grey histograms), after 2 min C5a stimulation (dashed lines) and after 10 min C5a stimulation (bold dashed lines). Relative change of phosphorylated p38 in unstimulated or C5a-stimulated purified NK cells from **(B)** WT or **(C)** C5aR2^{-/-} mice. Values show the mean \pm SEM. n=6; *p<0.05; ***p<0.001 (ANOVA) 80

Figure 36: NKp46 expression levels in NK cells from spleen and peritoneal cavity of WT, C5aR1^{-/-} and C5aR2^{-/-} mice. **(A)** NKp46 expression in NK cells from the spleen (left) and peritoneal cavity (right) of WT (grey histograms), C5aR1^{-/-} (solid line) and C5aR2^{-/-} mice (dashed line). **(B)** Shown is the NKp46 expression as mean fluorescence intensity (MFI) on NK cells from WT, C5aR1^{-/-} and C5aR2^{-/-} mice in the spleen (left) and peritoneal cavity (right). Values show the mean \pm SEM. n=5. **p<0.01, ****p<0.0001 (ANOVA) 82

Figure 37: NKp46 expression is higher in tdTomato-C5aR2⁺ NK cells than in tdTomato-C5aR2⁻ NK cells from spleen and peritoneal cavity, but not in the blood. Shown is the Δ MFI of NKp46 expression on tdTomato-C5aR2⁺ and tdTomato-C5aR2⁻ NK cells in **(A)** blood, **(B)** peritoneal cavity and **(C)** spleen. Δ MFI = MFI_{tdTomato-C5aR2⁺} - MFI_{WT}; Values show the mean \pm SEM. n=5-9. ****p<0.0001 (unpaired student t test) 83

Figure 38: VCAM1 and CD11a expression in DCs and NK cells and frequencies of VCAM1⁺ or CD11a⁺ DCs or NK cells in WT, C5aR1^{-/-} and C5aR2^{-/-} mice. Shown is the MFI **(A, C)** or frequency **(B, D)** of DCs **(A, B)** or NK cells **(C, D)**. Values show the mean \pm SEM. n \geq 13-16; *p<0.05; **p<0.01; ***p<0.001 (ANOVA) 84

Figure 39: Gab3^{R27C} mice showed increased susceptibility and higher cyst counts in the brain during *T. gondii* infections. **(A)** Relative weight loss. **(B)** Survival of WT and Gab3^{R27C} mice during first 30 days after infection. **(C)** Survival of WT and Gab3^{R27C} mice between day 22 and day 30 after infection. **(D)** Gab3^{R27C} mice show significantly increased parasite burden in the brain 30 days p.i. The data are from

three independent experiments; values show the mean \pm SEM. n=10-15; Data were analyzed by ANOVA (A), by Log-rank (Mantel-Cox) (B+C) and by unpaired student t-test (D). * $p \leq 0.05$ *** $p < 0.001$

.....86

Figure 40: Cytokine and chemokine levels from WT and $Gab3^{R27C}$ mice in serum were comparable between day 1 and day 7 p.i. with 50 cysts of *T. gondii* i.p. Cytokine levels were analyzed using Bio-Plex® multiplex system (Bio-Rad Laboratories GmbH, Munich). Values show the mean \pm SEM. n=3; * indicates significant differences during the observation period within the WT group, # indicates significant differences during the observation period within the $Gab3^{R27C}$ group, + indicates differences during the observation period between the WT and $Gab3^{R27C}$ group; # * $p \leq 0.05$; ** $p < 0.01$; *** $p < 0.001$ **** $p < 0.001$. Data were analyzed by ANOVA.....87

Figure 41: Immune cells predominantly differentiate from $CD45.1^+$ WT donors. Results obtained with mixed BM chimeric mice using WT $CD45.1^+$ and $CD45.2^+$ recipients and WT ($CD45.1^+$) as well as $Gab3^{R27C}$ ($CD45.2^+$) donors. The graphs depict immune cells differentiated either from WT or $Gab3^{R27C}$ cells in the peritoneal cavity 30 days after transfer. **(A)** Cell frequencies of $CD45.1^+$ WT and $CD45.2^+$ $Gab3^{R27C}$ cells. **(B)** Frequencies of myeloid and lymphoid cell populations in the peritoneal cavity that differentiated from either $CD45.1^+$ WT or $CD45.2^+$ $Gab3^{R27C}$ donor cells in $CD45.1^+$ (left) and $CD45.2^+$ (right) WT recipients. Values in B show the mean \pm SEM. n=489

Figure 42: C5aR2 stimulation leads to blockade of p38 phosphorylation. Schematic figure illustrating the function of C5aR2 on **(A)** WT and **(B)** $C5aR2^{-/-}$ NK cells. C5a stimulation of C5aR2 results in decreased phosphorylation of p38 MAPK and consequently in reduced IFN- γ production after IL-12/18 stimulation in WT NK cells. $C5aR2^{-/-}$ NK cells lack this regulatory mechanism and are hyperresponsive to IL-12/18 stimulation and produce more IFN- γ97

Figure 43: Schematic figure showing the impact of the *Gab* mutation $Gab3^{R27C}$ during the acute and chronic phase of *T. gondii* infection. **(A)** In the WT mice immediate innate immune cell activation drives effective elimination of tachyzoites. The development of an appropriate adaptive immune response converts the remaining tachyzoites into tissue cysts residing preferentially in the brain. **(B)** In the $Gab3^{R27C}$ mice, a delayed or impaired innate immune response results in ineffective elimination of tachyzoites in the acute phase of the infection which leads to increased tissue cyst production that cannot be efficiently controlled by the adaptive immune system.101

6.3 Tables

Table 1: Overview of C5a-mediated effects on immune cells via C5aR1 and C5aR2. Modified from (Lee et al., 2008).	9
Table 2: Mouse Strains. B6 = C57BL/6J, cg = congenic, tg = transgenic, tm = targeted mutation.....	29
Table 3: Chemicals and reagents	29
Table 4: Stimulants	31
Table 5: Buffers, solutions and media	31
Table 6: Antibodies. AF = Alexa Fluor®, APC = Allophycocyanin, BV = Brilliant Violet, Cy = Cyanin, FITC = Fluorescein isothiocyanate, PE = Phycoerythrin, PerCP = Peridinin-chlorophyll-protein complex, hamster = Armenian hamster	32
Table 7: Plastic ware and disposable items	34
Table 8: Commercially available kits	35
Table 9: Laboratory equipment	35
Table 10: Computer Software	37

Oral Presentations

NDI3 - New Developments in Immunology, Inflammation and Infection, Borstel (2017)

“C5aR2 is expressed in NK cells during acute *Toxoplasma gondii* infection and controls NK cell function in vitro”

6.4 List of publications

“Monitoring C5aR2 Expression Using a Floxed tdTomato-C5aR2 Knock-In Mouse.” Karsten CM, Wiese AV, **Mey F**, Figge J, Woodruff TM, Reuter T, Scurtu O, Kordowski A, Almeida LN, Briukhovetska D, Quell KM, Sun J, Ender F, Schmutde I, Vollbrandt T, Laumonnier Y, Köhl J.

J Immunol. 2017 Nov 1;199(9):3234-3248. doi: 10.4049/jimmunol.1700710

6.4.1 Congress contributions

Poster Presentations

International Cluster Symposium, Kiel (2015)

“The role of C5a-mediated cross-talk between natural killer cells and dendritic cells in *Toxoplasma gondii* infection”

1st International Symposium on Immunoregulation in Allergy and Infection, Luebeck (2016)

“Role of C5a/C5aR in the activation of natural killer cells”

16th European Meeting on Complement in Human Disease, Copenhagen (2017)

“C5aR2 is expressed in NK cells during acute *Toxoplasma gondii* infection and controls NK cell function in vitro”

47th Annual Meeting German Society for Immunology, Erlangen (2017)

“C5aR2 is expressed in NK cells during acute *Toxoplasma gondii* infection and controls NK cell function in vitro”

Annual Immunology Retreat Cincinnati Childrens Hospital Medical Center, Cincinnati (2017)

*“C5aR2 is expressed in NK cells during acute *Toxoplasma gondii* infection and controls NK cell function in vitro”*

NDI3 - New Developments in Immunology, Inflammation and Infection, Borstel (2017)

“C5aR2 is expressed in NK cells during acute *Toxoplasma gondii* infection and controls NK cell function in vitro”

7 ACKNOWLEDGEMENTS

This thesis wouldn't be possible without the help and support of several people who I would like to express my gratitude:

Prof. Dr. med. Jörg Köhl for the opportunity to work in his institute for the past 3,5 years and for taking over supervision for my thesis.

Dr. Christian Karsten and Dr. Julia Figge for all the time they invested during the progress of this thesis, for inspiring discussions during the past years and the great atmosphere in the lab and outside. Thanks for great Christmas parties, "Why am I (un)happy"-meetings, lab meetings with lots of cake and all the HSV jokes.

PhD Kasper Hoebe and PhD Edith Janssen for a great time I spent in Cincinnati, where I learned so many things and enjoyed being there. Special thanks to Kasper for all his time for our – more or less – regular skype meetings and the helpful discussions. Also, thanks to **all team members** of both labs. You all made my stay in Cincinnati memorable!

Prof. Dr. Norbert Tautz for being head of the examination board.

Prof. Dr. Tamas Laskay for taking part in the yearly reports as the 3rd supervisor of my project.

Prof. Dr. med. Dirk Schlüter for sharing his expertise regarding *T. gondii* experiments and providing of parasite cultures.

Prof. Dr. Ulrich Schaible for being the second referee for my thesis.

Dr. Tillman Vollbrandt for his patience while sorting millions of NK cells for me and for some great Squash lessons.

All the students I was allowed to work with: **Birte Ohm, Lilit Grygorjan, Sebastian Wenzel, Caroline Hennig, Lucia Grandison**. I really enjoyed working with all of you and I hope that I could awaken your interest in research, the complement system and at least a little bit in soccer 😊.

Lana Pohle for her excellent work and help during long infection experiment days, also on weekends. Also, thanks to **Gabriele Köhl** and **Esther Strerath** for assistance regarding animal management and ordering. **Claudia Delfs** for assistance with organizing and paperwork.

To **all present and past ISEF colleagues** for a great working atmosphere, coffee breaks, birthday cakes and legendary "Sekt"-Fridays.

Special thanks to my parents **Heidi and Udo Mey** who always supported me during my study, work and in every situation in my life. It makes everything easier, if you know that you have your support from home. And home is where your heart is!

Another special thanks to **Melissa!** You were “stupid” enough to choose a scientist, but for over 7 years you are always at my side to support, motivate or solace me. That’s not taken for granted and I really appreciate that!

8 CURRICULUM VITAE

FABIAN MEY

Königstr. 69
32427 Minden, Germany
+49 151 70068044
fabianmey@gmx.de



Personal Profile:

Young PhD with expertise in biomedicine and infection models; skills in molecular methods and techniques; advanced experience in supervision and project management, ability to work in a team with good self-organization and high motivation.

Professional Experience

- 12/2018 – now **Project Manager: Quality control at the LOMAPHARM GmbH, Emmerthal**
- 02/2015 – 08/2018 **PhD Student at the Institute for systemic inflammation research (ISEF), Luebeck**
Project B2 - The role of C5a-mediated cross-talk between natural killer cells and dendritic cells in *Toxoplasma gondii* infection
- 02/2016 – 08/2016 **Exchange student at Division of Immunology, laboratory of Kasper Hoebe, PhD**
Cincinnati Children's Hospital Medical Center and University of Cincinnati College of Medicine
Role of Gab3 proteins during *Toxoplasma gondii* infections
- 05/2012 **Assistant at the University of Osnabrueck, department of animal physiology**
Responsible for the students during the practical course, correct protocols and conduct oral exams

Education:

- 10/2012 – 10/2014 **Master of Science in Cell and Molecular Biology at University Osnabrueck**
Final mark: 1.3
Master's thesis: "Localisation of protein trap transposons within the „Morin“-collection: Lines 110-707, 110-710, 110-726, 110-853" (*mark: 1.5*)
- 10/2009 – 9/2012 **Bachelor of Science in Cell and Molecular Biology at University Osnabrueck**
Final mark: 2.2
Bachelor's thesis: "Electrophysical investigations of the membrane potential on the marine ciliate *Euplotes vannus*" (*mark: 1.8*)
- 07/1999 – 05/2008 **Abitur at Staedtisches Gymnasium Petershagen, Petershagen**

Abitur, final mark: 2.7

Focus subjects: Biology, History

Further examination subjects: English, Sports

Voluntary Activities:

- 04/2010 – 09/2014 **Active member of the student association,**
Department: Biology/Chemistry of the University of Osnabrueck
- 04/2011 – 03/2013 **Member of the study commission,**
Department: Biology/Chemistry of the University of Osnabrueck
- 01/2011 – 12/2011 **Member of the council of the student association,**
Department: Biology/Chemistry of the University of Osnabrueck
- 06/2008 – 09/2009 **Coach and responsible person of the U19-Soccerteam**
TuS Petershagen Ovenstaedt

Skills:

- Animal handling: Surgical dissection, harvesting of tissues, blood sampling, oral gavage, i.p. and s.c. injections,
Toxoplasma gondii infection models
- Flow cytometry: Isolation of murine immune cells from peritoneal cavity, spleen, lymph nodes, brain, lung.
 FACS and MACS cell enrichment, sorting and purification. Intracellular and extracellular stainings for flow cytometry, multicolor panel design, flow cytometry (LSRII, FACSAria III)
- Cell culture: bone-marrow derived dendritic cells, macrophages, peritoneal macrophages, splenic DCs, LAK cells, cultivation of *T. gondii* in eukaryotic cells
- Microscopy: Laser scanning confocal microscopy (Olympus FV1000), vital imaging of cells in vitro
- Histology: OCT embedding, processing and cryosectioning, H&E and immunofluorescent staining
- Techniques: Genomic DNA and RNA extraction, protein and nucleic acid quantification, PCR/RT qPCR, SDS-PAGE, ELISA, multiplex assays (Biolegend LEGENDplex, AYOXXA Lunaris)
- Supervision: Supervision of 2 medical students (1 year each, Luebeck), 2 master student (6 months each, Luebeck), 1 RISE student (3 months, Luebeck), 1 summer student (3 months, Cincinnati) during PhD student period

Language German: Native
 English: Fluent

IT MS Office Very Good
 Open Office Very Good
 Photoshop Good
 ImageJ Good

FlowJo	Very Good
GraphPad	Very Good
Imaris	Good

Other skills efficient, organized, reliable, highly motivated, learning receptivity

Interests:

Soccer I have been playing competitive soccer for several years and currently play for the TuS Petershagen/Ovenstaedt. Apart from keeping me fit, it also teaches me about the importance of teamwork.